UNIVERSITY OF SOUTHAMPTON

Faculty of Natural and Environmental Sciences

School of Chemistry

# Synthesis of dimeric pyridylguanidinium based supramolecular structures stable in polar and aqueous solvent systems

by

Biniam Fessehaye Tesfatsion

Doctor of Philosophy

December 2011

*To My Dad, Fessehaye Tesfatsion Gebru*

UNIVERSITY OF SOUTHAMPTON

# ABSTRACT

FACULTY OF NATURAL AND ENVIRONMENTAL SCIENCES

SCHOOL OF CHEMISTRY

Doctor of Philosophy

## Synthesis of dimeric pyridylguanidinium based supramolecular structures stable in polar and aqueous solvent systems

by Biniam Fessehaye Tesfatsion

This thesis describes the synthesis of a series of pyridyl guanidinium-carboxylates. Dilution and spectroscopic studies are made thus affording information concerning the molecular forces controlling their dimerisation. Chapter I provides an introduction to the thesis and discusses, in the main part, the thermodynamics of self-assembly with particular focus given to guanidinium-carboxylates. Chapter II describes the syntheses and dimerisation studies undertaken and Chapter III contains the experimental procedures and results. The dimerisation of the pyridylguanidinium-carboxylates was investigated in DMSO and $H_2O$/DMSO mixtures using isothermal calorimetric and NMR dilution techniques and the relative importance of H-bonding, π- π stacking, electrostatic and hydrophobic interactions in constructing a dimeric self-assembled system in polar and aqueous environment has been investigated.While most of the guanidinium-carboxylates show excellent dimerisation in DMSO (~ $K_{dim}$ = 7692±1124 $M^{-1}$) and 10% $H_2O$/DMSO (~ $K_{dim}$= 2695±151 $M^{-1}$), some of them exhibit entropy driven dimerisation in an aqueous environment containing up to 50% (~$K_{dim}$= 55±8 $M^{-1}$) and 75% (~$K_{dim}$= 27±7 $M^{-1}$) $H_2O$ in DMSO.

# Table of contents

# Preface

The research contained within this thesis was undertaken under the supervision of Professor J.D.Kilburn at the University of Southampton between October 2007 and August 2011. No part of this thesis has previously been submitted to this or any other university.

# Acknowledgments

My special thanks goes to my supervisor Professor Jeremy D Kilburn for giving me the opportunity to work in his lab and being supportive and encouraging in the whole course of this PhD research work. I am very much indebted to Dr.Sally Dixon who has been the integral part of this PhD work from the inception till the completion the thesis writing. I would like to extend my gratitude to my advisor Professor Philip Gale for the advice and guidance he offered.

I am grateful to Neil Wells for the excellent NMR services; John Langley and Julie Wright for the quality mass spec services; Mark Light for the X-ray crystallography services and the store facility. And I am very thankful to ORS and the School of Chemistry of the University of Southampton for funding this PhD work.

This PhD research work would not have been possible had it not been for the devotion and determination of Janet and John Mellor, who fought hard to sort out the visa problem I initially encountered in coming to the UK. I am very grateful to John and Janet for sponsoring the lengthy court proceeding and for their continuous care and support in the difficult times. I again want to mention the support I had from Professor Jeremy D Kilburn at this difficult juncture. I want to thank my dear friends Biniam Dawit and Kibrom Tewolde, for making things easy during my stay in Nairobi, Kenya on my way coming to the UK.

I would like to extend my gratitude to Kilburn group past (Luke, Jean, Irfan, Jariya Junxiu) and present (Aleksandra, Will, Emma and Boris). I specially want to thank William Nesbit for being helpful in and outside the lab and for his invaluable comments in the course of the thesis writing.

My special thanks goes to my beloved wife Feven Tesfabrhan Abraham for making my life so special and for the continuous love and care she cherished me.

The support and care from my beloved friends, Manny Zewdu and Michael Fitsumbrhan, has been very instrumental in overcoming all the challenges of doing this PhD research work.

And finally, I would like to express my gratitude to my family (My mum Gabriela, My sisters Almaz, Selam, Aster, Eden and my brother Tedros) for their love and support.

# Abbreviations used

AA: Amino acid

Ala: Alanine

Boc: Di-*t*-butyl dicarbonate

Cbz: Benzyloxycarbonyl

CC: Column chromatography

DCM: Dichloromethane

DEAD: Diethyl azodicarboxylate

DMSO: Dimethylsulfoxide

DMF: *N*, *N*-dimethyl formamide

EtOAc: Ethyl acetate

EtOH:Ethanol

$Et_3N$: Triethyl amine

EDC: 1-Ethyl-3-(3-dimethylaminopropyl) carbodiimide hydrochloride

ESI-MS: Electrospray ionization mass spectrometry

Gua: Guanidiniocarbonyl pyrrole cation

Gly: Glycine

HOBT: 1-Hydroxybenzotriazole

Ile: Isoleucine

ITC: Isothermal titration calorimetry

Leu: Leucine

$Me_3SiOK$: Potassium trimethylsilanolate

MeOH: Methanol

NMR: Nuclear magnetic resonance

NMM: N-Methylmorpholine

NaOMe : Sodium methoxide

NOESY: Nuclear Overhauser Effect Spectroscopy

PE: Petroleum ether

PyBop: Benzotriazol-1-yl-oxytripyrrolidinophosphonium hexafluorophosphate

Pd/C: Palladium/carbon

PEG: Polyethleneglycol

Phe: Phenylalanine

rt: Room temperature

Trp: Tryptophane

Tyr: Tyrosine

THF: Tetrahydrofuran

TFA: Trifluoroacetic acid

Val: Valine

# 1. Introduction

Supramolecular chemistry has significantly advanced in recent years both in terms of prospective applications and in its relevance to biological systems. The formation and function of supramolecular complexes is orchestrated through non-covalent binding forces that usually occur in multiplicity in a given system.[1] The study of non-covalent interactions is crucial to understanding many biological processes that depend on these forces for structure and function. Weak, non-covalent, intermolecular interactions responsible for the binding and self-assembly of supramolecular structures include hydrogen bonds, coordination bonds in ligands and complexes, ionic interactions, dipolar interactions, van der Waals forces and hydrophobic interactions. Hydrogen bonding is the favourite intermolecular force in self-assembling systems by virtue of its directionality, specificity, and its abundance in biological systems.[2] Many protein structures in water are held together by hydrogen bonding.[3] Monomeric structures can self assemble with the help of hydrogen bonding since the energy stored in an intermolecular hydrogen bond is large enough to overcome the intermolecular thermal energy (30 kJ mol $^{-1}$ *vs* 4 kJ mol $^{-1}$).

## 1.1 The biological significance of non-covalent bond interactions

All physiological processes in biological systems involve non-covalent bond interactions of one or more types and alterations or disruptions of the nature of the non-covalent binding forces in a given system are likely to be followed by a change in the physiological processes. Cell division, enzyme substrate binding, hormonal regulations, antigen-antibody binding, transportation of macromolecules in the blood, intercellular communications, neurotransmitter activities and intracellular signal transduction processes are only a few of the activities in our body which are crucially dependent on non-covalent binding forces operating among macromolecules involved in the particular process. With this in mind, it is not unexpected that physiological and anatomical malfunctions resulting in alteration of features important in the non-covalent binding processes of a given biological system will result in pathological conditions. In most of the circumstances the underlying causes for the alteration are unknown but are believed to be of genetic origin. Understanding the disease processes and hence coming up with a therapeutic intervention strategy requires a profound and

deep knowledge of the binding phenomena occurring among biomolecules involved in the given system.

### 1.1.1 Diseases of protein aggregation

Protein aggregation is a very common phenomenon in biological systems and significantly involved in numerous physiological and pathological processes. Partial folding of protein intermediates which may arise as a result of genetic alterations is believed to be the cause of the formation of protein aggregates. These intermediates are susceptible to aggregation due to the exposure of the hydrophobic core which usually lies in the inside core of a tertiary and secondary protein structure. *In vitro* studies done by exposing proteins to solvent environments similar to those of biological systems have established this generic property of proteins.[4] A detailed analysis of amino acid-amino acid interactions in protein structures especially those of the side chains of non-polar residues is very important if we wish to have a better understanding of disease processes which are the direct result of abnormal protein aggregations.

In human etiology, more than 20 different devastating human diseases have been reported to be associated with protein aggregation. It is increasingly being established that neurodegenerative diseases such as Alzheimer's disease (AD), Parkinson's disease (PD), Huntington's disease (HD), amyotrophic lateral sclerosis (ALS) and prion diseases are characterized by molecular mechanisms resulting in the formation of protein aggregates. The aggregates are made up of fibres containing misfolded protein with a ß-sheet conformation, termed an amyloid. Accumulation of these abnormal proteins in tissues is believed to play the crucial part in the disease process by causing cell degeneration. These visible protein aggregates are the end result of a molecular cascade of several steps and are directly associated with the pathogenesis of the particular neurodegenerative disease. Protein aggregation diseases have been the centre of intense research and a lot of research activities are being undertaken to understand the pathways and the mechanisms involved in protein aggregation. Understanding protein aggregation at molecular level will pave the way to rational therapeutic strategies for neurodegenerative diseases which are now collectively one of the leading causes of mortality in the developed world. [5]

### 1.1.2 Non-covalent bond interactions and drug design

Apart from their importance in explaining enzyme kinetics and various physiological and pathological phenomena, non-covalent interactions are widely recognized for their paramount importance in the processes of molecular recognition. Various kinds of supramolecular structures have been designed and exploited for their usage as molecular recognition entities by virtue of their ability to make selective binding with the desired target substances. [6] This concept is hugely important in drug design as drugs should have the optimum bioavailability only at the desired site of action thereby minimizing undesired effects of the drug resulting mainly from interaction with non-target receptors in other tissues.[7] Pharmacokinetics and tissue drug distribution are also hugely affected by the reversible non-covalent bond interactions occurring between the drug molecule and the transporter macromolecule inside our body.[8] The huge potential of supramolecular chemistry in revolutionizing therapeutics is being exploited and can be exemplified by the developments of supramolecular capsules, nanoparticles and liposomes which are opening the door for the concept of targeted drug delivery.[9] Commercial preparations of liposomes are now available to fight life-threatening diseases.[10] Liposomes are formed spontaneously through the self-assembly of phospholipids when placed in an aqueous medium. The vesicles consist of simple lipid bilayers that resemble biological membranes, in the form of a spherical shell. It is their particle entrapping ability that makes liposomes drug carrier structures.[11] They are potential drug carriers for small molecular weight drugs, therapeutic proteins, and diagnostic agents.

### 1.1.3 Supramolecular chemistry and biological processes

One very common feature of supramolecular and biological systems is the fact that the function of both is crucially dependent on non-covalent interactions operating in the systems. Some attempts have been made to simulate biological processes through synthetic supramolecular structures.[12] However, this is severely restricted to nonpolar solvent systems because of the very limited usage of synthetic supramolecular systems in solvents of high polarity. This research project will attempt to throw a light on this by synthesizing supramolcular structures that can maintain stability in polar environment. These pyridoguanidinium based supramolecular structures to be

considered in this project would permit investigation of some biologically pertinent amino acid amino acid interactions.

## 1.2 Binding mechanisms in supramolecular systems

### 1.2.1 Non-covalent bond interactions

As mentioned previously, at the heart of most biological processes and molecular recognition events is the concept of non-covalent interactions. A non-covalent interaction can simply be described as an interaction between two species that does not involve the sharing of pairs of electrons, but rather involves more dispersed electromagnetic interactions. Associations of this nature cover a variable range of energies (2 $kJmol^{-1}$ in London dispersion forces to 350 $kJmol^{-1}$ in ionic-interactions) and depend explicitly on the structure and functionality of the species involved in the non-covalent bonding and also on the local environment in which the bonding is happening.[13] Though the magnitude of individual non-covalent bonds is much less than covalent bonds, additive interactions involving a multitude of binding centres in reversibly formed supramolecular complexes can lead to binding strengths approaching those of covalent bonds. This is due to what is referred as the 'chelate effect' or 'multivalency'.[14] The table below lists the major types of non-covalent interactions important in biological systems.[15]

| **Interaction type** | **Properties** |
|---|---|
| Charge-charge | Attractive or repulsive, distance dependent, ranges 100-350 $kJ.mol^{-1}$ |
| Charge-dipole | Attractive, distance dependent, ranges 50-200 $kJ.mol^{-1}$ |
| Dipole-dipole | Attractive or repulsive, distance dependent, short range interactions, ranges 5-50 $kJ.mol^{-1}$ |
| Nonpolar – nonpolar (London dispersion energy) | Attractive, distance dependent |
| Hydrogen bond | Directed interaction, responsible for the special properties of water and biological macromolecules, ranges 5-30 $kJ.mol^{-1}$ |
| Hydrophobic | Does not arise as a result of a direct interaction between the non-polar molecules, comparable in energy to hydrogen bonds |

**Table 1** *Types of non-covalent bond interactions*

As seen from table 1, most of the interactions are attractive in nature. There are circumstances when charge-charge and dipole-dipole might be repulsive. This depends on the signs of the charges and the relative angular orientation of the dipoles. Permanent and induced dipoles cause an attractive interaction by accommodating the forces acting upon them. Species with no charge or dipole associated with them can still attract each other due to Van der Waals forces (non polar-non polar interactions) caused by the polarizability of the group. All types of non-covalent bond interacting forces are distance-dependent. The dielectric constant of the medium through which the interaction is happening greatly influences the strength of the non-covalent bond interaction. A solvent with a high dielectric constant, such as water and DMSO, will greatly reduce interaction energies. The dielectric constant also explains the difference between the magnitudes of these forces in solution versus the gas phase, where the dielectric effect of the solvent is not present. It is also established that energies of interactions based on charge-non polar, dipole- non polar and non polar- non polar events are expected to increase as the effect of solvation is removed. This is due to the decrease of the polarizability of the interacting species in the presence of solvent molecules. An exception to this is a hydrophobic interaction between two non polar units, where the presence of water increases the attraction between these moieties. Hydrogen bonding interactions, hydrophobic interactions and ion pair interactions, which are the dominant binding forces in supramolecular complexes and which will be exploited in this PhD research project are further explained below.

### 1.2.2 Hydrogen bonds

A hydrogen bond is an attractive force of interaction between hydrogen attached to an electronegative atom of one molecule and an electronegative atom of a different molecule. Hydrogen bonds have been traditionally defined by the formalism D-H…A, where donor D and acceptor A are both electronegative atoms, such as N, O, or F.[16] Currently, even weaker donor atoms, such as carbon, are also found to contribute to the formation of hydrogen bonding in many binding systems. It has to be noted that a hydrogen bond is largely electrostatic in nature; but it does not involve actual ionization. Electrostatic and exchange-repulsion terms are considered to account for more than 80% of the hydrogen-bond interaction, with the other 20% made up of dispersive and polarization energies.[17] It is also observed that hydrogen bonds show a

tendency toward more cooperative effects through mutual polarization of the interacting groups participating in the hydrogen bonding.[18] The nature of the solvent molecules greatly influences the extent of these interactions, since they may have hydrogen-donor and -acceptor character as well and hence create a competitive environment. The contribution of the hydrogen bond can be reduced dramatically in solution due to entropic effects, solvation, or dielectric conditions.[19]

One very important feature of hydrogen bonding is that the degree of interaction is critically dependent not only on the distance, but also on the orientation or alignment of the hydrogen bonding groups.[20] The directionality of hydrogen bonds is a very important characteristic for the process of selective molecular recognition. Classic examples include synthetic receptors such as **1** used for the selective complexation of carboxylates. In DMSO, carboxylates are bound by **1** with K $>10^3$ $M^{-1}$, but sulfates or halides with only K$<$ 50 $M^{-1}$.[21]

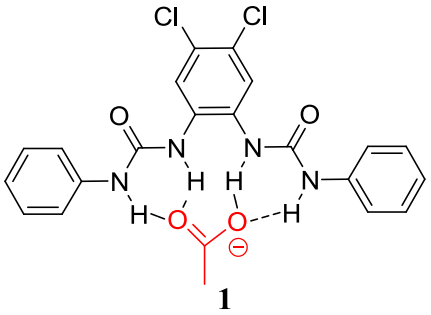


**1**

Though individual H-bonds are weak, a strong, positive cooperative effect has been observed when there are a multitude of hydrogen bonds in a given supramolecular complex. This property of hydrogen bonds can be exploited in the development of receptors for drug molecules. Hamilton *et al.* have designed receptors **2** for barbiturates and studied the effect of multiple hydrogen bonding on the binding affinity of the receptor. [22]

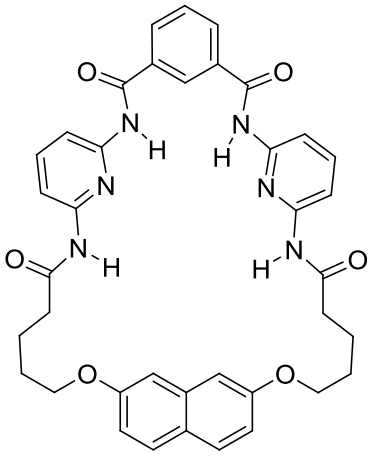

**2**

The selectivity of receptor **2** for various derivatives of barbiturates (**3**-**7**) was investigated and marked selectivity ($K_{ass}$~$10^5$ $M^{-1}$ in DCM) was observed for barbital **3** which contains additional hydrogen accepter sites as compared with barbitals **4**, **5** and **7** (Fig1).

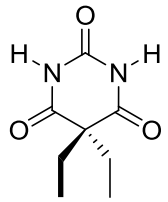

**3**

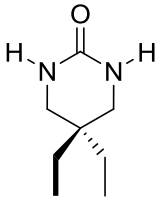

**4**

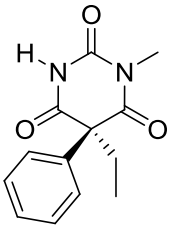

**5**

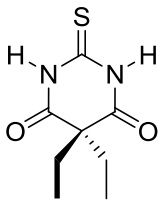

**6**

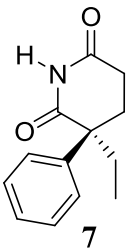

**7**

Steric factors also contributed for the less efficient binding of barbitals **5** and **7**. Though all the six H-bonding sites are present in **6,** the binding is 350-fold weaker. This is consistent with the weaker H-bond accepting characteristics of sulfur (compared to oxygen) as well as its larger size, inhibiting binding into the cavity.

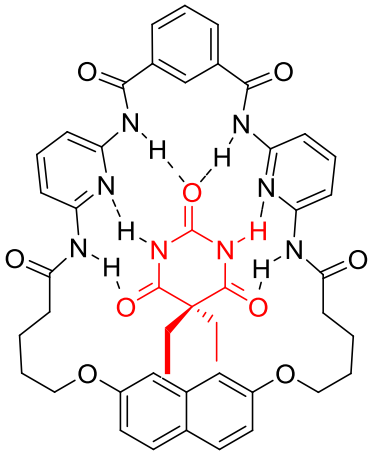

**Fig 1** *Binding of barbital **3** with the macrocyclic receptor **2***

Hydrogen bonding is seen to be one of the dominant forms of non-covalent binding forces being exploited by supramolecular chemists in developing synthetic receptors and self-assembled systems. The self-assembled systems designed in this research project will be crucially dependent on the intermolecular bidentate hydrogen bonding between the guanidinium moiety and the carboxylate anion.

## 1.2.3 Hydrophobic interactions

Solvophobicity is a phenomenon that explains the interaction between polar solvent molecules and non-polar solutes. Hydrophobicity is the most commonly observed solvophobic phenomenon owing to the ubiquitous nature of water.[13] The hydrophobic effect originates from the disruption of the highly structured hydrogen bond network among water molecules upon mixing with non-polar solutes. Water exhibits a much stronger solvophobic effect than other solvents. This is due to the fact that a large number of solvent molecules are required to solvate a given substrate and water, owing to its small size, does the job more efficiently than other common solvents. In addition, the heavily structured nature of water molecules through hydrogen bonding plays a crucial role in creating favourable theromodynamics for the solvation process.

The classical Frank–Evans model illustrates the hydrophobic effect as an entropic advantage upon the association of lipophilic substrates, which arises through the release of water molecules surrounding the lipophilic molecules. When a lipophilic molecule is put in water it results in increased ordering of the surrounding water

molecules forming the solvation sphere. This leads to significant losses in translational and rotational entropy of water molecules and makes the process unfavorable in terms of the free energy of the system. Upon coalescence of two or more substrate molecules, less water molecules are required to form the solvent sphere surrounding the resulting aggregate than were previously necessary. This is simply due to the decrease in surface area. This new system will experience less significant loss in entropy as compared to the previous one and hence a favourable free energy of formation. [23]

.

Hydrophobic interactions play a major role not only in biologically important interactions, but also in many biomimetic synthetic complexes. The hydrophobic effect plays an important role in protein aggregation, lipid bilayer formation, membrane protein structuring and protein-small molecule interactions. [24]

### 1.2.4 Electrostatic or ion pair interactions

Ion pairs and electrostatic interactions play a very significant role in the formation of both biological and supramolecular complexes. It is one of the most dominant forces that operate in enzyme-substrate interactions and is largely responsible for the selective and specific binding of a substrate with an active site of an enzyme.The contribution of these types of interactions for the stabilization of the secondary and tertiary structure of peptides and proteins is also of paramount importance in nature. [25]

The free energy of interaction accompanying two charged groups in a vacuum is purely enthalpy driven. But this is not the case when there are solvent molecules accompanying the charged species. The free energy of interaction between charged groups in water is often dominated by entropy. This is due to reconfiguration of water molecules surrounding the charges in response to the association or interaction of the charged species. And the effect of the solvent is correlated with the dielectric constant and is expected to be high in solvents like water and DMSO.[25]

The free energy of interaction ($\Delta G$) between two charged species in solution is given by the following relation:

.

$\Delta G = e^2 z1z2/4\pi E_o Er$, where z1, z2 = The number of charges, $E_o$ = The dielectric permittivity in vacuum, E = The relative permittivity of the solvent

It is evident from the equations above that the dielectric constant (E) of the solvent through which the interaction between the charged species is happening directly affects the free energy of the binding process. The interaction between two charged species in organic solvents of low dielectric constant is enthalpy driven as opposed to the entropy driven interaction of the same charged species in solvents of high dielectric constant like water.

In this PhD research work, we will attempt to use a combination of the above mentioned non-covalent interactions in order to access dimeric supramolecular structures in solvents of high polarity and dielectric constant (DMSO and DMSO-$H_2O$ mixture). Analysis of the thermodynamic behaviour of these supramolecular systems might enable us to better understand these interactions in polar and aqueous solvent systems and enrich our knowledge of numerous biologically important processes which depend on non-covalent bond interactions for their function.

## 1.3 Solvent effect on the binding phenomena

Solvent effect on the binding process is very crucial and should never be understated. If binding between two complimentary interacting molecules is to occur, first and foremost solvation of the chemical groups should happen. This is a must if the molecules are to be dissolved by the solvent in which the binding study is to be undertaken. Once dissolved, the molecules should diffuse through the medium and approach each other. The solvent will help in moderating the temperature of the binding process either by absorbing heat as in the case of exothermic processes or releasing heat if it is an endothermic one.

One of the main challenges of supramolecular chemistry is to design a host guest system that can function in a solvent medium which mimics a biological environment, *i.e* very high polarity and dielectric constant. Binding is greatly hampered in such kind of competitive solvent systems due to the solvent molecule's ability to form hydrogen bonding with the interacting sites which makes the binding event enthalpically unfavourable. If binding occurs in such media, it is often entropy driven which arises

from the liberation of the solvent molecules upon association of the molecules. The enthalpic loss should be well compensated by entropy if the binding is to be feasible thermodynamically. It is the overall balance of enthalpy and entropy that will eventually decide the thermodynamic feasibility of the binding process. [26] This is what is referred to as the enthalpy-entropy compensation.[27]

## 1.4 Free Energy of Binding

The free energy of binding in a given physico-chemical process is given by the Gibbs-Helmholtz equation: $\Delta G = \Delta H - T\Delta S$, where $\Delta G$ is the Gibbs free energy, $\Delta H$ is enthalpy, T is temperature in Kelvin, and $\Delta S$ is entropy. For a binding process to proceed spontaneously $\Delta G$ should be less than zero. The more negative the value of $\Delta G$, the more favourable is the binding process, and this is associated with either a negative value of $\Delta H$ or a positive value of $\Delta S$, or both.

The thermodynamic feasibility of a given binding process depends on the balance of contributions made by each species upon complexation. These contributions can be negative or positive and arise due to the modification of the solvation of the host and/or guest, the modification of the degrees of freedom of the host and/or guest, the electrostatic interactions, the hydrophobic interactions, the hydrogen bonding, the π–π interactions, *etc*.[28] It is impossible to dissect the enthalpic and entropic contribution of all the components in a given supramolecular complex. However, some general trends can be anticipated in a given binding process. In water for example, ion pairing is entropically driven while long-range coulombic bonds or hydrogen bonds are generally enthalpically driven. It was also noted that π– π interactions give a negative (favorable) contribution to $\Delta H$ where as hydrophobic interactions give a positive contribution to $T\Delta S$. However, a clear elucidation of the overall interplay of all the factors to give either a positive or negative $\Delta G$ value is a daunting task awaiting a very formidable research endeavour.

## 1.5 Quantification of non-covalent interactions in synthetic systems

Quantification of a specific non covalent bond interaction from an array of interactions in a given system is a very difficult task and is a current challenge for supramolecular chemists. [30] Some degree of success has been registered in developing supramolecular models which could be used to study specific non-covalent interactions among a multitude of interactions operating in a given supramolecular structure. The double-mutant cycle (DMC) method, which is now a standard practice for the quantification of non-covalent interactions in proteins [29], is also valuable to study individual functional group interactions present in other synthetic systems. [30, 31] A simplified schematic representation of the DMC cycle was proposed by Fersht in 1994 (Fig 2).[32] If the change in free energy upon making a single X mutation ($\Delta G_{XY \rightarrow X'Y}$) differs from the free energy change when the same mutation is made to a single Y mutant protein ($\Delta G_{XY' \rightarrow X'Y'}$), then there must be an interaction between the mutated residues X and Y. The extent of any direct and indirect interaction of X and Y is given by:

$$\Delta\Delta G = \Delta G_{XY \rightarrow X'Y} - \Delta G_{XY' \rightarrow X'Y'} = \Delta G_{XY \rightarrow XY'} - \Delta G_{X'Y \rightarrow X'Y'}$$

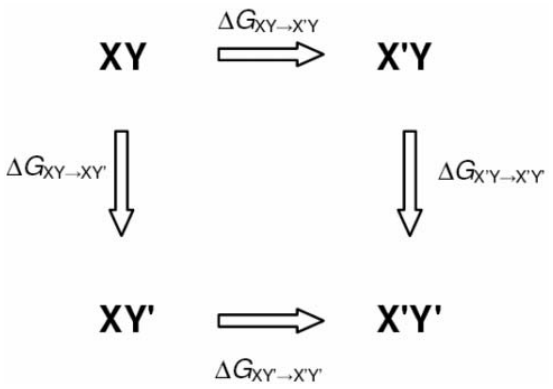


**Fig 2** *Schematic representation of the double mutant cycle* [30]

However, the following criteria should be met for the validity of the DMC approach to be accurate for such a purpose.

- The mutant substitutions should be non-interacting

- ❖ There should be no differences in the conformation of each member of the cycle
- ❖ The molecular framework should remain intact as it might be an essential part of the molecular recognition event

Synthetic systems which fulfilled the above mentioned requirements have been synthesized and exploited using the concept of DMC approach to quantify a number of non-covalent bond interactions.[33] Edge-to-face aromatic interactions (Fig.3), aromatic–cation interactions, aromatic–halogen interactions, aromatic–carbohydrate interactions and aromatic stacking interactions have been successfully investigated by this approach.

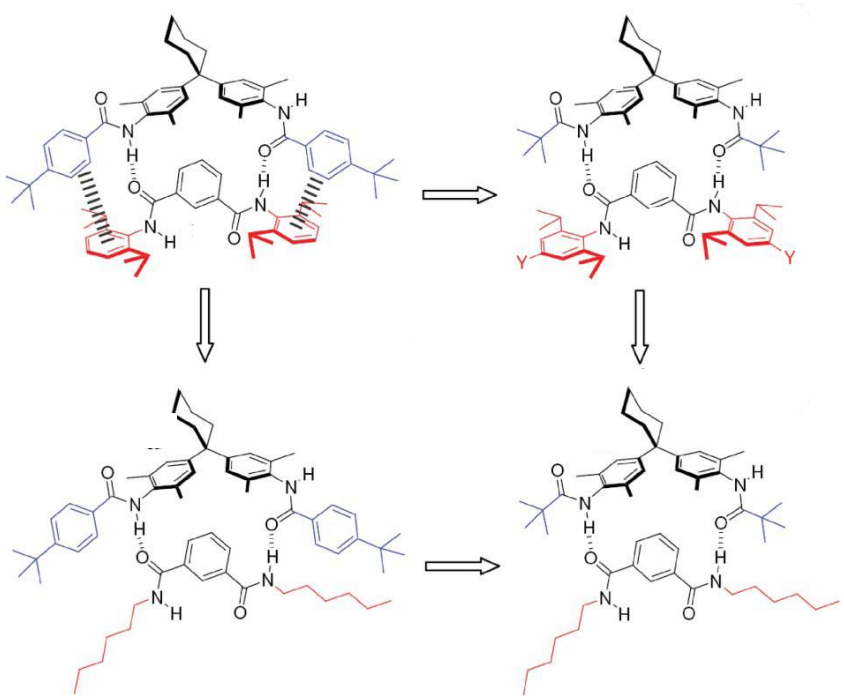

**Fig 3** *A double-mutant cycle for determining the magnitude of the two terminal edge-to-face aromatic interactions* [30]

Based on this approach the magnitude of one of the edge-to-face aromatic interactions in $CDCl_3$ was found to be -1.3 $kJmol^{-1}$.

The principle of quantification of non-covalent interactions however has been limited mostly to non-polar solvent systems. [17, 34, 35] In contrast to covalent bonding, non-covalent bond interactions are highly dependent upon external parameters such as solvent composition, polarity and temperature.[36] In this context water as a solvent is the most challenging one. Electrostatic interactions (H-bonding and ion pair), which

are well-exploited in artificial supramolecular systems, are very weak in aqueous solvent systems. [37]

Hydrophobic and aromatic stacking interactions, which can be rather strong in aqueous solvents, are much more difficult to deliberately design and use in synthetic receptors. [38, 39] However, it is very desirable to design systems that will be useful to quantify non-covalent bond interactions in aqueous and polar solvents like water and DMSO by employing supramolecular systems stable under these conditions. This is important to simulate the working environment of the natural biological system.[40] This is one of the current challenges facing the field of supramolecular chemistry. In this PhD research work, we will try to develop synthetic pyridoguanidinium based supramolecular structures which are stable in polar solvent systems. Achieving this might pave the way to use the DMC approach in quantifying non-covalent interactions in polar and aqueous solvent systems.

## 1.6 Analytical methods for quantification of non-covalent bond interactions

Several techniques have been forwarded by chemists to measure the strength of non-covalent bond interactions in supramolecular complexes. NMR dilution/titration, isothermal calorimetric dilution/titration, ionization mass spectrometry [41] and UV dilution/titration techniques [42] are some of the methods which have been successfully used to study non-covalent bond interactions in biological and supramolecular systems. NMR and ITC techniques are discussed below as they are the most widely exploited techniques in studying supramolecular complexes and are the ones to be used in this research project.

### 1.6.1 NMR dilution experiments

NMR is the most widely reported technique in the literature to study non-covalent interactions in supramolecular complexes. NMR experiments are used to follow binding events by observing the change in the resonance signals of magnetically active nuclei, such as $^{1}H$, $^{13}C$, and $^{15}N$, in a host or guest molecule.[43] The concentration-dependent change in the chemical shift value of the protons involved in the hydrogen bonding between the host and guest molecules is correlated with the

stability/binding constant of the host-guest (self-assembled) complex. This information can also be used to study the thermodynamic properties associated with the complex formation. NMR techniques have been previously used to study the structures of nucleic acids. The base pairing between guanosine and cytidine was first studied by Katz and Penman using an NMR titration technique.[44] Though the accuracy of the method is debatable [45], NMR studies can be used to figure out the thermodynamic profile of binding phenomena. Thermodynamic determinations of $\Delta G_{ass}$, $\Delta H_{ass}$, and $\Delta S_{ass}$ can be done using NMR experiments through the construction of a van't Hoff plot. Performing NMR studies of a binding process at different temperatures and plotting the natural logarithm of the equilibrium constant versus the reciprocal temperature gives the van't Hoff plot. This curve can then be analysed to deduce the enthalpy and entropy of binding involved in complex formation.[46] In addition to getting direct information about the association or dissociation constant of a supramolecular complex, NMR techniques (NOEs and DOSY) are also useful for gathering precise knowledge of solution-phase binding phenomena. [47]

### 1.6.2 Isothermal titration calorimetry

Isothermal titration calorimetry (ITC) is becoming the method of choice for the determination of the thermodynamic parameters associated with the non-covalent interaction of two (or more) molecules. ITC is the only technique available to date that can directly measure both the stability constant (K) and enthalpy (ΔH) of a binding process. [48] The experiment involves titration of one of the binding partners into the other binding partner contained in a calorimetric sample cell at a constant temperature. After each addition of a small aliquot of titrant, the heat released or absorbed in the sample cell is measured with respect to a reference cell filled with a buffer solution. The heat change (ΔH) is expressed as the electrical power required to maintain a constant temperature difference between the sample cell and the reference cell, which are both placed in an adiabatic jacket.[49] The amount of complex formed (extent of dissociation) at each injection is directly proportional to the heat given out and this heat of interaction is used as a probe of the course of the binding process as one component is titrated into the other. This will allow for the amount of free and bound ligand to be determined at any point in the titration process. From this the observed equilibrium binding (association) constant, KB (KB = 1/dissociation

constant, 1/KD) can be determined. Once these parameters are at hand a full thermodynamic characterization of the binding event can be determined from the relationships below.[50, 51, 52, 53.]

The change in free energy, $\Delta G$ is related to the $K_B$ by:

$K_B = e^{-\Delta G/RT}$

where R is the gas constant and T is the experimental temperature.

The change in entropy, $\Delta S$ is related to the $\Delta H$ by:

$\Delta H = \Delta G + T\Delta S$

ITC is becoming the method of choice in binding studies ranging from drug design to polymer chemistry and from cellular biology to nanotechnology.[54] The ITC binding study technique offers numerous advantages over NMR and other techniques. The method is more sensitive and accurate and it allows the dissection of association free energies into the enthalpic and entropic components. As previously mentioned, determination of the enthalpic and entropic component of the binding phenomena using NMR technique is very laborious and error prone.

### 1.6.3 ITC investigation of dimeric suprmaolecular systems

The principles of the ITC technique in a binding study can be extended to investigate the dimerisation process of a supramolecular system.[55, 56] The dimerisation characteristics of all the pyridoguanidinium carboxylates considered in this project were primarily investigated using the isothermal titration calorimetry (ITC) technique. A reasonably concentrated solution of the guanidinium carboxylate which is believed to contain a higher proportion of the dimeric form of the compound is sequentially injected from a syringe into a blank solvent contained in the calorimeter cell. This results in dissociation of the dimer which is usually accompanied by a heat uptake from the surrounding environment. [57] This results in endothermic heat signals. The magnitude of the endothermic heat signals decreases non-linearly with successive injections and this is due the build up of concentration of the compound in the cell thereby shifting the equilibrium of dimer dissociation to the left (Fig 4).


**Fig 4** *Monomer-dimer equilibrium*

The series of the endothermic heat pulse data is then fitted to a monomer-dimer equilibrium model used for estimating $K_{diss}$ and $\Delta H_{diss}$ directly. The inverse of these parameters will give the $K_{dim}$ and $\Delta H_{dim}$ and the other thermodynamic parameters $\Delta G_{dim}$ and $T\Delta S_{dim}$ can be calculated using the Gibbs-Helmholtz equation.

## 1.7 Carboxylate binding by guanidinium derivatives

### 1.7.1 Significance of the guanidinium group

The guanidinium group has served as an excellent 'work horse' for supramolecular chemists because of its important role in nature.[58] It is widely found in nature and mediates a variety of specific non-covalent interactions in biological systems.[59] The guanidine moiety of the arginine amino acid mediates the interaction of many negatively charged anionic species (phosph[on]ates, sulf[on]ates, and carboxylates) or electron rich aromatic moieties found in substrates with enzymes or receptors.[60] Nature often uses simple alkyl guanidinium cations in the form of the amino acid arginine for the binding of oxyanions.[61] A large number of natural products and drugs contain a guanidinium moiety and this is believed to be responsible for the bioactivity of many drug molecules. The guanidinium-carboxylate binding has been found to form the basis for the biological activity of quite a number of alkaloids and toxins such as ptilomycalin A (Fig 5) and related guanidinium natural products.[62, 63]

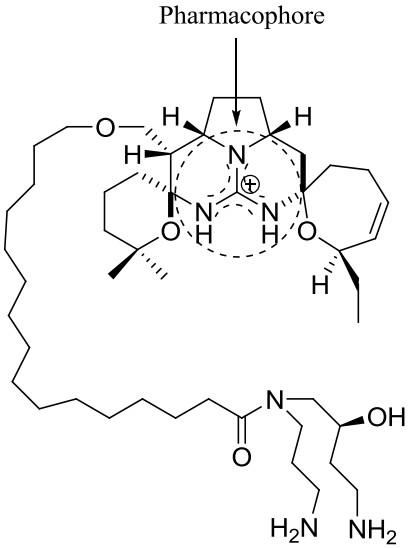


**Fig 5** *Ptilomycalin A which has anti tumour, antifungal and antimicrobial activity*

The guanidinium functionality has exceptionally high stability in an aqueous environment due to resonance stabilization.[64] All the resonance structures have six potential hydrogen bond donors and the positive charge is distributed equally to the three nitrogen atoms (Fig 6).

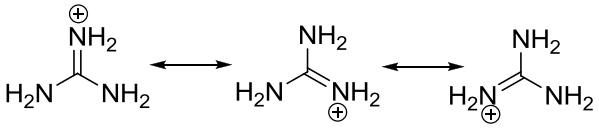


**Fig 6** *Resonance stabilization of a guanidinium functionality*

Guanidine has a pKa value of ~ 13.5 in water. This makes it protonated over a wide pH range. Substitution of one or two of the hydrogens by an alkyl group decreases the pKa as is observed in arginine which has a pKa value of 12.5. The extent of lowering of the pKa value by mono substitution depends on the nature of the neighbouring group (substituent). In general, it was observed that the pKa lowering effect was acyl > phenyl > alkyl in mono substituted guanidines. An X-ray crystal structure has revealed that the C-N single bond length in an alkylguanidine is shorter than the normal C-N bonds. In guanidine, all three bond lengths and bond angles are nearly equal with an average of 1.33 Å and 120°, respectively.

The reason for the strong binding of guanidiniums with oxoanions is due to the binding pattern featuring two parallel hydrogen bonds augmented by electrostatic attraction (Fig 7), a structural motif that can be found in many crystal structures of enzyme complexes with oxoanionic substrates.[65, 66]

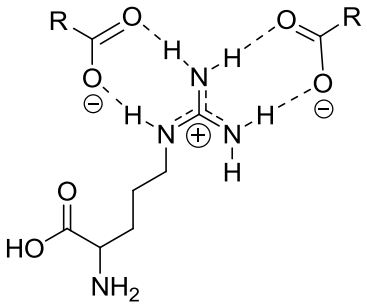


**Fig 7** *Binding modes of the guanidinium group of arginine with carboxylates* [67]

In biological systems, this binding usually occurs in the hydrophobic pockets of enzymes, thereby avoiding solvation effects of the water molecules. Exploiting the guanidinium functionality for carboxylate binding in artificial receptor systems however is hampered by the very effective solvation of the guanidinium functionality in water leading to weaker electrostatic interactions. In spite of these setbacks, the guanidinium group has served as a basis for the development of an appreciable number of artificial guanidinium-based receptors for anions.[68]

## 1.7.2 Synthetic guanidinium receptors

Inspired by nature's use of arginine, a variety of host systems based on guanidinium cations have been designed.[69] However, most of the receptors developed so far are functional only in non-polar solvents. The current challenge of designing guanidinium receptors focuses on issues like utility of the receptor in aqueous media and enhancement of enantioselectivity of the receptor.

Designing a guanidinium based receptor that can function in an aqueous environment is a very difficult task. This however is circumvented in nature by the overall hydrophobic character of the binding pockets in the enzymes. This enhances the strength of the enzyme substrate interaction.[70] Supramolecular chemistry has employed this concept and some guanidinium based receptors showing appreciable

binding strength in aqueous environments have been reported in the literature. A bisguanidinium-based receptor **8** developed in 1992 by Hamilton *et al* is one of the pioneering works in developing guanidinium based receptors for anion binding in aqueous solvent systems. Receptor **8** was developed with the idea of mimicking the active site of staphylococcal nuclease which is important in accelerating phosphodiester cleavage in RNA. Another related work by Hamilton *et al* has reported a well characterized bisguanidinium receptor **9** with an intramolecular distance of 4-5 $A^o$ for recognition of the aspartate group. [71]

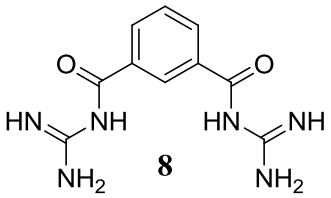


**8**

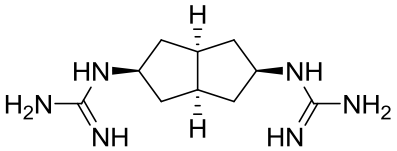


**9**

Hamilton *et al* made an in depth analysis of the thermodynamic behaviour of the binding phenomena of guanidinium groups and carboxylate anions in competitive solvent systems such as water. They have clearly established the fact that decreased stability of the guanidinium-carboxylate complex is attributed to solvation of the hydrogen bond forming sites by the water molecules. The modest binding observed in water was entropy driven as opposed to the enthalpy driven binding in DMSO.

Other notable works in the development of guanidinium based anion receptors include; the bicyclic guanidinium receptor **10** for enantioselective recognition of anions developed by De Mendoza *et al* [72], the ditopic receptor **11** which is able to bind tetrahedral anions such as phosphate in chloroform and in water developed by Schmidtchen *et al* [73], pyrrole guanidinium-based receptors **12** with a high binding affinity for carboxylates in water developed by Schmuck *et al* [61], and pyrido-guanidinium based receptors and tweezers (**13**) which showed enantioselective recognition for carboxylates in DMSO/water systems developed by Kilburn *et al.*[74]

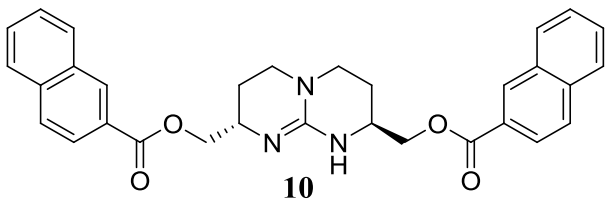


**10**

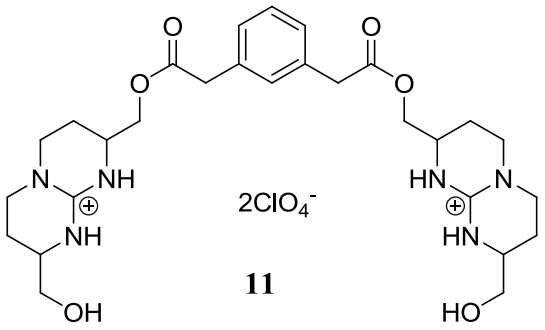


**11**

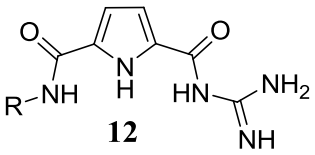


**12**

R = ethyl, butyl, amidomethyl, 1-amido-2-methylpropyl

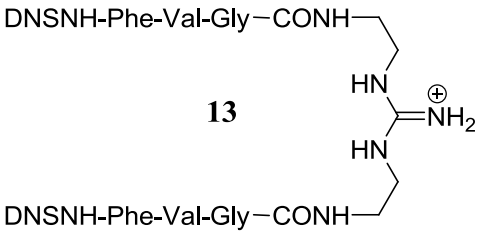


**13**

A relevant work by Schmidtchen *et al* has focused on the design of guanidinium-based receptors capable of overcoming the enthalpic penalty for association in competitive media.[75] This approach is similar to nature's strategy of enhancing enzyme substrate binding through creating an overall hydrophobic environment in the form of binding pockets in the enzymes. With this concept, Schmidtchen *et al* have developed receptors of the type **14** wherein the receptor site is lined with aromatic residues to reduce the solvation in the vicinity of the binding site.

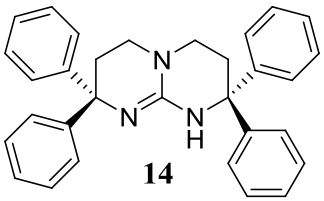


**14**

Pyrrole and pyridine based guanidinium receptors have been extensively studied by Schmuck and Kilburn respectively and these systems are discussed below as they are pertinent to this research project.

## 1.7.3 Pyrrole acyl guanidiniums as carboxylate receptors

Schmuck's approach of developing receptors for carboxylates is based on substituted 2-(guanidiniocarbonyl)-1*H*-pyrroles (Fig 8). Important features have been installed in this scaffold to enhance the complexation of carboxylates in aqueous solvents.[76] The pKa values of acyl guanidiniums (7–8) are lower than those of simple guanidiniums (~13). This enhances the acidity of the guanidinium protons which consequently increases its binding affinity for the formation of hydrogen bonded ion pairs with carboxylate guests.[76] In addition to the ion pairing with the guanidinium, the hydrogen bonding from the pyrrole NH is also believed to be crucial in enhancing the binding strength. Another advantage of this carboxylate receptor motif is the fact that the binding cleft is planar and rather rigid and therefore ideally preorganised for the binding of planar anions such as carboxylates. [76]

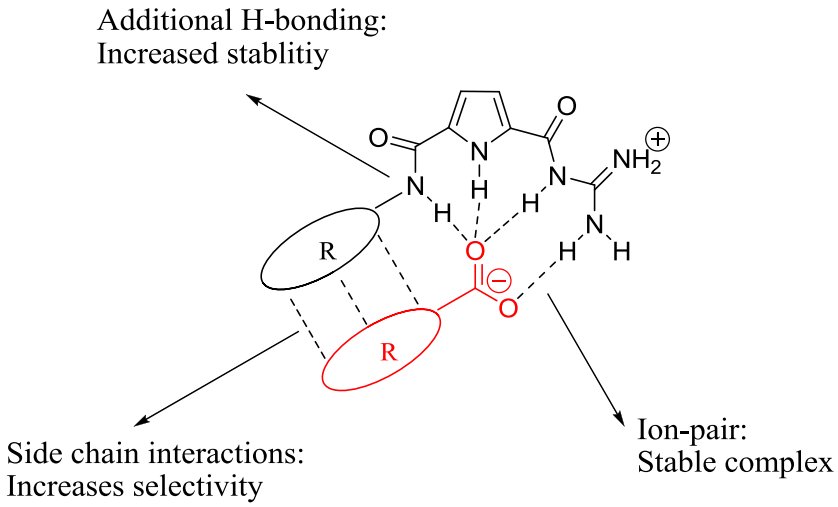


**Fig 8** *Carboxylate binding by 2-(guanidiniocarbonyl)-1H-pyrroles*

These properties of 2-(guanidiniocarbonyl)-1*H*-pyrroles have made them superior to simple guanidinium cations in binding carboxylates effectively even in polar solvent systems. Variation of the amide side chain R allows fine tuning of the binding selectivity of the receptor for different substrates. Incorporating chiral amino acids in the side chain has been utilized for chiral substrate recognition processes. Sterioselective recognition has been achieved through this approach.[77] Making use of the above concept, Schmuck *et al* synthesized many potent carboxylate receptors derived from the 2-(guanidiniocarbonyl)-1*H*-pyrrole scaffold. The ethylamide receptor **15** and the L-valine derived receptor **16** have been found to bind *N*-acetyl

alanyl carboxylates with binding constants of 770 $M^{-1}$ and 1610 $M^{-1}$ respectively in 40% $H_2O$/DMSO.[76]

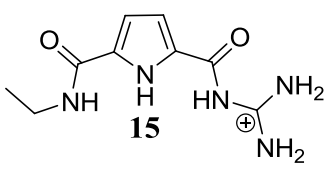


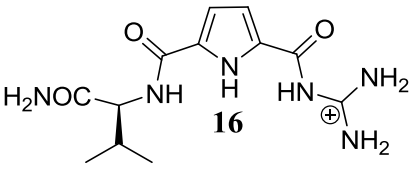


The chiral, L-valine derived receptor **16** shows not only side chain selectivity but also moderate stereoselectivity. [76] The superiority of receptor **16** compared to receptor **15** is owing to the additional hydrogen bond from the terminal carbonyl group. The ability of receptor **16** to discriminate between D-alanine (K = 730 $M^{-1}$) and L-alanine (K = 1610 $M^{-1}$) lies in the fact that there is an unfavorable steric repulsion between the methyl group of the D-amino acid and the isopropyl side chain of the receptor which is not present in the complex with the L-enantiomer where the methyl group points away from the isopropyl group (Fig 9).

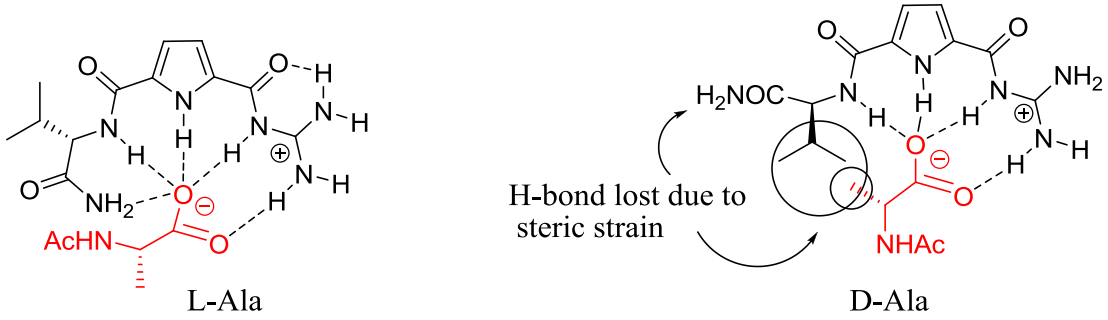


**Fig 9** *Proposed binding mode of L and D-alanine by receptor **16***

One important feature of Schmuck's guanidiniocarbonyl pyrrole receptors is that the improved binding properties in aqueous solvents are solely based on electrostatic interactions without the need of creating hydrophobic cavities. A remarkable improvement of the receptor's ability to bind Ala in an aqueous environment was achieved by the introduction of a third positive charge in the form of a primary ammonium group in receptor **17**. This was designed with the expectation of enhancing the electrostatic interactions which is proved to be crucial for the binding efficiency in water.[78] Receptor **17** showed appreciable binding affinity (K = 2100 $M^{-1}$) for carboxylates in nearly pure water (10% DMSO).

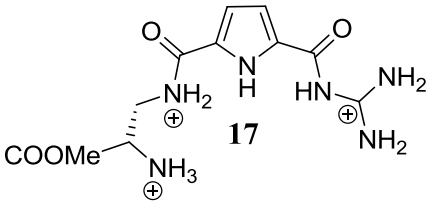

**17**

Schmuck *et al* have further exploited the guanidiniocarbonyl pyrrole scaffold to design receptors for larger substrates such as peptides and oligopeptides. Using molecular mechanics approach dipeptide receptor **18** was designed which is expected to form a hydrogen bonded ion pair with the carboxylate, and show additional hydrogen bonding with the dipeptide backbone. As seen by NMR- and UV-titration experiments, this receptor indeed binds anionic dipeptides very efficiently in buffered water ($K \approx 5\times10^4\ M^{-1}$) Table.

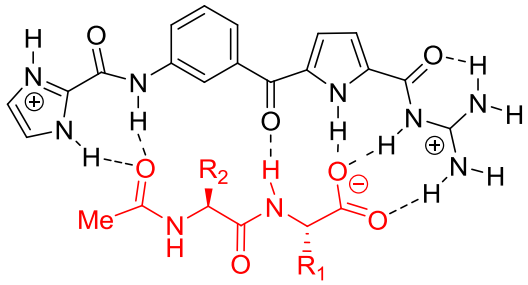

**18**

| **Carboxylate** | **K [$M^{-1}$]** |
|---|---|
| Gly-Gly | 15900 |
| Ala-Ala | 30600 |
| Val-Ala | 43800 |
| Val-Val | 54300 |
| Ala | 7400 |
| Gly | 5200 |

The increase in stability for the dipeptides as compared with simple amino acids must be due to the additional binding sites within the complex (the H-bonds between the backbone amides and interactions with the imidazole group).

## 1.7.4 Pyridoguanidiniums as carboxylate receptors

Kilburn *et al* have extensively utilized the guanidinium motif for the purpose of carboxylate recognition. Similar to the principle of peptide recognition used by Schmuck, Kilburn has earlier synthesized a guanidinium based tweezer receptor **19** which showed 95% selectivity for binding with tripeptides having valine at the carboxy terminus and 40% selectivity for binding with tripeptides having Glu(OtBu) at the amino terminus. An ITC aided binding study has shown that receptor **19** binds with Cbz-Glu(OtBu)-Ser(OtBu)-Val-OH with a binding constant of $K_{ass} = 4 \times 10^5\ M^{-1}$ in 17% DMSO/$H_2O$ buffered at pH = 9.2.[38]

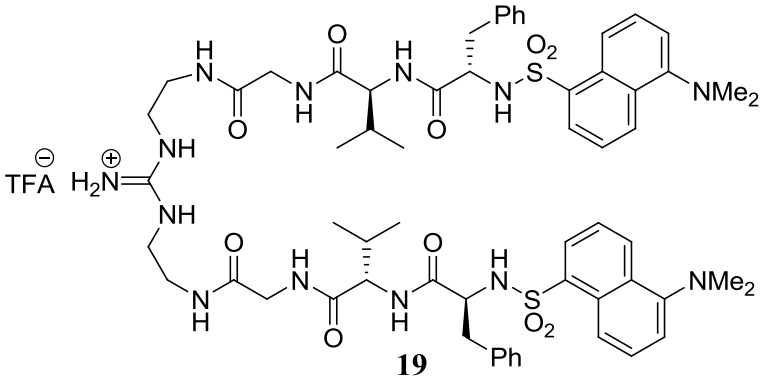

**19**

This tweezer receptor has the potential to form both hydrophobic and β-sheet like hydrogen bonding interactions with the backbone of the incoming peptide substrate. Ion pairs and hydrogen bonding are primarily responsible for the binding energy. In addition to contributing to the binding process, hydrophobic interactions play an important role in imparting selectivity to the receptor.[79]

Kilburn *et al* have recently synthesized a chiral bisguanidinium macrocycle **20** which binds strongly with biscarboxylates in a highly competitive aqueous solvent system. [80] This macrocycle has shown enantioselectivity in binding with N-Boc- glutamate amino acids. It shows preference in binding with N-Boc-L-glutamate ($K = 3.8 \times 10^4$ $M^{-1}$) over N-Boc-D-glutamate ($2.9 \times 10^3$ $M^{-1}$) in 50% $H_2O$–DMSO (using a tris buffer). There is a precise and tight fit within the macrocyclic cavity for the preferred guest, *N*-Boc-L-glutamate, with strong hydrogen bonding interactions to both carboxylate groups of the glutamate.

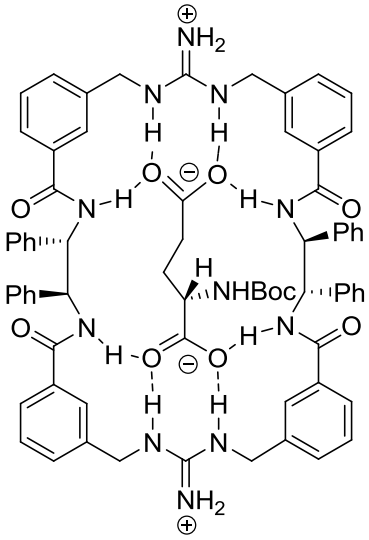

**20**

Following this, Kilburn *et al* have introduced pyridylguanidinium motifs for the purpose of carboxylate binding. Using the pyridine scaffold has the potential advantage of preorganizing the binding cavity into the desired conformation by the weak intramolecular H-bonding between the pyridine N-lone pair electrons and the amide NH and/or guanidine NH. This property of the pyridine carboxyamide motif has been exploited to preorganize macrocyclic and acyclic receptors. However, possible electrostatic repulsions between the pyridyl nitrogen and the incoming anionic guest might create a setback in the binding process (Fig 10). Whether the favourable preorganization effect outweighs the unfavourable electrostatic repulsion or not might depend on the size and electronic structure of the incoming carboxylate guest.

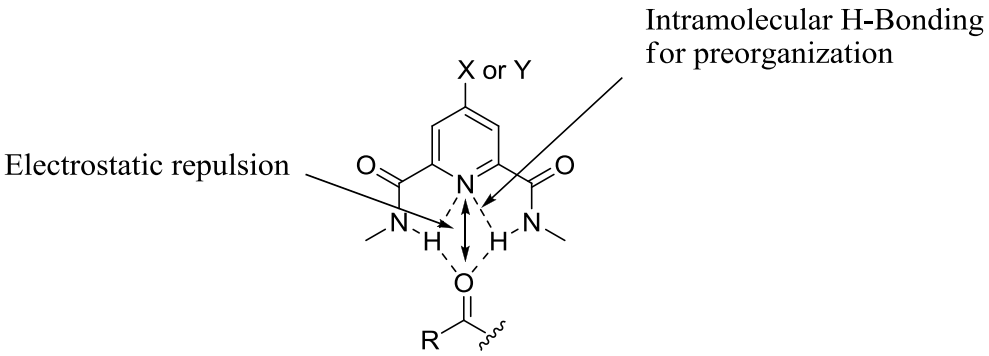


**Fig 10** *Possible electrostatic repulsions between the pyridyl nitrogen of tetralactam macrocycles and the incoming carbonyl oxygen of guest*

The deleterious effect of the electrostatic repulsion between the electron density at the pyridine nitrogen and the negative charge of the incoming anionic guest can be minimized by introducing electron withdrawing groups ($NO_2$, Cl) into the pyridine ring.[81]

A number of efficient pyrido guanidinium based receptors which showed excellent binding with carboxylates have been developed by Kilburn *et al*.[59] The most recent of these is the carboxylate receptor **21** which was found to efficiently bind acetate ($K_{ass}$= 22000 $M^{-1}$) in a highly polar solvent system, DMSO. The thermodynamic data of the binding shows that the binding is entropy driven ($\Delta G$ = -24.8 kJ $mol^{-1}$, $\Delta H$ = - 8.0 kJ $mol^{-1}$, $T\Delta S$ = 16.8 kJ $mol^{-1}$) and this confirms that the preorganisation effect of the pyridine N is indeed very important in creating the binding cleft. The preorganisation is as a result of two intramolecular hydrogen bonds between the pyridine lone pair and adjacent guanidinium/amide protons. The receptor has maintained some of its

carboxylate binding property even in more aqueous solvent systems. It binds acetate with K = 480 $M^{-1}$ in 30% $H_2O$/DMSO with the entropic component still the driving force ($\Delta G$ = -15.3 kJ $mol^{-1}$, $\Delta H$ = - 2.0 kJ $mol^{-1}$, $T\Delta S$ = 13.3 kJ $mol^{-1}$).This dramatic decline from 22,000 $M^{-1}$ to 480 $M^{-1}$ upon changing the solvent system from pure DMSO to 30% water/DMSO is as a result of the competitive solvation of hydrogen and electrostatic bond donor and acceptor sites by the water molecules. This is not unexpected and is one of the current challenges of supramolecular chemistry. However, it has to be noted that the 480 $M^{-1}$ binding constant is highly encouraging for future development of efficient carboxylate binding receptors in water using the pyridine scaffold.

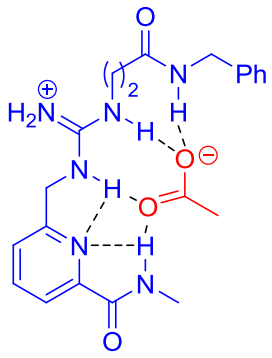

**21**

To further substantiate the importance of preorganization by the pyridine nitrogen, compound **22** in which the pyridine moiety was replaced with a benzene ring was synthesized and its acetate binding properties were investigated under the same conditions as compound **21**. It was found that the binding constant falls dramatically to 5300 $M^{-1}$ and the thermodynamic parameters of the binding ($\Delta G$ = -21.2 kJ $mol^{-1}$, $\Delta H$ = - 19.4 kJ $mol^{-1}$, $T\Delta S$ = 1.8 kJ $mol^{-1}$) showing the binding process is enthalpy driven.

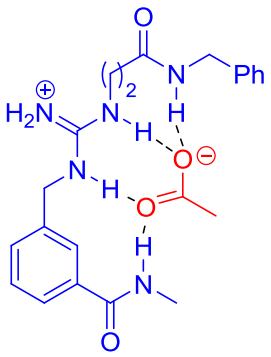

**22**

### 1.7.5 Importance of guanidinium functionality in self-assembly

As previously mentioned guanidiniums are very versatile functionalities in biological systems and found abundantly in many protein structures and enzymes. Numerous biological processes are mediated through them. This makes guanidiniums very good candidates to be exploited for the purpose of developing self assembled supramolecular systems which can mimic biological functions. This research project will try to make use of this concept and aim to develop self-assembled systems built on guanidinium motifs.

## 1.8 Self-assembly and molecular recognition

### 1.8.1 Principles of self-assembly

Over the past few years, intense research has been directed towards gaining an understanding of the concepts and principles that govern the processes of self-assembly.[82] The self-assembly of molecules can lead to the formation of highly complex and fascinating structures from simple monomeric building blocks. Self-assembly can offer ways of making very complex structures which otherwise would have been very difficult and/or uneconomical to synthesize using covalent synthesis. The core principle of self-assembly lies in the fact that the spontaneous assembly is dictated by the supramolecular information encoded in the interacting sites of the simple building block. [83] This principle is very widely used in nature, as exemplified by the molecular architecture of the tobacco virus, the formation of protein plaques in Alzheimer's disease, the formation of the DNA double helix [84] and the association of microtubuli during mitosis.[85, 86] The units forming these super structures spontaneously self-assemble in aqueous media by ingeniously employing multiple non-covalent interactions such as electrostatic interactions, hydrogen bonding, dipole-dipole interactions, and hydrophobic association.[87]

Supramolecular chemistry has recently been successful in using the principle of programmed self-assembly of simple synthetic molecules to get a detailed understanding of the formation of complex supramolecular structures. Structurally diversified and exciting self-assembled systems have been reported in the literature.

These include dimers [88], capsules [89], oligomers [90], polymers, and nanostructures [91] such as micelles, vesicles and nanotubes.

One important feature of self-assembly is the reversibility of the process. As the process is entirely governed by non-covalent interactions, external factors such as polarity of the solvent, pH and temperature should be closely monitored to fine tune the formation of the desired system. This control over the formation of the self-assembled system offers some advantage over the kinetically controlled synthesis of complex covalent structures such as polymers in which defects in the final structure cannot be rectified. The responsiveness of the self-assembled systems to the surrounding environment and their ability to communicate with thier surroundings is another advantage over covalent structures.[92]

### 1.8.2 Self-assembly in polar solvents based on specific interactions

Most self-assembled systems described to date show stability only in the solid state or in organic solvents such as chloroform. H-bonds are the main non-covalent interactions used due to their directionality and complementarity in non-polar solvent systems.[93] The disadvantage of these H-bond based assemblies is that they work beautifully only in solvents of low polarity but not in aqueous solvents due to the competitive solvation of donor and acceptor sites by the solvent molecules.[94]

However, it is very desirable to have access to self-assembling systems that also function in more polar solvents such as DMSO or water. This requires a strategy to circumvent the problem of solvation by seeking ways to enhance covalent bond interactions in such kind of solvents. Metal-ligand complexes have been used to achieve strong complexation in aqueous solvent systems. But this approach is of limited use for biological purpose owing to bio-incompatability of metals and/or unfavorable complexation kinetics. [95]

Another plausible approach to design a self assembled-system is to exploit the enhanced strength of hydrophobic-hydrophobic or aromatic-aromatic stacking interactions in aqueous solvent systems. However, to deliberately encode supramolecular information in monomeric structures using these types of interactions is very difficult because they are not as directional and specific as H-bonding. Hence,

the sole use of these kinds of solvophobic interactions in constructing a self-assembled system is improbable. Self-assembly in polar solvent systems requires a combination of several non-covalent interactions in the system. A combination of H-bonds and hydrophobic/aromatic stacking interactions has been previously employed for such a purpose but only with limited degree of success. It has recently been revealed that H-bonded ion pairs like guanidinium-carboxylate complexes have been proven useful in maintaining the systems in polar and aqueous environments. [61] Another factor that should be taken into account when designing a monomeric structure for the purpose of self-assembly is careful analysis of the propensity of the molecule to make intra versus intermolecular interactions. Intramolecular interactions might hamper the self-assembly process. In line with this is molecular rigidity of the monomer as it is very crucial in maintaining the self-assembled system.[92] Using the concepts above, some developments are being made in designing synthetic self-assembled systems in polar solvents like DMSO, MeOH or even water.[96]

## 1.8.3 Self-assembling systems based on guanidine derivatives

Schmuck *et al* have synthesized pyrrole based guanidinium compounds which are excellent supramolecular architectures from the point of view of both binding strongly with carboxylate anions and forming well elaborated dimers in polar solvent systems. The zwitterionic compound 5-(guanidiniocarbonyl)-1*H*- pyrrole-2-carboxylate (**23**) self assembles to form dimers ($K_{ass}$ =$10^{12}$ $mol^{-1}$) (Fig 11), which are stable in DMSO at 170 $^{o}$C and at concentrations of 0.001 mM. [97] This system has also been found to show some degree of stability even in pure water ($K_{ass}$ = 170 $M^{-1}$).

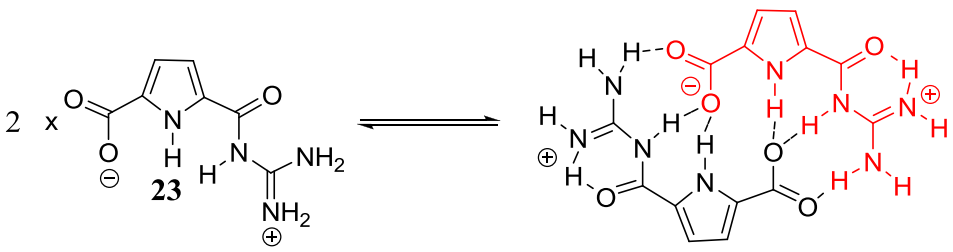


**Fig 11** *Dimerisation of 5-(guanidiniocarbonyl)-1H- pyrrole-2-carboxylate*

Schmuck has predicted that the surprisingly high stability of the zwitterionic dimer is most likely due to a combination of both ion pairing and the formation of a directed

H-bond pattern. To probe the importance of the electrostatic interaction, an analogue of 5-(guanidiniocarbonyl)-1*H*- pyrrole-2-carboxylate with an amidopyridine group replacing the guanidinium cation was synthesized with the intention of switching off the electrostatic interaction in the dimeric structure. ESI-MS and NMR dilution studies confirmed that compound **24** dimerizes in solution (Fig 12)

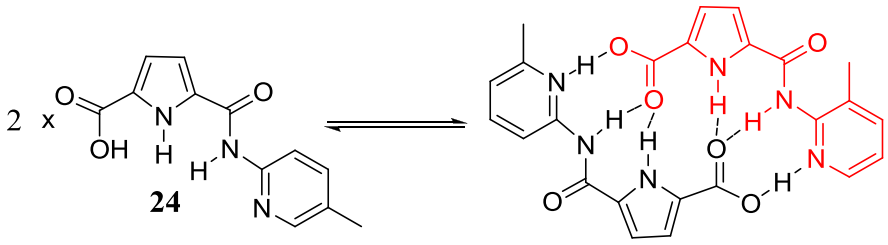


**Fig 12** *Dimerisation of compound **24***

The X-ray crystal structure reveals that in the solid state the structure of this dimer is identical to the zwitterionic 5-(guanidiniocarbonyl)-1*H*-pyrrole-2-carboxylate. Comparing the stability of the two dimers shows that the neutral dimer is only stable in chloroform ($K_{ass}>10^4$ $M^{-1}$). It shows no dimerisation at all in pure DMSO thereby underlining the fact that the charge interaction in **23** is absolutely necessary for stable self-assembly in polar, protic solutions. [97]

Another important factor which needs proper attention in the design of a self-assembling system is rigidity of the monomeric unit. Schmuck has synthesized derivatives of the 5-(guanidiniocarbonyl)-1*H*- pyrrole-2-carboxylate (**25**) in which the carboxylate is not directly attached to the guanidiniocarbonyl pyrrole but with a spacer.[137]

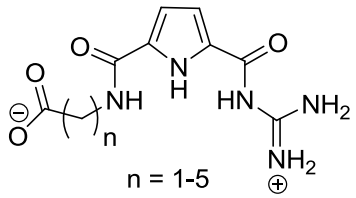


**25**

It was observed that the degree of self-assembly was found to decrease as the number of carbons in the spacer increases. For n = 1, large aggregates were observed even at a very low concentration. Whereas a very large concentration of the monomeric unit

was required for n = 3-5, for any detectable self-assembling system to be formed. The differences between the five zwitterions can be explained based on the extent of intramolecular charge interaction within the monomers. Any intramolecular interaction between the binding sites within the monomer weakens the intermolecular self-assembly. In addition, increased intermolecular motion might also be responsible for the weakening of the self assembly.[98]

Following this Schmuck has reported one of the most efficient self-assembling systems in water reported so far. In water compound **26** was found to dimerise with an association constant of 170 $M^{-1}$.[97] The binding is again attributed to the ion-pair formation between the complementary guanidinium and carboxylate groups.

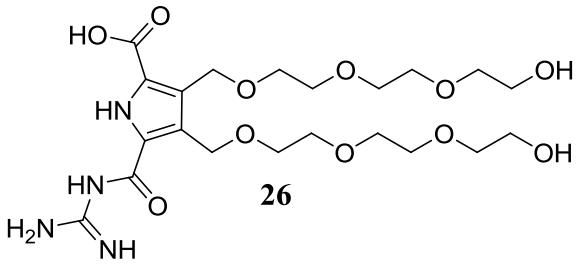


**26**

Kilburn has recently synthesized self-assembled dimeric structures based on the previous pyridoguanidinium motif used for the purpose of carboxylate binding. A carboxylic functionality was incorporated into the pyridoguanidinium receptor **22** with the idea of inducing head-to-tail self association primarily based on the complimentary carboxylate-guanidinium intermolecular interaction (Fig 13).[88]

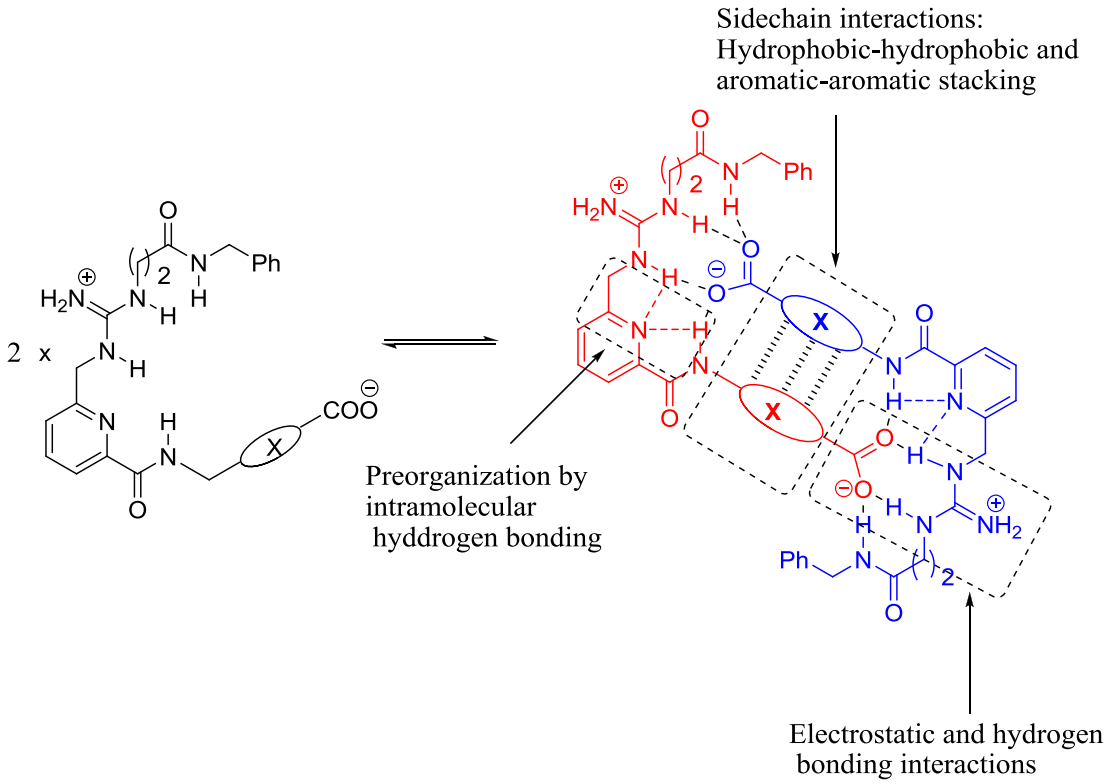


**Fig 13** *Proposed dimerisation mode of a pyridoguanidium-carobxylate*

The bidentate hydrogen bonding and electrostatic interactions between the carboxylate and the guanidinium functionalities are believed to be crucial in maintaining the dimeric structure in polar and aqueous solvent system. Additional non-covalent interaction furnishing sites (X) are encoded/installed in the building block to impart further stability into the dimeric structure. In addition, the monomeric zwitter ion is designed in such a way that it is easily amenable/tunable for structural manipulation and hence potentially makes this supramolecular system serve as a platform to investigate any chosen covalent interaction like hydrophobic-hydrophobic interactions in peptides and aromatic aromatic stacking interactions.

Kilburn *et al* have exploited this approach to investigate the strength of aromatic stacking interactions and the biologically important Val-Val and Leu-Leu hydrophobic interactions. ITC aided dimerization study of compound **27** shows that it forms a stable dimer in DMSO solution ($K_{dim}$ = 11876 $M^{-1}$, $\Delta G_{dim}$ = -23.2 kJmol $^{-1}$, $\Delta H_{dim}$ = -10.0 kJmol $^{-1}$, $T\Delta S_{dim}$ = 13.2 kJmol $^{-1}$). Upon changing the solvent system to 10% $H_2O$/DMSO, the dimerisation constant has declined dramatically ($K_{dim}$ = 532 $M^{-}$

[1], $\Delta G_{dim}$ = -15.6 kJmol $^{-1}$, $\Delta H_{dim}$ = -11.5 kJmol $^{-1}$, $T\Delta S_{dim}$ = 4.1 kJmol $^{-1}$) due to the expected solvation effect by the water molecules. It was unexpected that the enthalpic contribution in the dimerisation process was more in 10% $H_2O$/DMSO than in pure DMSO. An entropy driven binding of the receptor with acetate was observed previously in DMSO/water systems.

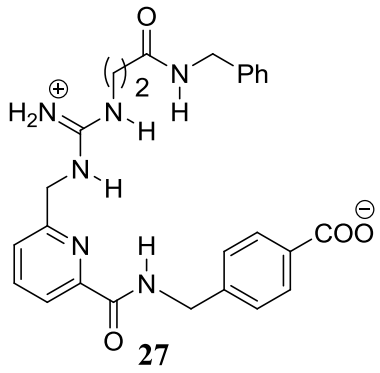


**27**

In the solid state, the dimer was found to be a well-defined structure with closely stacked aromatic rings and a water molecule bridging a hydrogen bonding between the amide hydrogen and the carboxylate (Fig 14). Though a solid state structure might not be extrapolated to the solution phase structure of the dimeric molecule, the constructive role of the water molecule in the solid state dimeric structure in mediating the hydrogen bonding might explain the unexpected increase in enthalpy in 10% water/DMSO system.

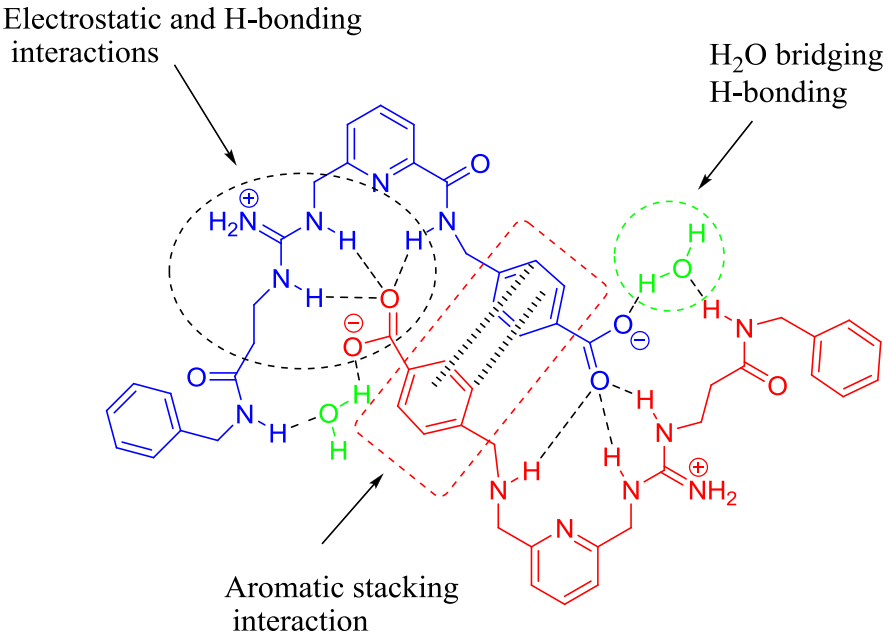


**Fig 14** *Schematic representation of the dimeric structure of compound* ***27***

### 1.8.4 Functional supramolecular structures using guanidinium derived receptors

In one of his recent works, Schmuck has taken a great stride towards the application of the guanidiniocarbonyl pyrrole carboxylate receptors in the field of medicine. The focus of the research was to design biosensors, targeting specific cellular processes in Alzheimer's disease. It is known that the self-aggregation of small peptides is responsible both in animals and humans for a variety of neuro degenerative diseases like Alzheimer's disease (AD). The senile plaques found within the brain of AD patients consist of an insoluble aggregate of a 39–42 residue peptide, called amyloid β-peptide (Aβ).[99] One possible therapeutic intervention in the pathogenesis of Alzheimer's disease (AD) is to prevent the Aβ self-aggregation.[100] Recently rifampcine and oligopeptides which contain fragments of the Aβ itself have been tested *in vitro* and showed encouraging results for the inhibition of Aβ aggregation.[101] However, nothing is known regarding the molecular basis of their interaction with Aβ and it is not even certain in some cases that a specific complexation between Aβ and the inhibitor actually occurs.[102] This lack of understanding of quantitative experimental binding data is a major setback in the design of more specific amyloid inhibitors for future therapeutic use. Having this in mind Schmuck *et al* have designed a supramolecular approach that helps to identify the structural and thermodynamic parameters that control the self-association and hence also possible interactions with aggregation inhibitors. Schmuck has synthesized a combinatorial receptor library based on the observation that the C-terminal sequence of Aβ (-Val39-Val40-Ile41-Ala42) is one of two domains mainly responsible for its self-aggregation.[103] This domain promotes the formation of aggregated β-sheets stabilized through a combination of H-bonds and hydrophobic interactions. Schmuck has chosen a tripeptide receptor library with the the idea of making an antiparallel β-sheet with the backbone of this Aβ tetrapeptide substrate. H-Bonding and hydrophobic interactions are believed to be the main dominant non-covalent bond forces to stabilise the β-sheet structure.

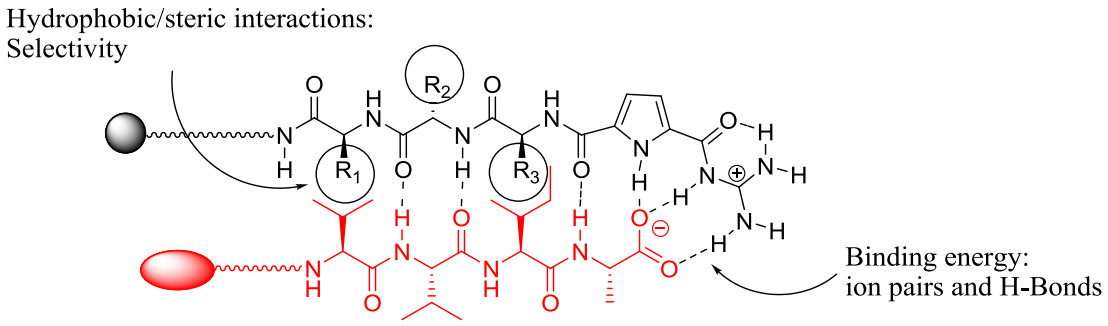


**Fig 15** *A tripeptide-based library of cationic guanidiniocarbonyl pyrrole receptors of the general structure Amino-TentaGel-AA**1**-AA**2**-AA**3**-Gua (AA = amino acid, Gua = guanidiniocarbonyl pyrrole cation) designed for the binding of L-Val-L-Val-L-Ile-L-Ala, a tetrapeptide representing the C-terminus of Aβ.* [104]

The functional application of a guanidiniocarbonyl pyrrole carboxylate receptor comes into picture here as the complexation process in polar solvents must be augmented by electrostatic interactions. H-bonding and hydrophobic interactions alone will not suffice to maintain the anticipated β-sheet structure in aqueous solvent system.Using the combinatorial synthesis approach, Schmuck has prepared 125 members of receptors which can bind with high affinity to a tetrapeptide representing the C-terminal end of the Alzheimer amyloid peptide Aβ. Analysis of selected receptors shows that the binding of the C-terminal Aβ fragment with the receptor is controlled by interplay between electrostatic and hydrophobic interactions.[104] This preliminary result is a way forward for the development of biosensors, targeting specific cellular processes (e.g., cancer, Alzheimer's disease, and bacterial infections), and the design of new therapeutics.

Functional self-assembled supramolecular structures have been synthesized using guanidiniocarbonyl pyrrole carboxylate zwitterions as building blocks. A possible vesicle membrane has been synthesized using a pyrroleguanidinium monomeric structure. The carboxylate group is separated from the guanidinium group by a chiral linker based on L-alanine leading to a rigid rod-like molecule with two oppositely charged ends and a less polar middle section (Fig 16). [105]

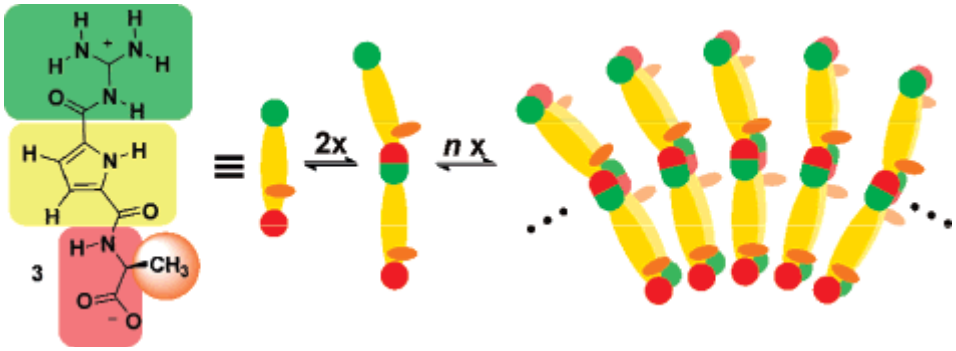


**Fig 16** *Suggested membrane formation via the self-assembly* [105]

## 1.8.5 Membrane transport using acyclic guanidinium receptors

Lehn *et al* have previously demonstrated that receptors based on lipophilic quaternary ammonium compounds were used to transport amino acids and dipeptides from one aqueous phase through a chloroform layer into another aqueous phase. [106] By a similar approach, Schmuck has recently reported efficient amino acid transporter using a guanidiniocarbonyl–pyrrole receptor. Amino acid transportation across membranes is the most widely happening phenomenon in biological processes. Movement of amino acids from one aqueous phase across a lipid bilayer membrane to another aqueous phase requires a host molecule (receptor) capable of efficiently binding the substrate under aqueous conditions. A guanidiniocarbonyl pyrrole motif, which has previously proved to be an efficient carboxylate receptor, was derivatised by introducing a lipophilic tris(dodecylbenzyl) group synthesized (**28**). The long alkyl chain imparts the desired solubility of the receptor in organic solvent systems (lipid bilayers). Where as the guanidinium groups will align themselves at the interface of the aqueous phase and ready to bind to carboxylates.

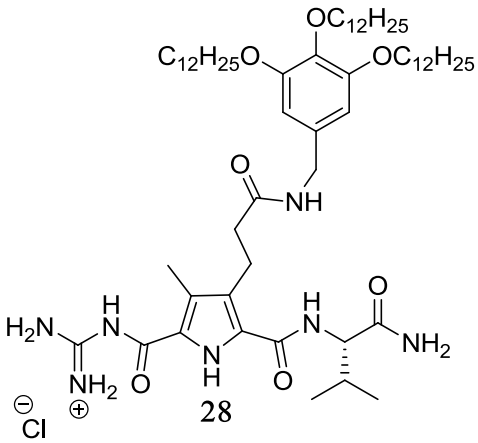


The pH gradient between the source and the receiving phase is the driving force for the symport of the amino acid carboxylate and the proton. (Fig 17)

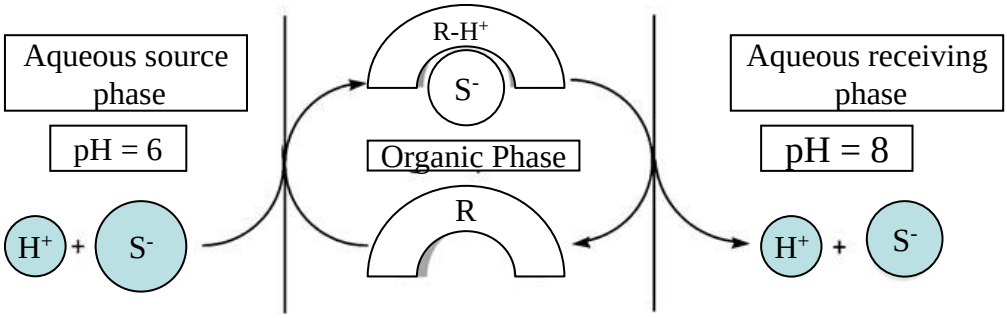


**Fig 17** *Transport of acetylated amino acid carboxylates (S) by receptor **29** (R).Only the protonated form RH+ of the receptor can bind the anionic substrate S and transport it across the bulk liquid membrane.* [107]

Transportation of N-acylated amino acids of alanine, valine, tyrosine, phenylalanine, and tryptophan was conducted in this experiment and it was observed that the receptor is capable of efficiently transporting the amino acids studied across the chloroform phase with the transportation efficiency in the order of Val > Phe >Ala >Trp >Tyr. The rate-determining step in the transportation process is not the binding of the substrate but its release upon contact with the receiving phase. The stronger a substrate binds, the higher is the energy barrier for its release from the receptor–substrate complex, in accord with the Bell–Evans–Polanyi principle.

# 2. Aim of the research project

Supramolecular chemistry has been successful in developing synthetic systems which could allow investigation of specific noncovalent bond interactions. However, most of the systems designed so far work reasonably well only in solvents of low polarity. The design of models that can function in polar and aqueous environments is a very difficult task for supramolecular chemists, owing to the weak nature of hydrogen bonding and ion pair interactions in such competitive solvent systems.

Kilburn *et al* have investigated several pyridylguanidinium based receptors for their carboxylate binding properties in polar and aqueous solvent systems. As a continuation of this well established research work, we have considered that incorporating carboxylate functionality into the pyridylguanidinium receptor will induce a complementary head-to-tail dimerisation process (Fig 18). This is based on the fact that self-assembly in polar solvents requires efficient self-complementary binding motifs.

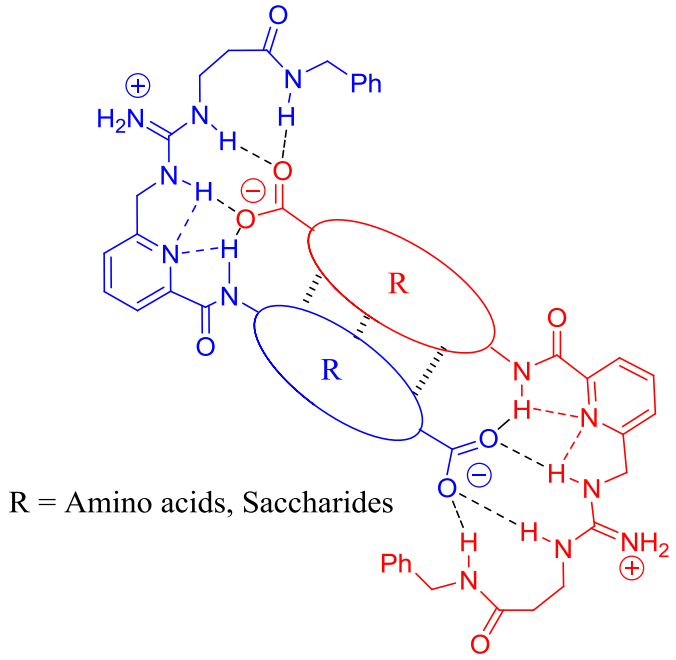


**Fig 18** *Proposed dimerisation mode of pyridoguanidinium-carboxylates*

The main driving force of the dimerisation process will be the combination of multiple non-covalent bond interactions (H-bonding, hydrophobic and electrostatic interactions) installed in the system. As seen from fig 18, at the heart of the proposed

dimeric structure will be the bidentate intermolecular hydrogen bonding-electrostatic interaction between the guanidinium and carboxylate functionalities. This interaction will be augmented by the preorganisation of the pyridine scaffold through intramolecular hydrogen bonding between the pyridine N and the adjacent amide and guanidine protons. Additional non-covalent bond interactions (π- π stacking and/or hydrophobic interactions) will be furnished into the system through the R group.

This PhD research project will primarily focus on the design and synthesis of pyridylguanidinium supramolecular structures stable in polar and aqueous environments. Synthesis of various pyridylguanidinium derivatives will be undertaken and this will be followed by investigation of their dimerisation properties using isothermal calorimetric (ITC) and NMR dilution techniques. This will allow direct determination of the thermodynamic parameters associated with the formation of the dimeric supramolecular structures.The magnitude of these parameters ($K_{dim}$, $\Delta G_{dim}$, $T\Delta S_{dim}$ and $\Delta H_{dim}$) will allow a direct measure and quantification of the strength of interactions between structural elements which lead to the formation of the dimeric supramolecular system. Crystal structure determination (when possible) will also be considered with the above mentioned binding study techniques and this will enable us to make a detailed structural analysis of dimerisation and self assembly.

The first part of our work will focus on structural optimisation with the aim of accessing the dimeric structure in polar solvent systems. The first approach will be through systematic replacement of the 'R' side chain with non-polar amino acid residues that can deliver hydrophobic-hydrophobic interactions into the dimeric supramolecular system. For this purpose, a series of pyridylguanidinium carboxylates containing β-Ala, Leu and Val amino acid residues in the side chain will be synthesized and their dimerisation properties will be investigated. This investigation will be vital to:

- Understand the importance of hydrophobic interactions in stabilizing the dimeric structures in aqueous environments.
- Investigate amino acid-amino acid interactions which are of biological significance.

Aims of the research project

Determination of Val-Val and Leu-Leu interactions will be attempted at the initial phase of this project since the two interactions are abundantly present in secondary and tertiary protein structures.

Once we optimize the conditions and have a better control of the dimerisation process, a series of peptide-pyridyl guanidinium derivatives will be prepared and their dimerization properties will be investigated (Fig 19).

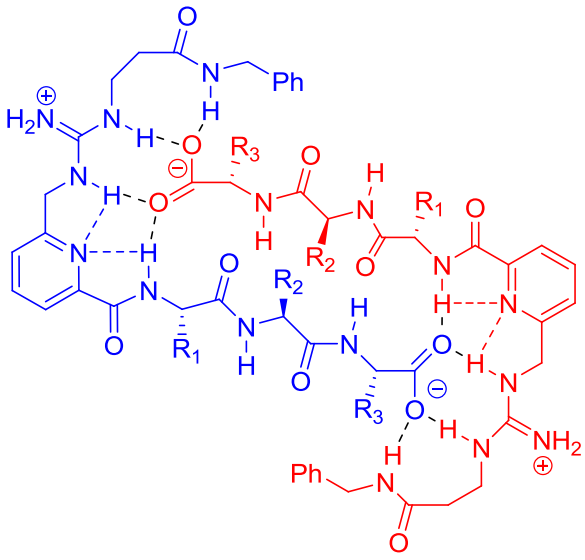


**Fig 19** *Proposed dimerisation mode of peptide containing pyridoguanidinium-carboxylates*

It is expected that once the desired degree of stability is achieved in polar solvent systems, our dimeric supramolecular structures can serve as a platform to investigate a chosen non-covalent bond interaction *via* tailoring of the structure of 'R'.

We have designed the dimeric supramolecular systems in this research project in order that they will meet the following criteria:

- ❖ Stable in polar environment
- ❖ Amenable to structural changes

Aims of the research project

- Designed in such a way that it will enable to mimic functions of biological systems
- Reasonably easy to synthesize

The outcome and the in-depth assessment of the dimerisation study results of the proposed guanidinium-carboxylates will help us to have a better understanding of the principles of self-assembly in polar and aqueous solvent systems. This in turn will enhance our understanding of the molecular recognition events and allow the future design of efficient carboxylate receptors which can function in aqueous systems.

# 3. Results and Discussion

## 3.1 Introduction

Several pyridylguanidinium based anion receptors have been investigated in our group for their amino acid binding properties in polar and aqueous solvent systems. A recent study showed that the pyridylguanidinium receptor **21** binds acetate strongly in 30% $H_2O$/DMSO making it an effective synthetic carboxylate receptor.[59]

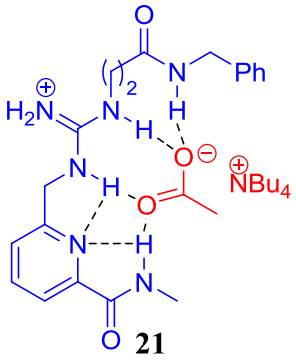


**21**

$K_{ass}$(DMSO) = 22000 $M^{-1}$
$K_{ass}$(30%$H_2O$/DMSO) = 480 $M^{-1}$

In subsequent studies by Kilburn *et al*, [88] a derivative of **21** incorporating carboxylate functionality (**27**) was designed to form dimers *via* an intermolecular head-to-tail self-assembly orchestrated by electrostatic and H-bonding interaction between the carboxylate with the guanidine moieties. Schmuck has used similar strategy to induce self-assembly of pyrroleguanidinium carboxylates. [97]

Compound **27** is found to dimerise strongly in polar solvent systems (DMSO and 10% $H_2O$/DMSO) with aromatic stacking interactions which are believed to contribute to the high binding energy of the dimeric structure as established by ITC dilution studies. This mode of dimer formation was also substantiated by evidence from the solid state X-ray structure (see page 81).

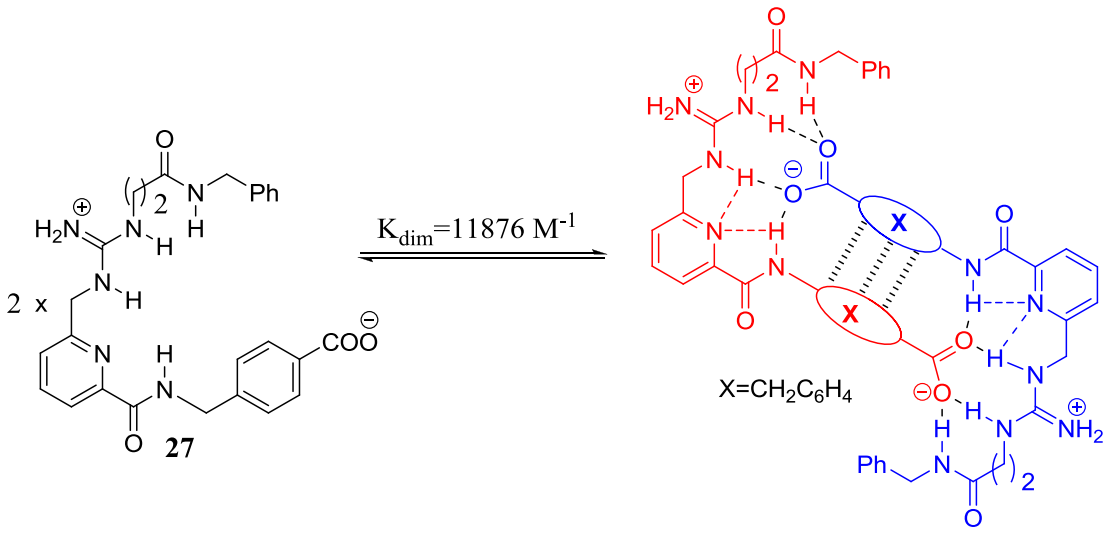


**Fig 20** *Dimerisation of compound **27** in DMSO*

With this in mind, optimisation of the dimerisation process was commenced with designing pyridylguanidinium derivatives **29** and **30** where the benzyl side chain is replaced with ß-Ala and l-valine amino acid residues respectively. This will help not only to understand the contribution of the possible aromatic-aromatic stacking interaction for the stability of the aforementioned dimer, but also to probe a Val-Val aminoacid interaction which is important in secondary and tertiary protein structure. Val and Leu are important in this regard and will be investigated in this research work.[108]

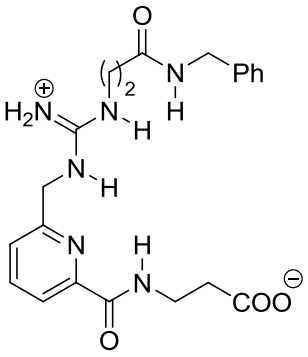
**29**

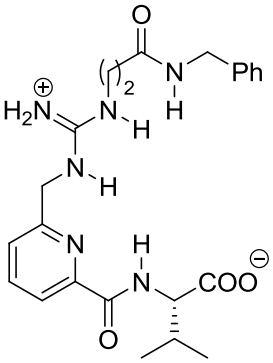
**30**

## 3.2 Synthesis of guanidine-carboxylates **29** and **30**

The syntheses of all the pyridoguanidine systems considered in this project involve syntheses of the basic pyridine scaffolds **35** and **36**. Syntheses of these scaffolds were

achieved by building upon the commercially available pyridine-2, 6-dicarboxylic acid (**31**). The scaffold was then functionalized appropriately to give the desired system.

Scheme1 describes the synthesis of the basic pyridine scaffold. Esterification of **31** was followed by reduction with sodium borohydride to give the alcohol **32**. The approach used to synthesize **34** is *via* activation of the hydroxyl group by converting it first into a good leaving group, mesylate or chloride. Subsequent $S_N2$ reactions with the nucleophile, $HNBoc_2$, gave compound **34** in a good yield.

**Scheme 1**

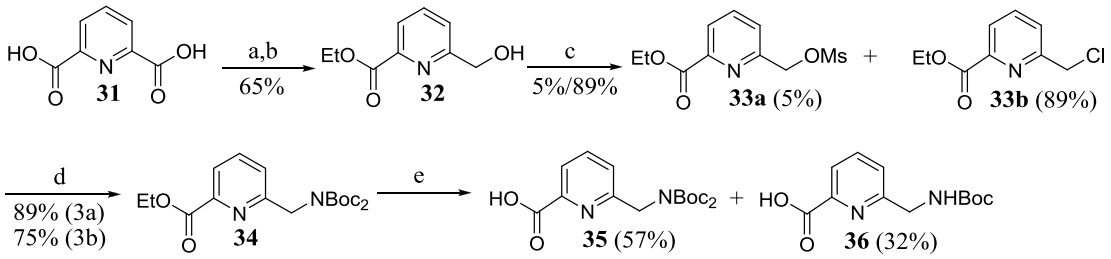


**Scheme 1**. Reagents and conditions: a) EtOH, $H_2SO_4$, reflux b) $NaBH_4$, EtOH, 0 °C c) MsCl, $Et_3N$, 0 °C d) DMF, $NHBoc_2$, $K_2CO_3$, 60 °C e) LiBr, $Et_3N$, $CH_3CN$ (2% v/v $H_2O$)

A Mitsunobu reaction was initially attempted to convert the primary OH group of **32** directly into the Boc protected product **34**. But it was accomplished in only 35 % yield.[109]

Ester hydrolysis of **34** was initially undertaken with $Me_3SiOK$ but it did not proceed with a good yield. The problem has been circumvented by using lithium salts for the hydrolysis procedure, a procedure which is recommended specially for ester functionalities containing a β-heteroatom.[110] Coordination of lithium to the ester carbonyl group and to the heteroatom at the β position makes the ester carbonyl centre more reactive to nucleophilic attack (Fig 21).

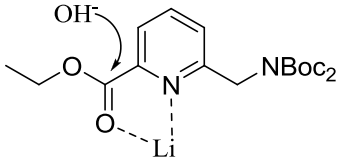


**Fig 21** *A proposed reaction mechanism of lithium mediated ester hydroysis*

Results and Discussion

Functionalization of the pyridine scaffold was undertaken by coupling reactions with β-alanine methyl ester and valine methyl ester to give compounds **37** and **38** respectively (Scheme 2).

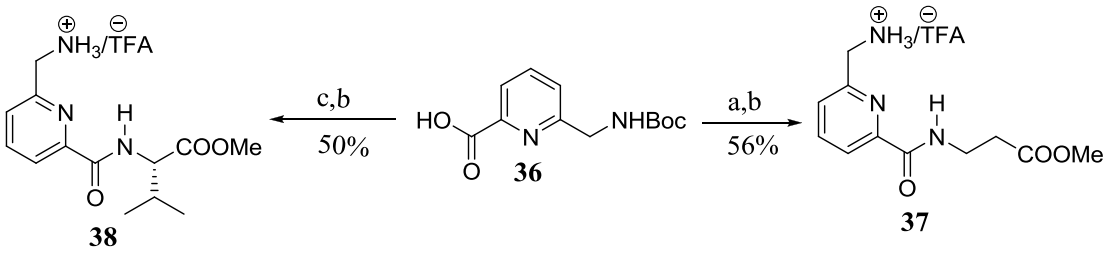


**Scheme 2**. Reagents and conditions: a) β-Alanine methyl ester, DIPEA, HOBt, EDC.HCl, DMF, DCM, rt. b) 20% TFA/DCM, rt. c) Valine methyl ester, DIPEA, HOBt, EDC.HCl, DMF, DCM, rt.

Scheme 3 depicts the synthesis of the Cbz activated thiourea compound **42** which will be used at a later stage to establish the guanidine functionality into the system. This synthetic route was previously used in our group [59] and exploited to synthesise various pyridyl guanidinium salts for the purpose of carboxylate binding in polar solvent systems. All the transformations in Scheme 3 were accomplished in reasonably good yields.

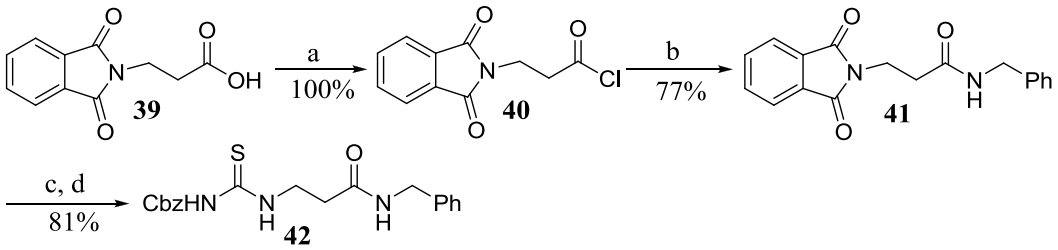


**Scheme 3**. Reagents and conditions: a) $SOCl_2$, Reflux. b) $BnNH_2$, $Et_3N$, 0 $^oC$-rt. c) $4H_2O.N_2H_4$, Reflux. d) CbzNCS, DCM, $Et_3N$, rt.

Scheme 4 shows coupling of compounds **37** with the thiourea compound **42** to give the corresponding Cbz protected compounds **43**. This procedure was followed by ester hydrolysis and hydrogenolysis steps leading to the synthesis of the carboxylate-guanidinium compound **29**.

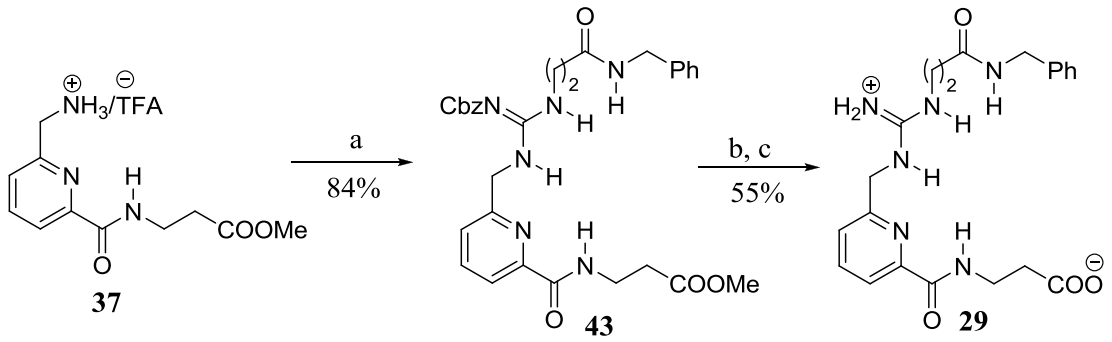


**Scheme 4**. Reagents and conditions: a) **42**, $Et_3N$, EDC.HCl, DCM, rt. b) $Me_3SiOK$,THF, rt. c) Pd/C, $H_2$, MeOH, rt.

Scheme 5 shows the similar approach used in scheme 4 that leads to the synthesis of the carboxylate-guanidinium compound **30**. The structures of these novel carboxylate-guanidinium compounds were fully characterized using spectroscopic (NMR, MS and IR) analysis.

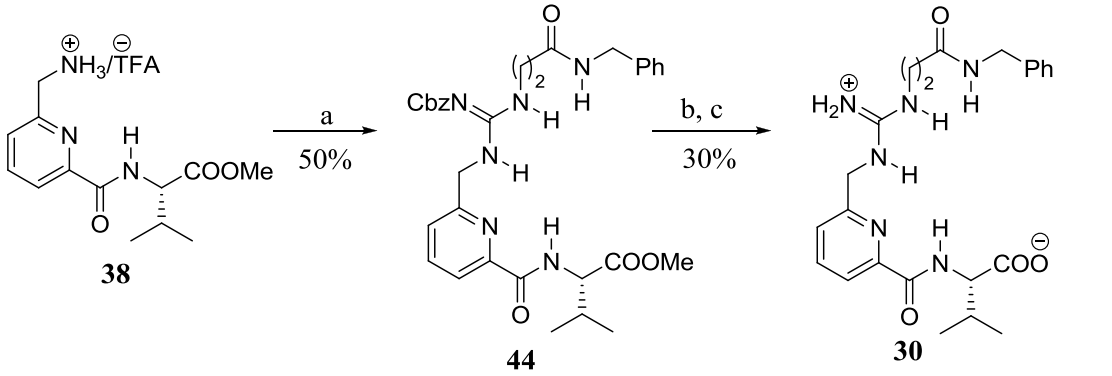


**Scheme 5**. Reagents and conditions: a) **42**, $Et_3N$, EDC.HCl, DCM, rt. b) $Me_3SiOK$,THF, rt. c) Pd/C, $H_2$, MeOH, rt.

## 3.3 Dimerisation studies of guanidnium-carboxylates **29** and **30**

### 3.3.1 Isothermal calorimetric dilution study of **29** and **30**

The initial dimerisation studies of **29** and **30** were performed in DMSO. DMSO was the solvent of choice to start the investigation owing to its similarity with water in terms of solvent properties, dipole moment and dielectric constant. Both water and DMSO can form hydrogen bonds owing to the strongly polarized O-H and S-O groups respectively. While water can accept and donate H-bonding, DMSO is capable of accepting hydrogen bonds. The initial dilution studies with these compounds have resulted in endothermic heat pulses as expected from dimer dissociation (Fig 22).

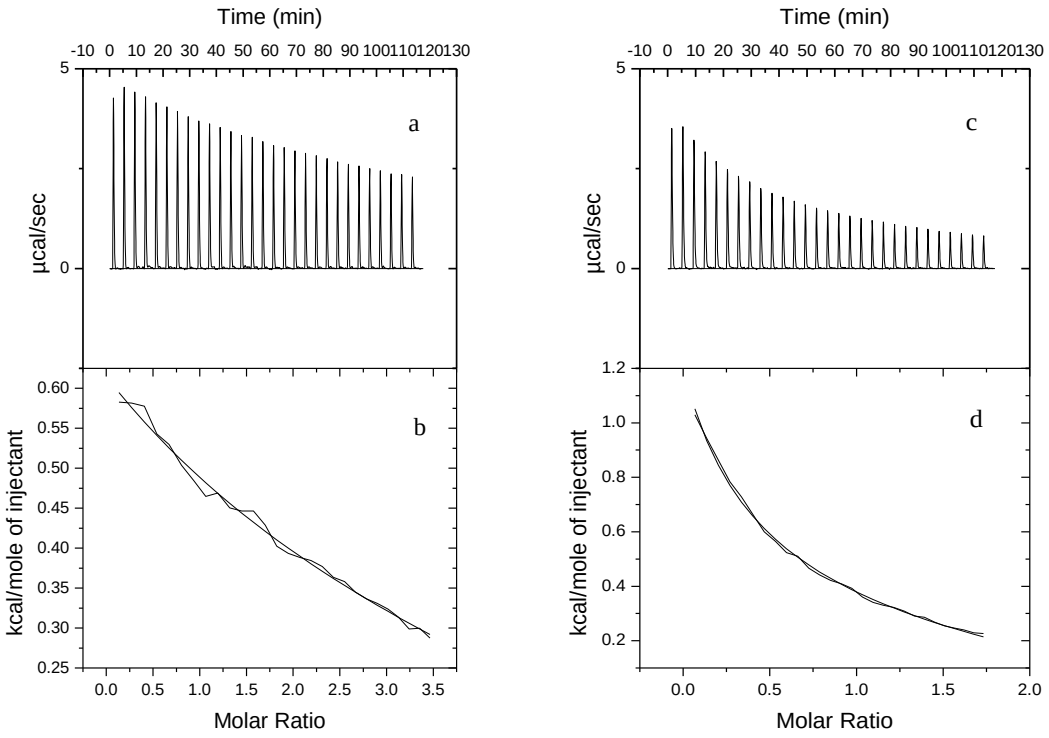


**Fig 22** *Calorimetric data obtained for ITC dilution studies of **29** (left) and **30** (right) in DMSO at 298K. a) c) Raw ITC data of **27** & **31** respectively in DMSO (29* x *10 µL injections); b) d) Non-linear curve fittings of the reference corrected data into the dimer-dissociation model*

Results and Discussion

The full thermodynamic profile of the dimerisation phenomena is tabulated below.

| Compound | $K_{dim}$ [$M^{-1}$] | $\Delta G_{dim}$ [kJ $mol^{-1}$] | $\Delta H_{dim}$ [kJ $mol^{-1}$] | $T\Delta S_{dim}$ [kJ $mol^{-1}$] |
|---|---|---|---|---|
| **29** | 79 ±14 | -9.0 | -6 ±0.3 | 3.0 |
| **30** | 400 ±22 | -14.8 | -11±0.1 | 3.7 |

**Table 2** *Energetics of dimerisations of compounds **29** and **30** (concentrations of 20 mM and 10 mM respectively) at 298 K in DMSO.*

The negative $\Delta G_{dim}$ values indicate the spontaneous and thermodynamically favoured formation of the dimeric complexes (Table 2).[57] Dissection of the free energy into its enthalpic and entropic components reveals that the dimerisation is driven by enthalpy although it can be seen that there is a modest positive entropic contribution. Compound **30** was found to form a more stable dimer in DMSO than compound **29** with an extra stabilization energy of -5.8 kJ $mol^{-1}$. This extra stability might be attributed to the van der Waals contact *via* Val-Val side chain interaction in the dimeric structure. But it should not be ruled out that the decreased stability of the dimeric structure from compound **29** might be due to possible deleterious intramolecular interactions leading to conformational changes resulting in decreased dimer formation. The more flexibility imparted to the monomer by the ß-Ala side chain could lead to this intramolecular interaction.

Investigation of the dimerisation in 10% $H_2O$/DMSO shows that there was complete disruption of the dimers. No endothermic heat pulse was observed. This is due to the competitive solvation of the hydrogen bond forming sites by the water molecules.[111] It was envisaged that a hydrophobic Val-Val side chain interaction might stabilise the dimer in 10% $H_2O$/DMSO, however either its effect was not detectable by the ITC or it did not materialise at all. Further dilution studies were made on compound **30** in 30, 40 and 50% $H_2O$/DMSO. Some degree of dimerisation was anticipated for compound **30** in the above solvent systems, considering the fact that hydrophobic interactions get stronger in a more aqueous environment. Nevertheless, no dimerisation was observed in these solvent systems.

Encouraging results have been registered for the initial structural optimisations made on compound **27**. It can be suggested that the possible Val-Val side chain interaction might be responsible for the improved dimerisation of compound **30** as compared with **29**. In addition, the results above are also important in highlighting the possible role of an aromatic-aromatic stacking interaction in dimer **27**.

## 3.4 Synthesis of guanidinium-carboxylates **45** and **46**

In order to undertake further structural optimization, compounds **45** and **46** were designed in which the phenylpropyl amide side chain in compounds **29** and **30** is replaced with a simple benzyl group. As guanidinium carboxylates **45** and **46** are more rigid, it is expected that they might dimerise more strongly. [92]

In addition, the dimerisation studies on these compounds will help to establish if the extra amide groups in the previous guandinium-carboxylates were important in stablising the dimeric structure.

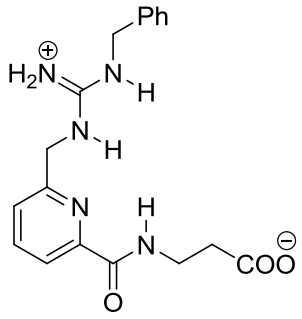


**45**

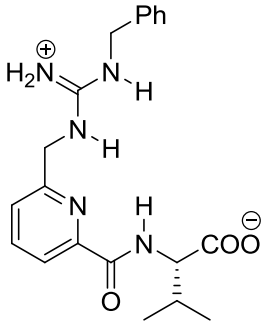


**46**

Scheme **6** outlines the synthesis of the thiourea compound which was used to install the benzyl-guanidine functionality into the system. Benzylchloroformate was converted into the corresponding thiocyanate derivative *via* a simple replacement of chloride with $SCN^-$. [112] This was followed by a coupling reaction with benzylamine to give the Cbz activated thiourea compound **49**. Compound **48** was found to be highly unstable with a propensity to decompose completely in a few hours if kept at room temperature.

**Scheme 6**

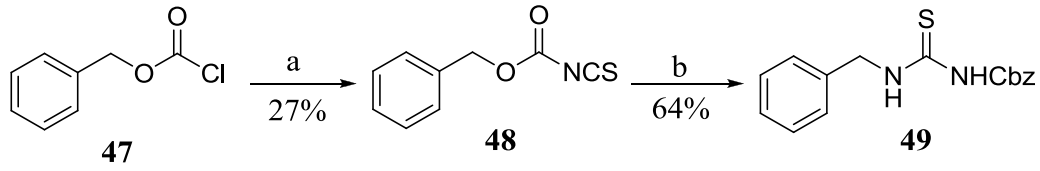


**Scheme 6**. Reagents and conditions: a) EtOAc, KCNS, 0 $^{o}$C b) $H_2NCH_2Ph$, DCM, rt.

Scheme **7** shows coupling of compound **37** with the thiourea compound **49** to give Cbz and ester protected form of the final carboxylate-guanidinium **45**. Final ester hydrolysis and Cbz deprotection steps then concluded the synthesis of guanidinium-carboxylate **45**.

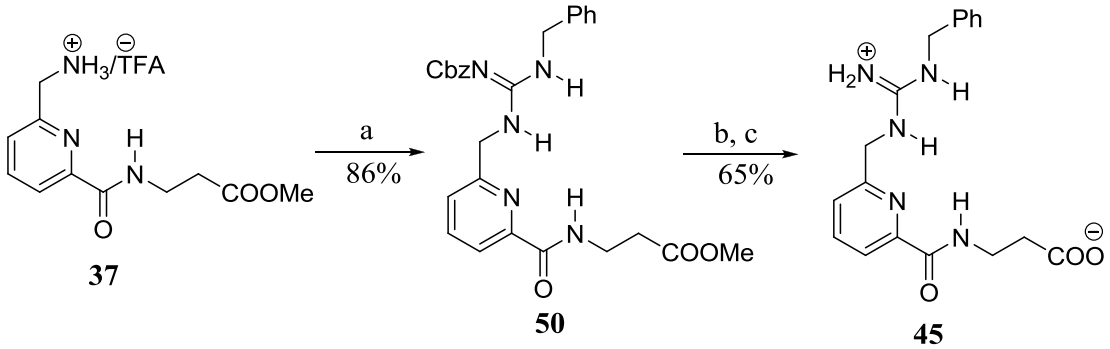


**Scheme 7**. Reagents and conditions: a) **49**, $Et_3N$, EDC.HCl, DCM, rt. b) $Me_3SiOK$, THF, rt. c) Pd/C,$H_2$, MeOH, rt.

Scheme **8** shows similar procedures leading to the synthesis of **46**. A lower yield was recorded for the valine functionalized derivative which might be due to a steric factor associated with the isopropyl side chain of valine during the methyl ester hydrolysis by $Me_3SiOK$.

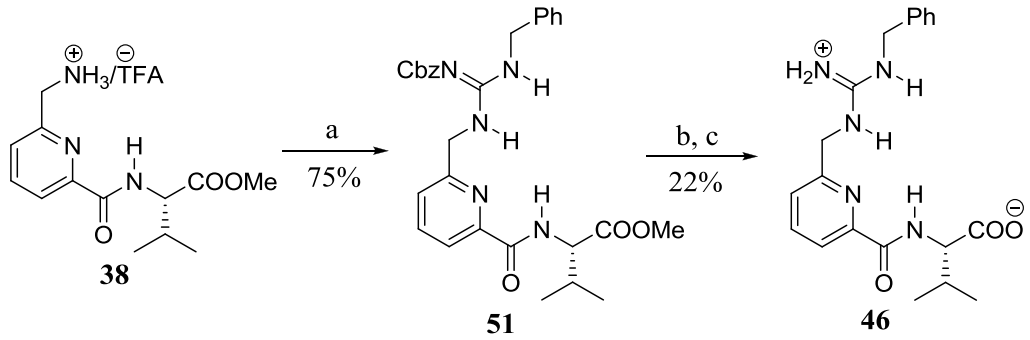


**Scheme 8**. Reagents and conditions: a) **49**, $Et_3N$, EDC.HCl, DCM, rt. b) $Me_3SiOK$, THF, rt. c) Pd/C,$H_2$, MeOH, rt.

The final compounds **45** and **46** were purified by repeated precipitation from methanol using diethyl ether. The high degree of polarity of the compounds precludes the use of normal phase chromatography as a means of purification.

## 3.4.1 Isothermal calorimetric dilution study of **45** and **46**

ITC dilution studies of compounds **45** and **46** were designed to look into the contribution of the propanamide side chain in the dimerisation process of compounds **29** and **30**, and were initially performed in DMSO (Fig 23). The studies also help to verify the importance of the Val-Val side chain interaction for the stability of the dimeric structure.

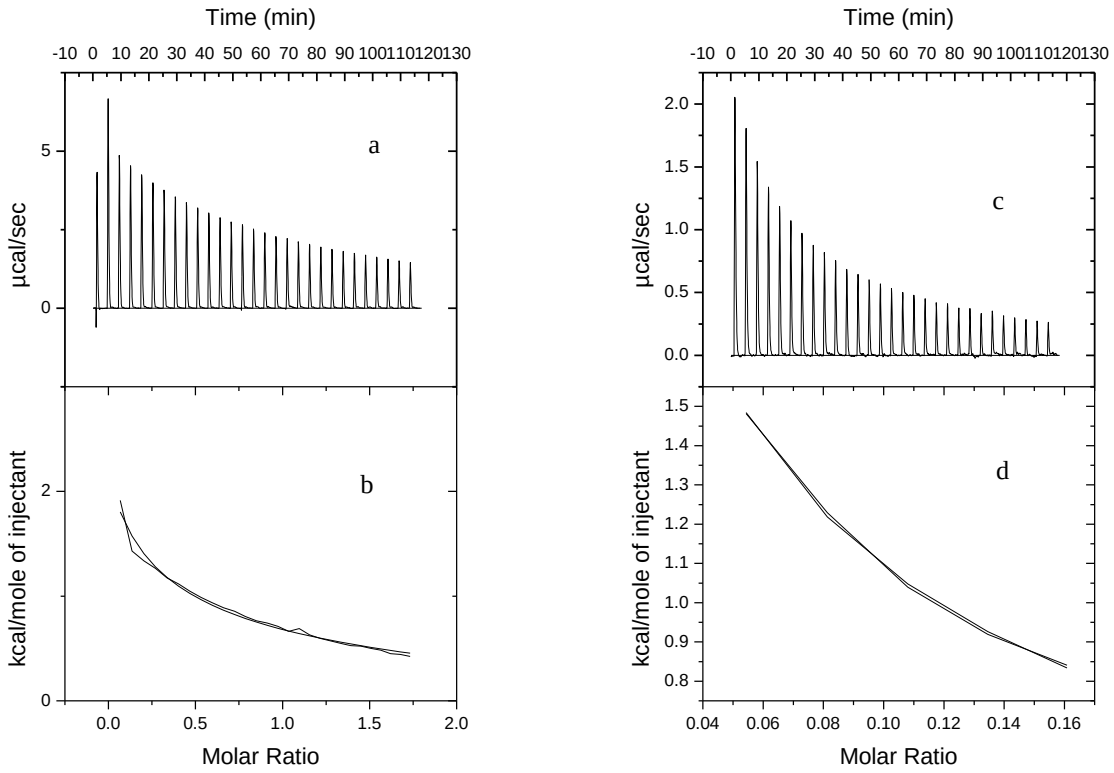


**Fig 23** *Calorimetric data obtained for ITC dilution studies of **45** (left) and **46** (right) in DMSO at 298 K. a & c) Raw ITC data (29* x *10 µL injections); b & d) Non-linear curve fitting of the reference corrected data into the dimer dissociation model*

The Val-functionalized compound **46** was found to form a very stable dimer in DMSO with a $K_{dim}$ of 4608±1954 $M^{-1}$. Dissection of the free energy of the dimerisation indicates that the process is primarily enthalpy driven (Table 3).

| Compound | $K_{dim}$ [$M^{-1}$] | $\Delta G_{dim}$ [kJ $mol^{-1}$] | $\Delta H_{dim}$ [kJ $mol^{-1}$] | $T\Delta S_{dim}$ [kJ $mol^{-1}$] |
|---|---|---|---|---|
| **45** | 180±30 | -12.9 | -24.4 ±0.4 | -11.4 |
| **46** | 4608±1954 | -20.9 | -21.8±1.1 | -0.9 |

**Table 3** *Energetics of dimerisations of compounds **45** and **46** (concentrations of 10 mM and 4 mM respectively) at 298 K in DMSO*

The possible contribution of a Val-Val non-polar interaction in the dimeric structure again comes into the picture. Compared to compound **45**, an extra stabilization energy of -5.1 kJ $mol^{-1}$ was observed for the dimer of compound **46** and this is similar to the

extra stabilization observed in the dimer of compound **30** compared with compound **29** which was -5.8 kJ $mol^{-1}$ (Fig 24). This consolidates the possibility of the role played by the Val side chain in enhancing the dimer stability.

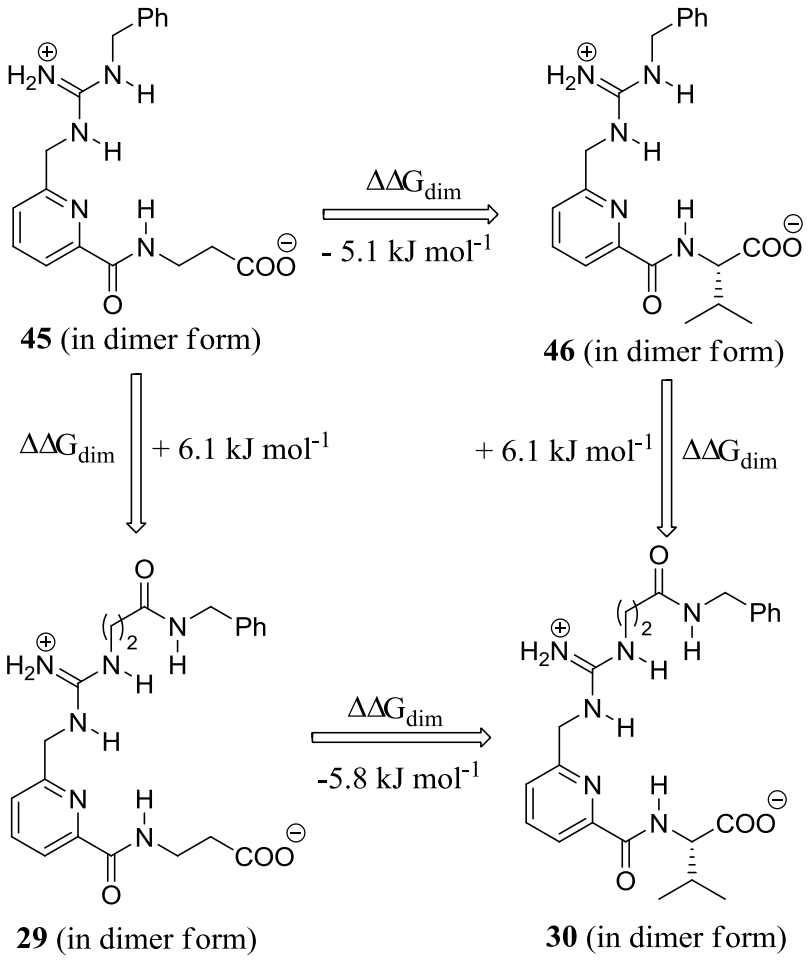


**45** (in dimer form) **46** (in dimer form)

**29** (in dimer form) **30** (in dimer form)

**Fig 24** *Comparison of the dimerisation energies of compounds **29**, **30**, **45** and **46***

In both ß-Ala (compounds **45** and **29)** and Val (compounds **46** and **30**) functionalized systems, the replacement of the phenyl propanamide side chain with a simple benzyl chain has resulted in an increase in $\Delta G_{dim}$ = -6.1 kJ$mol^{-1}$. Both systems indicate the possible deleterious effect of the propanamide side chain in the dimerisation process. However, in another set of compounds which contain aromatic side chains, it was the benzylpropane amide analogue rather than the simple benzyl one which was found to form a more stable dimer.[88] Compound **52** is an analogue of **27** in which the benzylpropane amide side chain was replaced with a benzyl group.

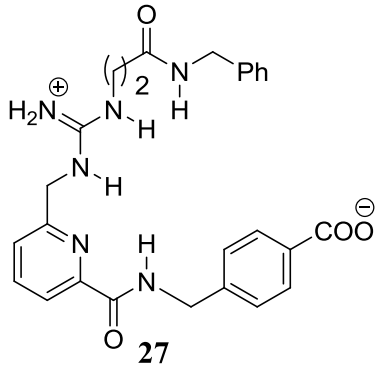

**27**

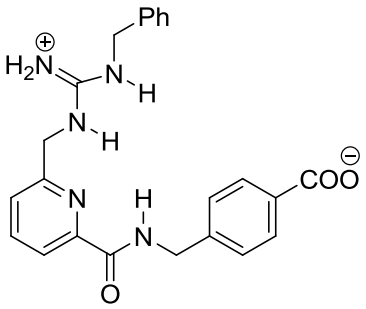

**52**

The dimers of both compounds are believed to be stabilized by aromatic-aromatic stacking interactions. However, it was noted that the dimer stability of **52** ($K_{dim}$ (DMSO) = 6622±2105 $M^{-1}$, $K_{dim}$ (10% $H_2O$/DMSO) = 148±31 $M^{-1}$) was found to be lower than that of **27** ($K_{dim}$(DMSO) = 11876±1692 $M^{-1}$ $K_{dim}$(10% $H_2O$/DMSO) = 532±23 $M^{-1}$). The constructive role of the benzyl propane amide moeity has also been observed in the binding of carboxylates by pyridoguandinium receptors incorporating this side chain.[59] The superiority of compound **27** is due to the possible involvement of the amide hydrogen in the dimerisation process. This is substantiated by the crystal structure evidences of **27** and **52**.[113] The dimer architecture of the guanidinium carboxylates with aliphatic side chains, however, might not allow the participation of the amide hydrogen in intermolecular hydrogen bonding as in the case of compound **27**.

Another plausible explanation for the weaker dimer stability of compound **45** vs **46** and compound **29** vs **30** is a possible non-covalent intramolecular interaction which can bring conformational changes affecting the intermolecular non-covalent interactions which are vital for dimer stability. A solid state X-ray structure of compound **45** substantiates this point (Fig 25).

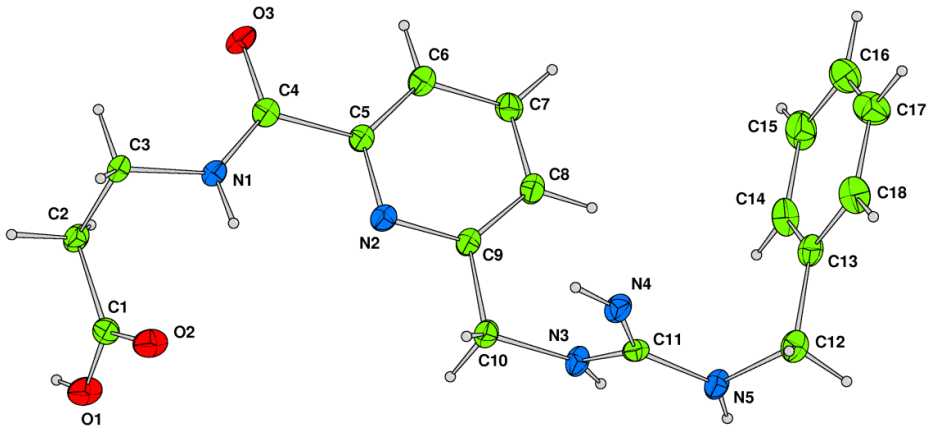


**Fig 25** *Solid state X-ray structure of compound **45***

The crystal structure analysis of **45** shows that there are four important inter and intra molecular hydrogen bonding interactions. Intramolecular H-bonding was observed between the amide NH and one of the carboxylate oxygens (N1–H···O2, 2.813 Å). Three important intermolecular hydrogen bonds between the guanidinium and carboxylate group were found in the X-ray structure. These guanidinium carboxylate interactions involve N3–H···O1 (2.772 Å), N5–H···O2 (2.749 Å) and O1–H···N4 (2.776 Å). The intermolecular H-bonding between the carboxylate and the guanidinium functionalities observed in the solid state are believed to be the driving force for the solution phase dimerisation of the compound (Fig 26). The flexibility of the β-Ala side chain in **45** allows intramolecular H-bonding between one of the carboxylate oxygens and the amide hydrogen. This may lead to conformational constraints which impede proper alignment for effective dimerisation in solution. The dimerisation process also requires breaking of the intramolecular H-bonds thus subtracting from the overall dimerisation energy. It is likely that the intramolecular hydrogen bonding will also be in the solution phase structure as intramolecular interactions are more likely to be preserved in solution compared to intermolecular ones.[114] However, it is has also to be in mind that solid state structures do not necessarily represent solution phase structures.[115]

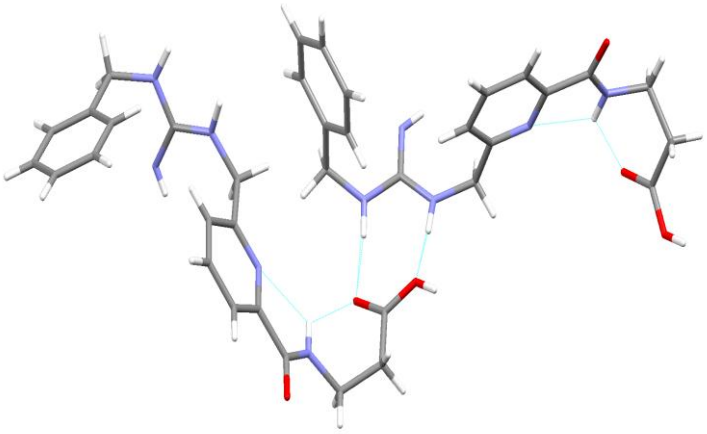

**Fig 26** *Self-association of compound **45** in the solid state*

The dimerisation of compounds **45** and **46** was further investigated in 10% $H_2O$/DMSO system (Fig 27).

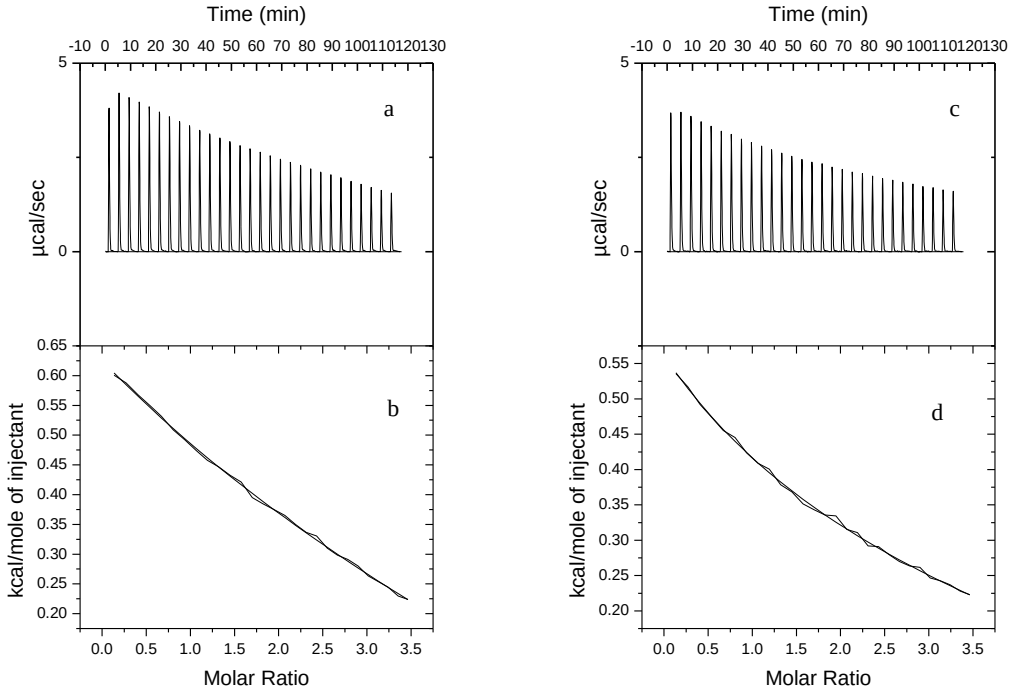


**Fig 27** *Calorimetric data obtained for ITC dilution studies of **45** (left) and **46** (right) in 10% $H_2O$/DMSO at 298 K. a & c) Raw ITC data (29 x 10 µL injections); b & d) Non-linear curve fitting of the reference corrected data into the dimer dissociation model*

The dimerisation of both compounds was found to be reduced significantly in 10% $H_2O$/DMSO. The marked difference in stability observed between the dimers from compounds **45** and **46** in DMSO was not apparent in 10% $H_2O$/DMSO (Table 4). This is unexpected as it was anticipated that the hydrophobic Val-Val interaction might help in preserving the dimerisation in an aqueous environment and hence bring considerable differences in terms of dimer stabilities between the two compounds.

| Compound | $K_{dim}$ [$M^{-1}$] | $\Delta G_{dim}$ [kJ $mol^{-1}$] | $\Delta H_{dim}$ [kJ $mol^{-1}$] | $T\Delta S_{dim}$ [kJ $mol^{-1}$] |
|---|---|---|---|---|
| **45** | 54±8 | -9.9 | -6.2±0.1 | 3.6 |
| **46** | 54±4 | -9.8 | -5.6±0.1 | 4.2 |

**Table 4** *Energetics of dimerisation of compounds **45** and **46** (concentrations of 20 mM each) at 298 K in 10% $H_2O$/DMSO*

It was also noted that the contribution of the entropic component of the free energy has significantly increased in 10% $H_2O$/DMSO. This is expected as hydrophobic interactions in aqueous environments are entropy driven. The ordered water molecules surrounding the monomeric structure are released into the bulk system during the dimerisation process and this directly results in increase of the entropy of the system. As expected, the entropic contribution is greater in compound **46** which might be due to the Val-Val hydrophobic interaction. It has to be noted however that ITC determination of enthalpy amd entropy is not reliable for processes with small binding constants.

In summary, by synthesizing compounds **45** and **46** and studying their dimerisation, we were able to undergo further analysis of dimer stability in DMSO and 10% $H_2O$/DMSO. In these two compounds, the negative role of the propane amide side chain and the positive role of the Val side chain in the stability of the dimeric structures were noted.

## 3.4.2 NMR dilution study of **29**, **30**, **45** and **46**

Having established the dimerisation of the above compounds using ITC, NMR dilution study was carried out to verify the self assembly process. This might not only confirm the stability constants of the dimer obtained from the ITC experiment but also give structural information regarding the dimerisation process in solution. The feasibility of undertaking an NMR dilution study was first assessed by calculating the concentration of any given monomer needed to prepare solutions which should contain a significant amount of dimer (9:1, dimer:monomer ratio) and a significant amount of the monomer (1:9, dimer:monomer ratio) in the given solvent system. These calculations were made using the $K_{dim}$ values obtained from the ITC studies. Out of the four compounds it was only compound **45** which could practically be studied by an NMR dilution experiment. In cases of the other compounds either the concentration required is beyond the solubility limits or is too dilute to be studied practically by NMR (Table 5).

| Compound | 90%[D*] | 85%[D*] | 50%[D*] | 20%[D*] | 15%[D*] |
|---|---|---|---|---|---|
| **29** | 487.80 | 204.70 | 10.8 | 1.69 | 1.12 |
| **30** | 102.15 | 42.90 | 2.30 | 0.35 | 0.23 |
| **45** | 54.60 | 22.90 | 1.20 | 0.19 | 0.13 |
| **46** | 7.50 | 3.10 | 0.17 | 0.02 | 0.01 |

[D*]= the concentration of the compound in mg/mL which contains the specified percentage of dimer in DMSO solution, calculated based on the $K_{dim}$ obtained from ITC dilution studies. $[D^*] = ([dimer]/K_{dim}* [monomer]^2)*MW$.

**Table 5** *Concentration needed to prepare solutions of compounds **29**, **30**, **45** and **46** in DMSO that is supposed to contain 90%, 85%, 50%, 20% and 15% dimeric structure*

A preliminary NMR dilution study was made by preparing a concentrated (10 mg/mL) and a dilute (1 mg/mL) solution of compound **45** in DMSO. The NMR spectra of these solutions show that there is a concentration dependent change in the chemical shift value of the NH protons (Fig 28). These concentration dependent changes of the chemical shift values are believed to be a direct result of the dimerisation process.

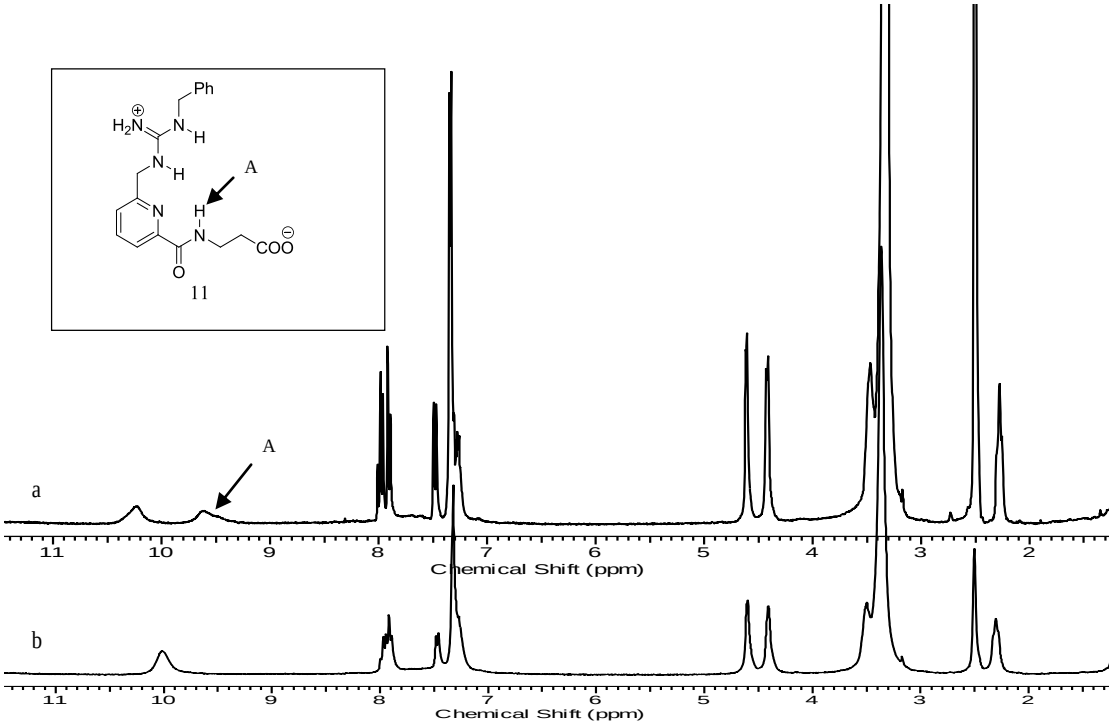


**Fig 28** *$^{1}H$ NMR spectra of compound **45** a) 1 mg/mL in DMSO b) 10 mg/mL in DMSO*

It can be seen from the NMR spectra above that two NH signals that resonate at the same chemical shift in the concentrated solution spectrum of compound **45** separated in the dilute solution spectrum. As we go from the dilute solution spectrum into the concentrated one, one of the NH signals shifts upfield and the other shifts downfield. The downfield shift is due to complexation of the guanidinium NH with carboxylate in the dimeric structure. However, the upfield shift could not justify the constructive involvement of the NH proton in the dimerisation process. This can be attributed to the fact that the amide NH might be involved in intramolecular H-bonding in the monomer, most probably with the carboxylate oxygen as observed from the X-ray structure (Fig 26), resulting in an upfield shift when the solution gets more concentrated. In dimer form, the carboxylate oxygen will be hydrogen bonded not only intramolecularly with the amide NH but also intermolecularly with the guanidinium NH. With increasing substrate concentration and as formation of the dimer begins, the strength of the intramolecular H-bonding decreases. This results in successive upfield shift of the amide proton signal as the concentration of the substrate increases.

This preliminary study was followed by a full NMR dilution study that would permit to make a full quantitative determination of the dimerisation constant in DMSO. [102] Diverging (one upfield and another downfield) shifts of the two NH proton signals were successively observed as the solution is increasingly diluted (Fig 29).

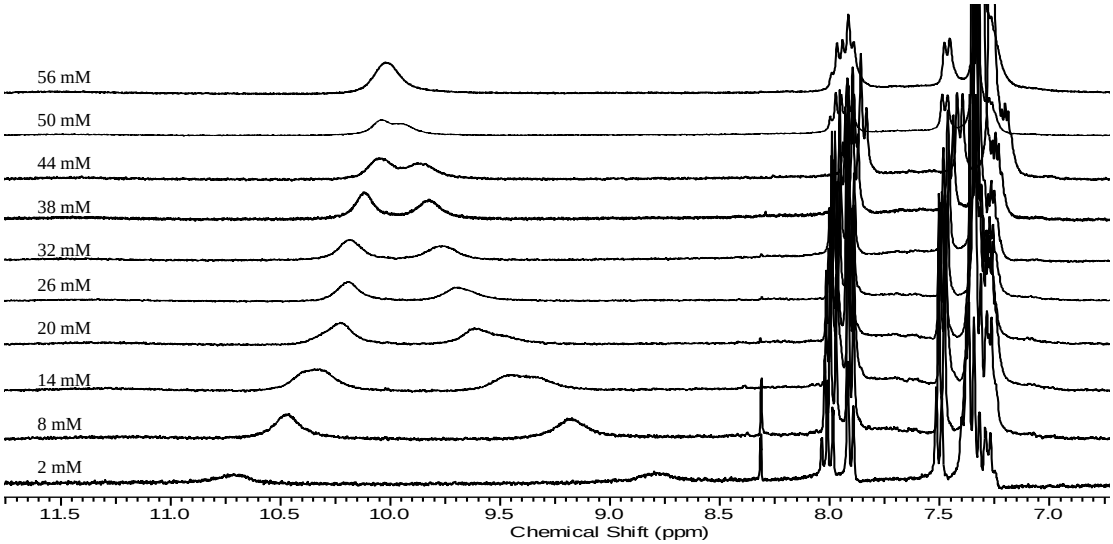


**Fig 29** *Part of $^{1}H$ NMR signals of compound **45** in DMSO along with the concentration of the sample at 298 K*

Plots of the observed chemical shifts versus concentration give two isothermic binding curves (Figure 30) and these concentration dependent changes of the two NH signals is correlated with the shift in the monomer-dimer equilibrium.

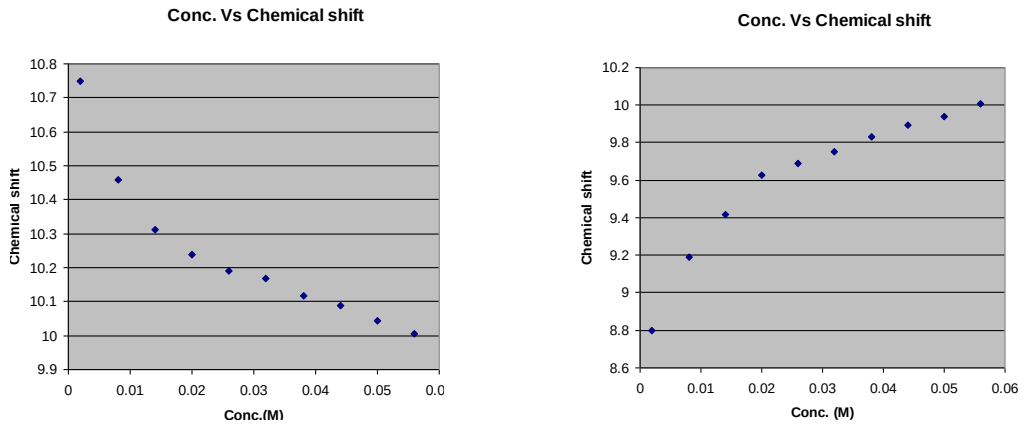


a b

**Fig 30** *a & b, Concentration versus chemical shift plots of the two NH protons signals which show concentration dependent chemical shift change in DMSO at 298 K*

The two NMR dilution data sets were analysed using nonlinear curve fitting to a dimerisation isotherm (NMRDil_Dimer) [30] and were found to have a $K_{dim}$ = 57.5 $M^{-1}$ using the dilution data obtained from the guanidine NH and $K_{dim}$ = 31.8 $M^{-1}$ using the dilution data obtained from the amide NH. These results are lower than the $K_{dim}$ (180 $M^{-1}$) obtained from the ITC study but are of the same order of magnitude. Results obtained with other dimers (vide infra) generally gave a consistent picture *i.e* dimerisation constants from NMR and ITC with the same order of magnitude.

Inaddition to verifying the ITC dimerisation figures, the NMR dilution study has helped us to observe the involvement of the guanidine and the amide protons in the dimerisation process in solution.

## 3.5 Synthesis of guanidinium-carboxylate **53**

Most of the compounds considered so far have shown good dimerisation in DMSO and 10% $H_2O$/DMSO systems. This has been well established by ITC dilution experiments. However, verification of the dimerisation process could not be made for most of the compounds using NMR dilution studies due to the fact that the concentration needed to span a 10%–90% range of dimer formation is not suitable for the NMR dilution experiment. However, it is desirable to verify the dimerisation by an NMR study and get more structural information on the dimer architecture and the binding event in solution.

Guanidine-carboxylate **53** is a compound previously synthesised in our lab which showed a $K_{dim}$ = 877±100 $M^{-1}$ in DMSO (Fig 31) as determined by ITC dilution study.

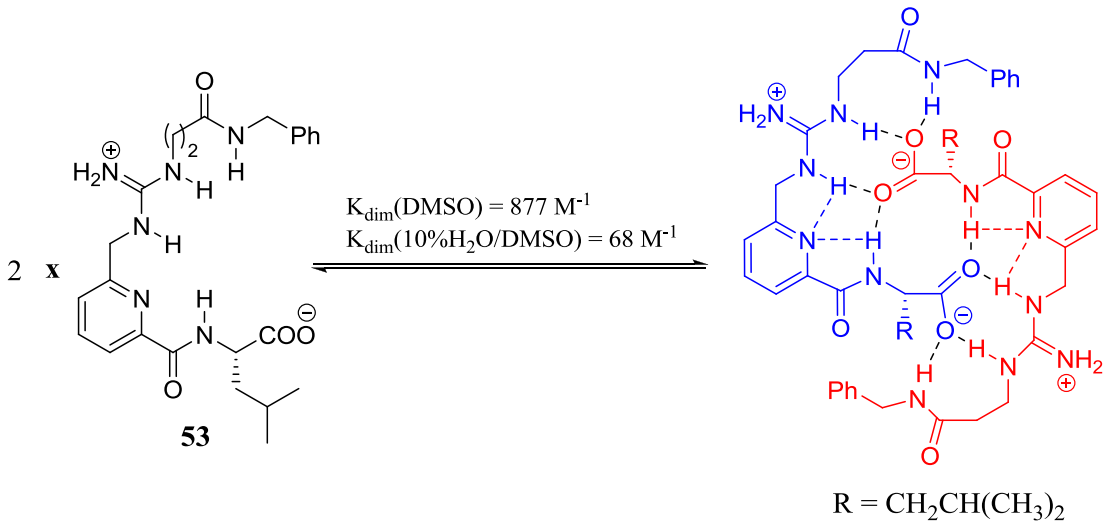


**Fig 31** *Schematic representation of the proposed dimerisation of compound **53***

Compound **53** is an analogue of compound **30** in which the Val amino acid side chain is replaced with Leu. Calculations based on ITC dimerisation data show that compound **53** is amenable to NMR dilution studies. The working concentration range of the proposed NMR dilution experiment was established based on the $K_{dim}$ value obtained from the ITC study result (Table 6).

| Compound | 85% [D*] | 80% [D*] | 50% [D*] | 15% [D*] | 10% [D*] |
|---|---|---|---|---|---|
| **122** | 20.20 | 10.7 | 1.10 | 0.11 | 0.07 |

[D*]= the concentration of the compound in mg/mL which contains the specified percentage of dimer in DMSO solution, calculated based on the $K_{dim}$ obtained from ITC dilution studies. [D*] = ([dimer]/$K_{dim}$* [monomer]$^2$)*MW.

**Table 6** *Concentration needed to prepare solutions of compounds **53** in DMSO that are supposed to contain 85%, 80%, 50%, 15% and 10% dimeric structure*

As seen from table 6, a concentration range that spans solutions containing 85:15 dimer:monomer ratio up to 15:85 dimer:monomer ratio can suitably be prepared thus making compound **53** a very good candidate for NMR dilution studies.

With this in mind, compound **53** was resynthesised and its dimerisation properties were fully investigated by ITC and NMR dilution experiments. Scheme **9** shows the synthesis of compound **53**. The pyridine scaffold **35** was coupled with the methyl ester of L-Leu amino acid to yield compound **54**. Boc deprotection of **54** followed by coupling with the Cbz activated thiourea compound **42** has then afforded compound

**55** which is the Cbz and methyl ester protected version of the final compound. In the previous synthesis procedure [88], a reverse order of coupling procedure was used to access compound **55**. Boc deprotected methyl ester of the pyridine scaffold **35** was coupled with the Cbz activated thiourea compound **42**. This was followed by methyl ester hydrolysis and coupling with Leu methyl ester to access compound **55**. The last two procedures, methyl ester hydrolysis and Cbz deprotection of **55**, are the same in both synthetic schemes and similar yields were recorded.

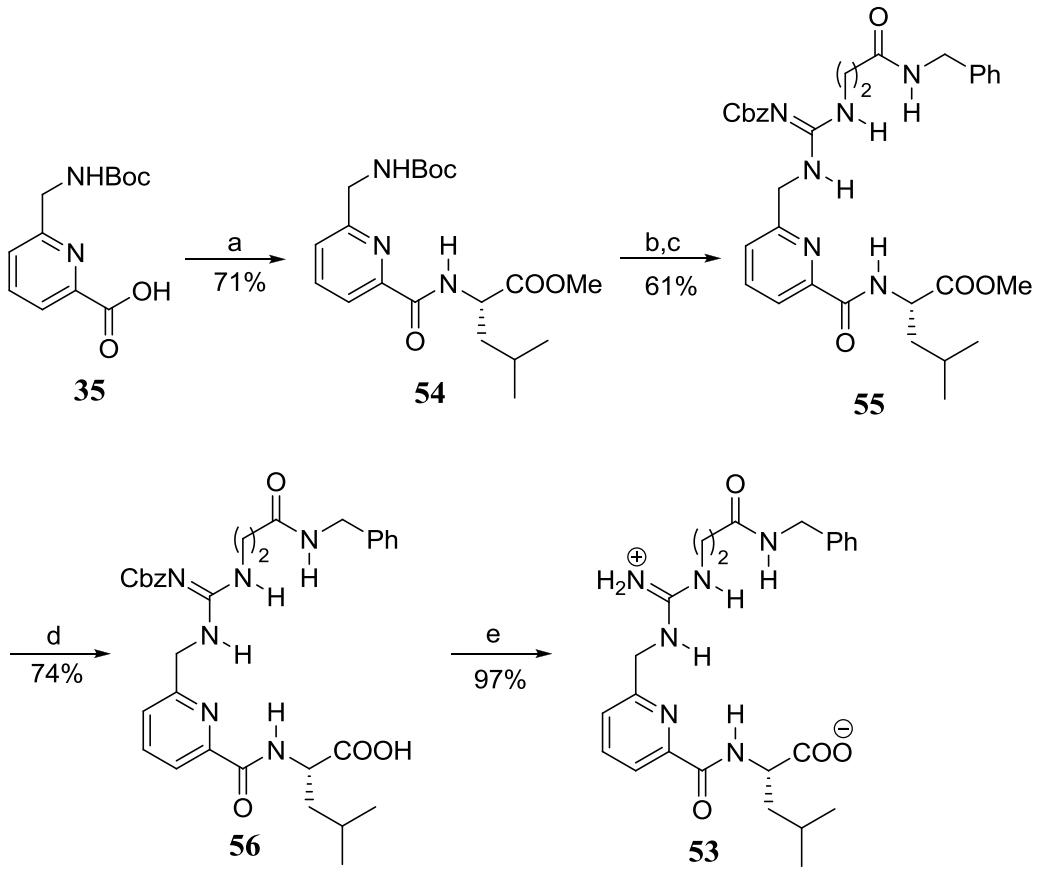


**Scheme 9**. Conditions and reagents: a) L-Leu-methyl ester, EDC.HCl, HOBt, DIPEA, DCM,rt. b) 20% TFA/DCM, rt. c) **42**, EDC.HCl, $Et_3N$, DCM, rt. d) $Me_3SiOK$, THF, rt. e) $H_2$, Pd/C, MeOH, rt.

Compound **53** was fully characterized and its purity established using spectroscopic analyses.

## 3.5.1 Isothermal calorimetric dilution study of **53**

Prior to performing NMR dilution experiments, an ITC dimerisation study of compound **53** was performed to verify the results from the previous ITC experiments and also to further investigate the dimerisation process in different solvent systems (Fig 32)

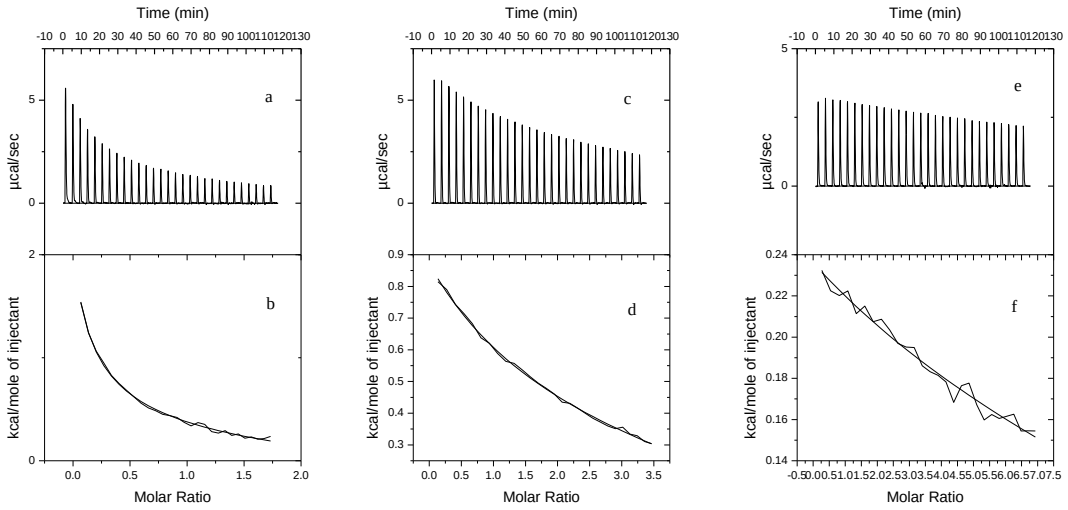


**Fig 32** *Calorimetric data obtained for ITC dilution studies of **53** in DMSO (left), 10% $H_2O$/DMSO (middle) and 50% $H_2O$/DMSO (right) at 298K. a, c & e) Raw ITC data (29 x 10µL injections); b, d & f) Non-linear curve fitting of the reference corrected data into the dimer dissociation model*

The full thermodynamic profile associated with the dimerisation of compound **53** is given below.

| Solvent | $K_{dim}$ [$M^{-1}$] | $\Delta G_{dim}$ [kJ $mol^{-1}$] | $\Delta H_{dim}$ [kJ $mol^{-1}$] | $T\Delta S_{dim}$ [kJ $mol^{-1}$] |
|---|---|---|---|---|
| DMSO | 952±64 | -17.0 | -16.7±0.2 | 0.3 |
| 10% $H_2O$/DMSO | 73±5 | -10.6 | -8.6±0.1 | 2.0 |
| 50% $H_2O$/DMSO | 55±8 | -6.4 | -1.8±0.2 | 4.6 |

**Table 7** *Energetics of dimerisation of compound **53** at 298 K in DMSO (3 mM), 10% $H_2O$/DMSO (10 mM) and 50% (20 mM)*

An enthalpy driven dimerisation was observed in DMSO ($K_{dim}$ [$M^{-1}$] = 952±64) and 10% $H_2O$/DMSO ($K_{dim}$ [$M^{-1}$] = 73±5). This is consistent with the previous ITC

dilution result ($K_{dim}$ = 877±100 $M^{-1}$ in DMSO). Compared with the Val analogue ($K_{dim}$ [$M^{-1}$] = 400±22 in DMSO), compound **53** produced a more stable dimer which might be attributed to the Leu-Leu side chain interactions in the dimeric system. Comparing with dimeric systems from compounds **29** and **30** (Fig 33), it is observed that the dimer stability enhances as the hydrophobicity of the side chain increases and this might explain the importance of hydrophobic-hydrophobic interaction in stabilizing the dimers from compounds **29** and **53**. It has been reported in the literature that non-polar pairings between amino acids (Ile-Ile, Val-Val, Leu-Leu) occurring in parallel β-sheets are of the dominant types of pairings occurring between adjacent peptide strands. The rationale behind this is the good van der Waals contacts obtained by nested arrangement.[116]

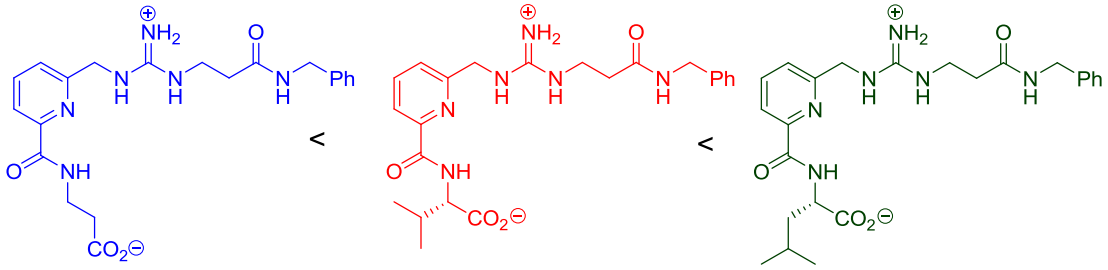


**29** (Dimer form)
$\Delta G_{dim}$ = -9.0 kJ $mol^{-1}$

**30** (Dimer form)
$\Delta G_{dim}$ = -14.8 kJ $mol^{-1}$

**53** (Dimer form)
$\Delta G_{dim}$ = -17.0 kJ $mol^{-1}$

**Fig 33** *The order of stabilities of the dimeric structures of compounds **29**, **30** and **53** in DMSO*

The superiority of the dimerisation of compound **53** over compounds **29** and **30** is once again demonstrated when the dimerisation studies were undertaken in 10% $H_2O$/DMSO system. The dimer of compound **30** was completely disrupted at 10% $H_2O$/DMSO while compound **53** maintains an enthalpy driven dimerisation of $K_{dim}$ = 73 ± 4.6 $M^{-1}$. It is also interesting to see that there was some dimerisation, which is essentially entropy driven, observed at 50% $H_2O$/DMSO level signifying the importance of the Leu-Leu hydrophobic interaction in enhancing dimer stability in aqueous environments. Encouraged by these results further studies were undertaken at 75% $H_2O$/DMSO system. Some qualitative evidence of dimerisation has been obtained in this system. As seen in fig 34 successive injections produced an endothermic heat pulse which is characteristic of dissociation of a dimer into the

monomeric structure. However, the error associated with the curve fitting is too large to make the estimated $K_{dim}$ a quantitatively valid result.

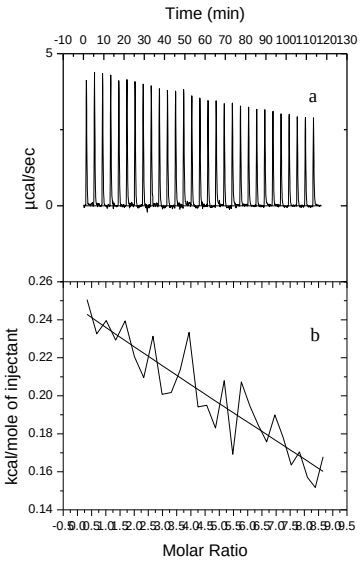


**Fig 34** *Calorimetric data obtained for ITC dilution studies of **53** in 75% $H_2O$/DMSO at 298 K. a) Raw ITC data (29* x *10µL injections); b) Attempted non-linear curve fitting of the reference corrected data into the dimer dissociation model*

## 3.5.2 NMR dilution study of **53**

A preliminary NMR dilution experiment using a concentrated (10 mg/mL) and a dilute (1 mg/mL) solution of compound **53** indicated that there is a concentration dependent change in the observed chemical shift value of the NH proton signals. A very noticeable change was observed for two of the NH protons (Fig 35). There is an upfield chemical shift of 0.64 ppm observed for the NH proton signal at **A** (9.45 ppm to 8.81 ppm) when the concentration of compound **53** was increased from 1 mg/mL to 10 mg/mL. The NH proton signal at **B** (8.28 ppm) was significantly shifted downfield where it moved from 7.61 ppm in the dilute solution spectrum and overlapped with the aromatic CH proton signals (7.81-7.90 ppm) in the concentrated solution spectrum. Spectral analysis of compound **53** has shown that the NH signal at A corresponds to the benzyl-amide NH proton whereas the signal at B corresponds to one of the guandine protons.

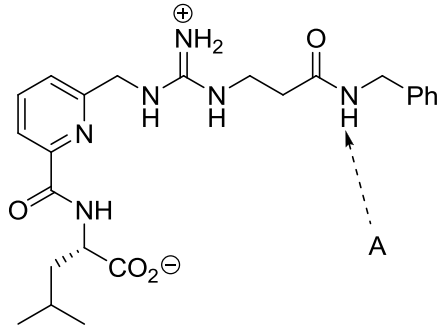


The $H^1$ NMR spectra of the concentrated and the dilute solution are shown below for comparison.

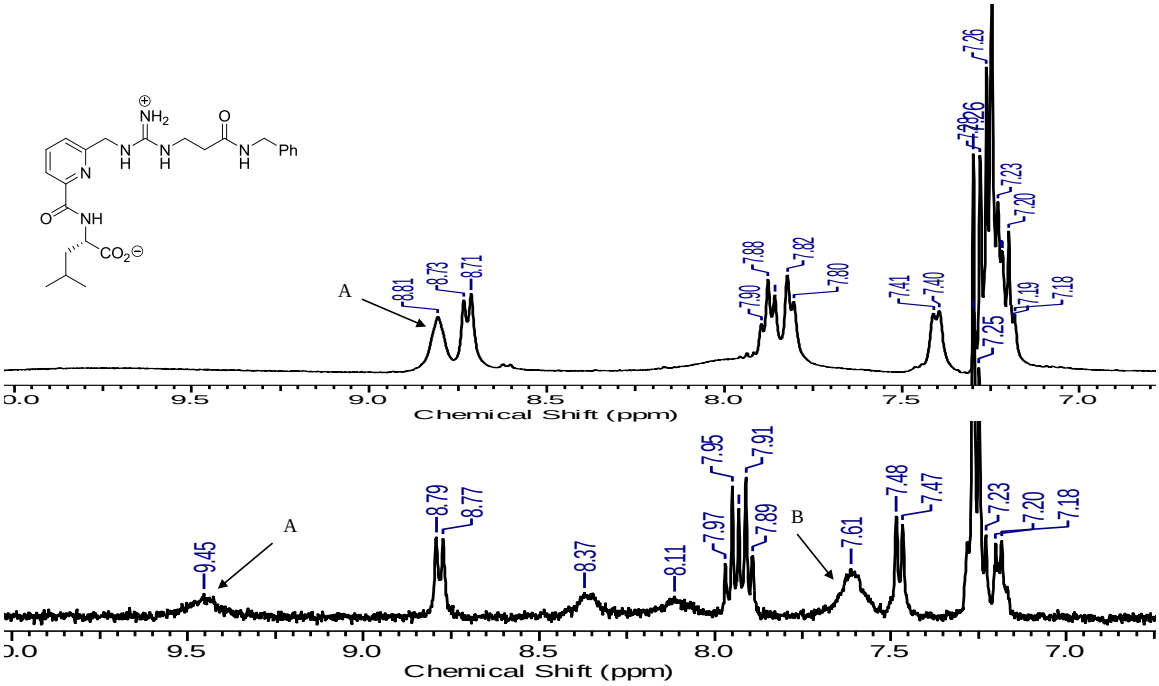


**Fig 35** *Part of $^1H$ NMR spectrum of compound **53** in DMSO. The spectrum above belongs to the concentrated solution (10 mg/mL) and below to the dilute solution (1 mg/mL) of compound **53***

Following this, the optimum concentration range of the samples needed for a full NMR dilution experiment were calculated based on the $K_{dim}$ value obtained from the ITC study result (Table 7).

Considering the solubility of the compound and the sensitivity of the NMR instrument, concentrations that contain 85:15 dimer:monomer ratio (19.01 mg/mL) and 10:90 dimer:monomer ratio (0.062 mg/mL) were chosen as the highest and the lowest

concentration limits respectively. Accordingly 15 dilutions (40.60 mM - 0.13 mM) were prepared from a stock solution of 19.01 mg/mL and their $^{1}$H NMR spectra were recorded (Fig 36).

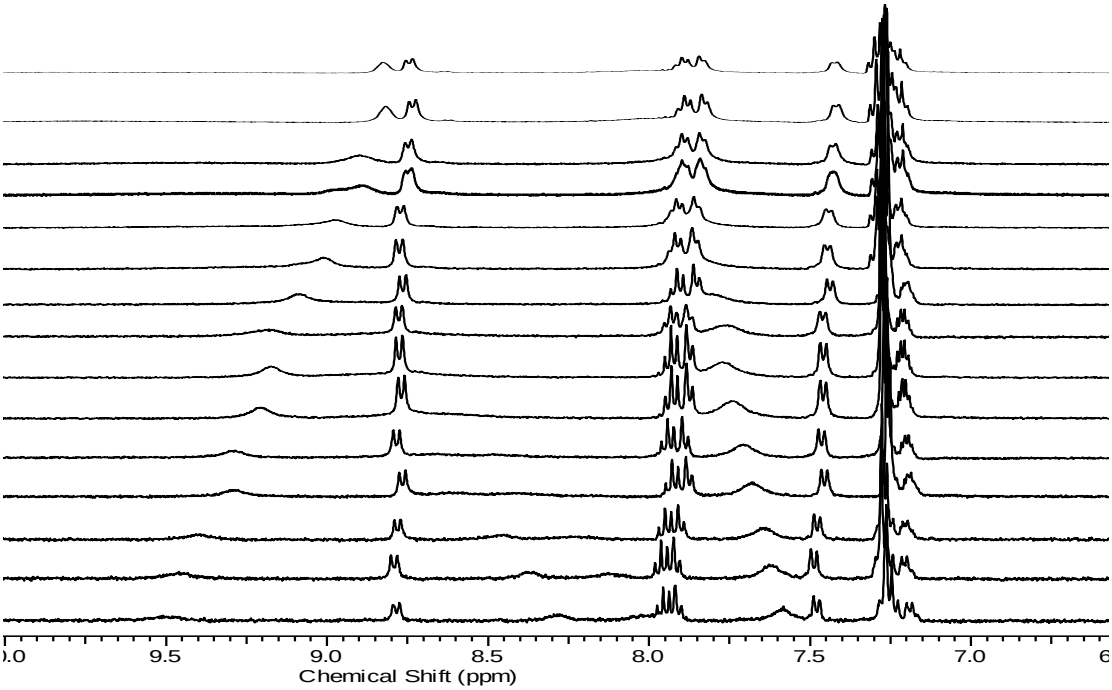


**Fig 36** *Parts of the $^{1}$H NMR spectra (400 MHz, 298 K) of **122** in DMSO showing the dimerization induced shift changes (Concentrations from bottom to top: 0.13, 0.23, 0.35,0.51, 0.72, 0.99, 1.35, 1.85, 2.55, 3.58 5.14, 7.70, 12.10, 20.60, 40.60 mM)*

The full NMR dilution experiment has demonstrated that there are indeed successive concentration dependent changes in the chemical shift value of the two NH proton signals mentioned above (Fig 36). As expected, the guanidine NH signal is downshifted as the concentration was sequentially increasing. This is expected to be the direct result of the head-to-tail complimentary complexation of the NH proton *via* hydrogen bonding with the carboxylate oxygen in the dimeric structure. However, the upfield shift of the amide proton signal with successive increments of concentration does not reflect the constructive intermolecular bond engagement of this proton. A plausible explanation for this is that the amide proton might be intramolecularly bonded with one of the carboxylate oxygens and the upfield shift of the amide proton with concentration increments would be due to weakening of this intramolecular hydrogen bond as a result of the dimerisation process.

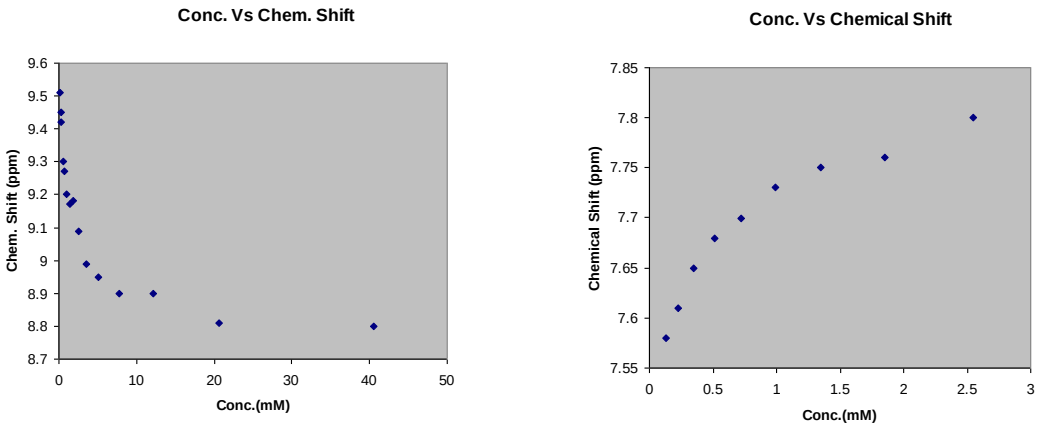


**Fig 37** *Plots of concentration versus observed chemical shift value of the amide and one of the guanidine NH protons of compound* ***53*** *in DMSO*

The two NMR dilution data sets were analysed using nonlinear curve fitting to a dimerisation isotherm (NMRDil_Dimer) (Fig 38) and gave $K_{dim}$ values of 647 $M^{-1}$ and 1110 $M^{-1}$. This is in good agreement with the dimerization constant obtained from the ITC study, which is 931 $M^{-1}$.

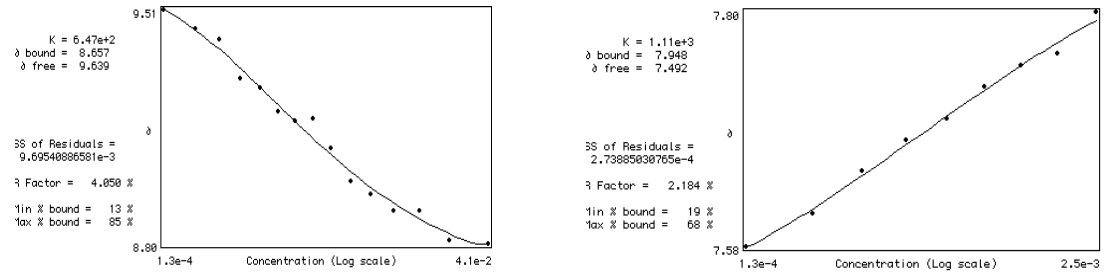


**Fig 38** *Nonlinear curve fitting of the NMR data to a dimerisation isotherm (NMRDil_Dimer) model*

In this experiment, we have demonstrated the good agreement of the $K_{dim}$ values determined by NMR and ITC dilution experiments. This can also be considered as a validation and verification of ITC determined $K_{dim}$ figures of compounds **46**, **29** and **30**. Furthermore the NMR dilution studies have revealed structural components of compound **53** which are involved in the solution phase intermolecular interaction.

## 3.6 Synthesis of guanidinium-carboxylate **57**

So far, we have uncovered some important structural features which play important roles in the dimerisation process. The main driving force of the dimeric architectures accessed so far in DMSO is the intermolecular complimentary H-bonding between the carboxylate and the guanidinium moieties. The effect of this H-bonding however was found to dramatically decline upon addition of even 10% $H_2O$ into the system. Fine tuning of the dimerisation process has been undertaken by introducing stabilizing non-covalent bond forming features into the system and significant progress has been made in this regard. It has been proved in our previous systems that π- π stacking interaction, Val-Val side chain interaction and Leu-Leu side chain interaction may contribute to additional stability in the dimeric system. However, none of the above interactions by themselves could effectively compensate for the loss of the guanidinium-carboxylate hydrogen bonding energy and maintain the dimeric structure in a more aqueous environment (>20% $H_2O$/DMSO), although it is noteworthy that compound **53,** which has a Leu amino acid side chain showed a quantitatively measurable dimerisation ($K_{dim}$ = 13±4.8 $M^{-1}$) in 50% $H_2O$/DMSO.

Based on the above encouraging result, it was envisaged that a pyridoguanidinium dimeric supramolecular system that encompasses a combination of the above mentioned features might show improved stability in an aqueous environment. With this in mind, compound **57**, which has a side chain containing a bis-aromatic moiety sandwiching a leucine amino acid residue, was designed.

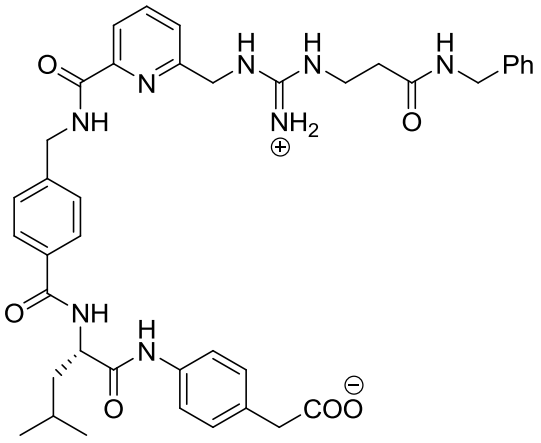


**57**

Considering the fact that Leu-Leu and aromatic-aromatic stacking interactions have been proved to be important features for dimer stability, it was thought that a compound such as **57** which simultaneously can furnish a bis aromatic-aromatic and a Leu-Leu hydrophobic intermolecular interaction will enhance the energetics of dimerisation in more aqueous environments (Fig 39). It was also expected that cooperativity among the non-covalent bonds would further strengthen the dimer stability.

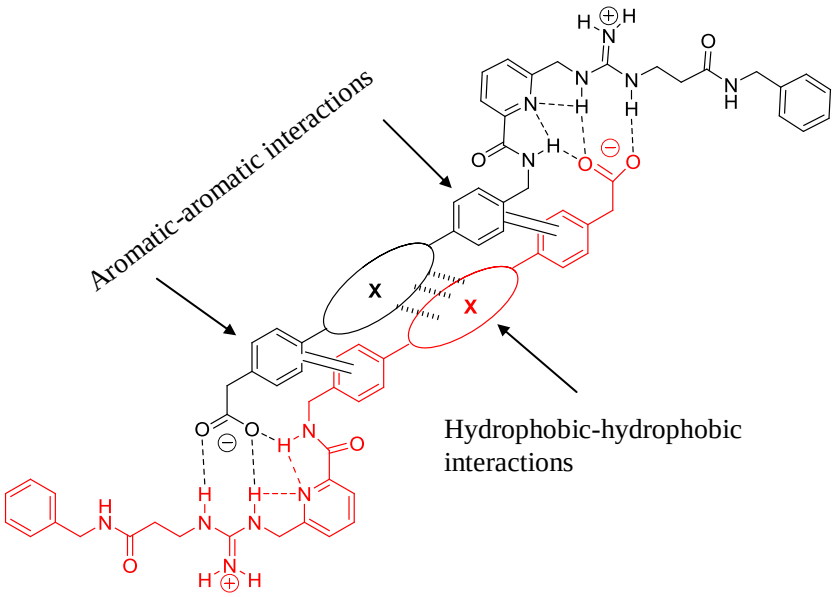


**Fig 39** *Expected dimer of compound **57** showing the possible intermolecular interactions contributing to the dimer stability.*

It was anticipated that the NOESY spectrum analysis of such compounds in solution might give us further structural information on the dimer structure as it is envisaged that a through space intermolecular interaction should occur between the aromatic protons which are expected to be in close proximity in the dimeric system.[117, 118]

The synthetic work undertaken initially was the large scale synthesis of the Cbz protected pyridoguanidine compound **59** (Scheme 10). This synthetic procedure was previously optimized in our group and has been used in creating versatile building block to make various pyridoguanidinium carboxylates.

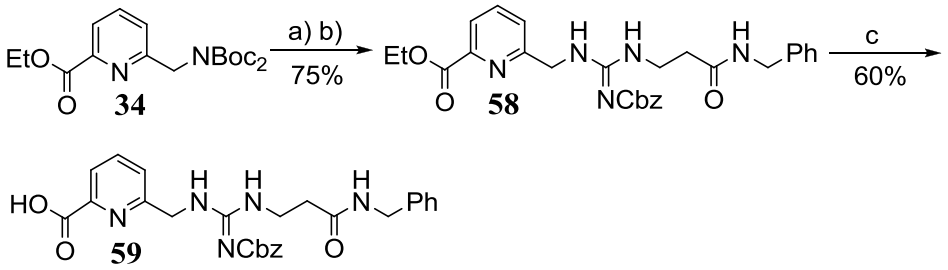


**Scheme 10**. Reagents and conditions: a) 20% TFA/DCM, rt. b) **42**, $Et_3N$, EDC.HCl, DCM, rt. c) $Me_3SiOK$, THF, rt.

The next synthetic scheme (Scheme 11) describes the synthesis of compound **64**, which is a peptide side chain containing the bis aromatic moieties sandwiching a leucine amino acid.

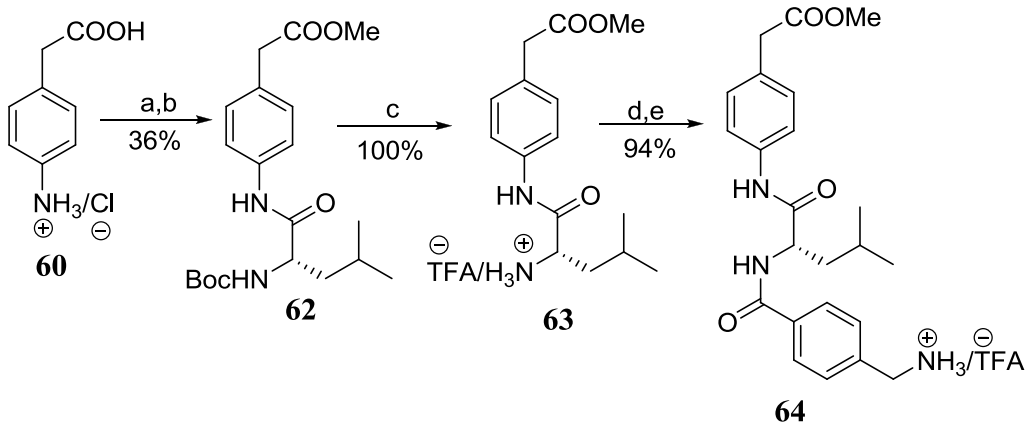


**Scheme 11**. Conditions and reagents: a) MeOH, HCl, reflux. b) Boc-Val-COOH, EDC.HCl, DIPEA, HOBt, DCM, rt. c) 20% TFA/DCM, rt. d) Boc-*p*-methylamino benzoic acid, EDC.HCl,DIPEA, HOBt, DCM, rt. e) 20% TFA/DCM, rt.

Compound **64** was then coupled to compound **59** using the standard peptide coupling procedure (Scheme 15). This results in the precursor **65** of the final compound which requires methyl ester hydrolysis and hydrogenolysis of to give guanidinium carboxylate **53**.

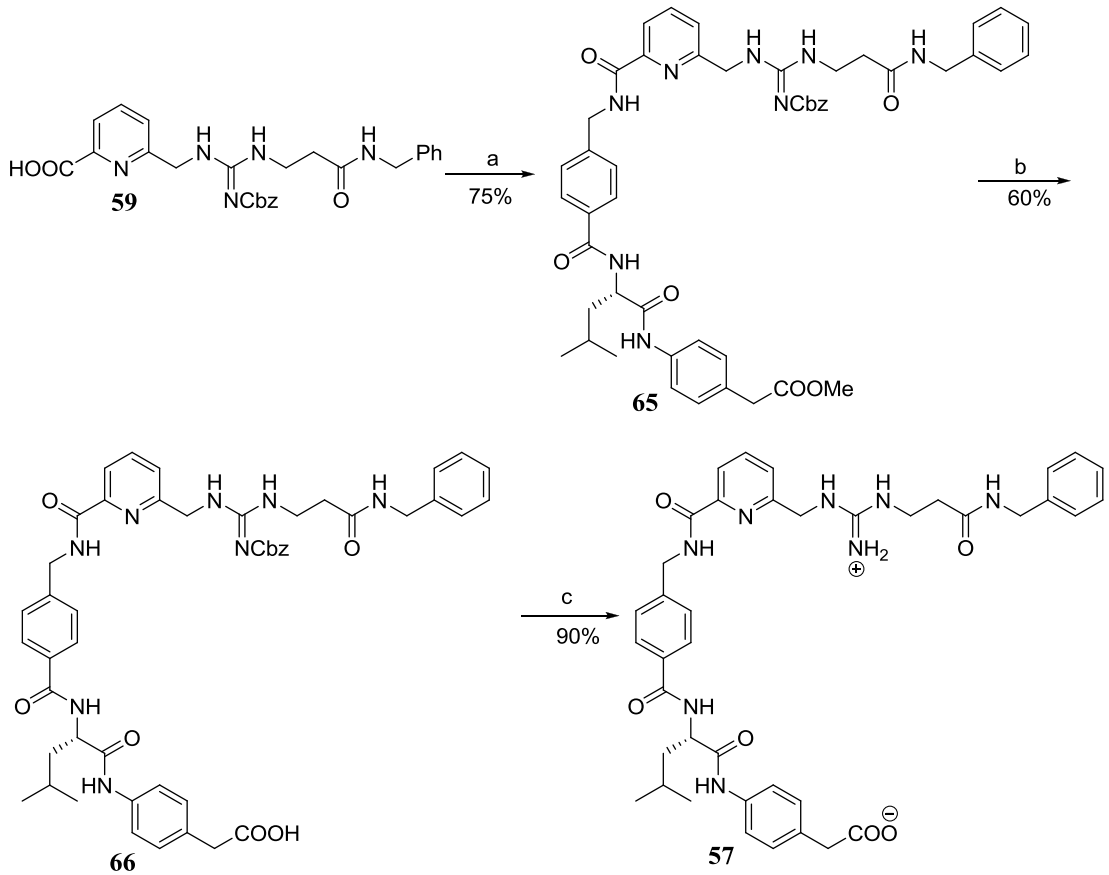


**Scheme 12**. Reagents and conditions: a) **64**, EDC.HCl, DIPEA, HOBt, DCM, rt. b) $Me_3SiOK$, THF, rt.c) $H_2$, Pd/C, MeOH, rt.

The last part of the synthetic procedure is identical to the synthesis of the previous guanidinium-carboxylates. However, the enhanced polarity of the system necessitates a tedious purification procedure by column chromatography. The final product from hydrogenolysis was further purified by precipitation from methanol using diethyl ether. Characterization of this novel compound was established with spectroscopic techniques, 1 D and 2 D NMR, MS and IR.

## 3.6.1 ITC dilution study of guanidinium carboxylate **57**

Following the successful synthesis of guanidinium carboxylate **57**, extensive ITC dimerisation studies were undertaken in solvent systems containing as much as 50% $H_2O$/DMSO (Table 8). The very poor solubility of the compound has precluded dimerisation studies in a more aqueous environment.

| Solvent | $K_{dim}$ [$M^{-1}$] | $\Delta G_{dim}$ [kJ $mol^{-1}$] | $\Delta H_{dim}$ [kJ $mol^{-1}$] | $T\Delta S_{dim}$ [kJ $mol^{-1}$] |
|---|---|---|---|---|
| DMSO | 4032±1789 | -20.6 | -13.8±0.9 | 6.8 |
| 10% $H_2O$/DMSO | 336±58 | -14.4 | -3.7±0.1 | 10.8 |
| 40% $H_2O$/DMSO | 0 | 0 | 0 | 0 |
| 50% $H_2O$/DMSO | 345±535* | -14.5 | -0.6±0.16 | 13.9 |

*Error is too big to make the dimerisation figure statistically significant.

**Table 8** *Energetics of dimerisations of compound **57** at 298 K in DMSO (3 mM),10% $H_2O$/DMSO (10 mM), 40% $H_2O$/ DMSO (10 mM) and 50% $H_2O$/ DMSO (10 mM)*

Dimer formation was observed for compound **57** in DMSO ($K_{dim}$ = 4032±1789). However, compared with compound **27** ($K_{dim}$ = 11876±1692) the stability of the dimer has decreased. This is the opposite of what we have initially envisaged. This difference, however, was not observed at 10% $H_2O$/DMSO where compound **57** has a $K_{dim}$ = 336±58 and compound **27** has $K_{dim}$ = 533±23 and this might suggest that the effect of the hydrophobic-hydrophobic interaction is stronger in the 10% $H_2O$/DMSO system. Nevertheless, the anticipated increase in dimer stability by introducing extra aromatic stacking and hydrophobic interaction was not achieved in DMSO and 10% $H_2O$/DMSO systems. Two possible reasons can be forwarded for this. One is the possibility of intramolecular interactions in flexible compounds like **57** thereby disrupting the conformational requirement required for effective dimerisation. In addition to or another explanation which might be responsible for the decrease of the $K_{dim}$ in DMSO is the possibility of increased intermolecular motion of the extended dimeric structure.[27] As the complex becomes loose, the enthalpy contribution of each individual interaction becomes less favourable and this might hinder effective enthalpy-entropy compensations required for maintaining the free energy of binding. It has been previously mentioned that rigidity of the monomeric compound is one of

the key structural features needed for effective self-assembly.[92] Schmuck *et al* have observed the deleterious effect of increased flexibility on dimerisation by synthesizing derivatives of the 5-(guanidiniocarbonyl)-1*H*- pyrrole-2-carboxylate (**25**) in which the carboxylate is not directly attached to the guanidiniocarbonyl pyrrole but with a spacer.[105] He noted that as the length of the spacer increases the degree of dimerisation decreases.

The ITC study was pursued in more aqueous environments (40% $H_2O$ and 50% $H_2O$). It was found that in 40% $H_2O$/DMSO there was no dimerisation observed. However, recovery of dimerisation which is entirely entropy driven was observed at 50% $H_2O$/DMSO suggesting the bis-aromatic-aromatic and the hydrophobic Leu-Leu interactions might have started to get stronger and hence stabilize the dimeric structure to a greater extent at 50% $H_2O$/DMSO than they do at lower water concentrations (Fig 40).

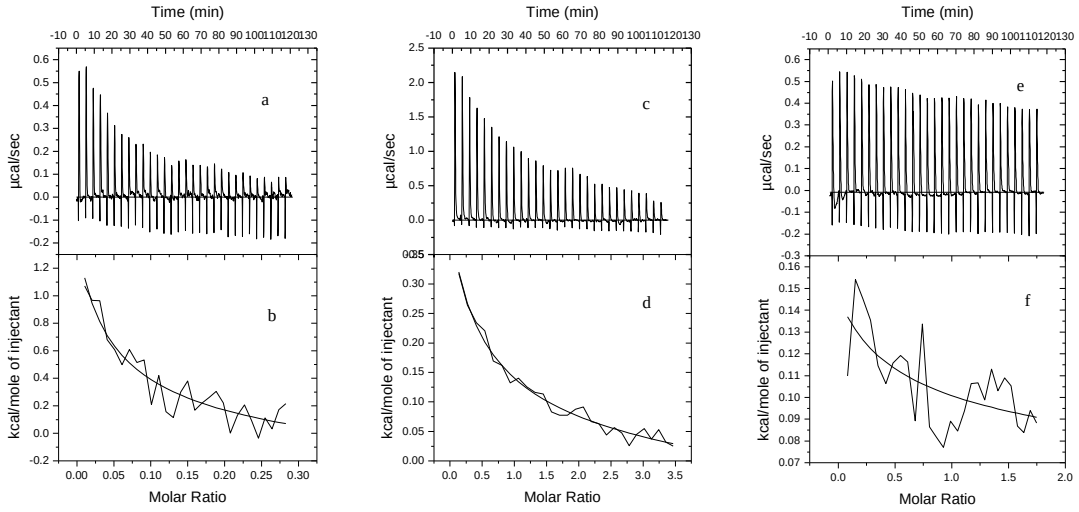


**Fig 40** *Calorimetric data obtained for ITC dilution studies of compound* ***57*** *in DMSO (left), 10% $H_2O$/DMSO (middle) and 50% $H_2O$/DMSO (right) at 298 K. a, c & e) Raw ITC data (29* x *10µL injections); b, d & f) Non-linear curve fitting of the reference corrected data into the dimer dissociation model*

Due to poor solubility of compound **57** in 50% $H_2O$/DMSO, the concentration of the solution prepared was not high enough to observe a good quality curve fitting and the error associated with $K_{dim}$ (345±535) determination was too big to make the dimerisation figure statistically valid. However, it shows that there is some qualitative

evidence of dimerisation occurring at 50% $H_2O$/DMSO. No dimerisation study could be undertaken in more aqueous systems due to solubility problems.

In summary, although the anticipated increase in dimer stability was not obsreved in DMSO and 10% $H_2O$/DMSO, it is encouraging that some evidence of dimerisation was observed in 50% $H_2O$/DMSO.

## 3.7 Synthesis of guanidinium-carboxylate **67**

One of the problems that preclude making ITC studies in more aqueous environments was the poor aqueous solubility of the guanidinium carboxylate compounds synthesized so far. Solubility was found to dramatically decline upon addition of 10% water in DMSO and as a result doing ITC dilution experiments in an increased percentage of water was very difficult.

Compound **67** incorporating a tetraethyleneglycol side chain was designed with the intention of imparting water solubility in order to undertake dimerisation studies in aqueous environments. Compound **67** is the water soluble analogue of compound **27**, which showed excellent dimerisation in DMSO ($K_{dim}$ = 11876 ± 1692$M^{-1}$). ITC study of compound **27** could not be made in an aqueous environment (> 20% $H_2O$/DMSO) with accuracy due to its poor solubility in an aqueous environment. The benzyl propanamide side chain was replaced with a tetraethyleneglycol side chain to enhance aqueous solubility.

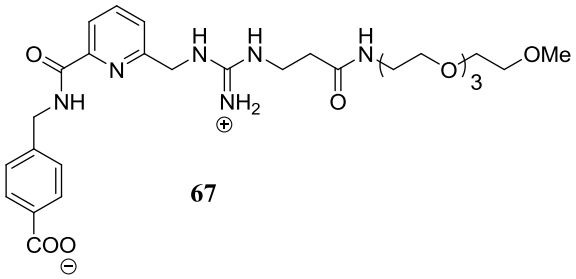


**67**

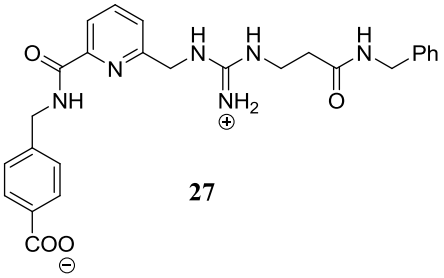


**27**

.

Amine **72** was synthesised (scheme 13) using a standard literature procedure [119] and coupled with the thiocyanate compound **18** to give the Cbz activated thiourea compound which is required to furnish the guanidine functionality into the final product. Tetraethylene glycol was asymmetrically mesylated to give compound **69**

with a 50% yield. A considerable amount of bis-mesylated side product was formed and this has contributed to the very low yield obtained. The purification of this step was found to be very tedious and time consuming due to the very similar polarity of the bis-mesylated side product, the mono-mesylated product and the unreacted tetra-ethylene glycol compounds. The next two steps, azide formation and reduction to amine, were accomplished in reasonably good yields.

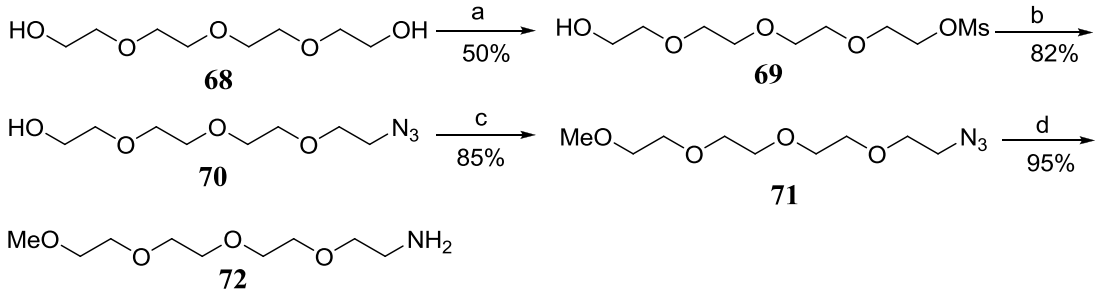


**Scheme 13**. Reagents and conditions: a) MsCl, $Et_3N$, THF, rt. b) $NaN_3$, $CH_3CN$, rt. c) MeI, NaH, DMF, rt. d) 1,3-propane-dithiol, $Et_3N$, MeOH, rt.

Coupling of amine **72** with phthalidoimidyl propanoyl chloride gave compound **73** (Scheme 14). The phthalidoimide group was removed with hydrazine hydrate and the resulting crude amine was coupled with CbzSCN to give the Cbz activated thiourea **74** incorporating a PEG chain.

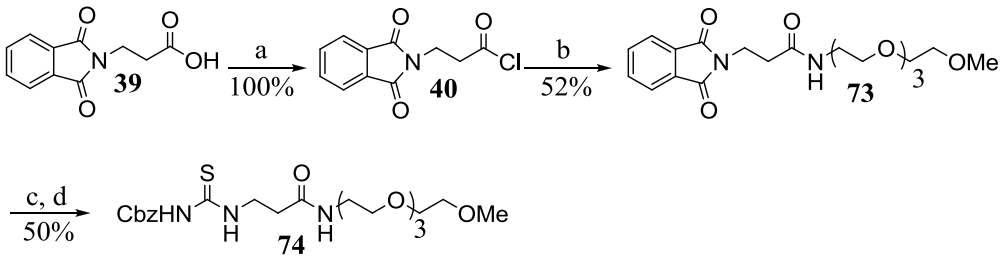


**Scheme 14**. Reagents and conditions: a) $SOCl_2$, Reflux. b) **72**, $Et_3N$, DCM, rt. c) 4 $H_2O$. $N_2H_4$ , EtOH, Reflux. d) CbzNCS, DCM, 0 $^oC$-rt.

The next synthesis procedure shows transformations leading to the target compound **67**. Similar strategies were used as before (Scheme 4) but employed the benzyl ester instead of the methyl ester of the 4-methylamino benzoic acid for the synthesis of compound **75**. This synthetic modification was vital as the final two steps of benzyl ester hydrolysis and Cbz deprotection could be undertaken simultaneously by hydrogenolysis. The penultimate methyl ester hydrolysis procedure in the previous

synthetic strategies was problematic as it involved a tedious and time consuming purification process and usually a very low yield was obtained. The final Cbz deprotected and benzyl ester hydrolysed product was purified by precipitation from methanol using diethyl ether.

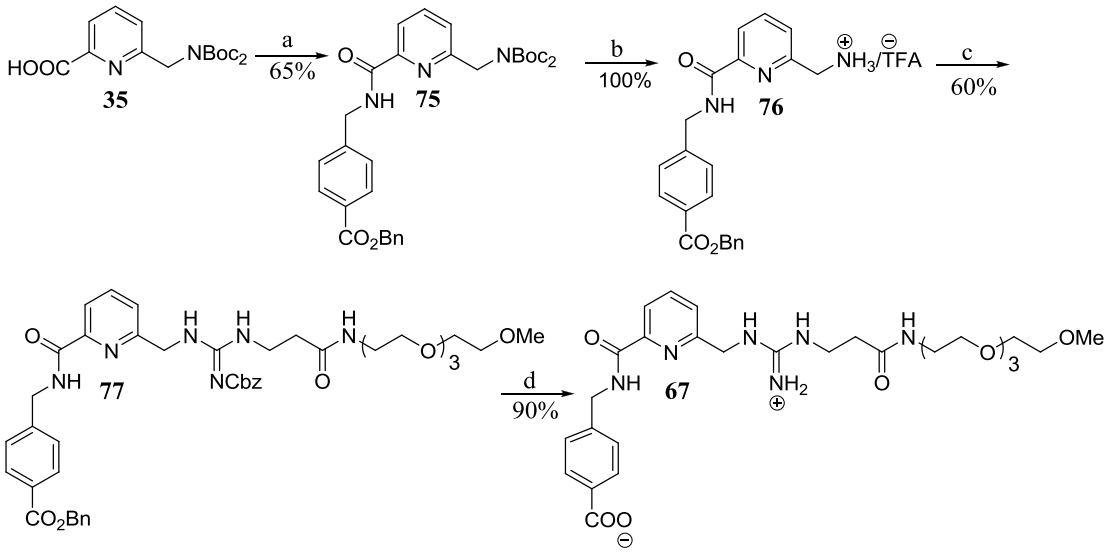


**Scheme 15**. Reagents and conditions: a) 4-Aminomethylbenzoic acid benzyl ester, EDC.HCl, HoBt, DIPEA, DCM, rt. b) 20% TFA/DCM, rt. c) **74**, EDC.HCl, $Et_3N$, DCM, 0 $^oC$ - rt. d) $H_2$, Pd/C, MeOH, rt.

## 3.7.1 Isothermal calorimetric dilution study of **67**

The objective of imparting aqeous solubility was successfully achieved and dimerisation studies could be undertaken even in essentially aqueous environments (DMSO, 10% $H_2O$/DMSO, 20% $H_2O$/DMSO, 50% $H_2O$/DMSO and $H_2O$) (Fig 41).

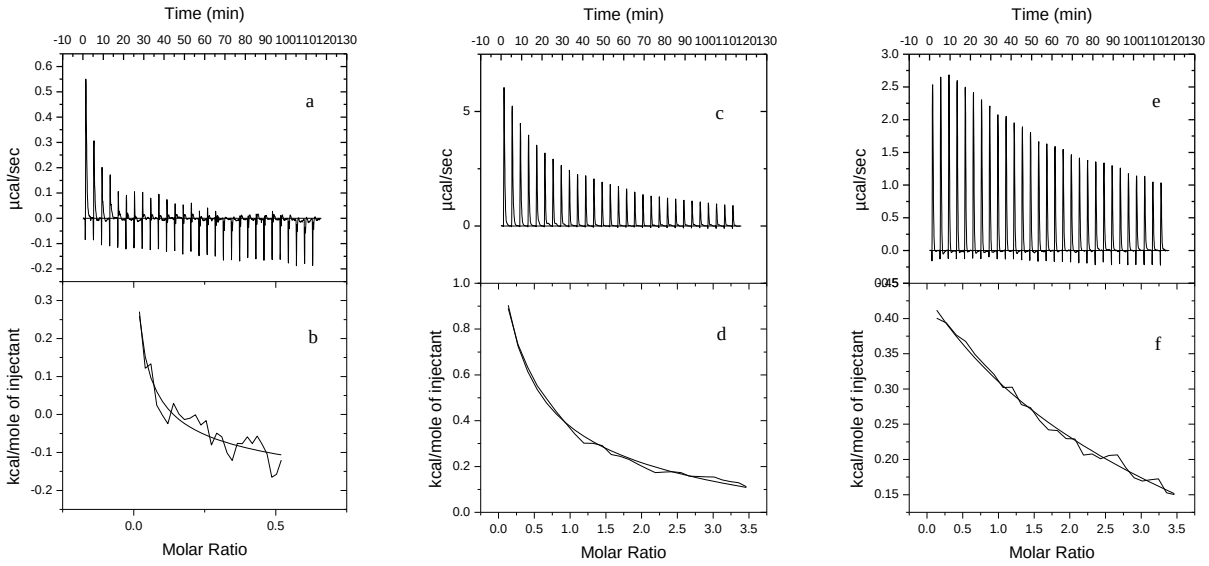


**Fig 41** *Calorimetric data obtained for ITC dilution studies of* ***67*** *in DMSO (left), 10% $H_2O$/DMSO (middle) and 20% $H_2O$/DMSO (right) at 298 K. a, c & e) Raw ITC data (29* x *10µL injections); b ,d & f) Non-linear curve fitting of the reference corrected data into the dimer dissociation model*

The full thermodynamic profile of the dimerisation study result of compound **67** is summarized in table **9**.

| Solvent | $K_{dim}$ [$M^{-1}$] | $\Delta G_{dim}$ [kJ $mol^{-1}$] | $\Delta H_{dim}$ [kJ $mol^{-1}$] | $T\Delta S_{dim}$ [kJ $mol^{-1}$] |
|---|---|---|---|---|
| DMSO | 7692±1124 | -22.2 | -4.7±1.6 | 17.5 |
| 10% $H_2O$/DMSO | 495±44 | -15.4 | -9.8±0.2 | 5.6 |
| 20% $H_2O$/DMSO | 57±9 | -10.0 | -4.6±0.2 | 5.4 |
| 50% $H_2O$/DMSO | 0 | 0 | 0 | 0 |
| $H_2O$ | 0 | 0 | 0 | 0 |

**Table 9** *Energetics of dimerisations of compound* ***67*** *at 298 K in DMSO (3 mM),10% $H_2O$/DMSO (20 mM), 20% $H_2O$/ DMSO (20 mM), 50% $H_2O$/DMSO (20 mM) and $H_2O$ (20 mM)*

Stable dimeric complexes of compound **67** were observed in DMSO, 10% $H_2O$/DMSO and 20% $H_2O$/DMSO (Fig **39**). In DMSO, the dimer stability of compound **67** ($K_{dim(67)}$ = 7692 ±1124) was slightly lower than that of compound **27**

($K_{dim(2)}$ =11876±1692 $M^{-1}$. It is believed that the aromatic-aromatic stacking interaction may still contribute to the dimer stability of compound **67**.[120] There are favourable enthalpy and entropy contributions for the dimerisation of both compounds though the enthalpic contribution is relatively greater in compound **27** ($\Delta G_{dim}$ = -23.2 kJ $mol^{-1}$, $\Delta H_{dim}$ = -10±0.4 kJ $mol^{-1}$ and $T\Delta S_{dim}$ = 13.2 kJ $mol^{-1}$), whereas the dimerisation of compound **67** is driven more by entropy ($\Delta G_{dim}$ = -22.2 kJ $mol^{-1}$, $\Delta H_{dim}$ = -4.7±1.6 kJ $mol^{-1}$ and $T\Delta S_{dim}$ = 17.5 kJ $mol^{-1}$). The slight decrease of the dimer stability associated with compound **67** might be attributed to the loss of some favourable intermolecular bonding that can potentially be mediated through the benzyl propanamide side chain as was observed in compound **27**. The crystal structure for **27** indicates that the dimeric form of the compound involves a complimentary head-to-tail guanidinium-carboxylate interaction with one of the carboxylate oxygens intermolecularly bonded to the amide hydrogen of the propanamide side chain through a bridging water molecule (Fig 42).[113] This also explains the greater enthalpic stabilisation of dimer **27** compared to dimer **67** which might lack this interaction. We could not explain the observation of the higher entropic contribution in the dimerisation of compound **67** in comparison with compound **27** and could not make any correlation between the introduction of the PEG chain and the increase in entropy.

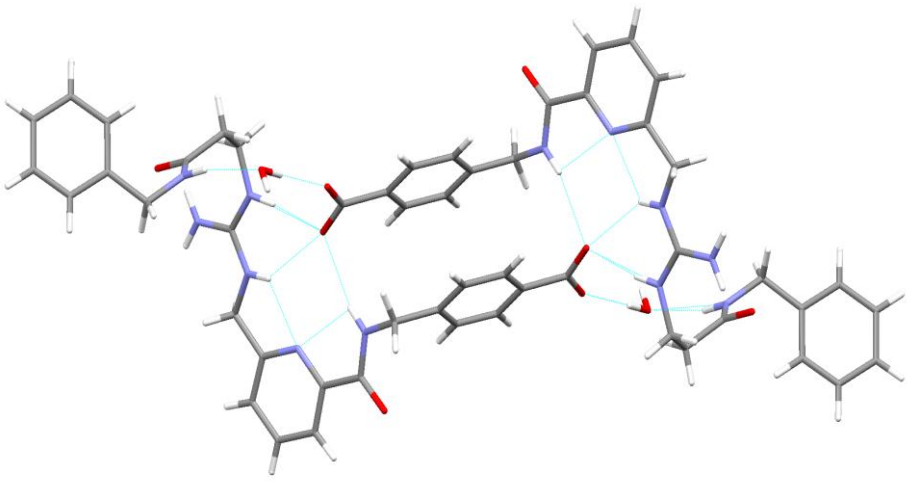

**Fig 42** *X-ray structure of compound 27*

Comparison of the thermodynamic parameters associated with dimerisation of compound **67** ($K_{dim(67)}$ = 495±44) with compound **27** ($K_{dim(2)}$= 532±23$M^{-1}$) in 10% $H_2O$/DMSO shows that introducing the tetraethylene glycol side chain has not resulted in any significant decrease of dimer stability. Hence, the objective of enhancing solubility while maintaining dimerisation intact has been attained in 10%

$H_2O$/DMSO. No dimerisation studies were undertaken on compound **27** in more aqueous medium due to its poor solubility and hence we could not compare its dimerisation profile with that of compound **67** in solvent systems containing more than 10% $H_2O$ in DMSO. A very dramatic fall of dimerisation ($K_{dim}$ = 57±9) was observed for compound **67** when the percentage of water was increased to 20%, and there was no dimerization observed at 50% and 100% $H_2O$/DMSO systems which suggests that the hydrogen bond forming entities are completely solvated by water leading to complete disruption of the dimeric system. It was anticipated that the π- π stacking interaction could get stronger in more aqueous media and might impart some stability to the dimeric system. The possibility of conformational changes of compound **67** in more aqueous systems should also not be ruled out. This might not allow efficient π- π stacking interaction and may lead to dimer disruption.[118]

## 3.8 Synthesis of guanidinium-carboxylate **78**

After the aqueous solubility of compound **67** was successfully enhanced without compromising its dimer stability, we decided to synthesise an analogue of compound **57** in which the benzyl propanamide side chain is replaced with a tetraethylene glycol moiety. At 50% $H_2O$/DMSO system, the ITC dilution data of compound **57** showed some dimerisation but the error associated with the curve fitting of the dilution data into the dimer dissociation model was too big to make a valid quantitative estimation of the thermodynamic parameters. The very poor solubility of compound **57** in 50% $H_2O$/DMSO makes it difficult to prepare a homogenous solution of compound **57**.

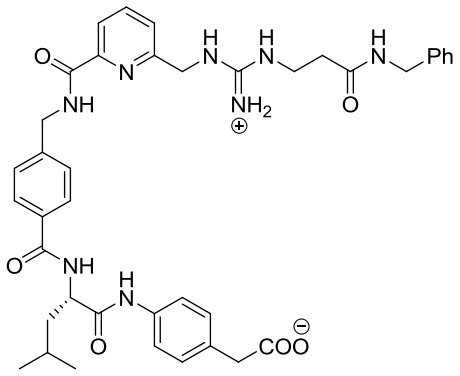

**57**

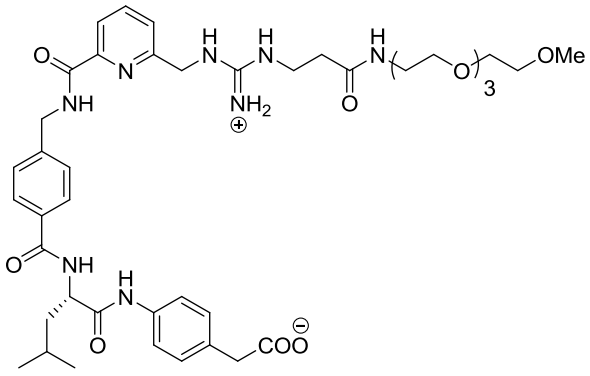

**78**

As with guanidinium-carboxylate **57**, it was hypothesised that **78** might use bis aromatic-aromatic interaction and hydrophobic Leu-Leu interaction in the dimeric

structure. It was envisaged that these combined non-covalent interactions in the system might get stronger in more aqueous environments and lead to a stable dimeric structure.Undertaking dimerisation studies of compound **78** in more aqueous systems will help to probe this hypothesis (Fig 43).

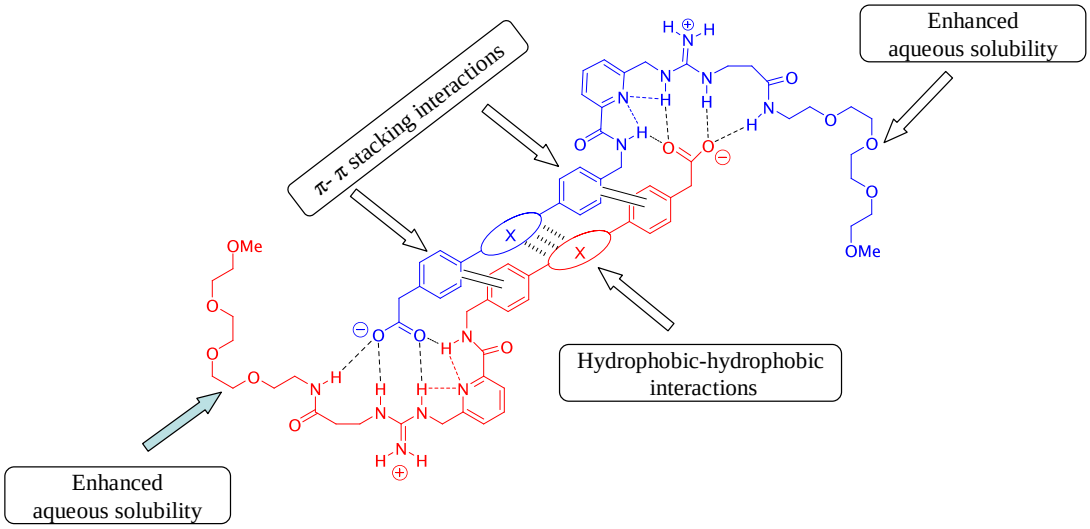


**Fig 43** *Expected dimerisation mode of compound* **78** *where X represents a Leu amino acid residue*

Scheme 16 shows the synthetic route undertaken to access guanidinium-carboxylate **78**. Unlike the case with the syntheses of the previous compounds, a relatively poor yield was observed in the coupling reaction of the Boc deprotected form of compound **72** with the thiourea compound **74**. The possible complexation of the PEG chain with ammonium ion might be responsible for the low yield.The ester hydrolysis reaction with compound **80** went to completion fairly quickly. However, repeated purification *via* column chromatography was needed to get acid **81**. The purification process at this stage must be done with maximum care as the final guanidinium–carboxylate compounds are too polar to be purified by normal phase column chromatography.

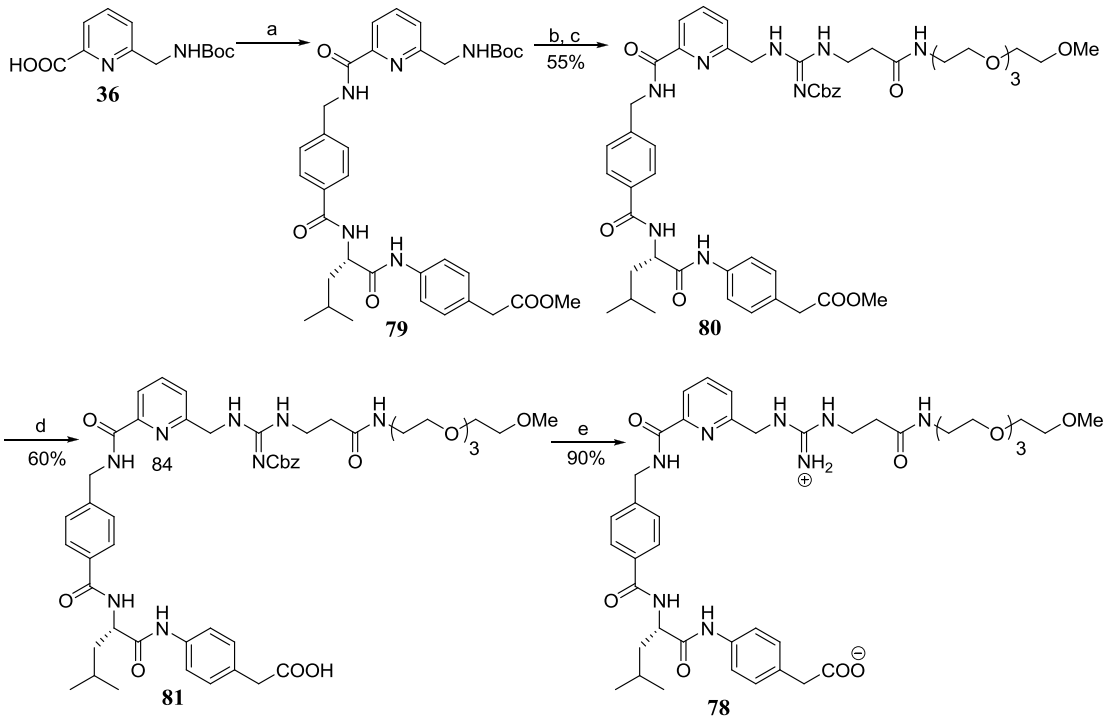


**Scheme 16**. Reagents and conditions: a) **64**, EDC.HCl, HOBt, DIPEA, DCM, rt. b) 20% TFA/DCM, rt. c) **74**, EDC. HCl, $Et_3N$, DCM, rt. d) TMSOK, THF, 40 $^oC$. e) $H_2$, Pd/C, MeOH, rt.

## 3.8.1 Isothermal calorimetric dilution study of **78**

The aqueous solubility of compound **78** was greatly improved compared to compound **53** and this has enabled dimerisation studies in 50% $H_2O$/DMSO and $H_2O$ (Fig 44).

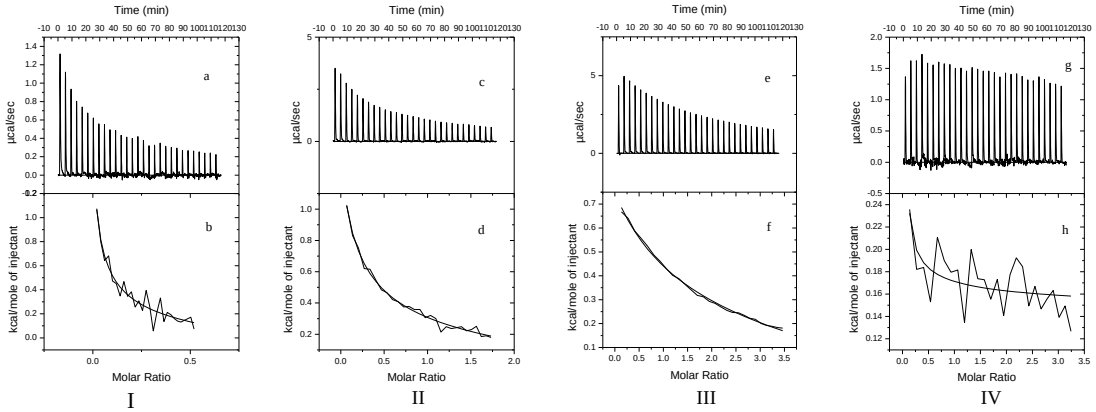


**Fig 44** *Calorimetric data obtained for ITC dilution studies of **78** in DMSO (I), 5% $H_2O$/DMSO (II), 10% $H_2O$/DMSO (III) & 50% $H_2O$/DMSO (IV) at 298 K. a, c, e & g) Raw ITC data (29 x 10 µL injections); b, d, f & g) Non-linear curve fitting of the reference corrected data into the dimer dissociation model*

It was observed that compound **78** exhibits a similar trend of dimerisation to compound **53**. There is a positive contribution of both the enthalpy and entropy parameters to the free energy of dimerisations in DMSO and 10% $H_2O$/DMSO. Upon increasing the aqueous level to 40%, the dimeric structure was completely disrupted and no measurable enthalpy change was detected. The full thermodynamic profile of the dimerisation process is given below.

| Solvent | $K_{dim}$ [$M^{-1}$] | $\Delta G_{dim}$ [kJ $mol^{-1}$] | $\Delta H_{dim}$ [kJ $mol^{-1}$] | $T\Delta S_{dim}$[kJ $mol^{-1}$] |
|---|---|---|---|---|
| DMSO | 5076±876 | -21.4 | -11.7±0.4 | 9.4 |
| 5% $H_2O$/DMSO | 862±104 | -16.8 | -10.3±0.2 | 6.5 |
| 10% $H_2O$/DMSO | 156±6 | -12.5 | -7.4±0.1 | 5.1 |
| 40% $H_2O$/DMSO | 0 | 0 | 0 | 0 |
| 50% $H_2O$/DMSO * | - | - | - | - |
| $H_2O$ | 0 | 0 | 0 | 0 |

*Error is too big to make the dimerisation figure statistically significant.

**Table 10** *Energetics of dimerisations of compound **85** at 298 K in DMSO (3 mM), 5% $H_2O$/DMSO (10 mM), 10% $H_2O$/ DMSO (20 mM), 40% $H_2O$/DMSO (20 mM), 50% $H_2O$/ DMSO (20 mM) and $H_2O$ (20 mM).*

The dilution study of **78** at 50% $H_2O$/DMSO shows similar results with compound **53**. Still the error associated with the curve fitting of the dilution data is too big to make the estimation of the thermodynamic parameters valid. It might be the case that the $K_{dim}$ is too small to be measured accurately. It has been reported in the literature that complexes should be reasonably stable for accurate and reliable ITC measurements.[27] The complete lack of dimerisation at 40% $H_2O$/DMSO and the recovery of some of the dimerisation energy at 50% $H_2O$/DMSO, has suggested that the hydrophobic and the aromatic-aromatic stacking interactions might get stronger in more aqueous environments. With this in mind, a dilution study was undertaken in pure water. But no noticeable dimerisation was observed. It is believed that the bis aromatic-aromatic stacking and the Leu-Leu hydrophobic interactions are still not strong enough to maintain the dimeric structure in aqueous environments. But again we should not rule out the possibility of conformational alterations which preclude the formation of the dimeric structure in more aqeous systems. Another possible disadvantage of extending

the side chain is that it may impart lack of rigidity to the system which will be obstructive in maintaining the supramolecular dimeric structure.

### 3.8.2 NMR dilution experiment of guanidinium carboxylate **78**

Considering the solubility of the compound and the sensitivity of the NMR instrument, 5% $H_2O$/DMSO was found to be the best solvent system to carry out the NMR dilution experiment (Table 11).

| Solvent | 90%[D*] | 80%[D*] | 30%[D*] | 20%[D*] | 10%[D*] |
|---|---|---|---|---|---|
| DMSO | 14.8 | 3.3 | 0.1 | 0.05 | 0.02 |
| 5%$H_2O$ | 83.5 | 19.5 | 0.6 | 0.3 | 0.12 |
| 10%$H_2O$ | 551 | 123 | 3.8 | 1.9 | 0.76 |

[D*]= the concentration of the compound in mg/mL which contains the specified percentage of dimer in DMSO, 5% $H_2O$/DMSO and 10% $H_2O$/DMSO solution, calculated based on the $K_{dim}$ obtained from ITC dilution studies. [D*] = ([dimer]/$K_{dim}$* [monomer]$^2$)*MW.

**Table 11** *Concentration needed to prepare solutions of compounds **78** in DMSO, 5% $H_2O$/DMSO & 10% $H_2O$/DMSO that is supposed to contain 90%, 85%, 50%, 20% and 15% dimeric structure*

A preliminary NMR dilution study performed using concentrated (30 mM) and dilute (0.15 mM) solutions of compound **78** in 5% $H_2O$/DMSO shows that there is indeed a concentration dependent chemical shift change of the NH protons. One of the NH protons (signal B) was shifted downfield from 9.36 ppm to 9.66 ppm and one of the other guanidine protons (signal C) has downshifted from 7.66 ppm and overlaps with the aromatic proton signals (7.83 ppm-8.01 ppm) upon changing the concentration from 0.15 mM to 30 mM.

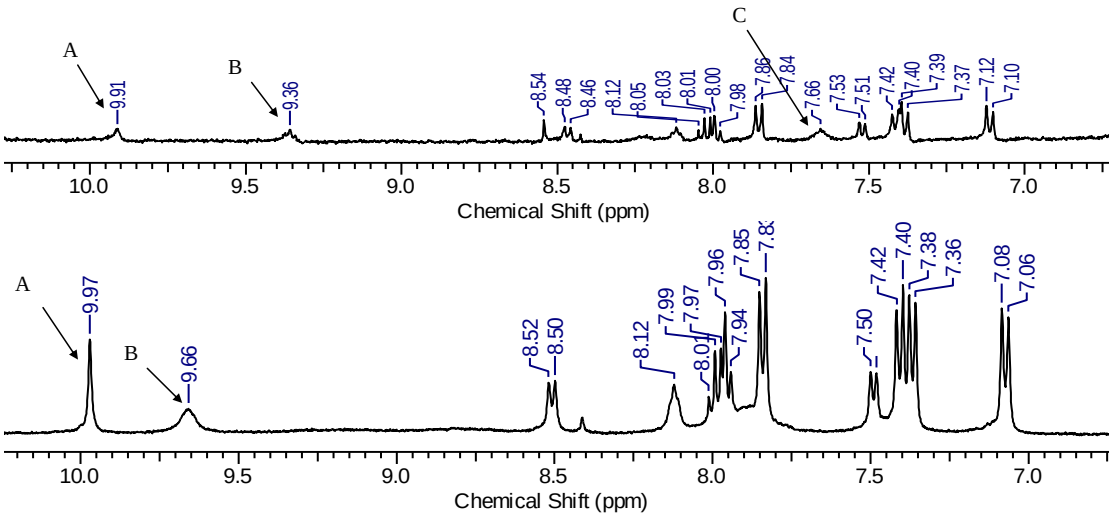


**Fig 45** *Part of $^{1}H$ NMR spectrum of compound **78** in 5% $H_2O$/DMSO at 298 K. The spectrum above belongs to the dilute solution (0.15 mM) and below to the concentrated solution (30 mM) of compound **78***

The full NMR dilution experiment of compound **78** shows the successive concentration dependent chemical shift changes of the NH proton signals noted above (Fig 45). The observed chemical shift of two of the NH proton signals has been successively downshifted as the concentration increases and this is believed to be the direct result of H-bond mediated complexation of the guanidine protons with carboxylate in the dimeric structure.

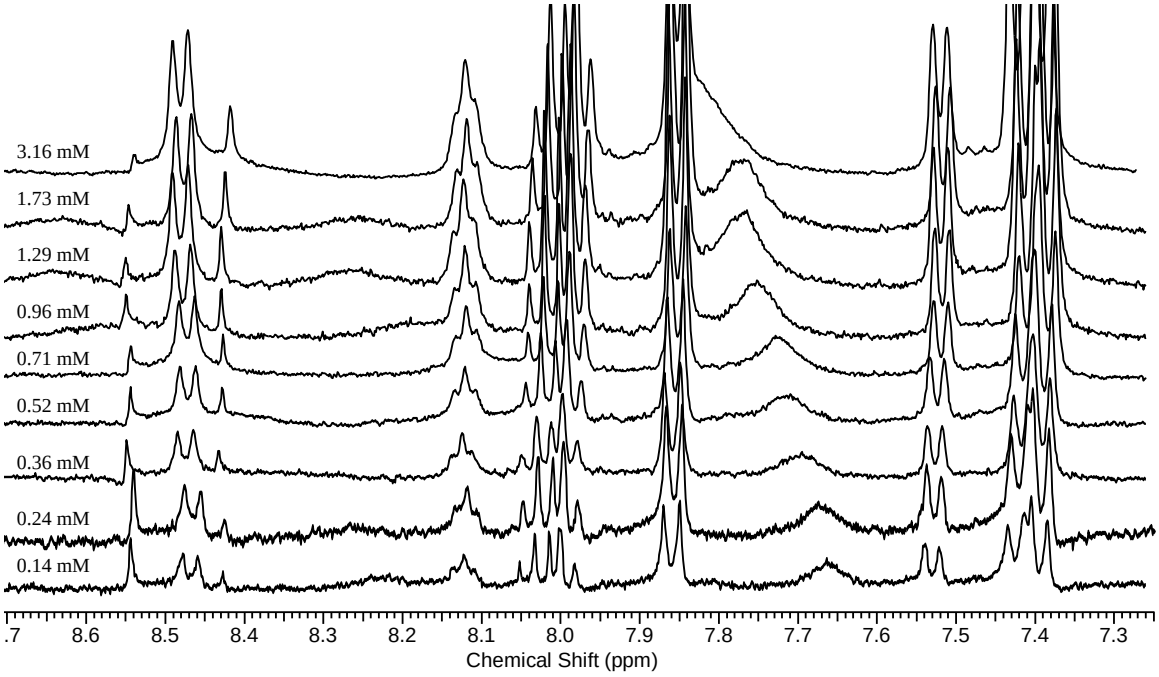


**Fig 46** *Parts of the $^{1}H$ NMR spectra (400 MHz, 298K) of **78** in 5% $H_2O$/DMSO showing the dimerisation induced shift changes*

Processing the NMR dilution data sets of the two guanidine proton signals using a 1:1 dimer dissociation model has given dimerisation constants of 305 $M^{-1}$ and 255 $M^{-1}$. This is consistent with the ITC measured dimerisation constant of **78** (860 $M^{1}$).

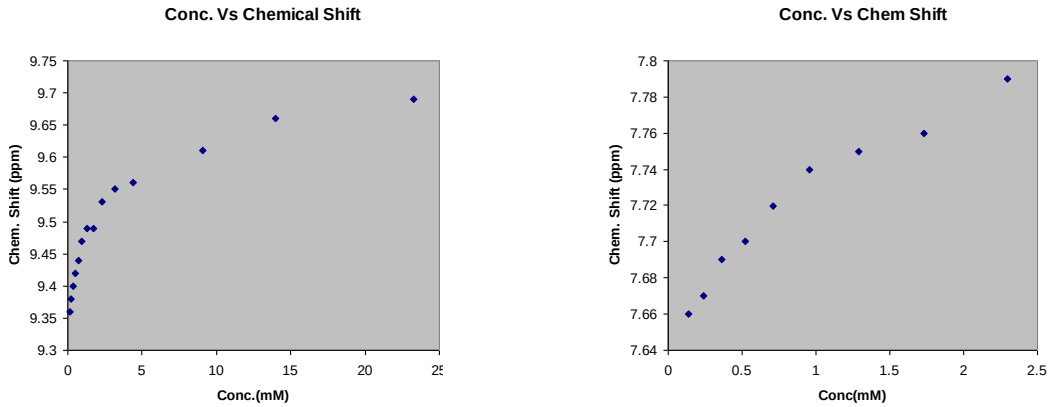


**Fig 47** *Plots of concentration versus observed chemical shift of the two NH protons*

The NMR dilution experiment has again substantiated not only the ITC study result but also the proposed mode of dimerisation orchestrated through complimentary

intermolecular head-to-tail complexation between the guanidinum protons and the carboxylates.

## 3.9 Synthesis of guanidinium-carboxylate **82**

After the dimerisation results of the previous compounds have been properly assessed, it was envisaged that strengthening the hydrophobic interaction might be an option to access the dimeric system in a more aqueous environment.The bis-aromatic compound **85** was not found to preserve the dimeric system in more aqueous systems (>50% $H_2O$). It might be the case that the bis aromatic-aromatic interactions were not strong enough to maintain the dimeric architecture. Hydrophobic-hydrophobic interactions might be more important than the aromatic-aromatic stacking interaction in a more aqueous solvent system and this can be illustrated by comparing the dimerisation properties of compounds **27** and **53**. It was found that compound **27** showed excellent dimerisation in DMSO ($K_{dim}$ = 11876±1692 $M^{-1}$) and 10% $H_2O$/DMSO ($K_{dim}$ = 532±23 $M^{-1}$). However, its water soluble analogue, compound **67**, showed no sign of dimerisation in a 50% $H_2O$/DMSO and in $H_2O$ which suggested that the aromatic-aromatic interaction was not strong enough to maintain the dimeric structure in these solvent systems. In contrast to this, compound **53** in which the aromatic side chain is replaced with Leu showed a $K_{dim}$ of 55±8 $M^{-1}$ in 50% $H_2O$/DMSO. However in DMSO the dimerisation of **53** ($K_{dim}$ = 952±64) is much less than that of compound **27**. Assuming both compounds have the same dimer architecture in solution, it can be sugested that aromatic-aromatic interactions are superior to the hydrophobic Leu-Leu interaction in DMSO and the reverse in 50% $H_2O$/DMSO system. However, making this assumption might be erroneous as the two compounds might have different conformations in different solvent systems and hence dissimilar modes of dimerisation. But the positive contribution of the Leu-Leu interaction in aqueous dimer stability is well noticed and with this in mind it was predicted that guanidinium-carboxylates that contain more hydrophobic moeties might lead to stable dimeric structures in aqueous environments. Compound **83** that features a Leu-Leu dipepetide side chain has previously been synthesised in a parallel PhD project within our research group [88] and its dimerisation property was investigated.

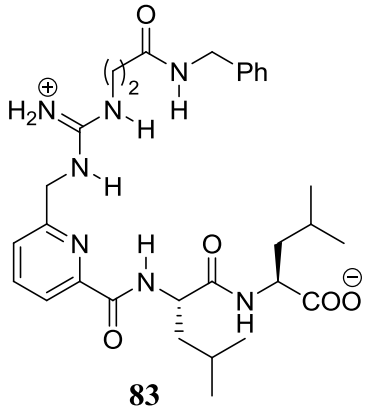

**83**

Guanidinium carboxylate **83** showed an entropy driven dimerisation ($K_{dim}$ = 50±10 $M^{-1}$, $\Delta G_{dim}$ = -9.7 kJmol$^{-1}$, $\Delta H_{dim}$ = -1.0±0.1 kJmol$^{-1}$ , $T\Delta S_{dim}$ = 8.7 kJmol$^{-1}$ ) in 50% $H_2O$/DMSO. It was expected that there would be improved dimerisation of compound **83** in aqueous environments by virtue of its enhanced hydrophobic side chain. However, it was found that the dimer from guanidinium carboxylate **83** in 50% $H_2O$/DMSO is slightly less stable than that from guanidinium carboxylate **53** ($K_{dim}$ = 55±8 $M^{-1}$, $\Delta G_{dim}$ = -9.9 kJmol$^{-1}$, $\Delta H_{dim}$ = -1.5±0.1 kJmol$^{-1}$ , $T\Delta S_{dim}$ = 8.4 kJmol$^{-1}$ ). Steric and electronic factors might have undermined the dimerisation process. Having this in mind, we designed compound **82** that contains a peptide sidearm with a Gly-Ile-Ala amino acid sequence. While the Gly residue merely functions as a linker, it is believed that the Ile-Ala sequence might furnish the desired degree of hydrophobic interaction by minimizing the possible steric and electronic clash in the dimeric structure. This peptide sequence has also some biological significance as it is frequently observed in some enzyme molecules and β-amyloid proteins. Sequence of aminoacids at the N-terminus of the virus protein responsible for foot-and-mouth disease has been found to contain the Gly-Ile sequence very frequently. [121]

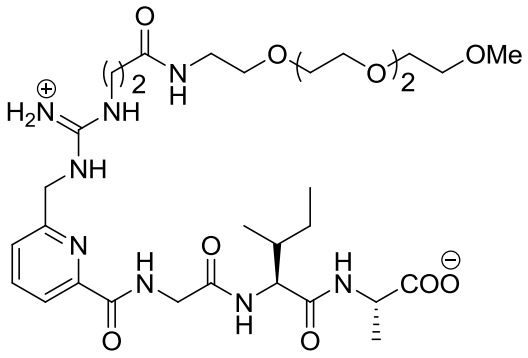

**82**

Results and Discussion

Standard peptide coupling procedures were used for the synthesis of the peptide (Gly-Ile-Ala) side arm that is to be tethered into the pyridine scaffold (Scheme 17).

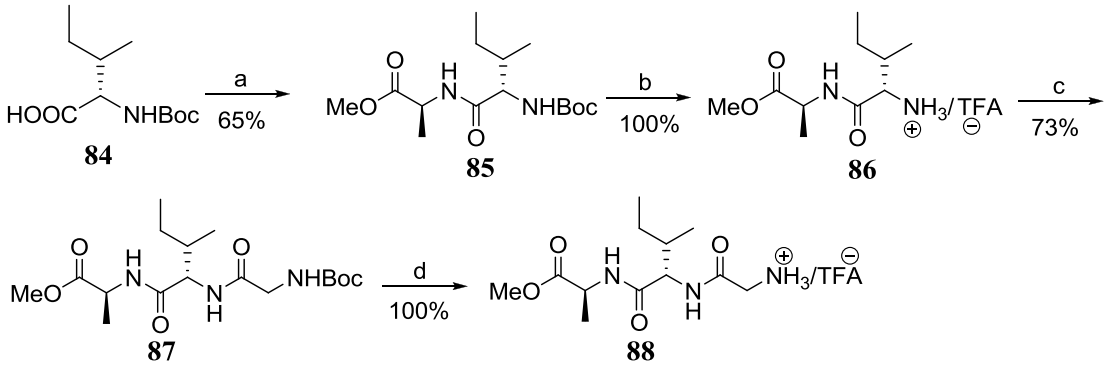

**Scheme 17**. Reagents and conditions: a) H-Ala-OMe, DCC, HOBt, DIPEA, DMF, rt. b) 20%TFA/DCM, rt. c) Boc-Gly-OH, DCC, HOBt, DIPEA, DM, rt. d) 20%TFA/DCM, rt.

The peptide arm **88** was then coupled to the pyridine scaffold to give compound **89** (Scheme 18). Boc deprotection of compound **89** was followed by a coupling reaction with the thiourea compound **74** to give **91**. Ester hydrolysis and Cbz deprotection procedures then afforded guanidinium carboxylate **82**.

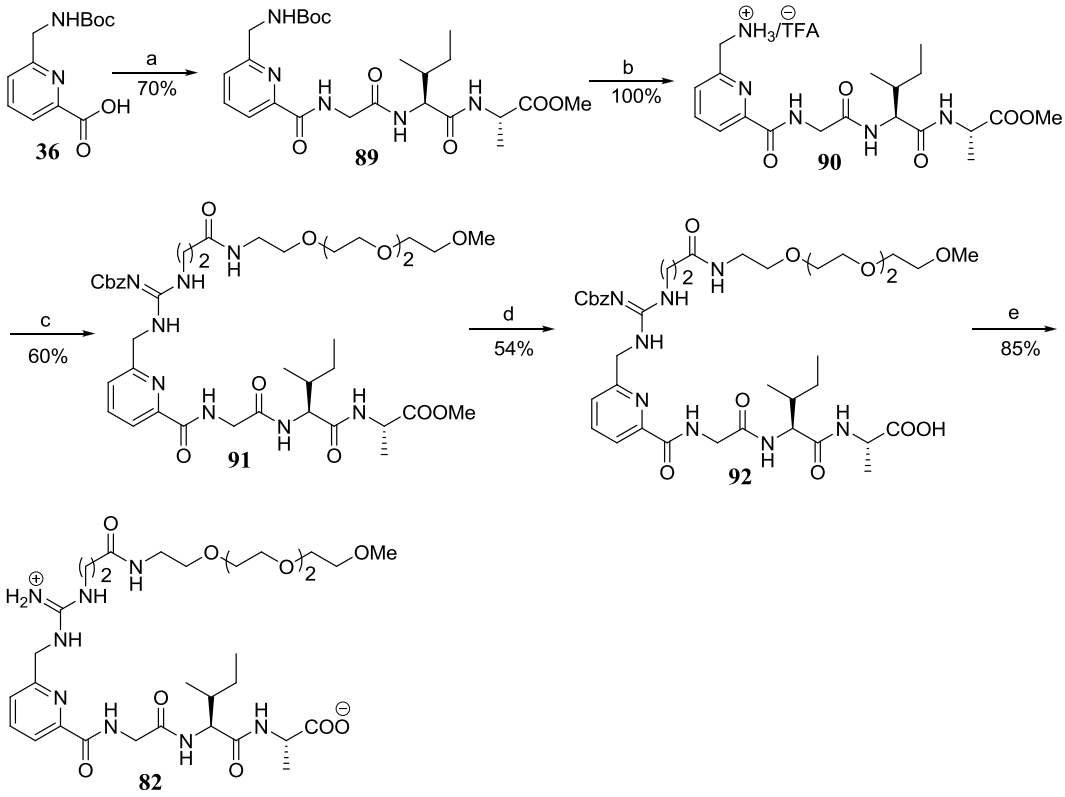

**Scheme 18**. Conditions and reagents: a) **88**, EDC.HCl, HOBt, DIPEA, DCM, rt. b) 20% TFA/DCM, rt. c) 74, EDC.HCl, $Et_3N$,DCM, rt. d) $Me_3SiOK$, THF, rt. e) $H_2$, Pd/C, MeOH, rt.

## 3.9.1 Isothermal calorimetric dilution study of **82**

ITC dilution studies were commenced in DMSO and then continued with 10% $H_2O$/DMSO and 50% $H_2O$/DMSO systems. In all the three systems endothermic heat pulses which characterize the dissociation of a dimer into a monomer were observed (Fig 48).

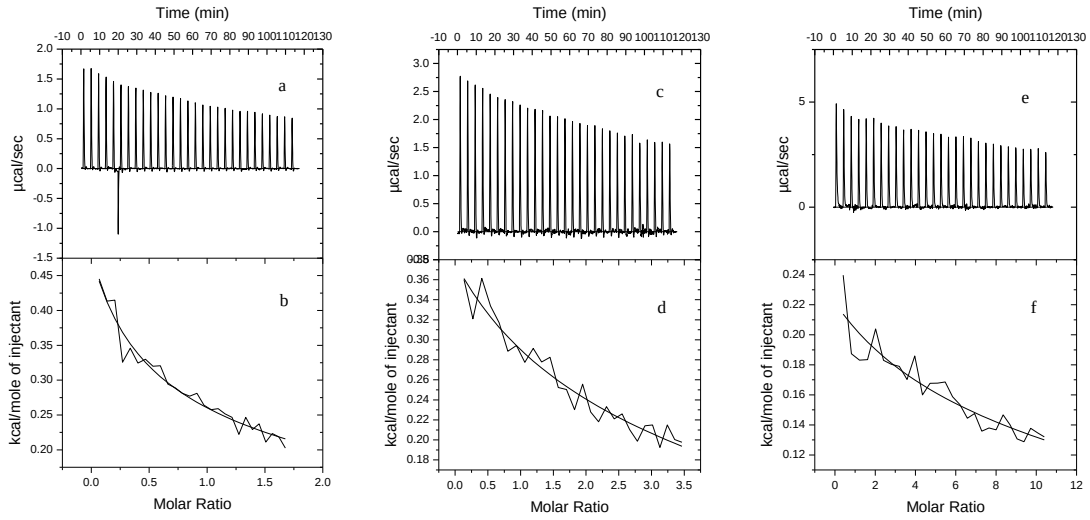


**Fig 48** *Calorimetric data obtained for ITC dilution studies of **82** in DMSO (left), 10% $H_2O$/DMSO (middle) and 50% $H_2O$/DMSO (right) at 298K. a, c & e) Raw ITC data (29 x 10µL injections); b, d & f) Non-linear curve fitting of the reference corrected data into the dimer dissociation model*

Compared with guanidinium carboxylate **78** ($K_{dim}$ = 5076±876 $M^{-1}$, $\Delta H_{dim}$ = -11.7±0.4 kJ $mol^{-1}$, $T\Delta S_{dim}$ = 9.4 kJ $mol^{-1}$ ) and **57** ($K_{dim}$ = 4032±1789, $\Delta H_{dim}$ = -13.8±0.9 kJ $mol^{-1}$, $T\Delta S_{dim}$ = 6.8 kJ $mol^{-1}$ ) in DMSO, the dimer stability of **82** (Table 12) is weaker in DMSO and this again highlights the strong possibility of the bis-aromatic-aromatic stacking interaction in the dimeric structure of compounds **57** and **78** in DMSO. Upon dissection of the free energy of dimerisation into its enthalpic and entropic components, it was noted that the dimerisation of **82** in DMSO is more entropy driven compared to **78** and **57**. The same is true in 10% $H_2O$/DMSO system.

| Solvent | $K_{dim}$ [$M^{-1}$] | $\Delta G_{dim}$ [kJ $mol^{-1}$] | $\Delta H_{dim}$ [kJ $mol^{-1}$] | $T\Delta S_{dim}$ [kJ $mol^{-1}$] |
|---|---|---|---|---|
| DMSO | 357±98 | -14.6 | -3.1±0.2 | 11.5 |
| 10% $H_2O$/DMSO | 78±30 | -10.8 | -2.7±0.3 | 8.1 |
| 50% $H_2O$/DMSO | 24±15 | -7.8 | -1.4±0.2 | 6.5 |

**Table 12** *Energetics of dimerisations of compound* ***82*** *at 298 K in DMSO, 10% $H_2O$/ DMSO and 50% $H_2O$/ DMSO*

The ITC study at 50% $H_2O$/DMSO has resulted in a statistically valid dimerisation figure ($K_{dim}$ = 24±15 $M^{-1}$). This might be an indication that the possible hydrophobic-hydrophobic interaction in 50% $H_2O$/DMSO in dimer **82** is more significant than the possible bis-aromatic-aromatic interactions in dimers **78** and **57**. But it has to be noted again that we are not making quantitative comparison of these interactions as they might have different conformations and modes of dimerisation in different solvent systems.[122]

## 3.9.2 NMR dilution experiment of compound **82**

ITC dilution study showed that guanidinium carboxylate **82** exhibits a moderate degree of dimerisation in DMSO. This was followed as before by an NMR dilution study. Apart from verifying the ITC result, the NMR study will give evidence regarding the structure of the dimer in solution thereby enabling us to infer the mode of dimerisation.

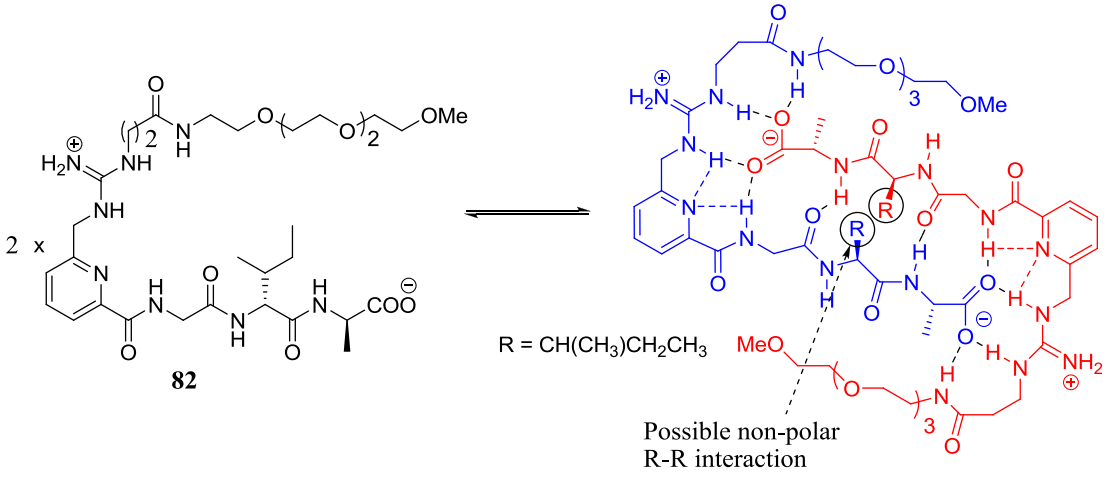


**Fig 49** *Proposed dimerisation of compound* ***82***

Results and Discussion

The suitability of compound **82** for an NMR dilution experiment in DMSO was initially confirmed. It was calculated, based on ITC results, that 24 mg/mL solution of compound **95** will have a 4:1 dimer:monomer ratio and a 0.4 mg/mL solution of compound **95** will have a 1:4 dimer:monomer ratio. By using these concentrations, a preliminary NMR dilution experiment was performed and showed the concentration dependent change of the chemical shift of some of the NH protons (Fig 50).

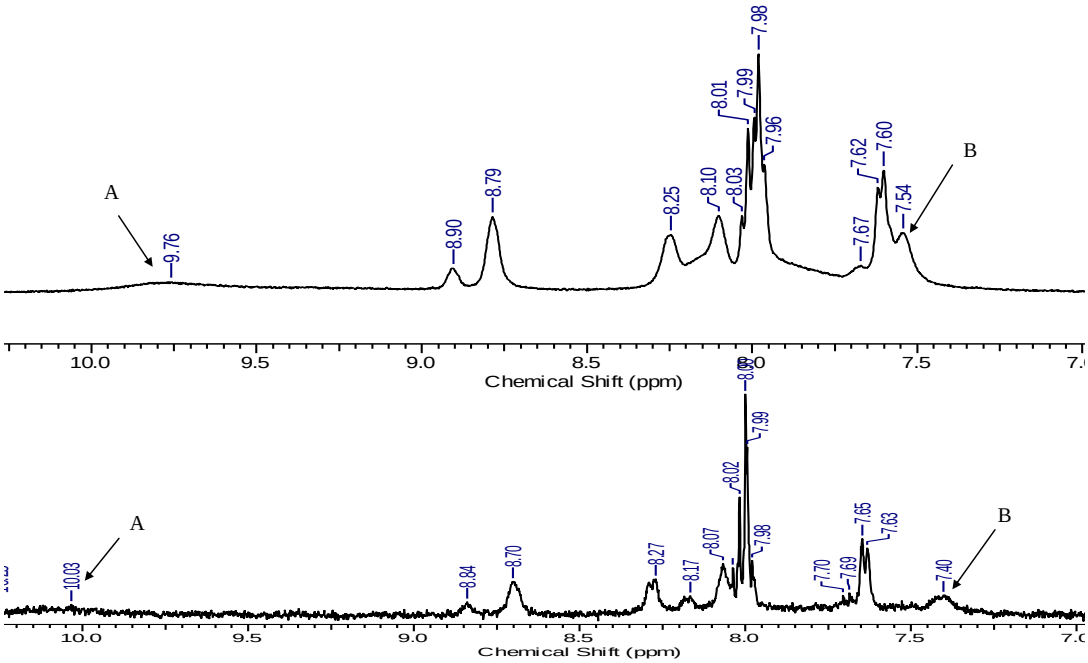


**Fig 50** *Part of $^{1}$H NMR spectrum of compound **82** in DMSO at 298 K. The spectrum above belongs to the concentrated solution (20 mM) and below to the dilute solution (0.3 mM) of compound **82***

The most noticeable change was observed for the guanidinium NH proton **B** which was shifted downfield from 7.40 ppm to 7.54 ppm. Whereas an NH proton at **A** has been shifted upfield from 10.03 ppm to 9.76 ppm. This might be attributed to some intramolecular H-bonding involvement of the NH proton at **A**.

A full NMR dilution experiment of compound **82** was carried out in which 10 dilutions (33.8 mM - 0.35 mM) were prepared from a stock solution of 23.6 mg/mL and their $^{1}$H NMR spectra were recorded (Fig 51).

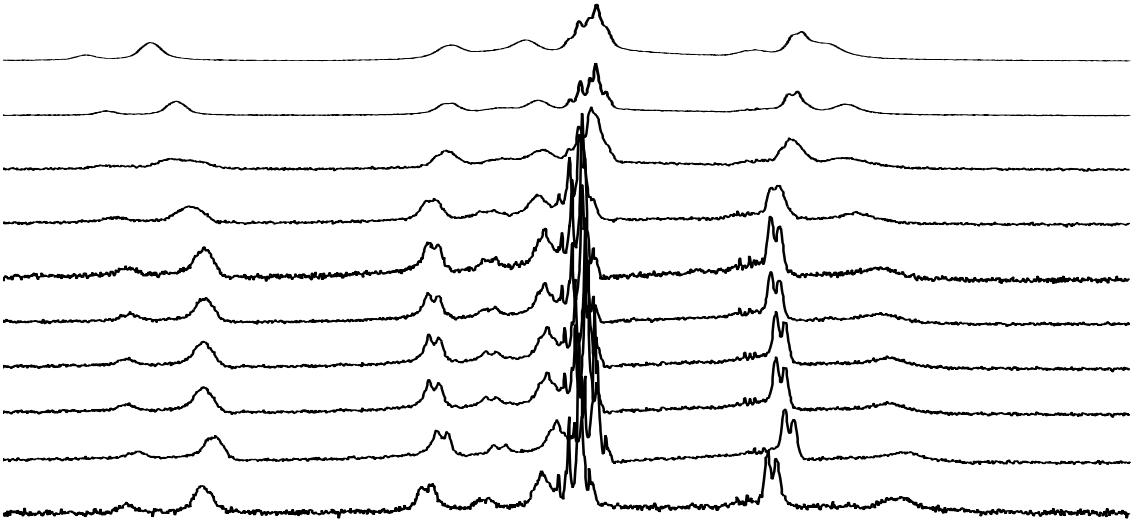

**Fig 51** *Parts of the $^{1}H$ NMR spectra (400 MHz, 298 K) of **82** in DMSO showing the dimerisation induced chemical shift changes (Concentrations from bottom to top: 0.35, 0.71, 1.2, 1.9, 0.72, 2.93, 4.47, 6.90, 11.0, 18.40 mM)*

A plot of the observed chemical shift versus concentration of the two NH protons gave isothermic binding curves. The curves indicate a concentration dependent change of the two NH signals which is attributed to the shift in the monomer-dimer equilibrium.

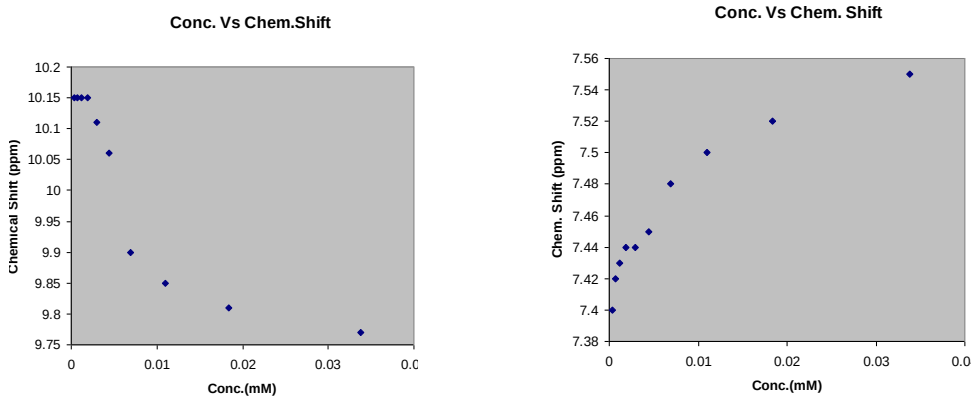


**Fig 52** *Plots of concentration versus chemical shift of the two NH protons*

The NMR dilution data were analysed to give a dimerisation constant of 287 $M^{-1}$. This is again in very good agreement with the ITC determined value 355 $M^{-1}$. The reliability of the ITC dilution technique in determining the thermodynamic parameters

associated with a self assembly process is once again well established using NMR dilution experiment.

## 3.10 Synthesis of guanidinium carboxylates **93** and **94**

It is clear from the dimerisation study results of the compounds synthesised so far that hydrophobic interactions can be very important in accessing the dimeric structures in more aqueous systems. In compounds **78** and **82**, some degree of dimerisation was observed at 50% $H_2O$/DMSO. It was considered that strengthening the hydrophobic interaction by introducing more non-polar amino acid residues into the system might enhance the stability of the dimeric structure in an aqueous environment. One possibility would be to make analogues of compound **85** in which the single Leu amino acid residue sandwiched between the bis-aromatic systems is replaced with a di-peptide and a tri-peptide moiety. With this in mind compounds **93** and **94** were designed and their syntheses were undertaken.

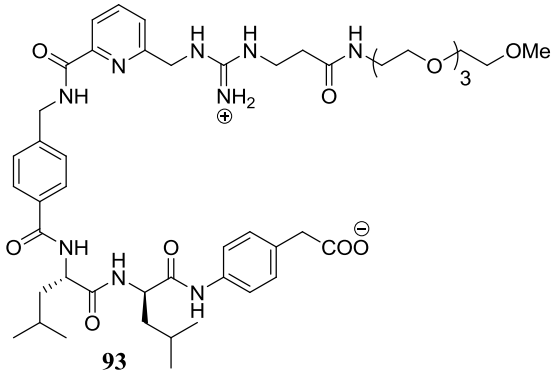

**93**

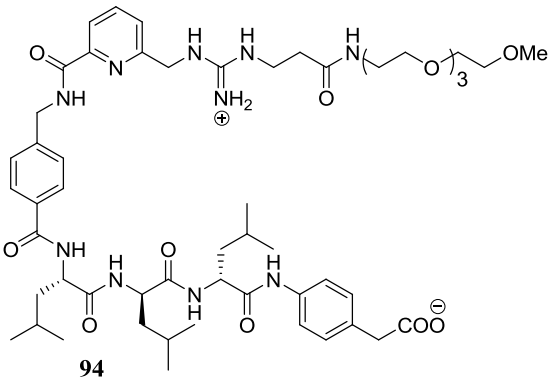

**94**

Scheme 19 depicts the synthesis of the peptide side chain **101** which contains a Leu-Leu dipeptide flanked between the two aromatic moieties. Standard peptide coupling procedures were used in this synthetic procedure.

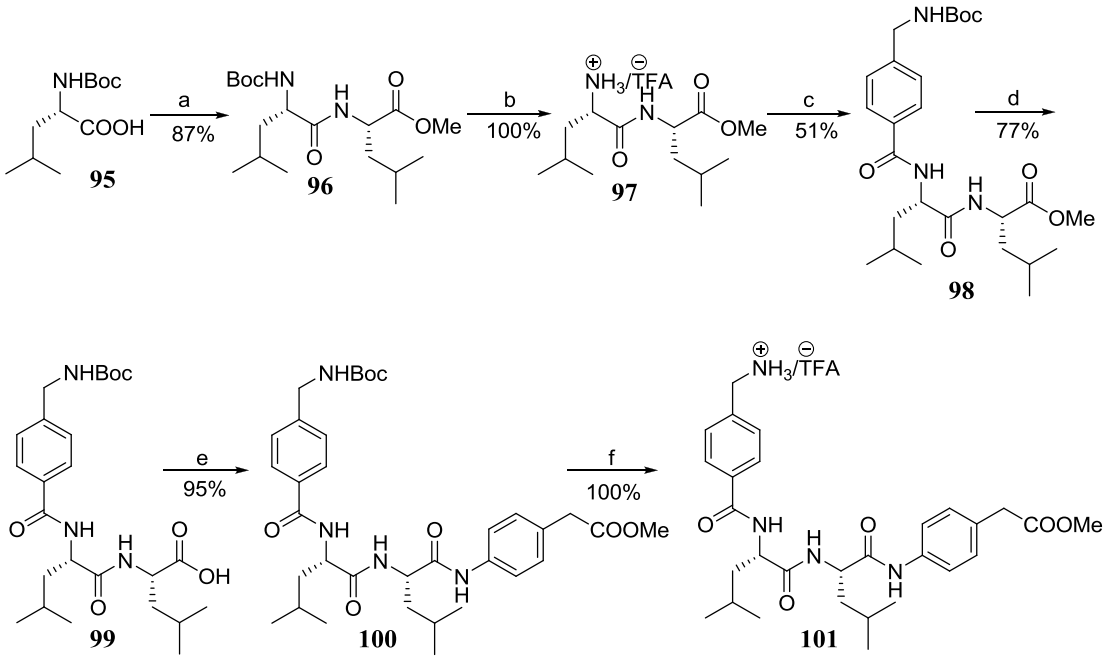


**Scheme 19**. Conditions and reagents: a) L-Leu-methyl ester, DCC, HOBt, DIPEA, DMF, rt. b) 20% TFA/DCM, rt. c) DCC, HOBt, DIPEA, DMF, rt. d) $Me_3SiOK$, THF, rt. e) *p*-amino benzylcarboxylic acid methyl ester, EDC.HCl, HOBt, DIPEA, DCM/DMF, rt. f) 20% TFA/DCM, rt.

The peptide side chain was then coupled with the pyridine scaffold **36** to give compound **102** (Scheme 20). Boc deprotection of compound **102** followed by coupling with thiourea **74** gave the precursor compound **104**. Ester hydrolysis of **104** and hydrogenolysis gave guanidinium-carboxylate **93**.

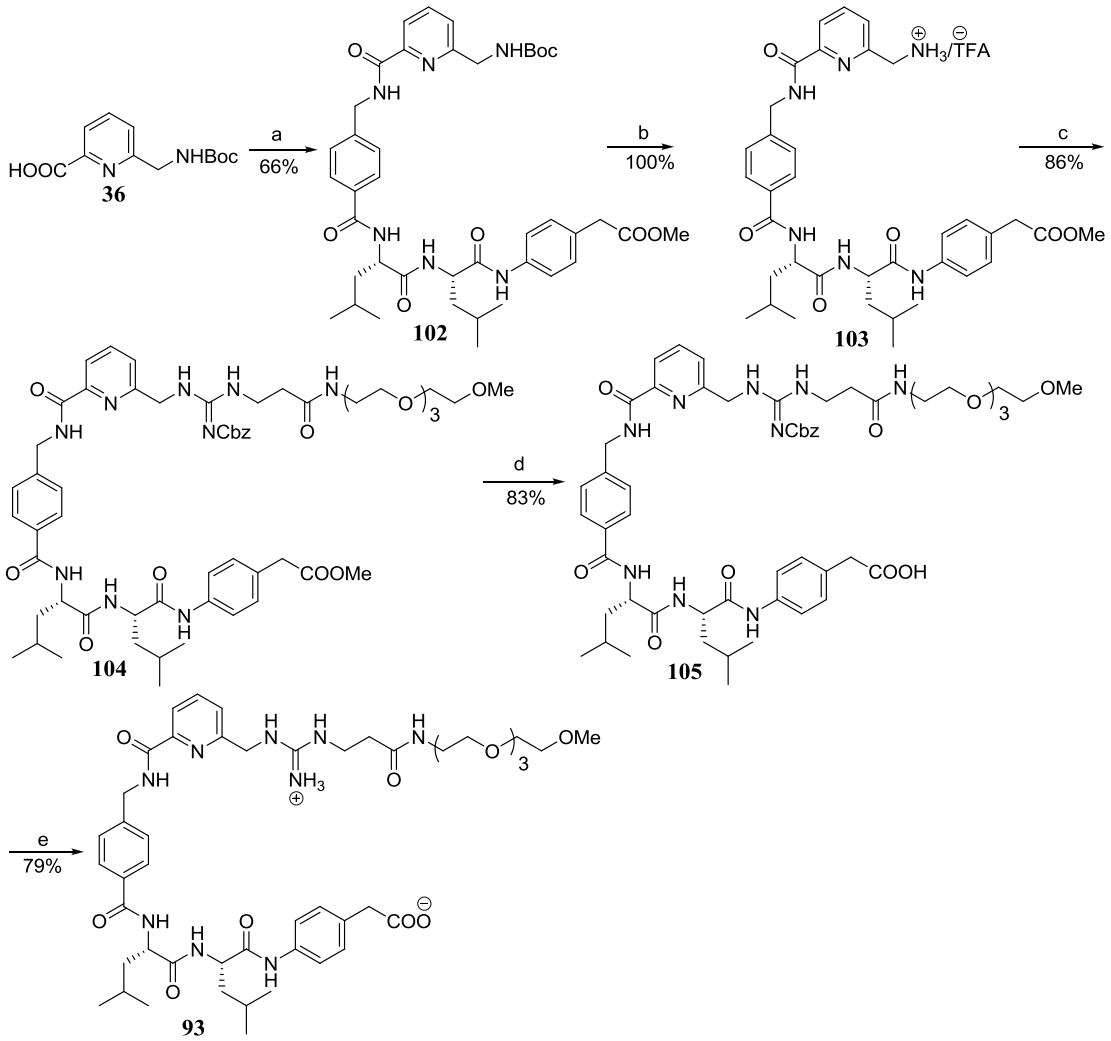


**Scheme 20.** Conditions and reagents: a) **101**, EDC.HCl, HOBt, DIPEA, DMF/DCM, rt. b) 20% TFA/DCM, rt. c) **74**, EDC.HCl, $Et_3N$, DCM, rt. d) $Me_3SiOK$, THF, rt.e) $H_2$, Pd/C, MeOH, rt.

The same strategy was used to synthesise compound **94** with the tripeptide Leu-Leu-Leu sandwiched between the two aromatic moieties, which was expected to further enhance the possible hydrophobic-hydrophobic interaction in the dimeric structure. Scheme **21** shows the synthesis of this peptide side arm.

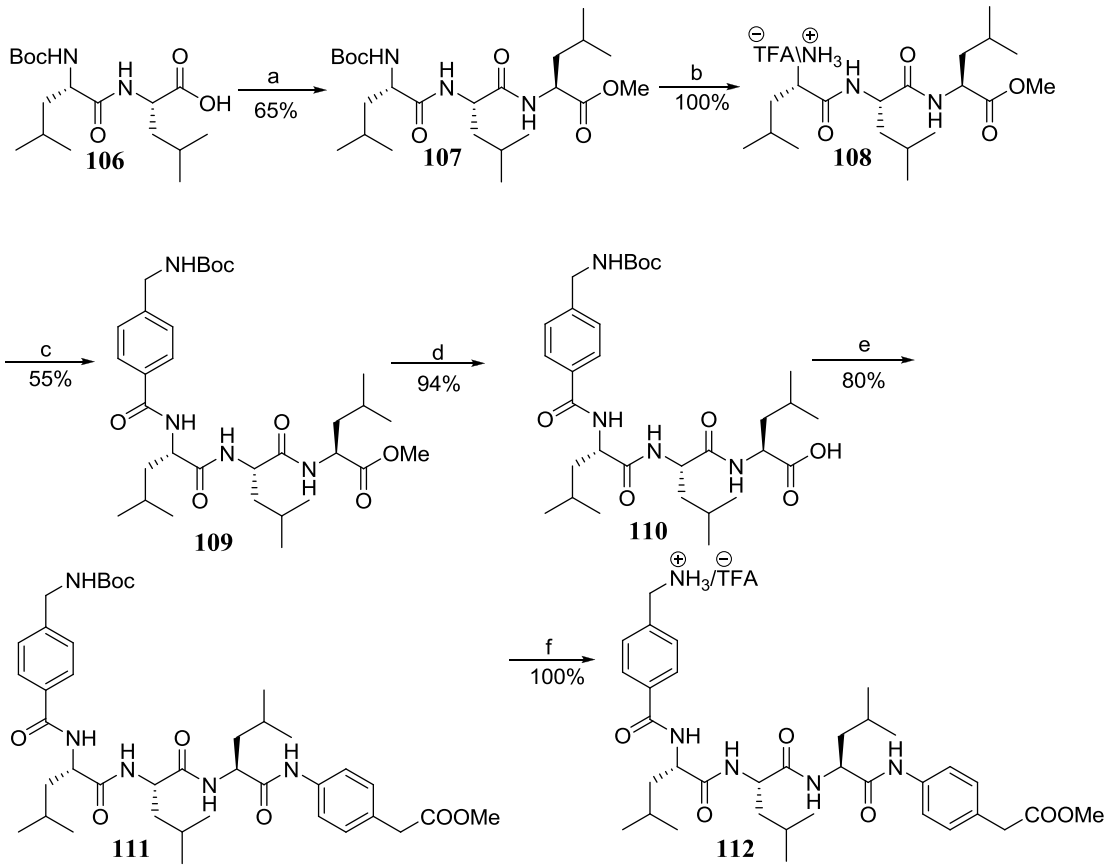


**Scheme 21**. Conditions and reagents: a) Leu-methyl ester, DCC, HOBt, DIPEA, DMF/DCM, rt. b) 20% TFA/DCM, rt. c) Boc- *p* -methyl aminobenzoic acid, EDC.HCl, HOBt, DIPEA, DMF/DCM, rt. d) $Me_3SiOK$, THF, rt. e) *p*-amino benzylcarboxylic acid methyl ester, EDC.HCl, HOBt, DIPEA, DMF/DCM, rt. f) 20% TFA/DCM, rt.

Transformations undertaken to access the final guanidinium-carboxylate compound **94** are shown in scheme 22. Purification of the final compound was carried out by precipitaion from a methanol solution using diethyl ether.

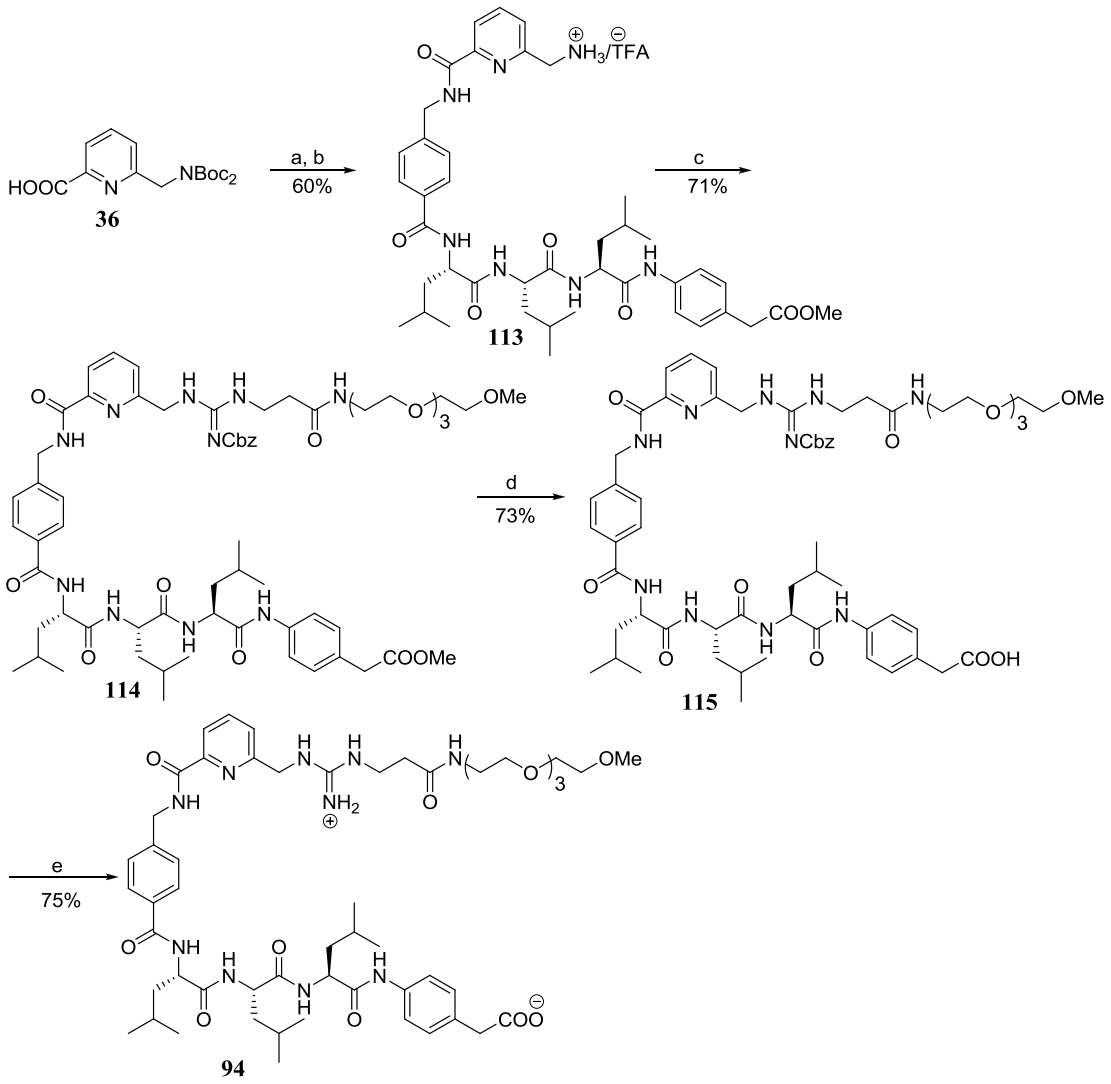


**Scheme 22**. Conditions and reagent: a) **112**, EDC.HCl, HOBt, DIPEA, DCM/DMF, rt. b) 20% TFA/DCM, rt. c) **74**, EDC.HCl, $Et_3N$, DCM, rt. d) $Me_3SiOK$, THF, rt. e) $H_2$, Pd/C, MeOH, rt.

## 3.10.1 Isothermal calorimetric dilution study of **93** and **94**

Though the hydrophobicity of compounds **93** and **94** was greatly enhanced, the aqueous solubility was maintained due to the PEG chain. ITC dilution studies were then undertaken in DMSO, 10% $H_2O$/DMSO, 50% $H_2O$/DMSO, 75% $H_2O$/DMSO and $H_2O$. Unfortunately, neither of the two compounds showed any measurable dimerisation in all of the solvent systems except in 75% $H_2O$/DMSO. Presumably conformational constraints preclude the formation of the anticipated dimeric

architecture in solution and this is most likely due to intramolecular interactions which are expected from very extended and flexible compounds like **93** and **94**. The hydrophobicity was imparted into the compounds at the expense of increasing flexibility.

In 75% $H_2O$/DMSO system some degree of dimerisation was observed for compounds **93** and **94** (Fig 53). The thermodynamic figures associated with the dimerisation of **93** ($K_{dim}$= 27±7 $M^{-1}$, $\Delta G_{dim}$ [kJ $mol^{-1}$] = -8.1, $\Delta H_{dim}$ [kJ $mol^{-1}$]= -4.2±0.4, $T\Delta S_{dim}$ [kJ $mol^{-1}$]= 3.9) suggested that the dimerisation is favourable both enthalpically and entropically. It could not be understood why particularly the 75% $H_2O$/DMSO system is conducive for the dimerisation process. It might be explained in simple terms by saying this solvent system might induce the right degree of hydrophobicity for the dimerisation processs while maintaining some degree of hydrogen bonding. An aqueous content more than 75% $H_2O$ is expected to enhance the hydrophobic effect more, however it might have been disruptive for dimer stability due to the increased degree of solvation of the hydrogen bond forming moieties.

A more rigorous analysis is needed from a physical chemistry point of view as to how this particular solvent system is conducive for the dimerisation process. It has been reported in the literature that water and DMSO form a non-ideal solution. Solvent properties like viscosities, densities, refractive indices, and enthalpies of mixing have found to deviate from ideality for aqueous DMSO solutions and this is attributed to association interactions between the molecules of water and DMSO. The degree of these interactions depends on the water:DMSO ratio in the solution and is found to be at a maximum when the water-DMSO molar ratio is 2:l. [123] In water-DMSO solutions, large amounts of water disrupts DMSO structure while small amounts of DMSO rigidify rather than break the H-bonding network among water molecules. We do not have a clear picture as to what extent the degree of interaction between water and DMSO influences the dimerisation process. It might be erroneous to simply correlate increased water percentage with enhanced solvation of the hydrogen bond forming moieties and hence decreased dimerisation. A specific ratio of water:DMSO solvent mixture might have its own unique property that may affect the dimerisation process

either positively or negatively. In the dimerisation of guanidinium-carboxylate **93** and **94**, the 75% $H_2O$/DMSO solvent mixture might have the proper balance of all the relevant solvent properties permissive for the dimerisation process.

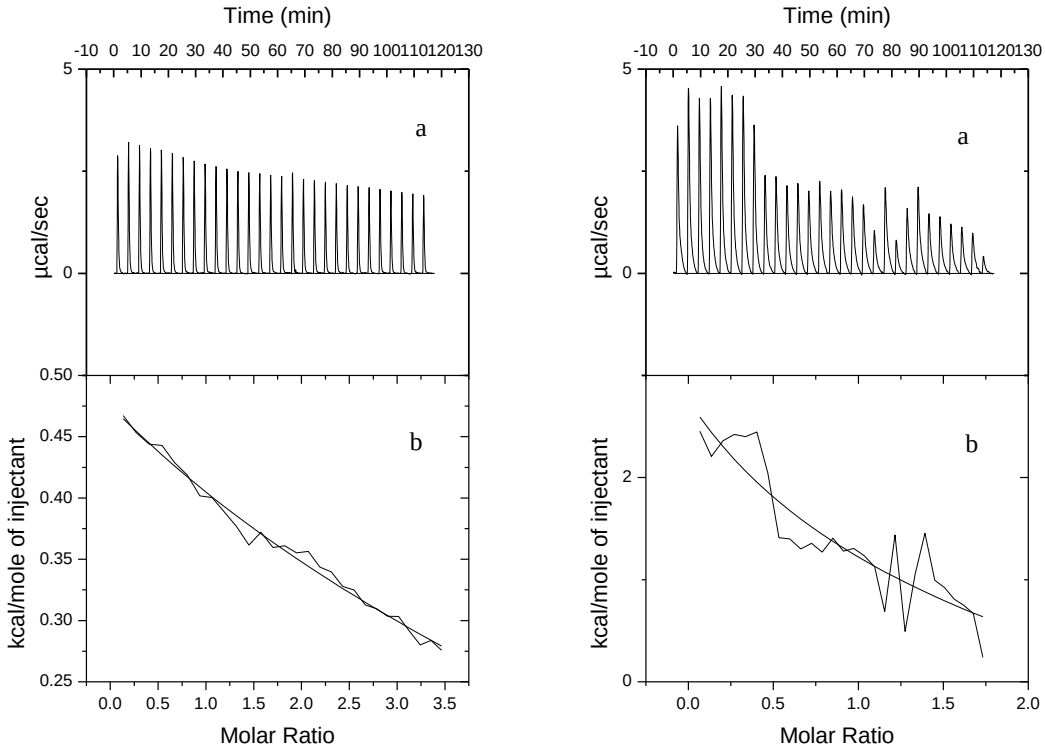


**Fig 53** *Calorimetric data obtained for ITC dilution studies of **93** (left) and **94** (right) in 75% $H_2O$/DMSO at 298K. a) Raw ITC data in 75%$H_2O$/DMSO (29x10µL injections) b) Non-linear curve fitting of the reference corrected data into the dimer dissociation model*

Investigation of the dimerisation of compound **94** in 75% $H_2O$/DMSO has also shown a positive result (Fig 51). The ITC data was fitted to the dimer dissociation model and gave a $K_{dim}$ =127± 100. The thermodynamic data ($\Delta G_{dim}$ [kJ mol$^{-1}$] = -12, $\Delta H_{dim}$ [kJ mol$^{-1}$]= -33±7, $T\Delta S_{dim}$ [kJ mol$^{-1}$]= -21.4) suggested the process is more enthalpy driven. The relatively big error associated with the $K_{dim}$ of **94** makes it difficult to make a comparison with the $K_{dim}$ of compound **93**.

## 3.11 Synthesis of guanidine-carboxylate **116**

One further structural modification which was thought to be worthy of consideration was introduction of a carbonyl functionality on the carbon between the guanidine N and the pyridine ring.

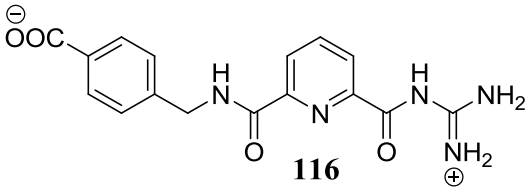

**116**

The acyl pyridoguanidinium derivatives are superior to simple alkyl and benzyl guanidines in their affinity for carboxylate anions and consequently a better stability of the dimeric structures in polar solvent systems.[61] Acyl guanidiniums have pKa values between 7 and 8 as compared to 13 for simple alkylguanidines. This increased acidity should further consolidate the strength of the hydrogen bonded ion pair complexes between the carboxylate and the guanidinium. An aromatic side chain was included in **116** to provide possible π- π interactions in the dimeric systems (Fig 54). The rigidity of the guanidine-carboxylate **116** is also an important criterion for making a dimeric structure in solution. The extreme flexibility associated with the previous systems is thought to be partly responsible for the weak dimerisation observed in more aqueous environments.

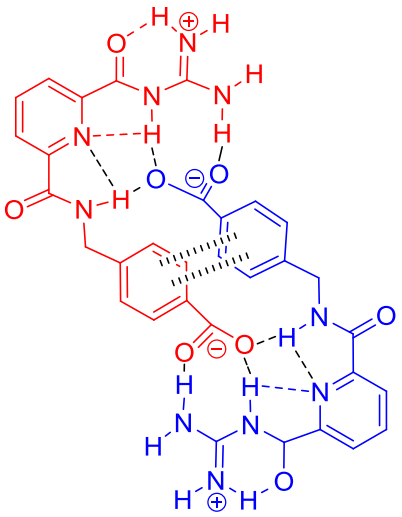

**Fig 54** *The proposed dimerisation mode of compound* ***116***

Scheme **23** illustrates the first route considered for the synthesis of compound **116**. A literature procedure was used to synthesize compounds **117** through **120**.[70] However in the final step, the methyl ester hydrolysis reaction of compound **121** did not proceed as smoothly as expected.

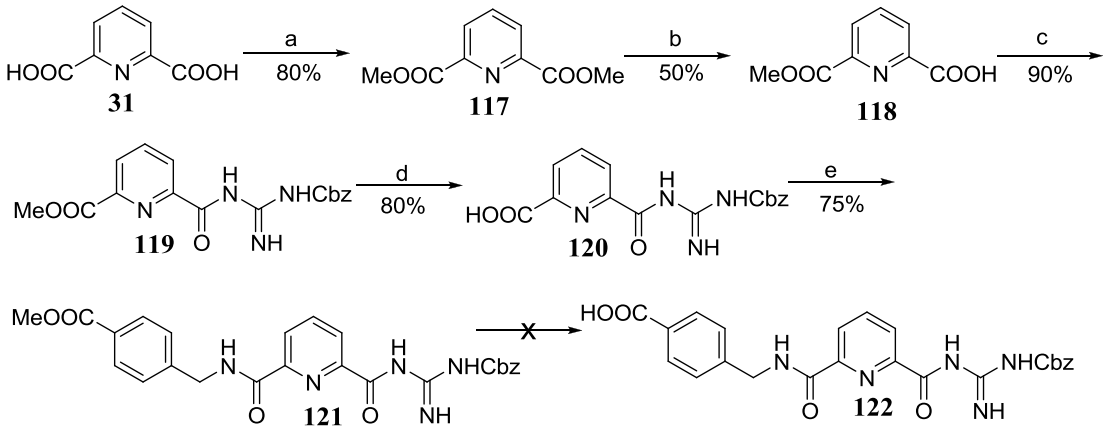


**Scheme 23**. Conditions and reagents: a) MeOH, $H_2SO_4$, Reflux. b) KOH, MeOH, 0 $^oC$. c) Cbz Guanidine, PyBOP, NMM, DMF, rt. d) LiBr, $Et_3N$, 2% $H_2O/CH_3CN$, rt. e) 4-(Aminomethyl) benzoic acid methyl ester, HOBt, EDC.HCl, DIPEA, DCM, rt.

Many ester hydrolysis procedures were attempted to prepare compound **122** but none were successeful for the selective hydrolysis the methyl ester. Instead preferred nucleophilic attack took place on the carbonyl carbon adjacent to the protected guanidine functionality resulting in cleavage of the Cbz guanidine from the pyridine scaffold.

To circumvent this problem, the synthetic scheme was redesigned so that compound **120** was coupled to the benzyl ester of 4–(aminomethyl) benzoic acid instead of the methyl ester (Scheme 24). Benzyl ester hydrolysis and Cbz deprotection procedures were carried out simultaneously giving the desired target compound **116**.

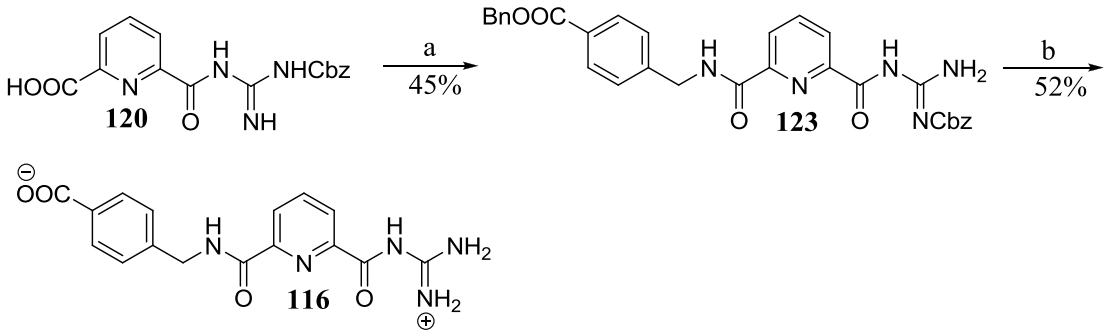


**Scheme 24**. Conditions and reagents: a) 4-(Aminomethyl) benzoic acid benzyl ester, HOBt, EDC.HCl, DIPEA, DCM, rt. b) $H_2$,Pd/C, MeOH/DCM, rt.

## 3.11.1 Isothermal calorimetric dilution study of **116**

The very poor aqueous solubility of compound **116** has restricted the dimerisation investigation only to DMSO and 10% water/DMSO. The study result indicates that compound **116** shows appreciable dimer formation in both solvent systems (Fig 55).

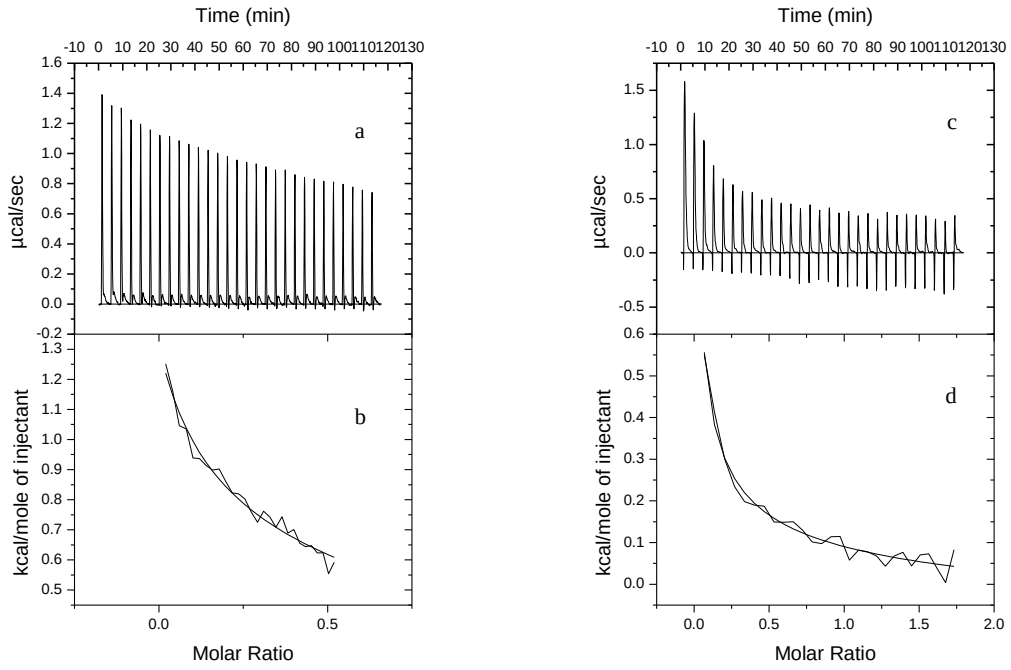


**Fig 55** *Calorimetric data obtained for ITC dilution studies of **58** in DMSO (left), and 10% $H_2O$/DMSO (right) at 298 K. a & c) Raw ITC data (29* x *10 µL injections); b & d) Non-linear curve fitting of the reference corrected data into the dimer dissociation mode*

Results and Discussion

The dimer stability of **116** is not as strong as the dimer of compound **27** ($K_{dim}$ = 11876 $M^{-1}$) in DMSO (Table **13**). An explanation may be that the dimer from compound **53 (116)** is too strained and hence some unfavourable electronic interactions might have been created. However, compound **58** has formed a strong dimer ($K_{dim}$ = 2695±151) at 10% $H_2O$/DMSO. Unlike the other systems investigated so far, the dimer stability in 10% $H_2O$/DMSO is stronger than in pure DMSO. This is the largest $K_{dim}$ value (at a 10% $H_2O$/DMSO) of all the guanidinium carboxylates investigated in this research project.

| Solvent | $K_{dim}$ [$M^{-1}$] | $\Delta G_{dim}$ [kJ $mol^{-1}$] | $\Delta H_{dim}$ [kJ $mol^{-1}$] | $T\Delta S_{dim}$ [kJ $mol^{-1}$] |
|---|---|---|---|---|
| DMSO | 1002±201 | -17.1 | -8.5±0.3 | 8.6 |
| 10% $H_2O$/DMSO | 2695±151 | -19.6 | -6.7±0.3 | 12.9 |

**Table 13** Energetics of dimerisations of compound **116** at 298 K in DMSO and 10% $H_2O$/ DMSO

We could not come up with a clear explanation as to how the 10% water added facilitated the dimerisation process. The presence of the carbonyl functionality might have enhanced the H-bond forming potential of the guanidinium protons. Schmuck has exploited this for the purpose of carboxylate binding by pyrrole guanidinium receptors in aqueous solvent systems.[124] Schmuck used the same principle to synthesize a dimeric structure based on pyrrole guanidinium carbonyl moiety which was stable in pure water (170 $M^{-1}$). This dimeric structure was stabilized solely by hydrogen bonding and an electrostatic interaction.[97] The enhanced ionic character of the guandinium moiety has formed a stronger ion-pair interaction with carboxylates. The possible contribution of a π- π stacking interaction for the high binding energy in 10% $H_2O$/DMSO should not be overlooked as well.

It is disappointing that the solubility of this compound is very poor and its dimerisation could not be investigated in more aqueous systems. It might be worth designing a water soluble analogue of this compound to undertake the dimerisation study in more aqueous environments. The improved dimerisation registered in 10% $H_2O$/DMSO compared to pure DMSO might be an indication that dimerisation could increase even in more aqueous environments.

## 3.12 Synthesis of guanidine-carboxylate **124**

The dimerisation results of compound **116**, especially in 10% $H_2O$/DMSO encouraged us to design the guanidino-carbonyl analogue of compound **27** which had shown excellent dimerisation in DMSO, but much weaker dimerisation in 10% $H_2O$/DMSO system. It was envisaged that similar to compound **116** compound **124** might show excellent dimerisation in 10% $H_2O$/DMSO and more aqueous environments.

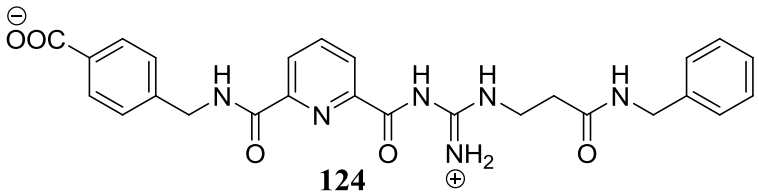


**124**

First, pyridine-2, 6-dicarboxylic acid was asymmetrically coupled with the benzyl ester of 4-aminomethyl benzoic acid (Scheme 25).

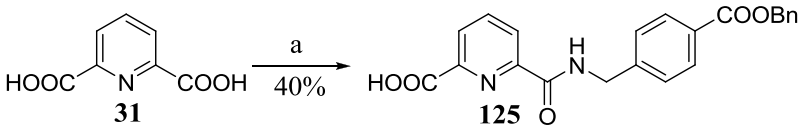


**31** **125**

**Scheme 25**. Conditions and reagents: a) 4-Aminomethyl benzylester, HOBt, EDC.HCl, DIPEA, DCM/DMF, rt.

Phenylpropanamide guanidine **130** was coupled with compound **125** to give **131**.[125, 126] The guanylating agent 1H-pyrazole-1-carboxamidine hydrochloride was first bis-Boc protected to give **128**. This reacted with N-benzyl B-alanine, a compound previously synthesized, to give the bis-Boc protected guanidine **129**. Boc deprotection with TFA afforded compound **130,** and coupling with **60** was attempted to give the precursor **131** of the final guanidinium-carboxylate. However this coupling procedure did not work. This may be due to the fact that the bases used in the coupling procedures are too weak to deprotonate the guanidinium ion. Alkylguanidiniums have pKa values of around 14 and it might be needed to use a strong base like NaOH to fully deprotonate the guanidinium carbocation and hence make it nucleophilic to permit the coupling reaction. However, direct use of a strong base like NaOH is not advisable as previous experience showed that the acyl pyridoguanidinium compounds are susceptible to hydrolysis.

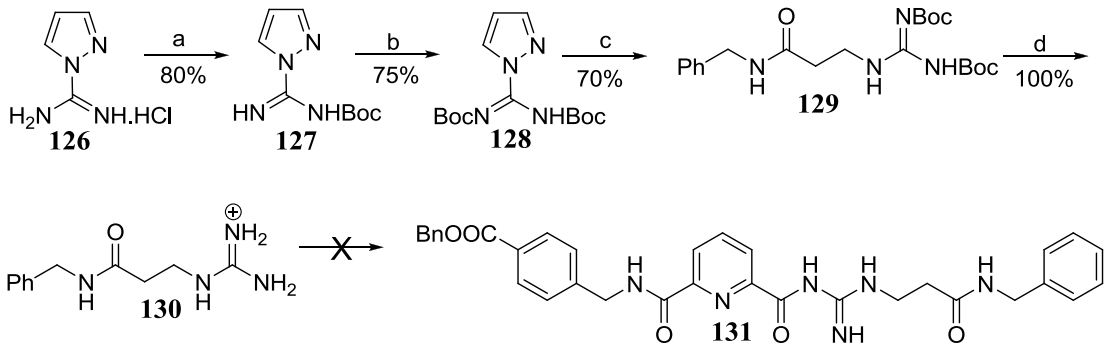


**Scheme 26**. Conditions and reagents: a) DIPEA,$(Boc)_2$, DMF, rt. b) NaH, $(Boc)_2$, THF, rt. c) $PhCH_2NHCOCH_2CH_2NH_2$, THF, DMF, rt. d) 20%TFA/DCM, rt.

The synthesis was redesigned so that a guanidine NH is protected with a Cbz group hence enhancing the basicity of the other $NH_2$ allowing the coupling in the standard coupling procedure. However, forming the Cbz protected compound was not feasible from a practical point of view. All the literature procedures recommend the use of excess (10 equivalent) of the guanidinium compound and this was found to be impractical. An attempt made to form the product by using 2-3 equivalents of compound **130** was not successful. Synthesis of compound **124** did not proceed from here.

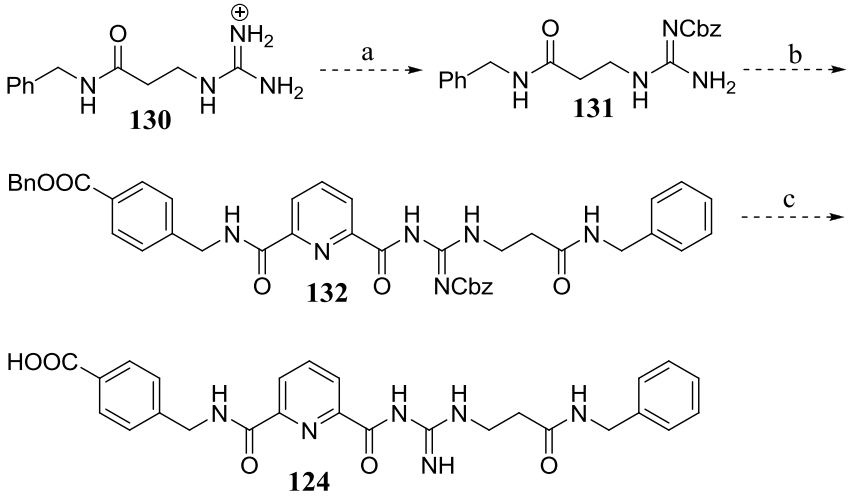


**Scheme 27**. Conditions and reagents: a) CbzCl, NaOH, Dioxane/water, 0 °C-rt. b) **125**, PyBop, NMM, DMF, rt. C) $H_2$, Pd/C, MeOH, rt.

## 3.13 Synthesis of guanidine-carboxylate **133**

The dimeric structures developed so far are based on a pyridine scaffold. We pondered the idea of employing a pyrrole scaffold instead of a pyridine scaffold so that a comparison could be made between the preorganization effect of the pyridine nitrogen and the hydrogen bond stabilization effect of the pyrrole NH proton with the incoming carboxylate oxygen (Fig 56). This comparison was intended to help in choosing the better scaffold for the future development of stable self assembling systems based on carboxylate and guanidinium functionalities.

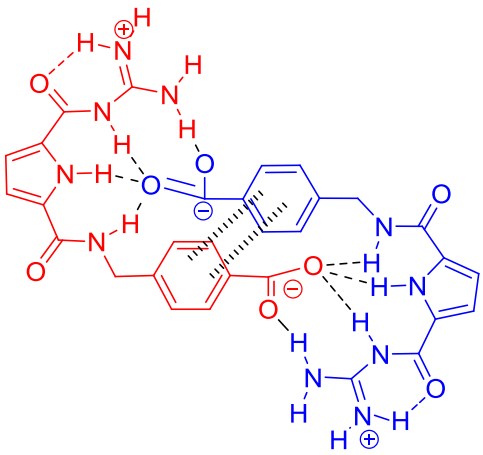

**Fig 56** *The proposed dimerisation mode of compound* ***59***

With this in mind we designed compound **133** which is an analogue of compound **116** incorporating a pyrrole scaffold instead of pyridine.

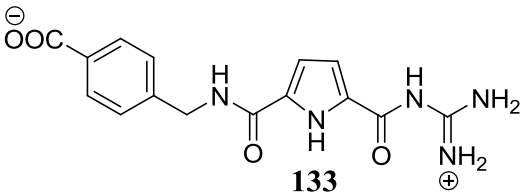

**133**

Initially scheme **28** was considered, and all the transformations were successfully achieved except the last one. Standard literature procedures were employed to undertake all the transformations leading to the synthesis of compound **141**.[61] **141** was then coupled with the methyl ester 4-aminomethyl benzoic acid to afford **142**. Methyl

ester hydrolysis of **142** gave the penultimate compound **143.** However, compound **143** was proved to be insoluble in any of the conventional solvents used for hydrogenolysis and hence the final Cbz deprotection step could not be undertaken.

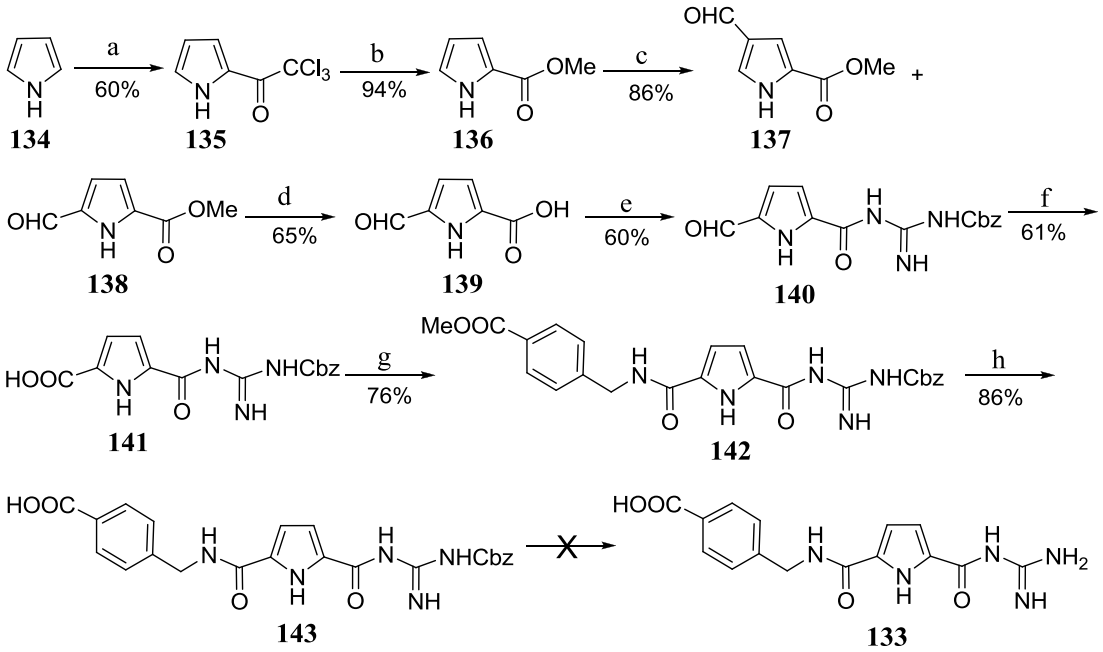


**Scheme 28**. Reagents and conditions: a) Trichloroacetyl chloride, $Et_2O$, rt. b) NaOMe, MeOH, rt. c) DMF/$POCl_3$, DCM, rt. d) KOH, Ethanol/water, rt. e) Cbz.Guanidine, NMM,DMF, PyBop, rt. f) $KMnO_4$, Aceton/Water, rt. g) 4-(Aminomethyl)benzoic acid methylester, EDC.HCl, HOBt, DIPEA,DCM, rt. h) $Me_3SiOK$, THF, rt.

To circumvent the solubility problem of compound **143**, the synthetic scheme was redesigned with the methyl ester replaced with a benzyl ester (Scheme **29**). Synthesis of the benzyl ester coupled product **144** was undertaken with standard peptide coupling conditions. Benzyl ester hydrolysis and Cbz deprotection were then successfully undertaken simultaneously *via* hydrogenolysis and resulted in the guanidinocarbonyl carboxylate **133**.

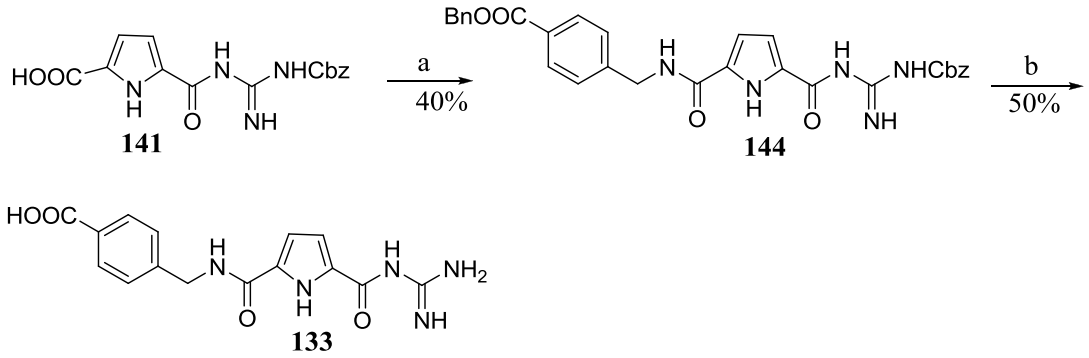


**Scheme 29**. Conditions and reagents: a) 4-(Aminomethyl)benzoic acid benzyl ester, EDC.HCl, HOBt, DIPEA, DCM, rt. b) $H_2$, Pd/C, MeOH/DCM, rt.

## 3.13.1 Isothermal calorimetric dilution study of **133**

As seen from table **14**, the pyrrole guanidocarbonyl compound exhibits strong dimerisation in DMSO and 10% $H_2O$/DMSO. The negative $\Delta G$ values indicate the spontaneous and thermodynamically favoured formation of the dimeric complexes.

| Solvent | $K_{dim}$ [$M^{-1}$] | $\Delta G_{dim}$ [kJ $mol^{-1}$] | $\Delta H_{dim}$ [kJ $mol^{-1}$] | $T\Delta S_{dim}$ [kJ $mol^{-1}$] |
|---|---|---|---|---|
| DMSO | 1767±364 | -18.5 | -19.5±1.5 | -0.9 |
| 10% $H_2O$/DMSO | 7634±3904 | -22.2 | -2.7±0.2 | 19.4 |

**Table 14** *Energetics of dimerisations of compound **133** at 298 K in DMSO and 10% $H_2O$/ DMSO*

As with compound **116**, there was more enhanced dimer stability in 10% $H_2O$/DMSO than in pure DMSO. Comparison between the dimer stabilities of compound **133** with that of compound **116** shows that the two systems have more or less similar stability in DMSO and 10% $H_2O$/DMSO systems.

Schmuck has demonstrated that guanidiniocarbonylpyrrole moiety is one of the most efficient carboxylate binding motifs known to date (Fig 8). He made a thorough investigation to indicate which of the multiple binding interactions present in complexes with carboxylates is responsible for its unique binding properties. The ion pair interaction has been proved to be crucial for the interaction. [76] Apart from that the actual impact of the pyrrole ring itself has been investigated and compared with guanidiniocarbonylpyridine receptors. By doing so Schmuck *et al* has tried to prove if

the pyrrole NH is actively involved in the binding or not, if the size and electronic structure of the aromatic ring are important or not and if the angle between the two adjacent amides is crucial for the binding. NMR binding studies of receptors **15** and **145** showed that the binding of Ala with the pyridine system (K = 360 $M^{-1}$) is generally less efficient than that with the pyrrole receptors (K = 1630 $M^{-1}$) in 40% $H_2O$/DMSO.[70]

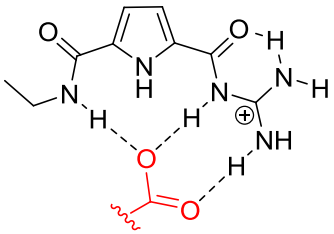

**15**

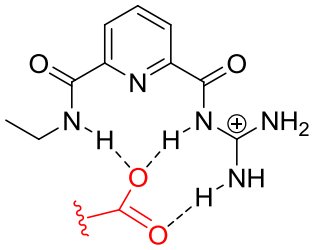

**145**

Calculations showed that in the pyridine system the complexation brings the carboxylate oxygen into close contact with the pyridine nitrogen (< 3Å). The resulting dipole repulsion between the lone pairs on the two heteroatoms could be the reason for the decreased complex stability in the pyridine receptor. One would expect the nitrogen lone pair to help orientate the two neighbouring amide NHs inwards, thereby favouring the specific receptor conformation needed for substrate binding. However, in the above pyridine system it has been observed that the unfavourable electronic repulsion dominates and resulted in the less efficient binding with carboxylates.

On the other hand, Kilburn *et al* [38, 127] has clearly demonstrated that the preorganisation effect of pyridine N is crucial in pyridoguanidinium receptors for binding with carboxylates. This has been discussed in chapter one of the thesis and exemplified by the more efficient binding of acetate by receptor **21** ($K_{ass}$ = 22,000 $M^{-1}$ in DMSO) compared with that of receptor **22** ($K_{ass}$ = 5300 $M^{-1}$ in DMSO) which lacks the preorganisation effect of the pyridine N.

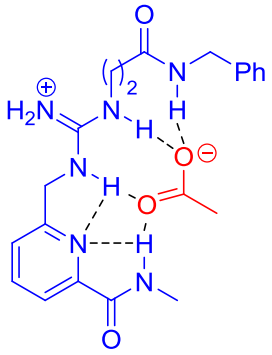

**21**

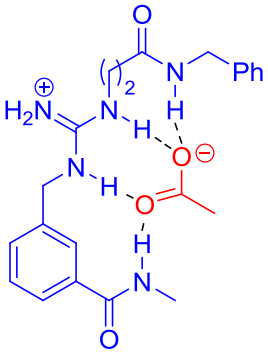

**22**

Kilburn *et al* has further investigated the importance of preorganisation in self assembely of dimeric systems developed based on pyridine (**27**) and benzene (**146**) scaffolds. Similar results were registered as **27** dimerises ($K_{dim}$ = 11876±1692 $M^{-1}$) more strongly than **146** ($K_{dim}$ = 1600±160 $M^{-1}$). This again shows that the preorganisation effect of the pyridine N is important in the formation of the dimeric structure.[136]

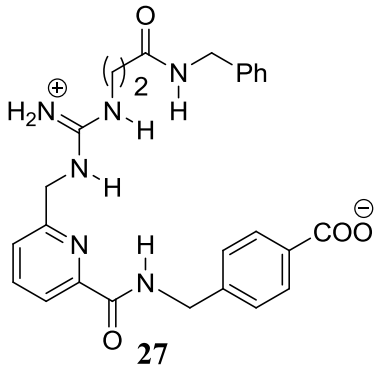

**27**

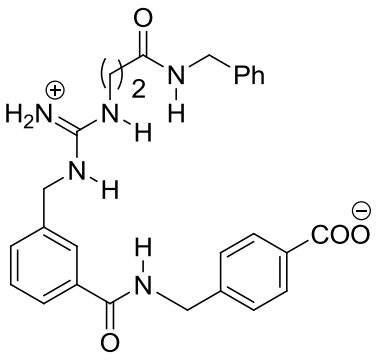

**146**

Considering their differences when the two scaffolds were used for the purpose of carboxylate binding, [124] it was anticipated that there would be some differences of stabilities between dimers of pyrrole (**133**) and pyridine (**116**) based compounds. Both systems have their own merits to function as scaffolds for the purpose of building a dimeric self assembling system. However, the differences observed between the two scaffolds in their usage as carboxylate receptors is not reflected when compounds **133** and **116** were used as self assembled dimeric systems. At this stage, we cannot suggest the preferability of using one scaffold over the other for the purpose of developing dimeric structures. More work is needed to investigate these systems thoroughly and suggest the preference of using one scaffold over the other.

Another observation in the dimeric system of compound **133** is the fact the dimerisation is reversed from enthalpy driven in DMSO into entropy driven in 10% $H_2O$/DMSO. That does not happen in compound **116**. It is indeed expected that the difference between these scaffolds will be more obvious when they are subjected to more aqueous environments. This is due to the fact that solvation effect by the surrounding water molecules will affect the hydrogen bonding between the pyrrole NH and the carboxylate more than it does the preorganization phenomenon in the pyridine system.

The poor solubilities of compounds **133** and **116** precluded dimerisation studies in more aqueous environments. Hence comparisons of these scaffolds in more aqueous solvent systems could not be made. At this juncture, we might not be able to suggest a pyridine scaffold is better than pyrrole in synthesising dimeric self assembled systems or *vice versa*.

# 4. General conclusions and future prospects

In this PhD project various pyridoguanidinium-carboxylate compounds were synthesized and investigated in terms of their ability to form dimeric self assembling systems in polar solvents (DMSO, DMSO-water mixtures and pure water). Considering the fact that there was not much literature precedent on the synthesis of self assembling systems in polar solvent systems that do not employ a metal ligand template, we believe that good progress has been made towards understanding the principles governing the process of self assembly in polar solvent systems.

In the first set of compounds **45**, **46**, **29** and **30**, features that are believed to furnish a combination of H-bonding and hydrophobic interactions have been encoded into the monomeric structures and their dimerisation properties were thoroughly investigated. All the four compounds showed significant dimerisation in DMSO and through this the concept of employing a combination of H-bonding, electrostatic and hydrophobic interactions in stabilizing a self assembled system have been clearly demonstrated. This is illustrated by the excellent dimerisation property of compound **46** in DMSO ($K_{dim}$ [$M^{-1}$] = 4608±1954). The guanidinium-carboxylate H-bonding and electrostatic interaction augmented by the Val-Val interaction is believed to be responsible in overcoming the high polarity and solvation properties associated with DMSO. The comparison of the dimerisation energies between the valine functionalized (**45** and **29)** and the β-Ala functionalized (**46** and **30)** compounds suggested that Val-Val interactions might be important in enhancing the stability of the dimeric structures in solution. The dramatic decrease of dimer stabilities in 10% $H_2O$/DMSO underscores the challenges and difficulties associated with the task of designing supramolecular self assembled systems in aqueous environments.

The superiority of guanidinium carboxylate **53** compared to compounds **29** and **30** in forming reasonably stable dimers in more aqueous environments demonstrates the possibility of utilizing hydrophobic interactions in creating self assembled systems in such competitive environments. The dimerisation of guanidinium carboxylate **53** in 50% $H_2O$/DMSO ($K_{dim}$ [$M^{-1}$] = 55±8) is a very good example in this regard and can be a stepping stone towards developing more stable systems in more aqueous

mediums. NMR dilution studies on **53** have not only verified the ITC dimerisation figures but also gave information regarding the structure of the dimer in solution.

The synthesis of compound **57** was undertaken to exploit the strength of a combined aromatic-aromatic stacking and hydrophobic-hydrophobic interactions in more aqueous environments. Some degree of dimerisation was observed in 50% $H_2O$/DMSO. However, the poor solubility of the compound has precluded a full investigation of the dimerisation property in more aqueous systems. The anticipated through space interaction of the aromatic protons was not observed in the NOESY spectrum analysis of this compound. This might not rule out the presence of the anticipated through space contact of the aromatic protons as a number of factors might interfere with getting a good quality NOESY spectrum. One possibility is the increased intermolecular motion in the dimeric structure which is typical of such extended monomeric systems.

The objective of synthesizing compounds **67** and **78** was basically to impart water solubility into the systems so that dilution studies could be undertaken in more aqueous mediums. This objective has been achieved without compromising the dimer strength. Aromatic-aromatic stacking interactions were once again proved to be vital for dimer strength as compound **67** exhibits a much stronger dimerisation in DMSO and 10% $H_2O$/DMSO than the previous aliphatic systems.

Compound **82** was designed to introduce more hydrophobic interactions into the dimeric system. In addition to the dimerisations observed in DMSO and 10% $H_2O$/DMSO, a reasonably stable dimeric structure was detected in 50% $H_2O$/DMSO. This illustrated once again the potential in utilizing intermolecular forces based on hydrophobic interactions in more aqueous environments. The suitability of compound **82** for NMR dilution studies has also helped in verifying the ITC dilution study results.

Encouraged by the results of compound **82** we have looked into more hydrophobic systems **93** and **94** and these systems have yielded dimeric structures with stability constants of 27±7 $M^{-1}$and 127± 100 $M^{-1}$ respectively in a 75% $H_2O$/DMSO system. It is for the first time that we observed dimerisation in this solvent system. This is important not only in terms of accessing the dimeric structures in such aqueous

environment but also in understanding the properties of hydrophobic interactions in aqueous media.

We investigated the importance of Val-Val, Leu-Leu, aromatic-aromatic stacking interactions in the dimerisation phenomena and recognized their pros and cons in the process and we looked into other structural features which might be important in improving dimer strength in aqueous systems. Introducing a carbonyl group in between the guanidine and the pyridine scaffold was observed to play a very constructive role in making compound **116** an excellent dimer in 10% $H_2O$/DMSO ($K_{dim}$ = 2695±151 $M^{-1}$).

In this PhD project, we have been able to access dimeric supramolecular structures stable in polar solvent systems. Virtually all the guanidinium-carboxylate compounds considered, exhibit excellent dimerisation in DMSO and 10% $H_2O$/DMSO. Some encouraging dimerisation results have also been registered in solvent systems containing 50% and 75% water in DMSO. All the pieces of information we gathered from each of the guanidinium-carboxylates can help us design systems which contain all the optimum structural features (hydrophobicity, aqueous solubility, rigidity, introduction of a guanidinocarbonyl functionality and aromatic moities) can pave the way for the design of a more efficient supramolecular system based pyrido guandinium-carboxylate for the future.

# 5. Experimental

## 5.1 General Experimental

Reactions requiring a dry atmosphere were carried out in oven dried glassware under a nitrogen atmosphere. Where degassed solvents were used, a stream of nitrogen was passed through them immediately prior to use. Solvents and reagents were of commercial grade and were used without further purification and where necessary, distilled prior to use. THF was distilled under argon from benzophenonone and sodium; DCM, $Et_3N$, PE and EtOAc were distilled from calcium hydride.TLC analysis was carried out using foil-backed sheets coated with silica gel (0.25 mm) and containing the fluorescent indicator $UV_{254}$. Flash column chromatography was performed on Sorbsil C60, 40-60 mesh silica.

## 5.2 Instrumentation

Proton NMR spectra were obtained at 300 MHz on a Bruker AC 300 and at 400 MHz on a Bruker DPX 400 spectrometer. Carbon NMR spectra were recorded at 75 MHz on a Bruker AC 300 and at 100 MHz on a Bruker DPX 400 spectrometer. Spectra were referenced to the solvent residual peak for the deuterated solvent. Chemical shifts are reported in ppm on the δ scale relative to the signal of the solvent used. Coupling constants (J) are given in Hz. Signal multiplicities were determined using the distortionless enhancement by a phase transfer (DEPT) spectral editing technique.

Infra-red spectra were recorded on a BIORAD Golden Gate FTS 135. All samples were run either as neat solids or oils. Melting points were determined in open capillary tubes using a Gallenkamp Electrothermal melting point apparatus and are uncorrected.

Optical rotations were measured on a PolAr2001 polarimeter using the solvent stated, the concentrations given are in g/100 mL. Mass spectra were obtained on a VG analytical 70-250 SE normal geometry double focusing mass spectrometer. All electron ionisation spectra were recorded on a ThermoQuest Trace MS single quadrupole GC-MS mass analyser with an electron ionisation ion source using DCM

as solvent. All electrospray (ES) spectra were recorded on a Micromass Platform quadrupole mass analyser with an electrospray ion source using acetonitrile as solvent. High resolution accurate mass measurements were carried out at 10,000 resolution on a Bruker Apex III FT-ICR mass spectrometer. Microanalysis wre performed by MEDAC Ltd., Surrey. Calorimetry experiments were performed on an Isothermal Titration Calorimeter from Microcal Inc., USA.

## 5.3 Experimental for ITC dilution studies

By directly measuring the heat evolved or absorbed as a function of time, ITC allows the determination of all the thermodynamic parameters associated with dissociation of self-assembled systems. In a single experiment the dissociation constant ($K_{diss}$), the stoichiometry (n) and the enthalpy ($\Delta H_{diss}$) of the dissociation process are determined. The association constant ($K_a$) of the self assembled system is simply the inverse of $K_{diss}$ and the relation between the enthalpy of the dissociation process ($\Delta H_{diss}$) and the association process ($\Delta H_a$), is:

$$\Delta H_{diss} = -\Delta H_a$$

From the association constant ($K_a$), it is possible to calculate the Gibbs free energy ($\Delta G_a$) according to:

$$\Delta G_a = -RT.\ln K_a$$

With $R$ = gas constant, $T$ = temperature, $K_a$ = association constant expressed in mole fraction units.

The entropy of the process is obtained using the Gibbs-Helmholtz relation:

$$T.\Delta S_a = \Delta H_a - \Delta G_a$$

A typical ITC dilution experiment begins with a degassed solvent in cell and controlled aliquots of known concentration sample solution are added through a syringe. As the dissociation begins, an endothermic or exothermic signal depending on the nature of dissociation is observed. As the concentration of dimer increases in the cell, we reach a plateau in terms of the amount of heat evolved or absorbed on further addition of dimer solution.

## 5.4 Method for obtaining calorimetric data

All dilution experiments were performed on an Isothermal Titration Calorimeter from Microcal Inc. (Northampton, MA). In a typical experiment, the degassed solvent

system used for the experiment is placed inside a calorimetric cell and a solution of receptor with a known concentration is introduced sequentially in 29 injections from a computer controlled syringe in 10 μL portion. The solution is continuously stirred at 310 rpm to ensure rapid mixing and the system is kept at 25$^{o}$C, through the combination of an external cooling bath and an internal heater. Dilution effects are determined by performing a blank experiment by adding solvent into solvent and subtracting it from the raw titration to produce the final dissociation curve. Dissociation parameters are found by applying a 1:1 dimer dissociation model, using the Origin 7.0 software provided. These methods rely on standard nonlinear least-squares regression (Levenberg-Marquard method) to fit the curves, taking into account the change in volume that occurs during the calorimetric dilution.

## 5.5 Experimental for NMR dilution studies

Obtaining dimerisation constants by $^{1}$H NMR dilution experiments involve preparation of a series of dilutions of the pyridoguanidinium compound which spans concentration ranges containing a predominantly dimeric form of the compound in one end and predominantly monomeric form of the compound in the other end. Upon complexation, protons in the pyridoguanidinium compounds may undergo a change in chemical shifts. In particular, protons involved in hydrogen bonding undergo a dramatic shift and therefore are used to determine association constants. After the data from the dilution experiment have been acquired, curve fitting software for a 1:1 dimer dissociation model (NMRDil_Dimer) is employed to determine the dimerisation constant.[135] The monomer and the dimer are in equilibrium.

## 5.6 Synthesis

### **Ethyl 6-(((methylsulfonyl) oxy) methyl) picolinate (33a)** and **ethyl 6-(chloromethyl) picolinate (33b)**

Compound **32** (5.00 g, 27.62 mmol) was dissolved in DCM (30 mL) at 0 °C. $Et_3N$ (7 mL, 50.34 mmol) and MsCl (5 mL, 52.20 mmol) were added and the resulting solution was stirred overnight at room temperature. *In vacuo* drying of the reaction mixture and purification of the resulting crude product by column chromatography ($SiO_2$, 1:9 EA/PE) afforded **33a** (334 mg, 5%) as a white solid and **33b** (4.50 g, 82%) as a yellowish oily liquid.

### **Ethyl 6-(((methylsulfonyl) oxy) methyl) picolinate (33a)**

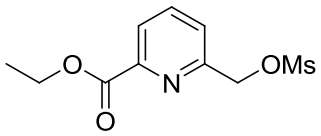


MP = 50-53°C; $^1$H NMR (300 MHz, $CDCl_3$): δ (ppm) = 8.03 (1 H, d, *J* = 7.9 Hz , CH), 7.86 (1 H, t, *J* = 8.5 Hz, CH), 7.60 (1 H, d, *J* = 8.5 Hz, CH ), 5.37 (2 H, s, C*H*$_2$S(O)$_2$CH$_3$), 4.40 (2 H, q, *J* = 7.9 Hz, C*H*$_2$CH$_3$), 3.13 (s, 3 H, CH$_2$S(O)$_2$C*H*$_3$), 1.36 (3 H, t, *J* = 7.9 Hz, CH$_2$C*H*$_3$); $^{13}$C NMR (75 MHz, $CDCl_3$): δ (ppm) = 164.7 (Cq), 154.4 (Cq), 148.1 (Cq), 138.2 (CH), 125.1 (CH), 124.8 (CH), 71.1 ($CH_2$), 62.1 ($CH_2$), 38.2 ($CH_3$), 14.3 ($CH_3$); ESMS: *m*/*z* = 321 $[M+Na]^+$; HRMS (ES): Calcd. for $C_{10}H_{13}NNaO_5S$ ($[M+Na]^+$) 282.0412, found 282.0408; FT-IR (solid): ν $_{max}$ $cm^{-1}$ = 2982 (m), 1736 (s), 1716 (s), 1589 (s) , 1456 (m), 1369 (m), 1315 (s), 1257 (s), 1226 (m), 1173 (s), 1131 (s), 747 (m), 696 (m).

Experimental

**Ethyl 6-(chloromethyl) picolinate**

**(33b)**

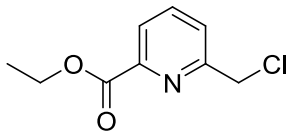


$^{1}$H NMR (300 MHz, $CDCl_3$): δ (ppm) = 8.02 (1 H, d, *J* = 8.53 Hz, CH), 7.89 (1 H, d, *J* = 8.53 Hz, CH), 7.68 (1 H, d, *J* = 8.73 Hz, CH), 4.74 ( 2 H, s, C*H*$_2$Cl), 4.44 (2 H, q, *J* = 8.0 Hz, C*H*$_2$CH$_3$), 1.39 (3 H, t, *J* = 7.2 Hz, CH$_2$C*H*$_3$); $^{13}$C NMR (75 MHz, $CDCl_3$): δ (ppm) = 164.8 (Cq), 157.2 (Cq), 147.7 (Cq), 138.1 (CH), 126.0 (CH), 124.3 (CH), 62.1 ($CH_2$), 46.3 ($CH_2$), 14.3 ($CH_3$); ESMS: *m*/*z* = 222 $[M+Na]^+$; FT-IR (liquid): ν $_{max}$ $cm^{-1}$ = 2982 (m), 1736 (s), 1716 (s), 1589 (m), 1455 (m), 745 (s), 694 (s).

***N, N*-Di-tert butyloxycarbonyl –N-[6-(ethoxy carbonyl) pyridn-2-yl] methaneamine**

**(34)**

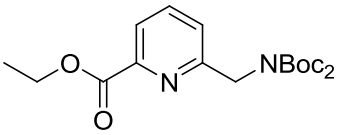


**33b** (4.25 g, 21.25 mmol) was dissolved in dry DMF (50 mL). $K_2CO_3$ (3.80 g, 27.00 mmol) and $NHBoc_2$ (5.90 g, 27.00 mmol) were added successively to the reaction mixture which was stirred for 24 hrs at 60 °C. The solvent was removed *in vacuo* and the resulting residue was dissolved in DCM (50 mL). The organic layer was washed with water (50 mL), brine (50 mL) and dried over $MgSO_4$. *In vacuo* removal of the organic solvent and purification of the resulting crude by column chromatography ($SiO_2$, 1:20 EtOAc/PE) afforded **34** (6.6 g, 75%) as a pale yellowish oily liquid. $^{1}$H NMR (300 MHz, $CDCl_3$): δ (ppm) = 7.95 (1 H, d, *J* = 8.5 Hz, CH), 7.75 (1 H, dd, *J* = 8.6 Hz, 8.5 Hz, CH), 7.31 (1 H, d, *J* = 8.7 Hz, CH), 4.99 (2 H, s, C*H*$_2$NBoc$_2$), 4.42 (2 H, q, *J* = 7.93 Hz, C*H*$_2$CH$_3$), 1.30-1.45 (21 H, m , 2 x C(C*H*$_3$)$_3$ + CH$_2$C*H*$_3$); $^{13}$C NMR (75 MHz, $CDCl_3$): δ (ppm) = 165.2 (Cq), 159.1 (Cq), 152.3 (Cq), 147.8 (Cq), 137.4 (CH), 123.3 (CH), 122.8 (CH), 82.9 (Cq), 61.8 ($CH_2$), 51.4 ($CH_2$), 30.0 ($CH_3$), 14.3 ($CH_3$); ESMS: *m*/*z* = 403 $[M+Na]^+$, 784 $[2M+Na]^+$; HRMS (ES): Calcd. for $C_{19}H_{28}N_2NaO_6$ ($[M+Na]^+$) 403.1845, found 403.1846; FT-IR (liquid): ν $_{max}$ $cm^{-1}$ = 2979 (m), 1717 (s), 1366 (m), 1141 (s), 1091 (s).

**6-((Di-(*tert*-butoxycarbonyl) amino) methyl) picolinic acid** (**35**) and 6-**(((*tert*-butoxycarbonyl) amino) methyl) picolinic acid**
(**36**)

Compound **34** (1.8 g, 4.74 mmol) was dissolved in $CH_3CN$ (20 mL) containing 2 % (v/v) of water. $Et_3N$ (2.2 mL, 15.80 mmol) and LiBr (4.60 g, 53.49 mmol) were added successively to the reaction mixture which was stirred vigorously at room temperature for 24 hrs. Water (100 mL) and EA (100 mL) were added and the mixture was directly acidified with 2M HCl until the pH of the reaction mixture was 2-3. The organic phase was washed with water (50 mL), dried over $MgSO_4$ and concentrated *in vacuo.* Purification of the resulting crude product by column chromatography ($SiO_2$, 1:20 MeOH/DCM) afforded compound **35** (0.95 g, 57 %) and compound **36** (0.38 g, 32 %) as white solids.

**6-((Di-(*tert*-butoxycarbonyl) amino) methyl) picolinic acid**
(**35**)

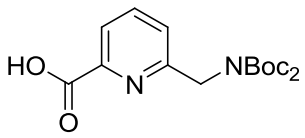


MP = 63-66 °C; $^1$H NMR (300 MHz, $CDCl_3$): δ (ppm) = 9.23 (1 H, s, COO*H*), 8.11 (1 H, d, *J* = 8.6 Hz, CH), 7.92 (1 H, t, *J* = 8.5 Hz, CH), 7.48 (1 H, d, *J* = 8.5 Hz, CH), 4.98 (2 H, s, C*H*$_2$ $NBoc_2$), 1.41 (18 H, s, 2 x C(C*H*$_3$)$_3$); $^{13}$C NMR (75 MHz, $CDCl_3$): δ (ppm) = 165.4 (Cq), 156.1 (Cq), 146.3 (Cq), 138.6 (CH), 125.6 (CH), 122.8 (CH), 81.5 (Cq), 53.4 ($CH_2$), 28.3 ($CH_3$); ESMS: *m*/*z* = 375 ($[M+Na]^+$); HRMS (ES): Calcd for $C_{17}H_{24}N_2NaO_6$ ($[M+Na]^+$) 375.1532, found 375.1521; FT-IR (solid): $\nu_{max}$ $cm^{-1}$ = 3566 (b), 2364 (m), 1733 (s), 1558 (m), 1507 (m), 1364 (m), 1113 (m).

**6-(((tert-butoxycarbonyl) amino) methyl)picolinic acid**
(**36**)

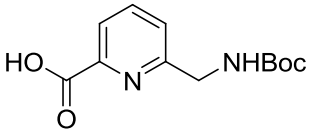

MP = 89-90 °C; $^{1}$H NMR (300 MHz, $CDCl_3$): δ (ppm) = 8.12 (1 H, d, *J* = 8.3 Hz, CH), 7.91 (1 H, t, *J* = 8.5 Hz, CH), 7.56 (1 H, d, *J* = 8.3 Hz, CH), 5.36 (1 H, s(b), N*H*Boc$_2$) 4.51 (2 H, d, *J* = 6.5 Hz, NHC*H*$_2$), 1.46 (9H, s, C(C*H*$_3$)$_3$ ); $^{13}$C NMR (75 MHz, $CDCl_3$): δ (ppm) =165.4 (Cq), 157.3 (Cq), 152.6 (Cq), 139.1 (CH), 124.9 (CH), 122.1 (CH), 83.3 (Cq), 50.1 ($CH_2$), 28.0 ($CH_3$); ESMS: *m*/*z* = 275 $[M+Na]^+$, HRMS (ES): Calcd for $C_{12}H_{16}N_2NaO_4$ ($[M+Na]^+$) 275.1008, found 275.1006; FT-IR (solid): $\nu_{max}$ cm$^{-1}$ = 3566 (b), 2364 (m),1733 (s).

**Methyl 3-(6-(((tert-butoxycarbonyl)amino)methyl)picolinamido)propanoate (37a)**

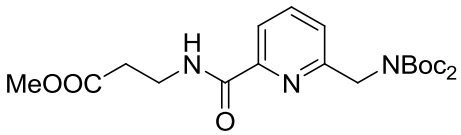


Compound **36** (3.40 g, 13.49 mmol) was dissolved in dry DCM (50 mL). *i*Pr$_2$NEt (4.42 g, 34.20 mmol), EDC (4.40 g, 28.39 mmol), HOBt (3.90 g, 28.89 mmol) and alanin-β-methyl ester (2.60 g, 19.40 mmol) dissolved in 25 mL DCM:DMF (4:1 mixture) were added successively to the reaction mixture which was stirred at room temperature for 72 hrs. *In vacuo* drying of the reaction mixture and purification of the resulting crude by column chromatography ($SiO_2$, 1:20 MeOH/DCM) afforded **37**a (2.30 g, 48%) as a white solid. MP = 60-62 °C; $^{1}$H NMR (300 MHz, $CDCl_3$): δ (ppm) = 8.30 (1 H, s, NH), 8.02 (1 H, dd, *J* = 8.5 Hz, 1.0 Hz, CH), 7.77 (1 H, t, *J* = 8.7 Hz, CH), 7.28 (1 H, dd, *J* = 8.5 Hz, 0.8 Hz, CH), 4.90 (2 H, s, C*H*$_2$NHBoc), 3.71 (2 H, t, *J* = 7.3 Hz, OCC*H*$_2$CH$_2$NH), 3.68 (3 H, s, OC*H*$_3$), 2.62 (2 H, t , *J* = 7.3 Hz, CH$_2$C*H*$_2$NH), 1.41 (18 H, s, C(C*H*$_3$)$_3$); $^{13}$ C NMR (75 MHz, $CDCl_3$): δ (ppm) = 172.3 (Cq), 164.3 (Cq), 156.9 (Cq), 152.5 (Cq), 149.0 (Cq), 137.9 (CH), 122.7 (CH), 120.5 (CH), 82.7 (Cq), 51.9 ($CH_3$), 50.1 ($CH_2$), 35.0 ($CH_2$), 34.1 ($CH_2$), 27.9 ($CH_3$); ESMS: *m*/*z* = 460 $[M+Na]^+$, 898 $[2M+Na]^+$; HRMS (ES): Calcd for $C_{16}H_{23}N_3NaO_5$ ($[M+Na]^+$) 460.2060, found 460.2051; FT-IR (solid): $\nu_{max}$ cm$^{-1}$ = 3397 (m), 2974 (s), 1743 (m), 1728 (s), 1680 (s).

Experimental

**(R)-Methyl 2-(6-(((tert-butoxycarbonyl)amino)methyl)picolinamido)-3-methylbutanoate**
**(38a)**

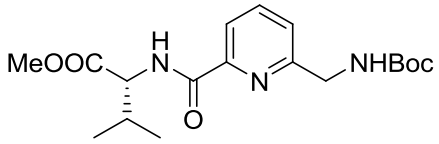


Compound **36** (100 mg, 0.36 mmol) was dissolved in DCM (25 mL). *i*$Pr_2$NEt (0.2 mL, 1.26 mmol), EDC.HCl (165 mg, 0.90 mmol), HOBt (146 mg, 1.08 mmol) and valine methyl ester (120 mg, 0.72 mmol) were added successively to the reaction mixture which was stirred at room temperature for 72 hrs. DCM (40 mL) and 1M $KHSO_4$ (40 mL) were added to the reaction mixture. The organic layer was separated, washed with sat $Na_2CO_3$ (30 mL) and brine (30 mL) successively, and dried over $MgSO_4$. *In vacuo* removal of the solvent and purification of the resulting crude product by column chromatography ($SiO_2$, 1:1 DCM/PE → 1:50 MeOH/DCM) afforded **38a** (80 mg, 50%) as yellowish oily liquid. $^1$H NMR (300 MHz, $CDCl_3$): δ (ppm) = 8.43 (1 H, d, *J* = 10.2 Hz, CHN*H*Boc), 8.04 (1 H, d, *J* = 8.5 Hz, CH), 7.80 (1 H, t, *J* = 8.5 Hz ,CH), 7.43 (1 H, d, *J* = 8.93 Hz , CH), 5.32 (1 H, s, $CH_2$N*H*), 4.70 (1 H, dd, *J* = 10.2 Hz, 5.7 Hz, CHC*H*(COOMe)NH), 4.48 (2 H, d, *J* = 6.5 Hz, NHC$H_2$), 3.79 (3 H, s, COOC$H_3$), 2.29 (1 H, m, $(CH_3)_2$C*H*CH), 1.45 (9 H, s, NHCOO(C$H_3$)$_3$), 1.01( 3 H, d, *J* = 2.5 Hz, CH(C$H_3$)$_2$), 0.99 (3 H, d, *J* = 2.5 Hz , CH(C$H_3$)$_2$); $^{13}$C NMR (75 MHz, $CDCl_3$): δ(ppm) = 172.3 (Cq), 164.1 (Cq), 157.2 (Cq), 156.0 (Cq), 148.8 (Cq) , 138.1 (CH), 124.2 (CH), 120.9 (CH), 79.8 (Cq), 57.3 (CH), 52.2 (CH), 45.7 ($CH_2$), 31.5 ($CH_3$), 28.4 ($CH_3$), 19.2 ($CH_3$), 17.9 ($CH_3$); ESMS: *m*/*z* = 388 $[M+Na]^+$; HRMS (ES): Calcd for $C_{18}H_{27}N_3NaO_5$ ($[M+Na]^+$) 388.1849, found 388.1841; FT-IR (liquid): $\nu_{max}$ $cm^{-1}$ = 3018 (w), 1671 (m), 1518 (m), 1214 (s), 745 (s).

**(R)-Methyl 2-(6-(aminomethyl)picolinamido)-3-methylbutanoate**
**(38)**

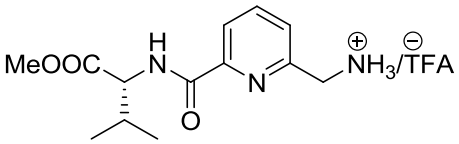

Experimental

Compound **38a** (56 mg, 0.15 mmol) was dissolved in DCM (10 mL). 20% (v/v) TFA/DCM (2 mL) was added to the reaction mixture which was stirred for 5 hrs at room temperature. *In vacuo* drying of the reaction mixture after the addition of toluene (3 x 2 mL) afforded **38** (30 mg, 72%) as a yellowish oily liquid. $^{1}$H NMR (300 MHz, $CDCl_3$): δ (ppm) = 8.59 (broad, NH & $NH_2$), 8.09 (1 H, d, *J* = 8.5 Hz, CH), 7.84 (1 H, t, *J* = 8.5 Hz , CH), 7.39 (1 H, d, *J* = 8.5 Hz, CH), 4.61 (1 H, dd, *J* = 10.0 Hz, 7.7 Hz, CHC*H*(COOMe)NH), 4.35 (2 H, s, C*H*$_2$NH$_2$), 3.70 (3 H, s, COOC*H*$_3$), 2.22 (1 H, m, $(CH_3)_2$C*H*CH), 0.95 (3 H, d, *J* = 3.0 Hz , CH(C*H*$_3$)$_2$), 0.93 (3 H, d, *J* = 3.0 Hz , CH(C*H*$_3$)$_2$); $^{13}$C NMR (75 MHz, $CDCl_3$): δ (ppm) = 174.2 (Cq), 164.2 (Cq), 150.9 (Cq), 149.1 (Cq), 138.9 (CH), 125.1 (CH), 122.8 (CH), 58.3 (CH), 52.4 (CH), 43.2 ($CH_2$), 31.0 ($CH_3$), 19.0 ($CH_3$), 18.2 ($CH_3$); ESMS: *m*/*z* = 266 $[M+H]^+$; HRMS (ES): Calcd for $C_{13}H_{20}N_3O_3$ ($[M+H]^+$) 266.1504, found 266.1495; FT-IR (liquid): ν $_{max}$ $cm^{-1}$ = 2961 (w), 1668 (m), 1594 (m), 903 (s), 728 (s).

. **N-Benzyl-3-(1,3-dioxoisoindolin-2-yl)propanamide (41)**

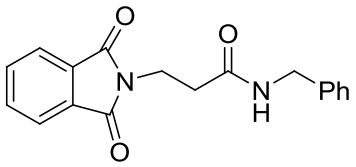


**40** (0.30 g, 1.26 mmol) was dissolved in DCM (25 mL) and added dropwise to a solution of benzylamine (1.0 mL) and $Et_3N$ (1.5 mL) in DCM (20 mL) at 0 °C. After an overnight stirring at room temperature, the reaction mixture was poured into ice cold 2M HCl (20 mL) and extracted with DCM (3 x 50 mL). The organic phases were combined, washed with brine and dried over $MgSO_4$. *In vacuo* removal of the organic solvent afforded **41** (0.30 g, 77%) as a white solid with no further purification. MP = 146-148 °C; $^{1}$H NMR (300 MHz, $CDCl_3$): δ (ppm) = 8.46 (1 H, t, *J* = 6.0 Hz, NH), 7.88-7.80 (4 H, m, CH ), 7.24-7.16 (5 H, m, CH), 4.21 (2 H, d, *J* = 6.5 Hz, $CH_2$), 3.82 (2 H, t, *J* = 8.0 Hz, NC*H*$_2$CH$_2$), 2.52 (2 H, t, *J* = 8.0 Hz, NCH$_2$C*H*$_2$); $^{13}$C NMR (75 MHz, $CDCl_3$): δ (ppm) = 169.4 (Cq), 167.6 (Cq), 139.3 (Cq), 134.3 (Cq), 131.7 (CH), 128.2 (CH), 127.1 (CH), 126.7 (CH), 123.0 (CH), 42.0 ($CH_2$), 34.4 ($CH_2$), 33.8 ($CH_2$); ESMS: *m*/*z* = 331 $[M+Na]^+$; HRMS (ES): Calcd for $C_{18}H_{16}N_2NaO_3$ ($[M+Na]^+$) 331.1059, found 331.1054; FT-IR (solid): ν $_{max}$ $cm^{-1}$ = 3290 (m), 1705 (s), 1631 (s), 1540 (m).

**[*N*-(*N*-Benzyl ethylamino carbonyl)-N-(benzyl formyl)]-thioguanidine (42)**

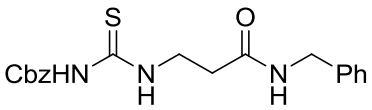

Compound **41** (0.30 g, 0.87 mmol) was suspended in EtOH (20 mL) and refluxed with hydrazine hydrate (76 µL) for 3 hrs and cooled to room temperature. Filtration of the reaction mixture and *in vacuo* drying of the resulting filtrate afforded compound **41a** (0.20 g, 100%) as a yellowish solid and was used for the next step with no further purification. Compound **41a** (0.23 g, 1.00 mmol) was dissolved in DCM (20 mL) and cooled to 0 $^{o}$C. $Et_3N$ (50 µL) and **48** (0.76 g, 2.0 mmol) were added to the reaction mixture which was stirred for 30 mins at 0 °C and then overnight at room temprature. *In vacuo* drying of the reaction mixture and purification of the resulting crude by column chromatography ($SiO_2$, 1:5 EA/PE) afforded **42** (0.31 g, 81%) as a white solid. MP = 137-139 °C; $^{1}$H NMR (300 MHz, DMSO-$d_6$): δ (ppm) = 10.16 (1 H, s, NH), 8.04 (1 H, s, NH), 7.34-7.23 (10 H, m, CH), 5.88 (1 H, s, NH), 5.19 (2 H, s, COC$H_2$Ar), 4.42 (2 H, d, *J* = 6.5 Hz, NHC$H_2$), 3.96 (2 H, t, *J* = 7.0 Hz, $CH_2$), 2.58 (2 H, t, *J* = 7.0 Hz, $CH_2$); $^{13}$C NMR (75 MHz, DMSO-$d_6$): δ (ppm) = 179.0 (Cq), 170.6 (Cq), 152.1 (Cq), 137.9 (Cq), 134.5 (Cq), 128.9 (CH), 128.8 (CH), 128.4 (CH), 127.9 (CH), 127.6 (CH), 68.2 ($CH_2$), 43.7 ($CH_2$), 41.6 ($CH_2$), 34.3 ($CH_2$); ESMS: *m*/*z* = 394.2 $[M+Na]^+$; HRMS (ES): Calcd for ($[M+Na]^+$) 394.1202, found 394.1197. FT-IR (solid): $\nu_{max}$ $cm^{-1}$ = 3290 (w) (b), 1718 (m), 1653 (m), 1647 (m), 1541(s), 1522 (s).

**Methyl 3-(6-((3-(3-(benzylamino)-3-oxopropyl)-2-((benzyloxy)carbonyl)guanidino)methyl)picolinamido)propanoate (43)**

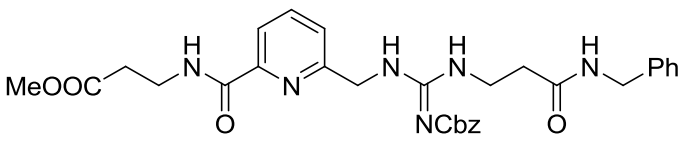

Compound **37a** (0.50 g, 1.48 mmol) was dissolved in DCM (50 mL). 20% (v/v) TFA/DCM (5 mL) was added to the reaction mixture which was stirred for 5 hrs at

room temperature. *In vacuo* drying of the reaction mixture after the addition of toluene (3 x 2 mL) afforded the TFA salt as a white gummy solid (0.37 g, quantitative) which used for the next step with no further purification. (0.23 g, 1.04 mmol) of the TFA salt was dissolved in DCM (40 mL). EDC.HCl (0.45 g, 2.13 mmol), $Et_3N$ (0.5 mL, 3.10 mmol) and **42** were added successively to the reaction mixture which was stirred for 3 days at room temperature. The reaction mixture was washed with 1M aq. $KHSO_4$ (50 mL) and brine, dried over $MgSO_4$ and concentrated *in vacuo*. Purification of the resulting crude product by column chromatography ($SiO_2$, 1:100 → 1:20 MeOH/DCM) afforded **43** (0.50 g, 84%) as a white solid. MP = 118-120 °C; $^1$H NMR (300 MHz, $CDCl_3$): δ (ppm) = 10.27 (1 H, s, NH), 9.30 (1 H, s(b), NH), 8.64 (1 H, s, NH), 8.12 (1 H, d, *J* = 5.4 Hz, CH), 7.86 (1 H, s, *J* = CH), 7.42-7.32 (11 H, m, CH), 5.31 (2 H, s, $CH_2$), 4.76 (2 H, s, $CH_2$), 4.39 (2 H, d, *J* = 5.0 Hz, $CH_2$), 3.73 (4 H, s, 2 x $CH_2$), 3.60 (2 H, s, $CH_3$), 2.72 (4 H, m, 2 x $CH_2$); $^{13}$C NMR (75 MHz, DMSO): δ (ppm) = 181.2 (Cq), 139.1 (Cq), 138.2 (Cq), 129.0 (CH), 128.3 (CH), 128.2 (CH), 127.9 (CH), 124.9 (Cq), 122.1 (Cq), 52.1 ($CH_3$), 46.4 ($CH_2$), 44.3 ($CH_2$), 38.5 ($CH_2$), 36.1 ($CH_2$), 34.5 ($CH_2$), 32.6 ($CH_2$); ESMS: *m*/*z* = 575.5 $[M+H]^+$; HRMS (ES): Calcd for $C_{30}H_{35}N_6O_6$ ($[M+H]^+$) 575.2618, found 575.2612; FT-IR (solid): $\nu_{max}$ $cm^{-1}$ = 1735 (m), 1637 (s), 1672 (s), 1594 (s).

**3-(6-((3-(3-(Benzylamino)-3-oxopropyl)-2-((benzyloxy)carbonyl)guanidino)methyl)picolinamido)propanoic acid (43a)**

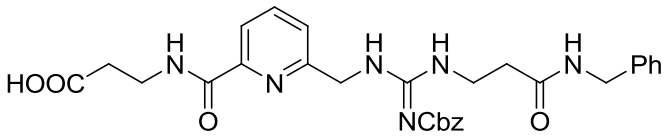


Compound **43** (0.45 g, 0.78 mmol) was dissolved in THF (30 mL) and added to $Me_3SiOK$ (100 mg, 0.78 mmol) suspended in THF (10 mL) under $N_2$. After overnight stirring at room temperature, DCM (50 mL) and $H_2O$ (50 mL) were added and the reaction mixture was cooled to 0 °C. Citric acid (0.1 M aqueous) was added dropwise until the pH was 6-7 and further stirred for 1 hr. *In vacuo* drying of the organic phase and purification of the resulting crude by column chromatography ($SiO_2$, 1:50 → 1:20 MeOH/DCM) afforded **43a** (0.30 g, 69%) as a white solid. MP = 215-217 °C; $^1$H NMR (300 MHz, DMSO-$d_6$): δ (ppm) = 12.30 (1 H, s, COO*H*), 10.50 (1 H, s, NH)

9.10 (1 H, s(b), NH), 8.78 (1 H, NH), 8.50 (1 H, s, NH), 7.92 (2 H, s, CH), 7.48 (1 H, d, *J* = 8.0 Hz , CH), 7.26-7.18 (10 H, m , CH), 4.96 (2 H, s, $CH_2$), 4.55 ( 2 H, d, *J* = 5.0 Hz, $CH_2$), 4.26 (2 H, d, *J* = 5.5 Hz, $CH_2$), 3.50 (4 H, s(b), 2 x $CH_2$), 2.54 (4 H, m, 2 x $CH_2$); $^{13}$C NMR (75 MHz, DMSO-$d_6$): δ (ppm) = 180.1 (Cq), 171.0 (Cq), 138.3 (Cq), 128.7 (CH), 128.1 (CH), 127.9 (CH), 127.7 (CH), 127.2 (CH), 66.0 ($CH_2$), 42.5 ($CH_2$), 35.6 ($CH_2$), 34.3 ($CH_2$), 32.1 ($CH_2$), 31.1 ($CH_2$); ESMS: *m*/*z* = 561 $[M+H]^+$; HRMS (ES): Calcd for $C_{29}H_{33}N_6O_6$ ($[M+H]^+$) 561.2461, found 561.2464. FT-IR (solid): $\nu_{max}$ $cm^{-1}$ = 3208 (m) (b), 2957 (m), 2927 (m), 2361 (m), 1728 (s), 1636 (s), 1573 (s),1518 (s), 1452 (m),1380 (s), 1271 (s).

**3-(6-((3-(3-(Benzylamino)-3-oxopropyl)guanidino)methyl)picolinamido)propanoic acid (29)**

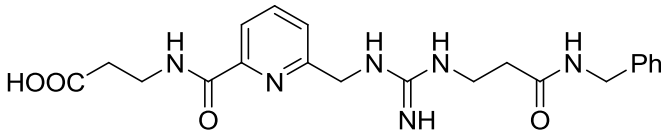


Compound **43a** (0.33 g, 0.58 mmol) was dissolved in MeOH (50 mL). Pd/C (60 mg, 0.58 mmol) was added and the reaction mixture was stirred for 48 hrs under hydrogen (1 atm) at room temperature. The reaction mixture was filtered through celite and dried *in vacuo*. Purification of the resulting solid by precipitation from MeOH using $Et_2O$ afforded compound **27** (0.20 g, 81 %) as a white solid. MP = 218-220 °C; $^1$H NMR (300 MHz, MeOD-$d_4$): δ (ppm) = 7.95-7.89 (2 H, m, CH), 7.46 (1 H, d, *J* = 8.9 Hz , CH), 7.25-7.06 (5 H, m, CH), 4.49 (2 H, s, $CH_2$), 4.28 (2 H, s, $CH_2$), 3.52-3.56 (4 H, m, 2 x $CH_2$), 2.58 (2 H, t, *J* = 7.0 Hz, $CH_2$), 2.43 (2 H, t, *J* = 7.0 Hz, $CH_2$); $^{13}$C NMR (75 MHz, MeOD-$d_4$): δ(ppm) = 177.0 (Cq), 170.8 (Cq), 162.9 (Cq), 156.6 (Cq), 152.0 (Cq), 149.5 (Cq), 139.9 (Cq), 139.3 (CH), 128.5 (CH), 127.5 (CH), 127.0 (CH), 124.4 (CH), 120.4 (CH), 55.4 ($CH_2$), 42.6 ($CH_2$), 38.9 ($CH_2$), 37.4 ($CH_2$), 36.6 ($CH_2$), 35.1 ($CH_2$); ESMS: *m*/*z* = 427 $[M+H]^+$; HRMS (ES): Calcd for $C_{21}H_{27}N_6O_4$ ($[M+H]^+$) 427.2094, found 427.2077; FT-IR (solid): $\nu_{max}$ $cm^{-1}$ = 3286 (w), 1644 (s), 1567 (s), 1537 (s), 697 (m), 607 (m).

**(R)-Methyl 2-(6-((3-(3-(Benzylamino)-3-oxopropyl)-2-((benzyloxy)carbonyl)guanidino)methyl)picolinamido)-3-methylbutanoate (44)**

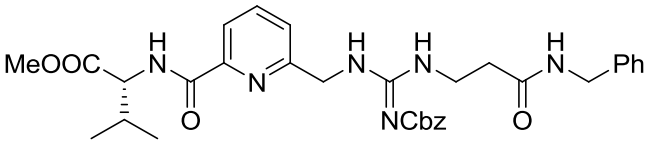


Compound **38** (0.46 g, 1.75 mmol) was dissolved in DCM (30 mL). EDC.HCl (0.84 g, 4.48 mmol), $Et_3N$ (0.74 mL, 5.25 mmol) and **42** (0.65 g, 1.75 mmol) were added successively and the resulting solution was stirred for 3 days at room temperature. The reaction mixture was washed with 1M aq. $KHSO_4$ (50 mL) and brine (40 mL), dried over $MgSO_4$ and concenterated *in vacuo*. Purification of the resulting crude product by column chromatography ($SiO_2$, 1:100 → 3:100 MeOH/DCM) afforded **44** (0.58 g, 50%) as a white solid. MP = 102-104 °C; $^1$H NMR (300 MHz, $CDCl_3$): δ (ppm) = 10.13 (1 H, s, NH), 9.24 (1 H, s, NH), 8.76 (1 H, s, NH), 8.57 (1 H, s, NH), 8.07 (1 H, s, CH), 7.79 (1 H, s , CH), 7.47-7.17 (11 H, m, CH), 5.08 (2 H, s, $CH_2$), 4.62 (3 H, m, $CH_2$ + CH), 4.30 (2 H, dt, *J* = 16.3 Hz, 7.0 Hz, NHC$H_2$$CH_2$), 3.29 (3 H, s, C$H_3$OOC), 2.48 (2 H, s, $CH_2$), 2.30 (1 H, m, C$H$($CH_3$)$_2$), 1.70 (2 H, s, $CH_2$), 0.95 (6 H, m, CH(C$H_3$)$_2$); $^{13}$C NMR (75 MHz, $CDCl_3$): δ (ppm) = 128.7 (CH), 128.3 (CH), 127.9 (CH), 127.7 (CH), 127.5 (CH), 66.5 ($CH_2$), 52.1 (CH), 50.8 (CH), 45.6 ($CH_3$), 38.9 ($CH_2$), 36.6 ($CH_2$), 35.1 ($CH_2$), 19.2 ($CH_3$), 19.2 ($CH_2$), 18.4 ($CH_3$); ESMS: *m*/*z* = 603.5 $[M+H]^+$; FT-IR (solid): $\nu_{max}$ $cm^{-1}$ = 3250 (m) (b), 1735 (m), 1637 (s), 1672 (s), 1594 (s).

**(R)-2-(6-((3-(3-(benzylamino)-3-oxopropyl)-2-((benzyloxy)carbonyl)guanidino)methyl)picolinamido)-3-methylbutanoic acid (44a)**

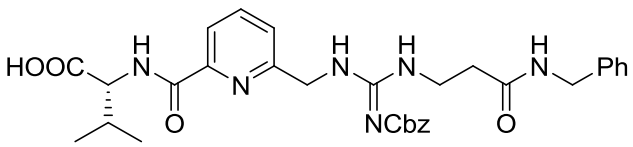


Compound **44** (0.47 g, 0.78 mmol) was dissolved in THF (30 mL) and added to $Me_3SiOK$ (133 mg, 1.04 mmol) suspended in THF (10 mL) under $N_2$. After overnight

stirring, DCM (50 mL) and $H_2O$ (50 mL) were added and the reaction mixture was cooled to 0 °C. Citric acid (0.1 M) was added dropwise until the pH was 6-7 and further stirred for 1hr. *In vacuo* drying of the organic phase and purification of the resulting crude by column chromatography ($SiO_2$, 3:100 → 1:10 MeOH/DCM) afforded **44a** (0.25 g, 54%) as a white solid. MP = 204-206 °C; $[\alpha]_D^{25}$ =-3.0 $^o$ (*c* 0.1, MeOH); $^1$H NMR (300 MHz, MeOD-*d*$_4$): δ (ppm) = 8.01 (1 H, d, *J* = 8.0 Hz, CH), 7.93 (1 H, t , *J* = 8.0 Hz, CH), 7.50 (1 H, d , *J* = 8.5 Hz, CH), 7.37-7.13 (10 H, m, CH), 5.13 (2 H, s, $CH_2$), 4.64 (2 H, s, $CH_2$), 4.48 (1 H, m, C*H*CH$(CH_3)_2$), 4.32 (2 H, s, $CH_2$), 3.66 (2 H, t, apparent triplet, NHC*H*$_2$CH$_2$), 2.58 (2 H, t, apparent triplet, NHCH$_2$C*H*$_2$), 2.35 (1 H, m, CHC*H*$(CH_3)_2$), 0.98 (6H, m, CH(C*H*$_3)_2$); $^{13}$C NMR (75 MHz, MeOD-*d*$_4$): δ (ppm) = 139.8 (Cq), 130.0 (CH), 129.9 (CH), 129.4 (CH), 129.0 (CH), 128.6 (CH), 126.2 (CH), 68.9 ($CH_2$), 47.0 ($CH_2$), 44.6 ($CH_2$), 39.6($CH_2$), 34.0 ($CH_2$), 20.4 ($CH_3$) (2CH peaks overlapped with solvent peaks); ESMS: *m*/*z* = 589.4 $[M+H]^+$; HRMS (ES): Calcd for $C_{31}H_{37}N_6O_6$ ($[M+H]^+$) 589.2774, found 589.2766; FT-IR (solid): $\nu_{max}$ cm$^{-1}$ = 3357 (m)(b), 2502 (w), 2072 (m), 1641 (s), 1593 (m), 972 (s).

**(R)-2-(6-((3-(3-(Benzylamino)-3-oxopropyl)guanidino)methyl)picolinamido)-3-methylbutanoic acid**
**(30)**

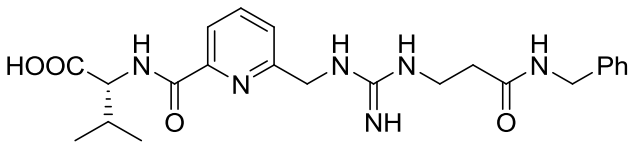


Compound **44a** (0.24 g, 0.41 mmol) was dissolved in MeOH (30 mL). Pd/C (43.4 mg, 0.41 mmol) was added and the reaction mixture was stirred for 48 hrs under hydrogen (1 atm) at room temperature. The reaction mixture was filtered through celite and dried *in vacuo*. Purification by precipitation from MeOH using $Et_2O$ afforded **30** (0.12 g, 55 %) as a white solid. MP = 242-244 °C; $[\alpha]_D^{25}$ =-18.0 $^o$ (*c* 0.7, MeOH); $^1$H NMR (300 MHz, MeOD-*d*$_4$): δ (ppm) = 8.02-7.92 (2 H, m, CH), 7.49 (1 H, d , *J* = 7.5 Hz, CH), 7.27-7.18 (5 H, m, CH), 4.48 (2 H, s, $CH_2$), 4.30 (1 H, d, *J* = 5.5 Hz, C*H*CH$(CH_3)_2$), 4.22 (2 H, s, $CH_2$), 3.45 (2 H, dt, *J* = 6.5 Hz, 2.5 Hz, NHC*H*$_2$CH$_2$), 2.48 (2 H, t, *J* = 7.5 Hz, NHCH$_2$C*H*$_2$), 2.10-2.24 (1 H, m, CHC*H*$(CH_3)_2$), 0.84-0.89 (6 H, m, CH(C*H*$_3)_2$). $^{13}$C NMR (75 MHz, MeOD-*d*$_4$): δ (ppm) = 173.4 (Cq), 165.6 (Cq),

158.8 (Cq), 156.5 (Cq), 151.2 (Cq), 140.3 (Cq) ,140.3 (Cq), 129.9 (CH), 129.0 (CH), 128.6 (CH), 126.1(CH), 122.6 (CH), 61.9 (CH), 47.0 ($CH_2$), 44.6 ($CH_2$), 39.6 ($CH_2$), 36.4 ($CH_2$), 33.9 (CH), 20.6 ($CH_3$), 19.0 ($CH_3$). ESMS: *m/z* = 455.4 $[M+H]^+$; HRMS (ES): Calcd for ($[M+H]^+$) 455.2407, found 455.2389; FT-IR (solid): $\nu_{max}$ $cm^{-1}$ = 3208w (b), 2957 (s), 2927 (s), 2858 (w), 2361 (s), 2342 (m), 1728 (s).

**_N_-(Benzylamino carbothiol) benzyloxycarbonyl amide**

**(49)**

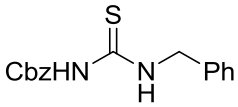


Compound **48** (0.80 g, 4.15 mmol) was dissolved in DCM (20 mL). Benzylamine (0.7 mL) was added under $N_2$ to the reaction mixture which was stirred overnight at room temperature. *In vacuo* drying of the reaction mixture and purification of the resulting crude product by column chromatography ($SiO_2$, DCM) afforded **49** (0.80 g, 64 %) as a white solid. MP = 56-58 °C; $^1$H NMR (300 MHz, $CDCl_3$): δ (ppm) = 9.8 (1 H, s, NH), 8.05 (1 H, s, NH), 7.23 (10 H, m, CH), 5.05 ( 2 H, s, $CH_2$), 4.74 (2 H, d, *J* = 5.5 Hz, $CH_2$); $^{13}$C NMR (75 MHz, $CDCl_3$): δ (ppm) = 179.1 (Cq), 152.4 (Cq), 136.2 (Cq) 134.4 (Cq), 128.9 (CH), 128.8 (CH), 128.3 (CH), 128.0 (CH), 127.9 (CH), 68.3 ($CH_2$), 49.7 ($CH_2$); ESMS: *m/z* = 301 $[M+H]^+$; HRMS (ES): Calcd for $C_{16}H_{16}N_2NaO_2S$ ($[M+Na]^+$) 323.0827, found 323.0827; FT-IR (solid): $\nu_{max}$ $cm^{-1}$ = 3689 (s), 3648 (s), 2563 (w), 1740 (s).

**Methyl 3-(6-((3-benzyl-2-((benzyloxy) carbonyl)guanidino)methyl)picolinamido)propanoate (50)**

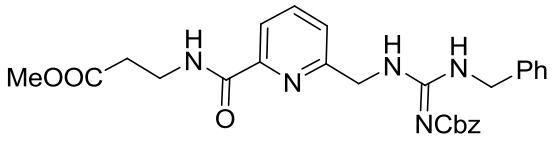


Compound **37** (0.50 g, 1.90 mmol) was dissolved in DCM (50 mL). $Et_3N$ (520 μL, 3.80 mmol) and EDC.HCl (0.73 g, 3.99 mmol) were added and the reaction mixture was stirred until it formed a clear solution. Compound **49** (*N*-(benzylamino carbothioyl) benzyloxycarbonyl amide) (0.52 g, 1.91 mmol) was added and the

reaction mixture was further stirred for 48 hrs at room temperature. *In vacuo* drying of the reaction mixture and purification of the resulting crude material by column chromatography ($SiO_2$, 3:100 MeOH/DCM) afforded **50** (0.43 g, 50%) as a white solid. MP = 74-76 °C; $^1$H NMR (300 MHz, $CDCl_3$): δ (ppm) = 10.45 (1 H, s, NH), 8.67 (1 H, s, NH), 7.76 (1 H, d, *J* = 8.1 Hz , CH), 7.52 (1 H, t, *J* = 8.1 Hz, CH), 7.09 (11 H, m, CH), 6.05 (1 H, s, NH), 4.97 (2 H, s, $CH_2$), 4.41 (4 H, m, 2 x $CH_2$), 3.52 (2 H, d, *J* = 6.5 Hz, $CH_2$), 3.44 (3 H, s, $CH_3$), 2.60 (2 H, t, *J* = 6.9 Hz, $CH_2$); $^{13}$C NMR (75 MHz, $CDCl_3$): δ (ppm) = 172.3 (Cq), 164.1 (Cq), 160.0 (Cq), 153.2 (Cq), 148.5 (Cq), 138.1 (Cq), 137.5 (CH), 128.6 (CH), 128.3 (CH), 128.1 (Cq), 127.7 (CH), 127.6 (CH), 127.3 (CH), 124.1 (CH), 120.7 (CH), 66.6 ($CH_2$), 51.7 ($CH_3$), 45.2 ($CH_2$), 44.9 ($CH_2$), 35.3 ($CH_2$), 33.8 ($CH_2$); ESMS: *m*/*z* = 526.3 $[M+Na]^+$, 1007.8 $[M+2Na]^+$; HRMS (ES): Calcd for $C_{27}H_{30}N_5O_5$ ($[M+H]^+$) 504.2247, found 504.2242; FT-IR (liquid): $\nu_{max}$ $cm^{-1}$ = 3355 (w), 3249 (w), 2359 (w), 2341 (w), 1733 (s), 1723 (s), 1668 (m), 1668 (m).

**3-(6-((3-Benzyl-2-((benzyloxy)carbonyl)guanidino)methyl)picolinamido)propanoic acid (50a)**

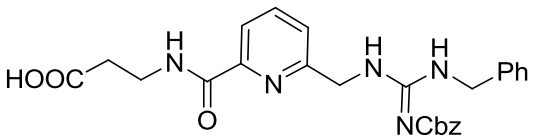


Compound **50** (0.40 g, 0.80 mmol) was dissolved in dry THF (25 mL) and added to a suspension of $Me_3SiOK$ (0.14 g, 1.04 mmol) in THF (25 mL) under $N_2$ which was stirred overnight at room temperature. DCM (50 mL) and $H_2O$ (50 mL) were added and the reaction mixture was cooled to 0 °C. Citric acid (0.1 M aqeous) was added until the pH was 6-7 and further stirred for 1 hr. *In vacuo* removal of the organic solvent and purification of the resulting crude by column chromatography ($SiO_2$, 1:50 → 1:20 MeOH/DCM) afforded **50a** (0.3 g, 77%) as a white solid. MP = 156-158 °C; $^1$H NMR (300 MHz, $CDCl_3$): δ (ppm) = 9.00 (1 H, s, NH), 8.49 (1 H, s, NH), 7.91 (1 H, d, *J* = 8.5 Hz , CH), 7.5 (1H, t, *J* = 7.7 Hz, CH), 7.27-7.22 (11 H, m, CH), 5.05 (2 H, s, $CH_2$), 4.46 (2 H, s, $CH_2$), 3.58 (2 H, m, $CH_2CH_2NH$), 2.53 (2 H, t, *J* = 6.9 Hz, $HOOCCH_2$), 1.38 (2 H, s, $CH_2$);$^{13}$C NMR (75 MHz, $CDCl_3$): δ(ppm) = 164.0 (Cq) , 149.0 (Cq) ,137.0 (CH), 128.9 (CH), 128.4 (CH), 127.9 (CH), 127.8 (CH), 127.2 (CH), 124.3 (CH), 67.0 ($CH_2$), 45.7 ($CH_2$), 45.3 ($CH_2$), 35.3 ($CH_2$), 34.3 ($CH_2$);

ESMS: *m/z* = 490 $[M+H]^+$; HRMS (ES): Calcd for $C_{26}H_{28}N_5O_5$ ($[M+H]^+$) 490.2090, found 490.2088; FT-IR (solid): $\nu_{max}$ $cm^{-1}$ = 3566 (w), 1714 (s), 1734 (s), 1717 (m), 1065 (m).

**3-(6-((3-benzylguanidino)methyl)picolinamido)propanoic acid (45)**

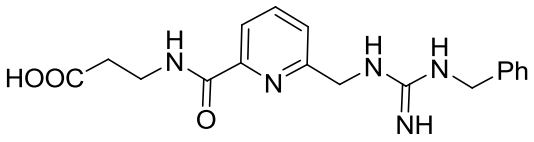


Compound **50a** (90 mg, 0.2 mmol) was dissolved in MeOH (20 mL). Pd/C (20 mg) was added and the reaction mixture was stirred for 48 hrs under $H_2$ (1 atm) at room temperature. The reaction mixture was filtered through celite and dried *in vacuo.* Purification of the resulting solid by precipitation from MeOH using $Et_2O$ afforded **45** (65 mg, 92%) as a white solid. MP = 276-278 °C; $^1$H NMR (300 MHz, DMSO): δ (ppm) = 10.34 (1 H, s, NH), 10.13 (1 H, s, NH), 8.18 (1 H, t, *J* = 5 Hz, CH), 8.11 (1 H, d, *J* = 5.0 Hz, CH), 7.68 (1 H, d, *J* = 5.0 Hz , CH), 7.55-7.46 (5 H, m, CH), 4.81 (2 H, s, $CH_2$), 4.62 (2 H, s, $CH_2$), 3.70 (2 H, t, *J* = 5.0 Hz, COOHC$H_2$), 2.50 (2 H, t, *J* = 5.0 Hz, $CH_2CH_2$NH); $^{13}$C NMR (75 MHz, DMSO): δ (ppm) = 181.2 (Cq), 176.6 (Cq), 163.3 (Cq), 156.7 (Cq), 149.7 (Cq), 138.8 (CH), 138.2 (Cq), 128.5 (CH), 127.3 (CH), 127.2 (CH), 124.0 (CH), 120.3 (CH), 45.5 ($CH_2$), 44.1 ($CH_2$), 38.5 ($CH_2$), 37.1 ($CH_2$); ESMS: *m/z* = 356 $[M+H]^+$; HRMS (ES): Calcd for $C_{18}H_{22}N_5O_3$ ($[M+H]^+$) 356.1723, found 356.1713; FT-IR (solid): $\nu_{max}$ $cm^{-1}$ = 3689 (s), 3675 (s), 3628 (b),1739 (m) ,1734 (s).

**(R)-Methyl 2-(6-((3-benzyl-2-((benzyloxy)carbonyl)guanidino)methyl)picolinamido)-3-Methylbutanoate (51)**

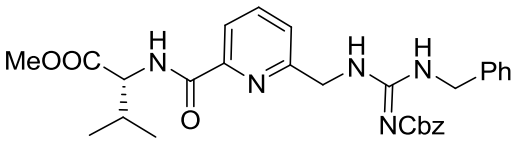


Compound **38** (0.90 g, 3.39 mol) was dissolved in DCM (15 mL). $Et_3N$ (0.1 mL), EDC.HCl (55 mg, 0.30 mmol) and **49** (67.5 mg, 0.2 mmol) were added successively

to the reaction mixture which was stirred for 3 days at room temperature. *In vacuo* drying of the reaction mixture and purification of the resulting crude by column chromatography ($SiO_2$, DCM → 3:100 MeOH/DCM) afforded **51** (1.35 g, 75% yield) as a white oily liquid. $^1$H NMR (300 MHz, $CDCl_3$): δ (ppm) = 10.20 (1 H, s, NH), 9.42 (1 H, s, NH), 8.35 (1 H, d, *J* = 9.8 Hz , CH), 7.98 (1 H, d, *J* = 8.1 Hz, CH), 7.72 (1 H, t, *J* = 8.5 Hz, CH), 7.34-7.18 (10 H, m , CH), 5.75 (1 H, s, NH), 5.05 (2 H, s, $CH_2$), 4.60 (3 H, m, C*H*CH$(CH_3)_2$ + $CH_2$), 4.49 (2 H, s, $CH_2$), 3.65 (3 H, s, COOC*H*$_3$ ), 2.20 (1 H, m, CHC*H*$(CH_3)_2$), 0.89 (3 H, d, *J* = 4.6 Hz, CH(C*H*$_3)_2$), 0.86 (3 H, d, *J* = 4.6 Hz, CH(C*H*$_3)_2$); $^{13}$C NMR (75 MHz, $CDCl_3$): δ(ppm) = 172.4 (Cq), 164.2 (Cq), 163.8 (Cq), 160.0 (Cq), 148.8 (Cq), 138.4 (CH), 137.5 (Cq), 128.9 (CH), 128.3 (CH), 128.0 (CH), 127.7 (CH), 127.5 (CH), 124.6 (CH), 121.4 (CH), 66.6 ($CH_2$), 57.4 (CH), 52.2 ($CH_3$), 45.4 ($CH_2$), 31.6 (CH), 19.1 ($CH_3$), 18.1 ($CH_3$); ESMS: *m/z* = 532 $[M+H]^+$; HRMS (ES): Calcd for $C_{29}H_{34}N_5O_5$ ($[M+H]^+$) 532.2560, found 532.2548; FT-IR (liquid): $\nu_{max}$ $cm^{-1}$ = 1713 (s), 1662 (m), 1523 (m).

**(Benzyl N-(3-benzylamino)-6-{[(2-hydroxycarbonyl)-isopropyl-1-amino] carbonyl}-[(2-pyridylmethyl) amino] methylenecarbamate) (51a)**

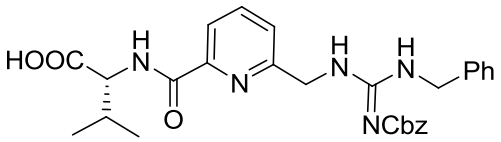


Compound **51** (0.35 g, 0.66 mmol) was dissolved in dry THF (25 mL) and added to a suspension of $Me_3SiOK$ (85 mg, 0.66 mmol) in THF (25 mL) which was stirred overnight at room temperature under $N_2$. DCM (50 mL) and $H_2O$ (50 mL) were added and the reaction mixture was cooled to 0 °C. Citric acid (0.1 M aqeous) was added dropwise until the pH was 6-7 and further stirred for 1 hr. *In vacuo* removal of the organic solvent and purification the resulting crude by column chromatography ($SiO_2$, 1:50 → 1:20 MeOH/DCM) afforded **51a** (0.15 g, 43%) as a white solid. MP =132-134 °C; $^1$H NMR (300 MHz, MeOD-*d*$_4$): δ (ppm) = 8.35 (1 H, d, *J* = 8.0 Hz, CH), 7.98 (1 H, d, *J* = 9.0 Hz, CH), 7.72 (1 H, t, *J* = 9.0 Hz, CH), 7.34-7.18 (10 H, m , CH), 5.05 (2 H, s, $CH_2$), 4.60 (2 H, s, $CH_2$), 4.49 (2 H, s, $CH_2$), 4.39 (1 H, d, *J* = 5.7 Hz, HOOCC*H*NH), 2.20 (1 H, m, C*H*$(CH_3)_2$), 0.91 (3 H, d, *J* = 2.5 Hz, CH(C*H*$_3)_2$), 0.89 (3 H, d, *J* = 2.5 Hz, CH(C*H*$_3)_2$); $^{13}$C NMR (75 MHz, MeOD-*d*$_4$) δ(ppm): 165.6 (Cq),

150.1 (Cq), 139.6 (CH) ,138.6 (Cq), 129.7 (CH), 129.4 (CH), 128.8 (CH), 128.4 (CH), 125.6 (CH), 121.8 (CH), 68.3 ($CH_2$), 60.4 (CH), 46.7 ($CH_2$), 46.0 ($CH_2$), 32.8 (CH), 20.1 ($CH_3$), 18.6 ($CH_3$); ESMS: *m/z* = 518.3 $[M+H]^+$; FT-IR (solid): $\nu_{max}$ $cm^{-1}$ = $cm^{-1}$ 3296 (w) (b), 1729 (m), 1599 (m), 733 (s).

**(R)-2-(6-((3-Benzylguanidino)methyl)picolinamido)-3-methylbutanoic acid (46)**

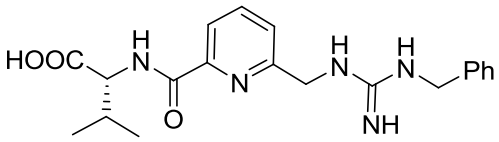


Compound **51a** (0.30 g, 0.58 mmol) was dissolved in MeOH (30 mL). Pd/C (64 mg) was added and the reaction mixture was stirred for 48 hrs at room temperature under hydrogen (1 atm). The reaction mixture was filtered through celite and dried *in vacuo.* Purification of the resulting solid by precipitation from MeOH using $Et_2O$ afforded **46** (110 mg, 50%) as a white solid. MP = 260-262 °C; $[\alpha]_D^{25}$ = -5.0 $^o$ (*c* 0.43, MeOH); $^1$H NMR (300 MHz, MeOD-*d*$_4$): δ (ppm) = 7.95 (1 H, t, *J* = 5 Hz, CH ), 7.90 (1 H, t, *J* = 6.0 Hz , CH), 7.43 (1 H, d, *J* = 6.0 Hz, CH) 7.28-7.21 (5 H, m, CH ), 4.60 (2 H, s, $CH_2$), 4.42 (2 H, s, $CH_2$), 4.34 (1 H, d, *J* = 4.0 Hz, HOOCC*H*NH), 2.19 (1 H, m, C*H*$(CH_3)_2$), 0.92 (3 H, d, *J* = 5.8 Hz, CH(C*H*$_3$)$_2$), 0.90 (3 H, d, *J* = 5.8 Hz, CH(C*H*$_3$)$_2$); $^{13}$C NMR (75 MHz, MeOD-*d*$_4$): δ (ppm) = 177.0 (Cq), 164.2 (Cq), 157.4 (Cq), 155.3 (Cq), 150.0 (Cq), 138.9 (CH), 136.7 (Cq), 128.9 (CH), 128.0 (CH), 127.3 (CH), 124.6 (CH), 121.2 (CH), 60.5 (CH), 45.7 (CH), 45.2 ($CH_2$), 32.5 ($CH_2$), 19.2 ($CH_3$), 17.6 ($CH_3$); ESMS: *m/z* = 384.4 $[M+H]^+$; HRMS (ES): Calcd for $C_{20}H_{26}N_5O_3$ ($[M+H]^+$) 384.2035, found 384.2036; FT-IR (solid): $\nu_{max}$ $cm^{-1}$ = 3188 (w) (b), 1651 (s), 1393 (m).

**(R)-Methyl 2-(6-(((tert-butoxycarbonyl)amino)methyl)picolinamido)-4-methylpentanoate (54)**

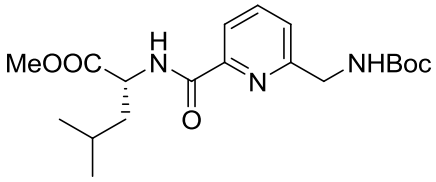

Experimental

Compound **35** (1.20 g, 4.76 mmol) was dissolved in DCM (30 mL). *i*$Pr_2$EtN (2.9 mL, 16.68 mmol), EDC.HCl (2.2 g, 12.02 mmol), HOBt (1.9 g, 14.07 mmol) and L-Leu-methyl ester (1.10 g, 6.05 mmol) were added successively and the resulting solution was stirred at room temperature for 72 hrs. DCM (20 mL) and aq. 1M $KHSO_4$ (20 mL) were added to the reaction mixture. The organic layer was separated, washed with sat. $Na_2CO_3$ (20 mL) and brine (20 mL) successively, and dried over $MgSO_4$. *In vacuo* removal of solvents and purification of the resulting crude product by column chromatography ($SiO_2$, 1:50 MeOH/DCM) afforded **54** (1.30 g, 71%) as a white solid. MP = 68 $^oC$ - 70 $^oC$; $^1H$ NMR (400 MHz, $CDCl_3$): δ (ppm) = 8.31 (1 H, d, *J* = 5.0 Hz, CHN*H*), 8.07( 1 H, d, *J* = 5.0 Hz, CH ), 7.82 (1 H, t, *J* = 5.0 Hz ,CH), 7.44 (1 H, d, *J* = 5.0 Hz, CH), 5.32(1H, s, N*H*Boc), 4.82-4.86 (1 H, m, $(CH_3)_2CHCH$), 4.49 (2 H, d, *J* = 5.0 Hz, $NHCH_2$ ), 3.77 (3 H, s, $COOCH_3$ ), 1.70-1.80 (3 H, m, $(CH_3)_2CHCH_2CH$ + $(CH_3)_2CHCH_2CH$), 1.46 (9 H, s, $NHCOO(CH_3)_3$, 0.98 (3 H, d, *J* = 5.0 Hz, $CH(CH_3)_2$, 0.96 (3 H, d, *J* = 5.0 Hz, $CH(CH_3)_2$; $^{13}C$ NMR (100 MHz, $CDCl_3$): δ(ppm) = 173.6 (Cq), 164.2 (Cq), 157.5 (Cq), 156.3 (Cq), 149.1 (Cq) , 138.4 (CH), 124.6(CH), 121.3 (CH), 80.1 (Cq), 52.6 (CH), 51.1 (CH), 46.0 ($CH_2$), 41.9 ($CH_2$), 28.7 ($CH_3$ ), 25.3 ($CH_3$ ), 23.2 ($CH_3$ ), 22.2 ($CH_3$); MSES: *m/z* = 402.2 $[M+Na]^+$; HRMS (ES): Calcd for $C_{19}H_{29}N_3NaO_5$ 402.2005 ($[M+Na]^+$), found 402.2004; FT-IR (solid): $\nu_{max}$ $cm^{-1}$ = 3018 (w), 1671(m), 1518 (m), 1214(s), 745(s).

**(R)-Methyl 2-(6-(aminomethyl)picolinamido)-4-methylpentanoate (54a)**

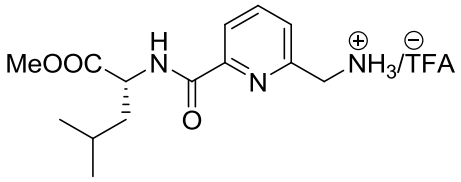


Compound **54a** (1.20 g, 3.16 mmol) was stirred in 20% v/v TFA/DCM (25 mL) at room temperature for 3h. *In vacuo* drying of the reaction mixture after the addition of toluene (3 x 3 mL) followed from precipitation by diethyl ether afforded the TFA salt of the target compound (1.20 g, quantitative yield) as a white solid compound. MP = 102-104 $^oC$ $^1H$ NMR (400 MHz, $CDCl_3$): δ (ppm) = 8.96 (1 H, d, *J* = 5.0 Hz, CHN*H*), 8.66 (1 H, s(b), $NH_2$), 8.09( 1 H, d, *J* = 5.0 Hz, CH), 7.83 (1 H, t, *J* = 5.0 Hz, CH), 7.35(1 H, d, *J* = 5.0 Hz, CH), 4.83-4.88 (1 H, m, CHC*H*(COOMe)NH ), 3.76 (3 H, s, $COOCH_3$), 3.49 (3 H, s, $NHCH_2$), 1.90-1.94 (1 H, m, $(CH_3)_2CHCH_2CH$ ), 1.71-1.74

(2 H, m, $CH_3)_2CHCH_2CH$), 0.91-0.96 (6 H, m, 2 x $CH(CH_3)_2$; $^{13}C$ NMR (100 MHz, $CDCl_3$): δ(ppm) = 176.2 (Cq), 164.6 (Cq), 151.3 (Cq), 149.4 (Cq), 139.1 (CH), 125.4 (CH), 123.0 (CH), 53.0 (CH), 51.6 (CH), 43.65 ($CH_2$), 40.4 ($CH_2$), 25.3 ($CH_3$), 23.0 ($CH_3$), 21.6 ($CH_3$).

**(R)-Methyl 2-(6-((3-(3-(benzylamino)-3-oxopropyl)-2-((benzyloxy)carbonyl)guanidino)methyl)picolinamido)-4-methylpentanoate (55)**

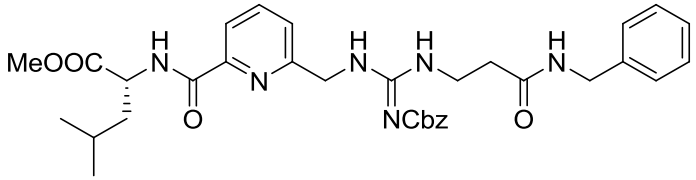


Compound **54a** (0.90 g, 3.20 mmol) was dissolved in DCM (50 mL). $Et_3N$ (1.40 mL, 9.6 mmol) and EDC.HCl (1.5 g, 8.0 mmol) were added to the reaction mixture which was stirred until it formed a clear solution. Compound **42** (1.20 g, 3.20 mmol) was added and the reaction mixture was further stirred for 24 hrs at room temperature. *In vacuo* removal of the solvent and purification of the resulting crude by column chromatography ($SiO_2$, 1:50 MeOH/DCM) afforded **55** (1.20 g, 61%) a white solid. MP = 60-62 ˚C; $^1H$ NMR (400 MHz, $CDCl_3$): δ (ppm) = 10.29 (1 H, s, NH), 9.27 (1 H, s, NH), 9.12 (1 H, s, NH), 8.71 (1 H, s, NH), 8.12 (1 H, s, CH), 7.83 (1 H, s , CH), 7.23-7.29 (11 H, m, CH), 5.13 (2 H, s, $CH_2$), 4.86-4.88 (1 H, m, CH), 4.66 (2 H, d, *J* = 5.0 Hz, $CH_2$), 4.36 (2 H, s, $CH_2$), 3.69 (5 H, m, $CH_2$ + $CH_3$), 2.52 (2 H, s, $CH_2$), 1.73-1.91 (3 H, m, $(CH_3)_2CHCH_2CH$ + $(CH_3)_2CHCH_2CH$), 0.93-0.96 (6 H, m, $CH(CH_3)_2$; $^{13}C$ NMR (100 MHz, $CDCl_3$): δ (ppm) = 173.5 (Cq), 172.1 (Cq), 164.0 (Cq), 148.8 (Cq),138.4 (Cq), 137.9 (Cq), 129.1 (CH), 128.6 (CH), 127.9 (CH), 127.9 (CH), 127.6 (CH), 127.5 (CH), 124.4 (Cq), 121.8 (Cq), 66.7 ($CH_2$), 52.2 ($CH_3$), 50.9 (CH), 45.6 ($CH_2$), 43.6 ($CH_2$), 40.8 ($CH_2$), 37.6 ($CH_2$), 24.9 (CH), 23.0 ($CH_3$), 21.7 ($CH_3$); MSES: *m*/*z* = 617.4 $[M+H]^+$; HRMS (ES): Calcd for $C_{33}H_{40}N_6NaO_6$ 617.3087, ($[M+Na]^+$), found 617.3076; FT-IR (solid): $\nu_{max}$ $cm^{-1}$ = 3308 broad, 2955 (w), 2360 (m), 1745 (m), 1635 (s), 1520 (s).

**(R)-2-(6-((3-(3-(Benzylamino)-3-oxopropyl)-2-((benzyloxy)carbonyl)guanidino)methyl)picolinamido)-4-methylpentanoic acid (56)**

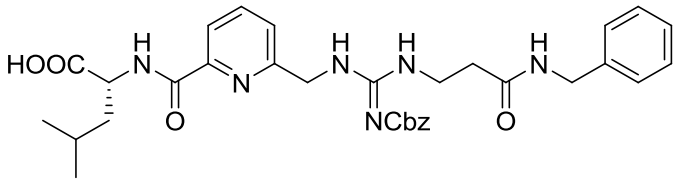


Compound **55** (1.1 g, 1.8 mmol) was dissolved in THF (40 mL) and added to $Me_3SiOK$ (0.35 g, 2.7 mmol) suspended in THF (30 mL) under nitrogen. After overnight stirring, DCM (30 mL) and $H_2O$ (20 mL) were added and the reaction mixture was cooled to 0 ˚C. Citric acid (0.1 M) was added dropwise until the pH was 6-7. *In vacuo* drying of the organic phase and purification of the resulting crude by column chromatography ($SiO_2$, 1:20 MeOH/DCM) afforded **56** (0.80 g, 74%) as a white solid. MP = 104-106 ˚C; $^1$H NMR (400 MHz, DMSO-$d_6$): δ (ppm) = 12.80 (1 H, s(b), COOH), 10.21 (1 H, s, NH), 9.04 (1 H, s(b), NH), 8.72 (1 H, d, *J* = 5.0 Hz, CH), 8.49 (1 H, s, NH), 7.96 (1 H, s, NH), 7.55 (1 H, d, *J* = 2.5 Hz, CH), 7.18-7.31 (11 H, m, CH), 4.98 (2 H, s, $CH_2$), 4.61 (2 H, d, *J* = 2.5 Hz, $CH_2$), 4.53-4.55 (1 H, m, $(CH_3)_2CHCH_2CH$), 4.27-4.28 (2 H, d, *J* = 2.5 Hz, $CH_2$), 3.53 (2 H, d, *J* = 2.5 Hz, $CH_2$), 2.46 (2 H, s, $CH_2$), 1.64-1.85 (3 H, m, $(CH_3)_2CHCH_2CH$ + $(CH_3)_2CHCH_2CH$), 0.85-0.98 (6 H, m, $CH(CH_3)_2$; $^{13}$C NMR (100 MHz, DMSO-$d_6$): δ (ppm) = 174.2 (Cq), 171.0 (Cq), 163.9 (Cq), 160.1 (Cq), 139.9 (Cq), 138.2 (Cq), 128.7 (CH), 128.7 (CH), 128.2 (CH), 128.0 (CH), 127.7 (CH), 127.2 (CH), 66.0 ($CH_2$), 50.9 (CH), 45.5 ($CH_2$), 42.5 ($CH_2$), 40.4 ($CH_2$), 37.7 ($CH_2$), 35.9 ($CH_2$), 25.0 (CH), 23.3 ($CH_3$), 21.8 ($CH_3$); MSES: *m*/*z* = 603.3 $[M+H]^+$; HRMS (ES): Calcd for $C_{32}H_{38}N_6NaO_6$ 603.2933, ($[M+Na]^+$), found 603.2933; FT-IR (solid): $\nu_{max}$ $cm^{-1}$ = 3246 (b), 1635 (m), 1593 (s), 1386 (m).

**(R)-2-(6-((3-(3-(Benzylamino)-3-oxopropyl)guanidino)methyl)picolinamido)-4-methylpentanoic acid**

**(53)**

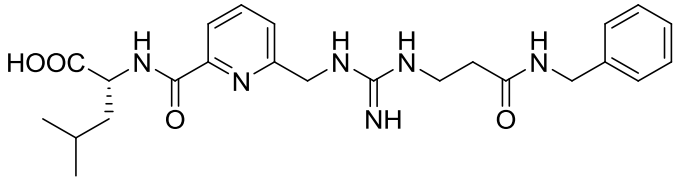


Compound **56** (0.2g, 0.33mmol) was dissolved in MeOH (30 mL). Pd/C (35 mg, 0.33 mmol) was added and the reaction mixture was stirred for 5 hrs at room temperature under hydrogen (1 atm). The reaction mixture was filtered through celite and dried *in vacou* to give **53** (0.15 mg, 97%) as a white solid. MP = 204-206 ˚C; $[\alpha]_D^{25}$ =-2.4 $^o$ (*c* 0.2, MeOH); $^1$H-NMR (400 MHz, MeOD-$d_4$): δ(ppm): 7.99-7.91 (2 H, m, CH), 7.49 (1 H, t, *J* = 7.52 Hz, CH), 7.26-7.17 (5 H, m, CH), 4.58 (2 H, s, PhC*H*$_2$NHCO), 4.56 (1 H, m, NHC*H*COOH), 4.35 (2 H, s, C*H*$_2$NHCNH), 3.56 (2 H, overlap with water peak, NHC*H*$_2$CH$_2$CO), 2.60 (2 H, t, *J* = 6.52 Hz, NHCH$_2$C*H*$_2$CO), 1.80-1.75 (1 H, m, (CH$_3$)$_2$C*H*), 1.74-1.66 (2 H, m, (CH$_3$)$_2$CHC*H*$_2$), 0.96 (6 H, m, 6.0 Hz, CH(C*H*$_3$)$_2$). $^{13}$C-NMR (100 MHz, MeOD-$d_4$): δ(ppm) = 176.7 (Cq), 170.7 (Cq), 162.8 (Cq), 157.3 (Cq), 156.2 (Cq), 150.1 (Cq), 139.8 (CH), 138.7 (Cq), 128.7 (CH), 127.6 (CH), 127.1 (CH), 124.10 (CH), 120.6 (CH), 53.4 (CH), 45.7 (CH$_2$), 43.2 (CH$_2$), 42.8 (CH$_2$), 38.3 (CH$_2$), 34.5 (CH$_2$), 24.7 (CH), 22.8 (CH$_3$), 22.7 (CH$_3$); MSES: *m*/*z* = 469.4 $[M + H]^+$; HRMS ($ES^+$): Calcd for $[M + H]^+$ $C_{24}H_{33}N_6O_4$ 469.2563; found: 469.2562. FT-IR (solid): $\nu_{max}$ cm$^{-1}$ = 3232 (b), 1651 (s), 1538 (s), 1392 (s).

**(R)-Methyl 2-(4-(2-((tert-butoxycarbonyl)amino)-4-methylpentanamido)phenyl)acetate**
**(62)**

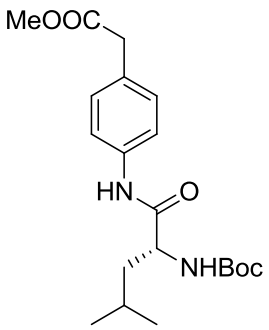

Experimental

Compound **61** (1.3 g, 7.88 mmol) was dissolved in DCM (50 mL). *i*$Pr_2$NEt (2.4 mL, 13.80 mmol), EDC.HCl (1.88 g, 9.82 mmol), HOBt (1.60 g, 11.85 mmol) and Boc-Leu-OH (0.90 g, 3.92 mmol) previously dissolved in DCM (25 mL) and DMF (1 mL), were added successively and the resulting solution was stirred at room temperature for 72 hrs. DCM (40 mL) and aq. 1M $KHSO_4$ (30 mL) were added to the reaction mixture. The organic layer was separated, washed with sat. $Na_2CO_3$ (30 mL) and brine (30 mL) successively, and dried over $MgSO_4$. *In vacuo* drying and purification of the resulting crude by column chromatography ($SiO_2$, 1:100 MeOH/DCM) afforded **62** (1.20 g, 72%) as an orange solid. MP = 46-50 ˚C; $^1$H NMR (300 MHz, DMSO-$d_6$): δ (ppm) = 9.91 (1 H, s, NH), 7.53 (2 H, d, *J* = 9.6 Hz, CH), 7.18 (2 H, d, *J* = 9.6 Hz, CH), 6.70 (1 H, d, *J* = 8.7 Hz, NH), 4.15 (1 H, m, C*H*$(CH_3)_2$), 3.59-3.61 (5 H, m, $CH_2$ + $CH_3$), 1.69 (1 H, m, $CH_2$C*H*), 1.37 (9 H, s, C(C*H*$_3)_3$, 0.95-0.98 (6 H, m, CH(C*H*$_3)_2$); $^{13}$C NMR (100 MHz, DMSO-$d_6$): δ (ppm) = 171.7 (Cq), 137.9 (Cq), 129.6 (Cq), 129.1 (Cq), 119.3 (CH), 78.0 (Cq), 51.6 (CH), 40.6 ($CH_2$), 39.5 ($CH_2$), 28.2 ($CH_3$), 28.1 ($CH_3$), 24.3 ($CH_3$), 22.9 ($CH_3$), 21.6 (CH); MSES: *m*/*z* = 401.20 $[M+Na]^+$, 779.5 $[2M+Na]^+$; HRMS (ES): Calcd for $C_{20}H_{30}N_2NaO_5$ 401.2053 ($[M+Na]^+$), found 401.2046; FT-IR (solid): $\nu_{max}$ $cm^{-1}$ = 3294 (w), 2956 (w), 1738 (s), 1662 (s), 1158 (s).

Compound **63**

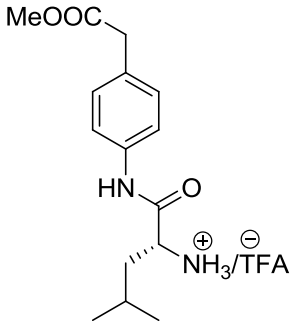


Compound **62** (1.6 g, 0.15 mmol) was dissolved in DCM (10 mL). 20% (v/v) TFA/DCM (5 mL) was added and the resulting solution was stirred for 5 hrs at room temperature. *In vacuo* drying of the reaction mixture after the addition of toluene (3 x 2 mL) afforded **63** (1.6 g, 100%) as a yellowish oily compound which was used for the next step with no further purification.

**(R)-Methyl 2-(4-(2-(4-(((tert-butoxycarbonyl)amino)methyl)benzamido)-4-methylpentanamido)phenyl)acetate**

**(64a)**

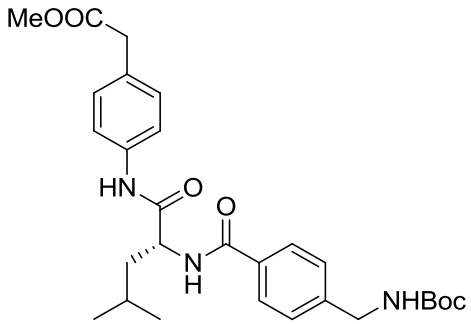


4-(*tert*-Butoxycarbonylamino-methyl)-benzoic acid (0.80 g, 3.19 mmol) was dissolved in DCM (50 mL). *i*$Pr_2$NEt (1.6 mL, 9.61 mmol), EDC.HCl (1.48 g, 7.97 mmol), HOBt (1.3 g, 9.6 mmol) and **63** (1.21 g, 3.22 mmol) were added successively and the resulting solution was stirred at room temperature for 48 hrs. DCM (40 mL) and aq 1M $KHSO_4$ (20 mL) were added to the reaction mixture. The organic layer was separated, washed with sat. $Na_2CO_3$ (20 mL) and brine (20 mL) successively, and dried over $MgSO_4$. *In vacuo* drying and purification of the resulting crude by column chromatography ($SiO_2$, 0.5:100 MeOH/DCM) afforded **64a** (1.60 g, 94%) as a white solid. MP = 68-70 $^oC$; $^1H$ NMR (300 MHz, DMSO-$d_6$): δ (ppm) = 8.94 (1 H, s, NH), 7.73 (2 H, d, *J* = 5.0 Hz, CH), 7.47 (2 H, d, *J* = 5.0 Hz, CH), 7.28 (2 H, d, *J* = 5.0 Hz, CH), 7.16 (2 H, d, *J* = 5.0 Hz, CH), 6.91 (1 H, d, *J* = 5.0 Hz, NH), 5.06 (1 H, s, NH), 4.85-4.91 (1 H, m, $CH_2CHNH$), 4.32 (2 H, d, *J* = 2.5 Hz, $CH_2NHBoc$), 3.65 (3 H, s, $CH_3COO$), 3.54 (2 H, s, $CH_2COOMe$), 1.70-1.88 (3 H, m, $(CH_3)_2CHCH_2CH$ + $(CH_3)_2CHCH_2CH$), 1.44 (9 H, s, $C(CH_3)_3$), 0.98-1.01 (6 H, m, $(CH_3)_2CH$); $^{13}C$ NMR (100 MHz, DMSO-$d_6$): δ (ppm) = 173.30 (Cq), 171.8 (Cq), 169.0 (Cq), 157.2 (Cq), 144.6 (Cq), 138.2 (Cq), 133.6 (Cq), 131.1 (Cq), 131.40 (CH), 128.8 (CH), 128.6 (CH), 122.4 (CH), 81.03 (Cq), 54.4 (CH), 53.3 ($CH_3$), 45.5 ($CH_2$), 41.1 ($CH_2$), 41.0 ($CH_2$), 28.8 ($CH_3$), 25.4 ($CH_3$), 23.3 ($CH_3$), 22.7 (CH); MSES: *m*/*z* = 534.3 $[M+Na]^+$, 1045.8 $[2M+Na]^+$; HRMS (ES): Calcd for $C_{28}H_{38}N_3O_6$ 534.2580 ($[M+H]^+$), found 534.2570; FT-IR (solid): $\nu_{max}$ $cm^{-1}$ = 3296(b), 1642 (s), 1522 (m), 1388 (s).

**(R)-(4-((1-((4-(2-Methoxy-2-oxoethyl)phenyl)amino)-4-methyl-1-oxopentan-2-yl)carbamoyl)phenyl)methanaminium**
**(64)**

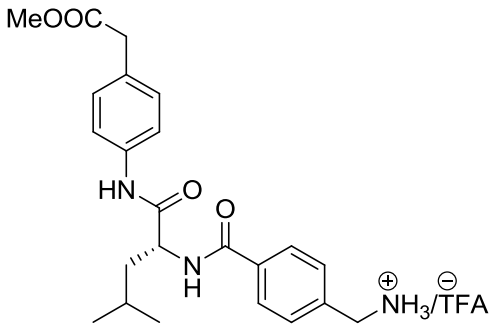


**64a** (1.60 g, 3.13 mmol) was dissolved in DCM (10 mL). 20% (v/v) TFA/DCM (10 mL) was added and the resulting solution was stirred for 5 hrs at room temperature. *In vacuo* drying of the reaction mixture after the addition of toluene (3 x 3 mL) afforded **64** (1.60, 100%) as a yellowish oily compound; $^{1}$H NMR (300 MHz, DMSO-$d_6$): δ (ppm) = 10.14 (1 H, s, NH), 8.63 (1 H, d, *J* = 5.0 Hz, CHN*H*CO), 8.30 (2 H, s(b), $NH_2$), 7.96 (2 H, d, *J* = 5.0 Hz, 2 x CH), 7.53-7.57 (4 H, m, 4 x CH), 7.19 (2 H, d, *J* = 5.0 Hz, 2 x CH), 4.63-4.69 (1 H, m, $CH_2CHNH$), 4.11 (2 H, s, $CH_2COOMe$), 3.60-3.61 (5 H, s, $CH_2NH_2$ + $CH_3COO$), 1.72-1.82 (2 H, m, $(CH_3)_2CHCH_2CH$) ), 1.59-1.72 (1 H, m, $(CH_3)_2CHCH_2$), 0.91-0.96 (6 H, m, $C(CH_3)_2$); $^{13}$C NMR (100 MHz, DMSO-$d_6$): δ (ppm) = 172.2 (Cq), 171.8 (Cq), 166.4 (Cq), 137.6 (Cq), 132.5 (Cq), 129.0 (CH), 129.0 (CH), 128.3 (CH), 119.8 (CH), 53.2 (CH), 52.1 (CH), 42.4 ($CH_2$), 40.6 ($CH_2$), 39.3 ($CH_2$), 23.8 ($CH_3$), 23.5($CH_3$), 21.1 (CH); MSES: *m*/*z* = 412.5 $[M+H]^+$; HRMS (ES): Calcd for $C_{23}H_{30}N_3O_4$ 412.2238 ($[M+H]^+$), found 412.2226; FT-IR (solid): $\nu_{max}$ $cm^{-1}$ = 3041 (w), 1779 (w), 1658 (m), 1144 (s).

**(S)-Methyl 2-(4-(2-(4-((6-((3-(3-(benzylamino)-3-oxopropyl)-2-((benzyloxy)carbonyl)guanidino)methyl)picolinamido)methyl)benzamido)-4-methylpentanamido)phenyl)acetate**
**(65)**

Experimental

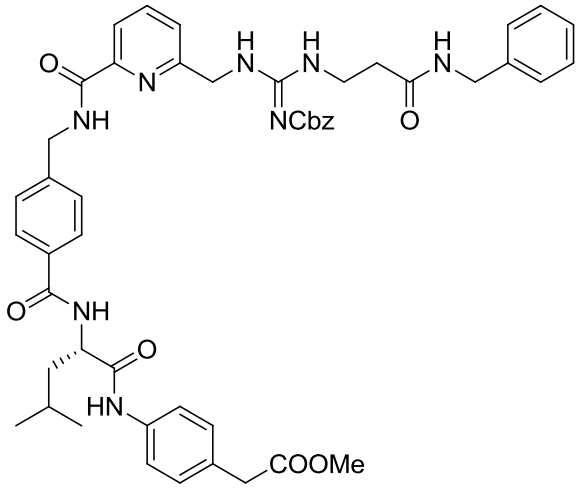


Compound **59** (0.52 g, 1.06 mmol) was dissolved in DCM (50 mL). *i*$Pr_2$NEt (0.6 mL, 3.71 mmol), EDC.HCl (0.48 g, 2.65 mmol), HOBt (0.43 g, 3.18 mmol) and **64** (0.48 g, 1.20 mmol) were added successively and the resulting solution was stirred at room temperature for 48 hrs. DCM (30 mL) and aq. 1M $KHSO_4$ (20 mL) were added to the reaction mixture. The organic layer was separated, washed with sat. aq. $Na_2CO_3$ (20 mL) and brine (20 mL), and dried over $MgSO_4$. *In vacuo* removal of the solvent and purification of the resulting crude product by column chromatography ($SiO_2$, 1:50 MeOH/DCM) afforded **65** (0.80 g, 75%) as a white solid. MP =128-130 ˚C;$^1$H NMR (300 MHz, DMSO-$d_6$): δ (ppm) = 10.08 (1 H, s, NH), 9.37 (1 H, apparent triplet, NH), 8.49 (2 H,d, *J* = 5.0 Hz, CH), 7.97 (2 H, s, 2 x NH), 7.86 (2 H, d, *J* = 7.5 Hz, CH), 7.55-7.57 (3 H, m, 3 x CH), 7.40 (2 H, d, *J* = 7.5 Hz, CH), 7.29-7.17 (12 H, m, CH), 4.89 (2 H, s, $CH_2$), 4.64-4.67 (1 H, m, $(CH_3)_2CHCH_2CH$)), 4.58 (4 H, m, 2 x $CH_2$), 4.26 (2 H, d, *J* = 2.5 Hz, $CH_2$), 3.61 (2 H, s, $CH_2$), 3.60 (3 H, s, $COOCH_3$), 3.51 (2 H, m, $CH_2$), 2.12 (2 H, s, $CH_2$), 1.70-1.81 (2 H, m, $(CH_3)_2CHCH_2CH$), 1.55-1.60 (1 H, m, $(CH_3)_2CHCH_2CH$), 0.90-0.94 (6 H, m, $(CH_3)_2CH$);$^{13}$C NMR (100 MHz, DMSO-$d_6$): δ (ppm) = 171.9 (Cq), 171.5 (Cq), 170.7 (Cq), 166.4 (Cq), 143.0 (Cq), 138.0 (Cq), 132.8 (Cq), 129.8 (CH), 128.4 (CH), 127.9 (CH), 127.4 (CH), 127.1 (CH), 126.9 (CH), 119.5 (CH), 65.6 ($CH_2$), 52.9 (CH), 51.8 (CH), 42.4 ($CH_2$), 42.3 ($CH_2$, 40.6 ($CH_2$), 37.4 ($CH_2$), 35.7 ($CH_2$), 24.7 ($CH_3$), 23.2 ($CH_3$), 21.7 ($CH_3$); MSES: *m*/*z* = 884.30 $[M+H]^+$; HRMS (ES): Calcd for $C_{49}H_{54}N_8NaO_8$ 905.3963 ($[M+Na]^+$), found 905.3941; FT-IR (solid): $\nu_{max}$ $cm^{-1}$ = 3289 (w), 1734 (w), 1632 (s), 1558 (m), 1312 (s).

Experimental

**(S)-2-(4-(2-(4-((6-((3-(3-(Benzylamino)-3-oxopropyl)-2-((benzyloxy)carbonyl)guanidino)methyl)picolinamido)methyl)benzamido)-4-methylpentanamido)phenyl)acetic acid**
**(66)**

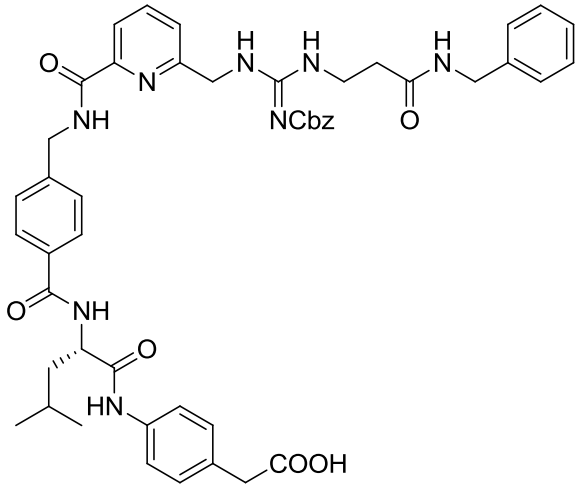


Compound **65** (0.6 g, 0.7 mmol) was dissolved in THF (25 mL) and added to $Me_3SiOK$ (0.35 g, 2.7 mmol) suspended in THF (25 mL) under an inert atmosphere. The reaction mixture was stirred overnight at room temperature. DCM (50 mL) and $H_2O$ (50 mL) were added and the reaction mixture was cooled to 0 ˚C. Citric acid (0.1 M aqeous) was added dropwise until the pH is 6-7 and further stirred for 1hr. *In vacuo* drying of the organic phase and purification of the resulting crude by column chromatography ($SiO_2$, 1:50 - 1:20 MeOH/DCM) afforded **66** (0.31 g, 60%) as a white solid. MP = 158 -160 ˚C; $^1$H NMR (400 MHz, DMSO-$d_6$): δ (ppm) = 10.06 (1 H, s, NH), 9.37 (1 H, t, *J* = 2.5 Hz, NH), 8.49 (2 H, d, *J* = 5.0 Hz, CH), 7.96 (2 H, s, NH), 7.85 (2 H, d, *J* = 5.0 Hz, CH), 7.53-7.56 (3 H, m, CH), 7.39 (2 H, d, *J* = 5.0 Hz, CH), 7.17-7.31 (12 H, m, CH), 4.88 (2 H, s, $CH_2$), 4.68-4.58 (5 H, m, 2 x $CH_2$ + CH), 4.25 (2 H, d, *J* = 5.0 Hz, $CH_2$), 3.49 (4 H, m, 2 x $CH_2$), 3.20 (2 H, overlap with water peak,$CH_2$), 1.74 (2 H, m, $(CH_3)_2CHCH_2CH$), 1.57 (1 H, m, $(CH_3)_2CH$), 0.90-0.94 (6 H, m, $(CH_3)_2CH$); $^{13}$C NMR (100 MHz, DMSO-$d_6$): δ (ppm) = 172.8 (Cq), 171.4 (Cq), 170.6 (Cq), 166.3 (Cq), 163.1 (Cq), 142.8 (Cq), 137.8 (Cq), 137.6 (Cq), 132.7 (Cq), 129.9 (CH), 129.6 (CH), 128.2 (CH), 127.7 (CH), 127.2 (CH), 127.0 (CH), 126.7 (CH), 119.3 (CH), 74.5 (CH), 65.9 ($CH_2$), 53.5 (CH), 45.6 ($CH_2$), 42.2 ($CH_2$ ), 42.1 ($CH_2$), 40.9 ($CH_2$), 40.6 ($CH_2$), 37.3 ($CH_2$), 24.6 ($CH_3$), 23.0 ($CH_3$), 21.5 (CH); MSES:

*m*/*z* = 870.8 $[M+H]^+$, 891.5 $[M+Na]^+$; HRMS (ES): Calcd for $C_{48}H_{53}N_8O_8$ 869.3986 ($[M+H]^+$), found 869.3959; FT-IR (solid): $\nu_{max}$ $cm^{-1}$ = 3273 (w), 1630 (w), 1508 (m).

**(S)-2-(4-(2-(4-((6-((3-(3-(Benzylamino)-3-oxopropyl)guanidino)methyl)picolinamido)methyl)benzamido)-4-methylpentanamido)phenyl)acetic acid**
**(57)**

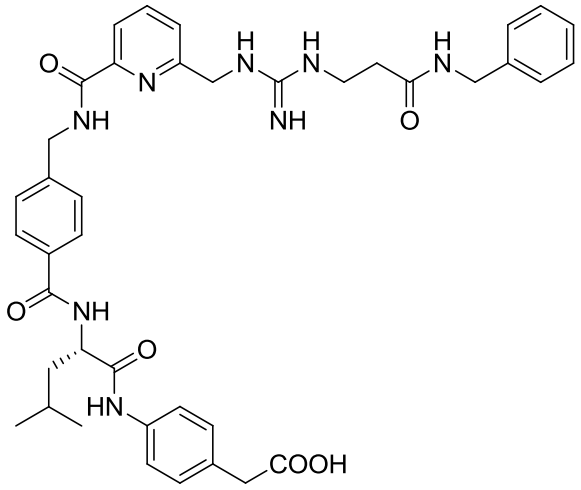


Compound **66** (100 mg, 0.12 mmol) was dissolved in MeOH (30 mL). Pd/C (30 mg, 0.12 mmol) was added and the reaction mixture was stirred for 4 hrs under hydrogen (1 atm) at room temperature. The reaction mixture was filtered through celite and dried *in vacuo*. Purification of the resulting solid by precipitation from $Et_2O$/MeOH afforded **57** (70 mg, 90%) as a white solid. MP > 250 ˚C; $[\alpha]_D^{25}$ =-5.4 $^o$ (*c* 0.2, MeOH); $^1$H NMR (300 MHz, DMSO-$d_6$): δ (ppm) = 10.09 (1 H, s, NH), 9.89 (1 H, broad, NH), 8.86 (1 H, broad, NH), 8.57 (2 H, s, NH), 7.96-8.03 (3 H, m, CH), 7.87 (2 H, d, *J* = 5.0 Hz, CH), 7.51 (3 H, t, *J* = 5.0 Hz, CH), 7.42 (2 H, d, *J* = 5.0 Hz, CH), 7.17-7.29 (4 H, m, CH), 7.14 (2 H, d, *J* = 5.0 Hz, CH), 4.56-4.68 (5 H, m, 2 x $CH_2$ + CH), 4.26 (2 H, d, *J* = 5.0 Hz, $CH_2$), 3.42 (4 H,overlap with water peak, 2 x $CH_2$), 2.46 (2 H, t, *J* = 5.0 Hz, $CH_2$), 1.68-1.74 (2 H, m, $(CH_3)_2CHCH_2CH$), 1.58 (1 H, m, $CH_3)_2CHCH_2$), 0.95-0.99 (6 H, m, $(CH_3)_2CH$); $^{13}$C NMR (100 MHz, DMSO-$d_6$): δ (ppm) = 171.2 (Cq), 170.1 (Cq), 166.2 (Cq), 163.7 (Cq), 156.3 (Cq), 154.5 (Cq), 149.2 (Cq), 143.0 (Cq), 139.2 (Cq), 139.1 (Cq), 138.6 (CH), 132.5 (Cq), 129.4 (CH), 128.2 (CH), 127.2 (CH), 127.1 (CH), 126.7 (CH), 124.2 (CH), 120.8 (CH), 119.1 (CH), 52.8 (CH), 45.3 ($CH_2$), 42.1 ($CH_2$), 41.5 ($CH_2$), 40.8 ($CH_2$), 37.6 ($CH_2$), 34.7 ($CH_2$), 24.6 ($CH_3$), 23.0 ($CH_3$), 21.5 (CH); (CH and Cq missing) MSES: *m*/*z* = 735.8 $[M+H]^+$, 757.6 $[M+Na]^+$;

HRMS (ES): Calcd for $C_{40}H_{47}N_8O_6$ 735.3618 ($[M+H]^+$), found 735.3603; FT-IR (solid): $\nu_{max}$ $cm^{-1}$ = 3274 (m) (broad), 1636 (s), 1539 (s).

**2-(2-(2-(2-Hydroxyethoxy)ethoxy)ethoxy)ethyl methanesulfonate (69)**

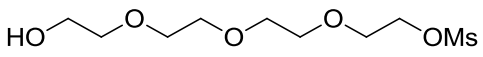


**68** (15.50 g, 80.00 mmol) was dissolved in THF (125 mL) under nitrogen. $Et_3N$ (11.2 mL, 80.00 mmol) was added and the reaction mixture was cooled down to 0 °C. Mesyl chloride (6.2 mL, 80.00 mmol) was added dropwise to the reaction mixture over a period of 10 mins. The reaction mixture was stirred at 0 °C for 2 hrs and then warmed to room temperature and left overnight. The resulting precipitate was filtered and washed with ethyl acetate. *In vacuo* concentration of the filtrate and purification of the resulting crude product by column chromatography ($SiO_2$, 4:1 EA:Hexane - EA) afforded **69** (7.0 g, 50%) as a clear oil. $^1$H NMR (300 MHz, $CDCl_3$): δ (ppm) = 4.39 - 4.36 (2 H, m, $CH_2$), 3.78-3.58 (14 H, m, $CH_2$), 3.07 (3 H, s, $CH_3$), 2.50 (2 H, s, OH); $^{13}$C NMR (100 MHz, $CDCl_3$): δ (ppm) = 72.3 ($CH_2$), 71.1 ($CH_2$), 71.1 ($CH_2$), 71.0 ($CH_2$), 71.0 ($CH_2$), 70.9 ($CH_2$), 70.4 ($CH_2$), 59.4 ($CH_3$), 51.1 ($CH_2$); MSES: *m/z* = 295.1 $[M+Na]^+$; FT-IR (liquid): $\nu_{max}$ $cm^{-1}$ = 3440 (w) (br), 2872 (m), 1346 (s), 1171 (s), 1103 (s).

**2-(2-(2-(2-Azidoethoxy)ethoxy)ethoxy)ethanol (70)**

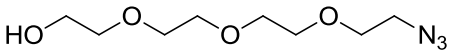


Compound **69** (7.0 g, 25.74) was dissolved in acetonitrile (50 mL) and stirred under nitrogen. $NaN_3$ (2.5 g, 38.17 mmol) was added and the reaction mixture was further stirred under reflux for 48 hrs. Water (60 mL) was added and the solution was extracted with DCM (3 x 100 mL) after the reaction mixture was cooled to room temperature. The organic extracts were combined and dried over $MgSO_4$. *In vacuo* concentration of the organic extracts and purification of the resulting crude product by column chromatography ($SiO_2$, EA) afforded **70** (5.50 g, 82%) as a clear oil. $^1$H NMR (300 MHz, $CDCl_3$): δ (ppm) = 3.70-3.67 (2 H, m, $CH_2$), 3.65-3.62 (8 H, m, 4 x $CH_2$), 3.58-3.56 (2 H, m, $CH_2$), 3.64-3.66 (2 H, m, $CH_2$), 3.69-3.72 (2 H, m, $CH_2$), 2.47 (1 H,

s, OH); $^{13}$C NMR (100 MHz, $CDCl_3$): δ (ppm) = 72.9 ($CH_2$), 71.1 ($CH_2$), 71.1 ($CH_2$), 71.0 ($CH_2$), 70.7 ($CH_2$), 70.4 ($CH_2$), 62.1 ($CH_2$), 51.1 ($CH_2$); MSES: *m/z* = 242.2 $[M+Na]^+$; FT-IR (liquid): $\nu_{max}$ $cm^{-1}$ = 3436 (w) (br), 2868 (m), 2098 (s), 1101 (s).

**13-Azido-2,5,8,11-tetraoxatridecane**
**(71)**

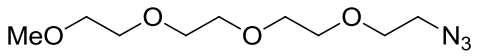


Sodium hydride (1.98 g, 49.6 mmol) was suspended in DMF (20 mL) and stirred for 15 mins under nitrogen. Compound **70** (5.5 g, 25.11 mmol) dissolved in DMF (10 mL) was added to the solution of sodium hydride. Methyl iodide (3.1 mL, 49.60 mmol) was added dropwise to the reaction mixture over a period of 5 mins. The reaction vessel was wrapped in aluminium foil and was stirred at room temperature overnight. Water (150 mL) was added, extracted with DCM (4 x 200 mL) and the organic phase was washed with brine (100 mL). The organic extract was combined and dried over $MgSO_4$. *In vacuo* concentration and purification of the resulting crude product by column chromatography ($SiO_2$, EA) afforded **71** (4.53 g, 85%) as clear oil, $^1$H NMR (300 MHz, $CDCl_3$): δ (ppm) = 3.72-3.66 (10 H, m, $CH_2$), 3.59-3.57 (2 H, m, $CH_2$), 3.58-3.56 (2 H, m, $CH_2$), 3.43-3.41 (5 H, m, $CH_3$ + $CH_2$); $^{13}$C NMR (100 MHz, $CDCl_3$): δ (ppm) = 72.3 ($CH_2$), 71.1 ($CH_2$), 71.1 ($CH_2$), 71.0 ($CH_2$), 71.0 ($CH_2$), 70.9 ($CH_2$), 70.4 ($CH_2$), 59.4 ($CH_3$), 51.1 ($CH_2$); MSES: *m/z* = 256.2 $[M+Na]^+$; FT-IR (liquid): $\nu_{max}$ $cm^{-1}$ = 2869 (m), 2098 (s), 1100 (s), 1103 (s).

**2,5,8,11-Tetraoxatridecan-13-amine**
**(72)**

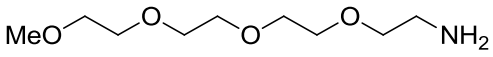


To a stirred solution of **71** (1.0 g, 4.29 mmol) in MeOH, was added $Et_3N$ (3 mL, 21.50 mmol). This was followed by 1, 3 - propane dithiol (2.15 mL, 21.50 mmol). The mixture was stirred at room temperature for three days. The residue was concentrated *in vacuo* and diluted with water (50 mL). The mixture was washed with diethyl ether (50 mL) to remove excess reducing agent. *In vacuo* concentration of the organic layer afforded **72** (1.0 g, 100%) as a yellowish liquid, $^1$H NMR (300 MHz, $CDCl_3$): δ (ppm) = 6.06 (2 H, s(broad), $NH_2$), 3.69-3.63 (12 H, m, $CH_2$), 3.57-3.55 (2 H, m, $CH_2$), 3.38

(3 H, s, $CH_3$), 3.06-3.03 (2 H, m, $CH_2$); $^{13}$C NMR (100 MHz, $CDCl_3$): δ (ppm) = 73.0 ($CH_2$), 71.5 ($CH_2$), 71.5 ($CH_2$), 71.3 ($CH_2$), 70.1 ($CH_2$), 60.1 ($CH_3$), 54.6 ($CH_2$), 41.0 ($CH_2$), 24.8 ($CH_2$); MSES: *m*/*z* = 208.20 $[M+H]^+$; HRMS (ES): Calcd for $C_9H_{22}NO_4$ 208.1551 ($[M+H]^+$), found 208.1544; FT-IR (liquid): $\nu_{max}$ $cm^{-1}$ = 3368 (w), 2872 (m), 2868 (m), 1097 (s).

**3-(1,3-Dioxoisoindolin-2-yl)-*N*-(2,5,8,11-tetraoxatridecan-13-yl)propanamide (73)**

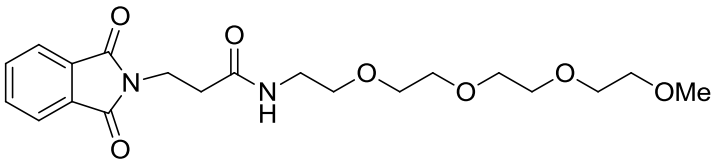


Compound **40** (1.10 g, 4.6 mmol) was dissolved in DCM (30 mL) and added dropwise to a solution of **72** (0.95 g, 4.61 mmol) and $Et_3N$ (1.3 mL) in DCM (20 mL) at 0 °C. The reaction mixture was stirred overnight at room temperature and poured into ice cold 2M HCl (30 mL) and extracted with DCM (3 x 50 mL). The organic phases were combined, washed with brine and dried over $MgSO_4$. *In vacuo* removal of the solvents afforded compound **73** (1.0 g, 52%) as a white solid. MP = 68-70 °C; $^1$H NMR (300 MHz, $CDCl_3$) δ (ppm): 7.82-7.84 (2 H, m, CH), 7.69-7.72 (2 H, m, CH), 6.65 (1 H, s(broad), NH), 4.01 (2 H, t, *J* = 2.5 Hz, $CH_2$), 3.61-3.64 (8 H, m, 4 x $CH_2$), 3.57-3.59 (4 H, m, 2 x $CH_2$), 3.51-3.54 (4 H, m, 2 x $CH_2$), 3.40-3.44 (2 H, m, $CH_2$) 3.34 (3 H, s, $CH_3$); $^{13}$C NMR (100 MHz, $CDCl_3$): δ (ppm) = 171.7 (Cq), 169.9 (Cq), 135.7 (CH), 134.0 (Cq), 125.1 (CH ), 73.7 ($CH_2$), 72.3 ($CH_2$), 72.2 ($CH_2$), 72.0 ($CH_2$), 71.6 ($CH_2$), 60.8 ($CH_3$), 41.7 ($CH_2$), 36.5 ($CH_2$), 36.3 ($CH_2$); HRMS (ES): Calcd for $C_{20}H_{29}N_2O_7$ 409.1975 ($[M+H]^+$), $C_{20}H_{28}N_2NaO_7$ 431.1795 ($[M+Na]^+$), found 409.1963, 431.1779; FT-IR (solid): $\nu_{max}$ $cm^{-1}$ = 3349 (m), 1759 (m), 1682 (m), 1518 (m), 1365 (m), 1155 (s).

Compound **74**

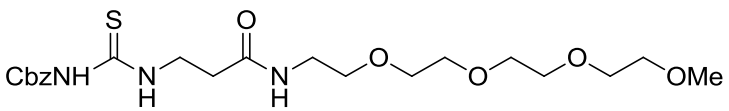

Experimental

Compound **76** (0.60 g, 2.20 mmol) was suspended in EtOH (20 mL) and hydrazine hydrate (120 μL) was added and the reaction mixture was refluxed for 8 hours. The solution was cooled to 0 $^{o}$C and stirred overnight. The reaction mixture was filtered off and the filtrate was dried *in vacuo* to give a yellowish solid residue. The resulting crude was dissolved in DCM and cooled to 0 $^{o}$C. $Et_3N$ (0.73 mL) and CbzNCS (0.40 g, 2.20 mmol) were added slowly and the reaction mixture was stirred for 30 mins at 0 °C and then overnight at room temperature. *In vacuo* drying of the reaction mixture and purification of the resulting crude product by column chromatography ($SiO_2$, 1:50 MeOH/DCM) afforded **74** (0.5 g, 50%) as a white gummy solid. $^{1}$H NMR (400 MHz, $CDCl_3$) δ (ppm): 11.30 (1H, s, NH), 10.10 (1H, t, *J* = 2.5 Hz, NH), 7.40-7.46 (5 H, m, CH), 5.23 (2 H, s, $CH_2$), 3.79-3.84 (2 H, m, $CH_2$), 3.55-3.58 (10 H, m, 5 x $CH_2$), 3.45-3.47 (4 H, m, 2 x $CH_2$), 3.25-3.28 (5 H, m, $CH_2$ + $CH_3$) 2.50 (2 H, t, *J* = 5 Hz, $CH_2$);$^{13}$C NMR (100 MHz, DMSO-$d_6$): δ (ppm) = 179.6 (Cq), 170.9 (Cq), 153.6 (Cq), 136.1 (Cq), 128.9 (CH), 128.7 (CH), 128.3 (CH), 71.7 ($CH_2$), 70.3 ($CH_2$), 70.2 ($CH_2$), 70.0 ($CH_2$), 69.5 ($CH_2$), 67.1 ($CH_2$), 58.5 ($CH_2$), 55.4 ($CH_3$), 39.0 ($CH_2$), 33.8 ($CH_2$); HRMS (ES): Calcd for $C_{21}H_{33}N_3NaO_7S$ 494.1937 ([M+Na]$^{+}$), found 494.1928; FT-IR (solid): $\nu_{max}$ cm$^{-1}$ = 3271 (m), 1713 (s), 1628 (m), 1378 (m), 1088 (m), 718 (s).

Compound **75**

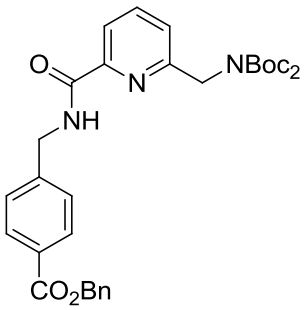


Compound **35** (0.50 g, 1.42 mmol) was dissolved in DCM (30 mL). *i*$Pr_2$EtN (0.86 mL, 5.00 mmol), EDC.HCl (0.65 g, 3.39 mmol), HOBt (0.58 g, 4.29 mmol) and 4-amino methyl benzoic acid benzyl ester (0.40 g, 1.70 mmol) were added successively and the resulting solution was stirred at room temperature for 48 hours. DCM (20 mL) and aq. 1M $KHSO_4$ (15 mL) were added to the reaction mixture. The organic layer was separated, washed with sat. $Na_2CO_3$ (15 mL) and brine (15 mL), and dried over $MgSO_4$. *In vacuo* removal of the solvent and purification of the resulting crude

product by column chromatography ($SiO_2$, 1:50 MeOH/DCM) afforded **75** (0.51g, 65%) as a white gummy solid; $^1$H NMR (400 MHz, $CDCl_3$): δ (ppm) = 8.41 (2 H, apparent triplet, NH), 8.13 (1 H, d, *J* = 5.0 Hz, CH), 8.05-8.07 (2 H, m, CH), 7.85 (1 H, t, *J* = 5.0 Hz, CH), 7.37-7.45 (8 H, m, CH), 5.37 (2 H, s, COOC$H_2$Ar), 4.74 (2H, d, *J* = 2.5 Hz, NHC$H_2$), 1.67 (2 H, s, C$H_2$NBoc$_2$), 1.43-1.46 (18 H, m, C(C$H_3$)$_3$); $^{13}$C NMR (100 MHz, $CDCl_3$): δ (ppm) = 166.6 (Cq), 164.6 (Cq), 157.5 (Cq), 156.4 (Cq), 149.4 (Cq), 144.1 (Cq), 138.8 (CH), 136.5 (Cq), 130.5 (CH), 129.7 (CH), 129.0 (CH), 128.5 (CH), 128.0 (CH), 124.8 (CH), 121.6 (CH), 80.3 (Cq), 67.1 ($CH_2$), 46.1 ($CH_2$), 43.5 ($CH_2$), 28.8 ($CH_3$), 28.6 ($CH_3$); MSES: *m*/*z* = 498.3 $[M+Na]^+$; FT-IR (solid): $\nu_{max}$ $cm^{-1}$ = 3379 (w), 2978 (w), 1716 (s), 1630 (s), 1094 (s).

Compound **76**

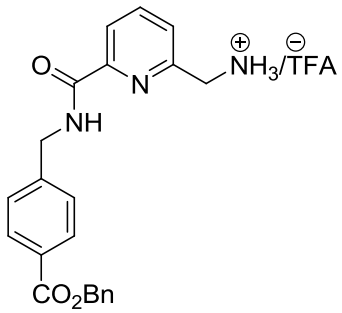


Compound **75** (0.6 g, 1 mmol) was dissolved in DCM (20 mL). 20 %( V/V) TFA/DCM (10 mL) was added and the resulting solution was stirred for 5 hrs at room temperature. *In vacuo* drying of the reaction mixture after the addition of toluene (3 x 2 mL) afforded **76** (0.6 g, quantitative yield) as a yellowish oily compound and was used for the next step with no further purification.

**Benzyl 4-((6-(3-(((benzyloxy)carbonyl)imino)-7-oxo-11,14,17,20-tetraoxa-2,4,8-triazahenicosyl)picolinamido)methyl)benzoate**
**(77)**

Experimental

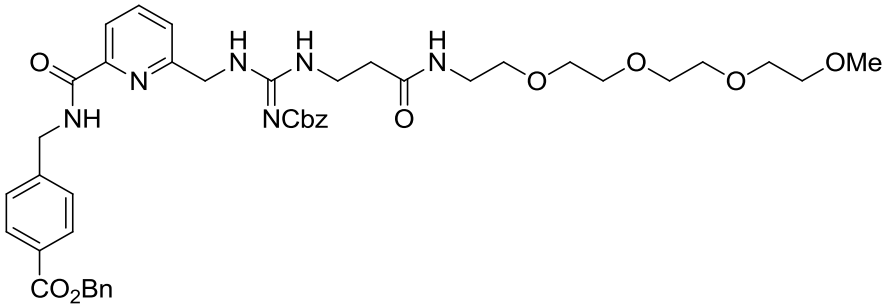

Compound **76** (0.40 g, 0.85 mmol) was dissolved in DCM (30 mL) and cooled to 0 $^{o}$C. $Et_3N$ (0.40 mL), EDC.HCl (0.40 g, 2.25 mmol) and **74** (0.40 g, 0.85 mmol) were added successively and the reaction mixture was stirred for 30 mins at 0 $^{o}$C and then overnight at room temperature. *In vacuo* removal of the solvent and purification of the resulting crude product by column chromatography ($SiO_2$, 3:100 MeOH/DCM) afforded **77** (0.40 g, 60%) as a white solid. MP = 74-76 $^{o}$C; $^{1}$H NMR (300 MHz, $CDCl_3$): δ (ppm) = 10.39 (1 H, s, NH), 9.75 (1 H, s, NH), 9.75 (1 H, s, NH), 9.07 (1 H, s, NH), 8.06 (1 H, d, *J* = 6.8 Hz, CH), 7.90 (1 H, d, *J* = 6.8 Hz, CH), 7.76 (1 H, s, CH), 7.35-7.16 (14 H, m, $CH_2$), 5.01-4.87 (2 H, m, $CH_2$), 4.63-4.44 (4 H, m, $CH_2$), 3.52-3.12 (23 H, m, 10 x $CH_2$ + $CH_3$), 2.33-2.23 (2 H, m, $CH_2$); $^{13}$C NMR (100 MHz, $CDCl_3$): δ (ppm) = 165.2 (Cq), 137.6 (CH), 135.1 (CH), 128.9 (CH), 127.9 (CH), 127.6 (CH), 127.3 (CH), 127.1 (CH), 126.6 (CH), 126.4 (CH), 70.8 ($CH_2$), 69.5 ($CH_2$), 69.3 ($CH_2$), 69.2 ($CH_2$), 68.7 ($CH_2$), 68.4 ($CH_2$), 65.6 ($CH_2$), 65.5 ($CH_2$), 57.9 ($CH_3$), 44.6 ($CH_2$), 42.06 ($CH_2$), 38.3 ($CH_2$), 36.3 ($CH_2$); MSES: *m*/*z* = 813.5 $[M+H]^+$; HRMS (ES): Calcd for $C_{43}H_{52}N_6NaO_{10}$ 813.3823, ($[M+Na]^+$), found 813.3806; FT-IR (solid): $\nu_{max}$ $cm^{-1}$ = 2914m, 1714s, 1611s, 1523s, 1405s, 1119s.

**4-((6-(3-Imino-7-oxo-11,14,17,20-tetraoxa-2,4,8-triazahenicosyl)picolinamido)methyl)benzoic acid (67)**

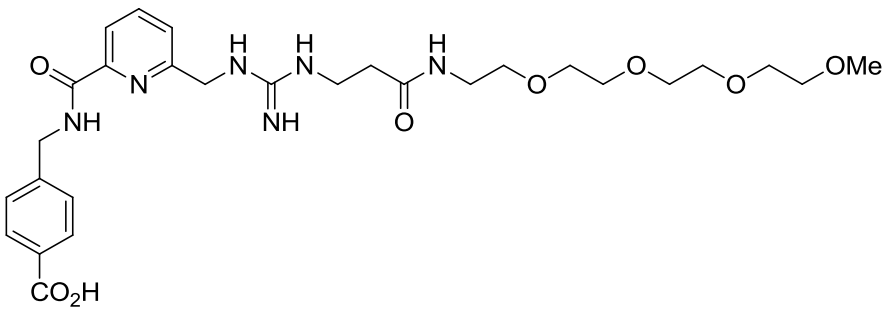

Experimental

Compound **77** (0.3g, 0.37 mmol) was dissolved in MeOH (30 mL). Pd/C (40 mg, 0.40 mmol) was added and the reaction mixture was stirred for 4 hrs at room temperature under hydrogen (1 atm). The reaction mixture was filtered through celite and dried *in vacuo*. Purification of the resulting solid by precipitation from MeOH using $Et_2O$ afforded **67** (0.20 g, 90%) as a white solid. MP = 102-105 $^oC$; $^1H$ NMR (400 MHz, DMSO-$d_6$): δ (ppm) = 9.69 (1 H, s, NH), 8.19 (1 H, s, NH), 8.01-7.94 (2 H, m, CH), 7.53-7.48 (3 H, m, CH), 6.78 (2 H, m, CH), 4.61 (2 H, s, $CH_2$), 4.37 (2 H, d, *J* = 3.2 Hz, $CH_2$), 3.48-3.21 (21 H, overlapped with water peak, 9 x $CH_2$ + $CH_3$), 2.40 ( 2 H, t, *J* = 4.4 Hz, $CH_2$); $^{13}C$ NMR (100 MHz, $CDCl_3$): δ (ppm) = 171.7 (Cq), 170.2 (Cq), 164.0 (Cq), 156.7 (Cq), 155.0 (Cq), 149.1 (Cq), 139.7 (CH), 138.2 (CH), 128.5 (CH), 125.0 (CH), 124.2 (Cq), 120.3 (CH), 70.9 ($CH_2$), 69.4 ($CH_2$), 69.3 ($CH_2$), 69.2 ($CH_2$), 68.6 ($CH_2$), 57.6 ($CH_3$), 44.9 ($CH_2$), 41.9 ($CH_2$), 38.2 ($CH_2$), 37.3 ($CH_2$), 34.5 ($CH_2$) (2 x $CH_2$ peaks are overlapped with DMSO peak); MSES: *m*/*z* = 589.4 $[M+H]^+$; HRMS (ES): Calcd for $C_{28}H_{40}N_6NaO_8$ 589.2986 ($[M+Na]^+$), found 589.2970; FT-IR (solid): $\nu_{max}$ $cm^{-1}$ = 3290 (w)(b), 2874 (m), 1644 (s), 1591 (s), 1527 (s), 1375 (s), 1089 (s).

**(S)-Methyl 2-(4-(2-(4-((6-(((tert-butoxycarbonyl)amino)methyl)picolinamido)methyl)benzamido)-4-methylpentanamido)phenyl)acetate**
**(79)**

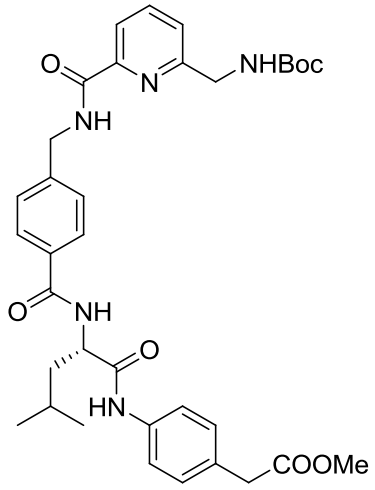


Compound **36** (1.10 g, 2.67 mmol) was dissolved in DCM (40 mL). *i*$Pr_2$EtN (1.64 mL, 9.45 mmol), EDC.HCl (1.24 g, 6.80 mmol), HOBt (1.10 g, 8.10 mmol) and compound **66** (0.68 g, 2.70 mmol) were added successively and the resulting solution

was stirred at room temperature for 48 hrs. DCM (30 mL) and aq. 1M $KHSO_4$ (20 mL) were added to the reaction mixture. The organic layer was separated, washed with sat. $Na_2CO_3$ (20 mL) and brine (20 mL), and dried over $MgSO_4$. *In vacuo* removal of the solvent and purification of the resulting crude product by column chromatography ($SiO_2$, 1:50 MeOH/DCM) afforded **79** (1.00 g, 57%) as a white solid. MP = 108 -110 ˚C; $^1$H NMR (400 MHz, $CDCl_3$): δ (ppm) = 9.13 (1 H, s, NH), 8.46 (1 H, t, *J* = 2.5 Hz, NH), 8.11 (1 H, t, *J* = 2.5 Hz, NH), 7.82 (1 H, t, *J* = 5.0 Hz, CH), 7.12 (1 H, d, *J* = 5.0 Hz, CH), 7.43-7.52 (4 H, m, CH), 7.27-7.30 (3 H, m, CH), 7.14 (2 H, d, *J* = 5.0 Hz, CH), 4.86-4.90 (1 H, m, $(CH_3)_2CHCH_2CH$), 4.64 (2 H, apparent doublet, $CH_2$), 4.45 (2 H, d, *J* = 2.5 Hz, $CH_2$), 3.67 (3 H, s,$COOCH_3$), 3.56 (2 H, s, $CH_2$), 1.84-1.94 (3 H, m, $(CH_3)_2CHCH_2CH$) + $(CH_3)_2CHCH_2CH$)), 1.42 (11 H, m, $C(CH_3)_3$ + $CH_2$), 0.95-0.99 (6 H, m, $(CH_3)_2CH$); $^{13}$C NMR (100 MHz, $CDCl_3$): δ (ppm) = 170.8 (Cq), 169.6 (Cq), 166.3 (Cq), 163.0 (Cq), 165.0 (Cq), 156.0 (Cq)154.8 (Cq), 147.8 (Cq), 141.1 (Cq), 137.0 (CH), 135.8 (Cq), 131.2 (CH), 128.4 (CH), 126.4 (CH), 125.2 (CH), 123.1 (CH), 119.8 (CH), 118.9 (CH), 78.6 (Cq), 52.0 (CH), 50.8 ($CH_3$), 48.0 ($CH_2$), 44.5 ($CH_2$ ), 41.8 ($CH_2$), 32.6 ($CH_2$), 27.1 ($CH_3$), 23.8 ($CH_3$), 21.7 ($CH_3$) 21.0 (CH); MSES: *m*/*z* =668.2$[M+Na]^+$; HRMS (ES): Calcd for $C_{35}H_{43}N_5NaO_7$ 668.3060 ($[M+Na]^+$), found 668.3043; FT-IR (solid): $\nu_{max}$ $cm^{-1}$ = 3308 (w), 2929 (w), 1716 (s), 1456 (s), 1164 (m).

**(S)-(6-((4-((1-((4-(2-Methoxy-2-oxoethyl)phenyl)amino)-4-methyl-1-oxopentan-2-yl)carbamoyl)benzyl)carbamoyl)pyridin-2-yl)methanaminium triflouro acetate**
**(80a)**

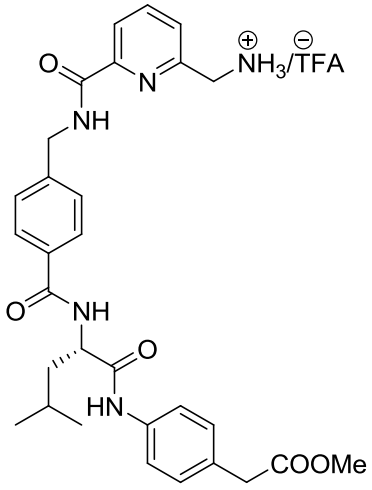

Experimental

Compound **79** (0.70 g, 1.09 mmol) was dissolved in DCM (20 mL). 20% (v/v) TFA/DCM (10 mL) was added to the reaction mixture which was stirred for 5 hrs at room temperature. *In vacuo* drying of the reaction mixture after the addition of toluene (3 x 2 mL) afforded **80a** (1.0 g, 100%) as a white solid. MP = 60 - 62 ˚C; $^{1}$H NMR (400 MHz, DMSO-$d_6$): δ (ppm) = 10.11 (1 H, s, NH), 9.69(1 H, t, *J* = 2.5 Hz, NH), 8.53 (1 H, t, *J* = 5.0 Hz, CH), 8.38 (2 H, s(b), $NH_2$), 8.04-8.10 (2 H, m, CH), 7.90 (1 H, d, *J* = 5.0 Hz, CH), 7.68 (1 H, d, *J* = 2.5 Hz, CH), 7.56 (2 H, d, *J* = 5.0 Hz, CH), 7.42 (2 H, d, *J* = 5.0 Hz, CH), 7.19 (2 H, d, *J* = 5.0 Hz, CH), 4.61-4.64 (3 H, m, $(CH_3)_2CHCH_2CH$ + $CH_2$), 4.34-4.36 (3 H, app doublet, $CH_2$), 3.60 (3 H, m, $COOCH_3$), 1.71-1.79 (2 H, m, $(CH_3)_2CHCH_2CH$)), 1.58-1.61 (1 H, m, $(CH_3)_2CHCH_2CH$), 1.09-1.12 (2 H, m, $CH_2$), 0.91-0.95 (6 H, m, $(CH_3)_2CH$); $^{13}$C NMR (100 MHz, DMSO-$d_6$): δ (ppm) = 170.9 (Cq), 170.6 (Cq), 165.4 (Cq), 162.8 (Cq), 151.6 (Cq), 148.0 (Cq), 142.0 (Cq), 138.2 (CH), 137.0 (Cq), 132.0 (CH), 128.8 (CH), 127.0 (CH), 126.1 (CH), 124.2 (Cq), 120.5 (CH), 118.5 (CH), 52.0 (CH), 50.9 ($CH_3$), 48.0 ($CH_2$), 41.3 ($CH_2$), 41.0 ($CH_2$), 40.9 ($CH_2$), 23.8 ($CH_3$), 22.2 ($CH_3$), 20.8 (CH); MSES: *m/z* =546.3 $[M+H]^+$; HRMS (ES): Calcd for $C_{30}H_{36}N_5O5$ 546.2716 ($[M+Na]^+$), found 546.2707; FT-IR (solid): $\nu_{max}$ $cm^{-1}$ = 3292 (w), 2956 (w), 1666 (s), 1537 (s), 1131 (m).

**(S)-Methyl 2-(4-(2-(4-((6-(3-(((benzyloxy)carbonyl)imino)-7-oxo-11,14,17-trioxa-2,4,8-triazaicosyl)picolinamido)methyl)benzamido)-4-methylpentanamido)phenyl)acetate**
**(80)**

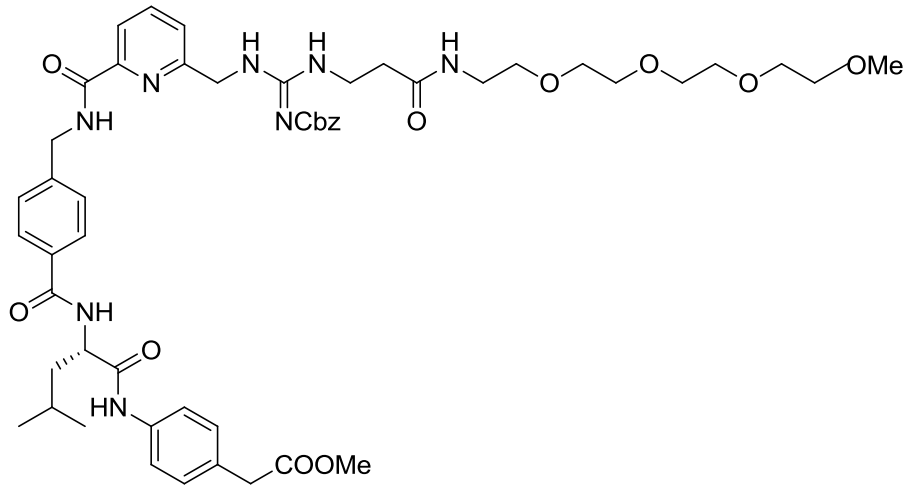

Experimental

Compound **80a** (0.70 g, 1.28 mmol) was dissolved in DCM (25 mL) and cooled to 0 $^{o}$C. $Et_3N$ (0.6 mL) and EDC.HCl (0.6 g, 3.28 mmol) were added to the reaction mixture. A DCM (20 mL) solution of **74** (0.6 g, 1.28 mmol) was added slowly and the reaction mixture was stirred for 30 mins at 0 $^{o}$C and then overnight at room temperature. *In vacuo* removal of the solvent and purification of the resulting crude product by column chromatography ($SiO_2$, 3:100 MeOH/DCM) afforded compound **80** (0.70 g, 55 %) as a white solid. MP = 98-100 $^{o}$C; $^{1}$H NMR (400 MHz, $CDCl_3$): δ (ppm) = 10.41 (1 H, s(b), NH), 9.67 (1 H, s(b), NH), 9.31 (1 H, s(b), NH), 9.15 (1 H, s(b), NH), 8.94 (1 H, s, NH), 8.14 (1 H, d, *J* = 5.0 Hz, CH), 7.84 (1 H, s(b), NH), 7.72 (2 H, d, *J* = 5.0 Hz, 2 x CH), 7.49 (2 H, d, *J* = 5.0 Hz, CH), 7.38-7.24 (9 H, m, 9 x CH), 7.16 (2 H, d, *J* = 5.0 Hz, CH), 5.08-4.99 (2 H, s, $CH_2$), 4.81-4.84 (1 H, m, CH), 4.68-4.59 (5 H, m, $CH_2$ + $CH_3$), 3.66-3.33 (21 H, overlap with water peak, 9 x $CH_2$ + $CH_3$), 2.45 (2 H, t, *J* = 3.8 Hz, $CH_2$), 1.87 (1 H, m, CH), (2 H, m, $CH_2$), 1.75 (2 H, m, $CH_2$), 1.32 (2 H, t, *J* = 3.8 Hz, $CH_2$), 0.97 (6 H, m, $CH(CH_3)_2$);$^{13}$C NMR (100 MHz, $CDCl_3$): δ (ppm) = 172.6 (Cq), 171.0 (Cq), 168.3 (Cq), 143.9 (Cq), 139.3 (Cq), 137.6 (Cq), 132.9 (Cq), 130.3 (CH), 129.2 (CH), 128.9 (CH), 128.2 (CH), 128.0 (CH), 127.9 (CH), 120.7 (CH), 72.4 ($CH_2$), 71.1 ($CH_2$), 71.0 ($CH_2$), 70.8 ($CH_2$), 70.4 ($CH_2$), 69.9 ($CH_2$), 67.2 ($CH_2$), 59.5 ($CH_3$), 53.7 ($CH_2$), 52.6 ($CH_3$), 46.2 ($CH_2$), 43.6 ($CH_2$), 42.3 ($CH_2$), 25.5 (CH), 23.5 ($CH_3$), 22.8 ($CH_3$), 9.08 (CH); MSES: *m*/*z* =1005.7 $[M+Na]^+$; HRMS (ES): Calcd for $C_{52}H_{70}N_8O_{12}$ 983.4879 ($[M+H]^+$), found 983.4864; FT-IR (solid): $\nu_{max}$ $cm^{-1}$ = 3287 (w), 2871 (m), 1646 (s), 1570 (s), 1540 (s), 310 (m), 1162 (m), 1021 (s), 799 (m), 696 (m).

**(S)-2-(4-(2-(4-((6-(3-(((Benzyloxy)carbonyl)imino)-7-oxo-11,14,17,20-tetraoxa-2,4,8-triazahenicosyl)picolinamido)methyl)benzamido)-4-methylpentanamido)phenyl)acetic acid**
**(81)**

Experimental

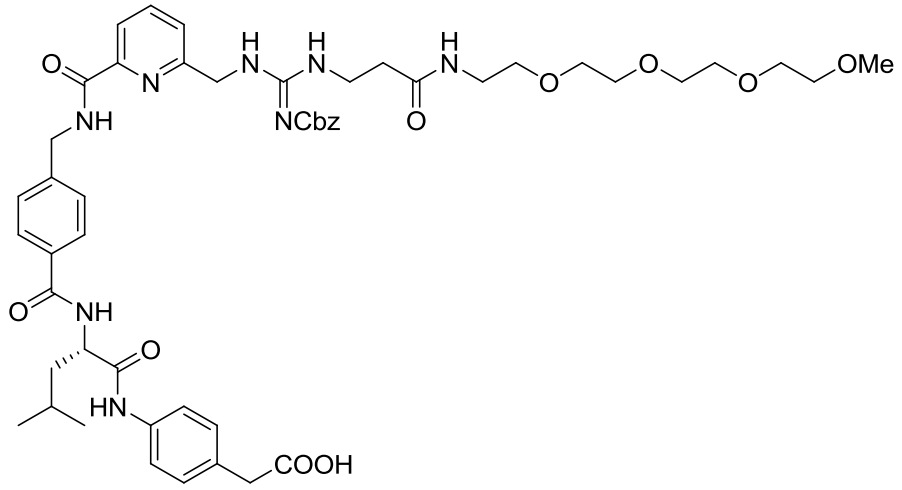


Compound **80** (0.25 g, 0.28 mmol) was dissolved in THF (30 mL) and added to $Me_3SiOK$ (54 mg, 0.42 mmol) suspended in THF (20 mL) under nitrogen. After overnight stirring, DCM (40 mL) and $H_2O$ (40 mL) were added and the reaction mixture was cooled to 0 °C. Citric acid (0.1 M) was added dropwise until the pH is 6-7 and further stirred for 1hr. *In vacuo* drying of the organic phase and purification of the resulting crude product by column chromatography ($SiO_2$, 3:100 MeOH/DCM → 1:20 MeOH/DCM) afforded **81** (0.17 g, 62%) as a white solid. MP = 130-132 °C; $^1$H NMR (400 MHz, DMSO-$d_6$): δ (ppm) = 12.24 (1 H, s, NH), 10.06 (1 H, s, NH), 8.49 (2 H, d, *J* = 5.0 Hz, CH), 7.99 (2 H, s(b), NH), 7.86 (2 H, d, *J* = 5.0 Hz, CH), 7.55 (3 H, d, *J* = 5.0 Hz, 3 x CH), 7.40 (2 H, d, *J* = 5.0 Hz, CH), 7.22-7.32 (5 H, m, CH), 7.18 (2 H, d, *J* = 5.0 Hz, CH), 4.88 (2 H, s, $CH_2$), 4.68-4.59 (5 H, m, CH + 2 x $CH_2$), 3.50-3.39 (18 H, m, 9 x $CH_2$), 3.22-3.16 (5 H, m, $CH_3$ + $CH_2$), 2.36 (2 H, s(b), $CH_2$), 1.74 (2 H, m, $CH_2$), 1.57 (1 H, m, CH), 0.90-0.94 (6 H, m, CH($CH_3$)$_2$); $^{13}$C NMR (100 MHz, DMSO-$d_6$): δ (ppm) = 173.2 (Cq), 171.8 (Cq), 171.1 (Cq), 166.7 (Cq), 143.2 (Cq), 138.2 (Cq), 138.2 (Cq), 133.1 (Cq), 130.3 (CH), 130.0 (CH), 128.7 (CH), 128.1 (CH), 127.9 (CH), 127.4 (CH), 119.7 (CH), 71.7 ($CH_2$), 70.2 ($CH_2$), 70.2 ($CH_2$), 70.0 ($CH_2$), 69.5 ($CH_2$), 65.9 ($CH_2$), 58.5 (CH), 53.1 ($CH_3$), 42.7 ($CH_2$), 40.9 ($CH_2$), 39.0 ($CH_2$), 37.7 ($CH_2$), 25.0 ($CH_3$), 23.5 ($CH_3$), 22.0 (CH ); MSES: *m*/*z* =991.7 $[M+H]^+$; HRMS (ES): Calcd for $C_{51}H_{68}N_8O_{12}$ 969.4723 ($[M+H]^+$), $C_{51}H_{67}N_8NaO_{12}$ 991.4542 ($[M+Na]^+$), found 969.4714, 991.4530; FT-IR (solid): $\nu_{max}$ $cm^{-1}$ = 3295 (m), 2870 (m), 1635 (s), 1307 (m), 1284 (m), 1149 (m), 1087 (m).

Experimental

**(*S*)-2-(4-(2-(4-((6-(3-Imino-7-oxo-11,14,17,20-tetraoxa-2,4,8-triazahenicosyl)picolinamido)methyl)benzamido)-4-methylpentanamido)phenyl)acetic acid**
**(78)**

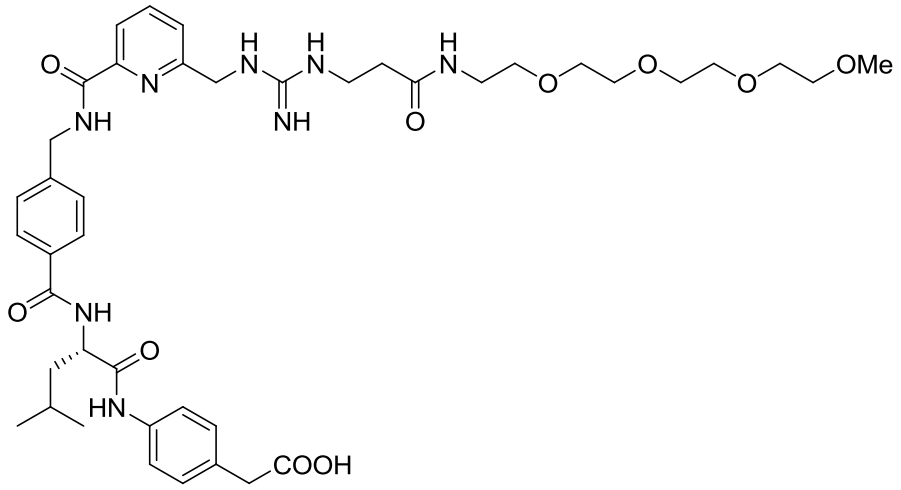


Compound **81** (100mg, 0.12 mmol) was dissolved in MeOH (25 mL). Pd/C (30 mg, 0.12 mmol) was added and the reaction mixture was stirred for 4 hrs at room temperature under hydrogen (1 atm). The reaction mixture was filtered through celite and dried *in vacuo*. Purification of the resulting solid by precipitation from MeOH using $Et_2O$ afforded **78** (70 mg, 69%) as a white solid. MP = 130-132 $^oC$; $[\alpha]_D^{25}$ =-17.1 $^o$ (*c* 0.2, MeOH); $^1H$ NMR (400 MHz, DMSO): δ (ppm) = $^1H$ NMR (400 MHz, DMSO-$d_6$): δ (ppm) = 12.24 (1 H, s, NH), 10.00 (1 H, s, NH), 8.61 (1 H, d, *J* = 5.0 Hz, NH), 8.14 (1 H, s, NH), 8.01-7.94 (2 H, m, CH), 7.87 (2 H, d, *J* = 5.0 Hz, CH), 7.42-7.36 (5 H, m, CH), 7.05 (2 H, d, *J* = 5.0 Hz, CH), 4.88 (2 H, s, $CH_2$), 4.64-4.53 (5 H, m, CH+ 2 x $CH_2$), 3.49-3.36 (16 H, m, 8 x $CH_2$ (overlap with water peak)), 3.22-3.16 (5 H, m, $CH_3$ + $CH_2$), 2.33 (2 H, s(b) $CH_2$), 1.71-1.68 (2 H, m, $CH_2$), 1.57-1.59 (1 H, m, CH), 0.88-0.93 (6 H, m, 2 x CH(C$H_3$)$_2$); $^{13}C$ NMR (100 MHz, DMSO-$d_6$): δ (ppm) = 170.9 (Cq), 170.3 (Cq), 166.0 (Cq), 163. 9 (Cq), 156.5 (Cq), 155.1 (Cq), 149.1 (Cq), 142.7 (Cq), 138.3 (CH), 136.2 (Cq), 133.8 (Cq), 132.4 (Cq), 128.9 (CH), 127.4 (CH), 126.6 (CH), 123.8 (CH), 120.4 (CH), 118.8 (CH), 71.0 ($CH_2$), 69.6 ($CH_2$), 69.4 ($CH_2$), 68.8 ($CH_2$), 57.8 (CH), 52.6 ($CH_3$), 45.2 ($CH_2$), 44.5 ($CH_2$), 42.0 ($CH_2$), 38.4 ($CH_2$), 37.4 ($CH_2$), 34.6 ($CH_2$), 24.4 ($CH_3$), 22.8 ($CH_3$), 21.4 (CH); MSES: *m*/*z* = 836.0 $[M+H]^+$, 857.6 $[M+Na]^+$; HRMS (ES): Calcd for $C_{43}H_{62}N_8O_{10}$ 835.4355 ($[M+H]^+$), $C_{43}H_{61}N_8NaO_{10}$ 857.4174 ($[M+Na]^+$), found 835.4340, 857.4179; FT-IR (solid): $\nu_{max}$ $cm^{-1}$ = 3300 (w) (broad)), 2900 (w), 2158 (m), 2035 (m), 1969 (w), 1652 (s).

**(2*R*, 5*S*, 6*R*)-Methyl 5-((*tert*-butoxycarbonyl)amino)-2,6-dimethyl-4-oxooctanoate (85)**

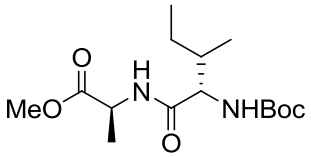


Compound **84** (4.00 g, 16.67 mmol) was dissolved in DMF (50 mL). *i*$Pr_2$NEt (10.40 mL, 59.82 mmol), DCC (7.00 g, 33.98 mmol), HOBt (7.00 g, 51.85 mmol) and alanine methyl ester (2.30 g, 16.67 mmol) were added successively and the resulting solution was stirred at room temperature for 48 hrs. The solid residue from the reaction mixture was filtered off and the DMF was removed *in vacuo*. The resulting crude was dissolved with DCM (70 mL) and washed successively with aq. 1M $KHSO_4$ (40 mL), sat. $Na_2CO_3$ (40 mL) and brine (20 mL), and dried over $MgSO_4$. *In vacuo* removal of the solvent and purification of the resulting crude product by column chromatography ($SiO_2$, 1:100 MeOH/DCM) afforded **85** (1.60g, 65%) as a white solid. MP = 118-120 $^oC$; $^1H$ NMR (400 MHz, $CDCl_3$): δ (ppm) = 6.51 (1 H, d, *J* = 5.0 Hz, N*H*Boc), 5.08 (1 H, d, *J* = 2.5 Hz, NH), 4.56-4.60 (1 H, m, CH), 3.96 (1 H, t, *J* = 5.0 Hz, CH), 3.74 (3 H, s, COOC$H_3$), 1.66-1.68 (1 H, m, $CH_2CHCH_3$), 1.44 (9 H, s, C($CH_3$)$_3$), 1.33 (3 H, d, *J* = 5.0 Hz, $CH_3$CHCOOMe(NH)), 1.08-1.18 (2 H, m, $CH_3CH_2CH$), 0.89-0.95 (6 H, m, $CH_3CH_2$ + CH$CH_3$); $^{13}C$ NMR (100 MHz, $CDCl_3$): δ (ppm) = 173.5 (Cq), 171.5 (Cq), 80.3 ($CH_3$), 59.6 ($CH_3$), 52.8 ($CH_3$), 48.4 (CH), 37.8 ($CH_3$), 34.3 ($CH_2$), 18.7 ($CH_3$), 15.9 (CH), 11.8 (CH); MSES: *m*/*z* = 339.1 $[M+Na]^+$; FT-IR (solid): $\nu_{max}$ $cm^{-1}$ = 3324 (s), 2928 (m), 1654 (m), 1521 (m), 1166 (m), 640 (m).

**(S)-Methyl 2-((2S,3R)-2-amino-3-methylpentanamido)propanoate (86)**

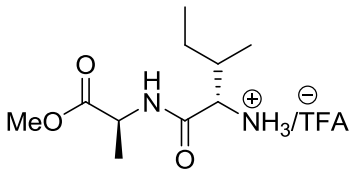


Compound **85** (1.60 g, 7.41 mmol) was dissolved in DCM (10 mL). 20% (v/v) TFA/DCM (10 mL) was added and the resulting solution was stirred for 5 hrs at room

temperature. *In vacuo* drying of the reaction mixture after the addition of toluene (3 x 3 mL) followed by crystallisation from diethyl ether afforded compound **86** (1.60 g, quantitative yield) as a white solid. MP = 134-136 °C; $^{1}$H NMR (400 MHz, DMSO): δ (ppm) = 8.84 (1 H, d, *J* = 2.5 Hz, NH), 8.16 (2 H, s(b), $NH_2$), 4.34-4.39 (1 H, m, CH), 3.63 (3 H, s, COOC$H_3$), 3.55-3.41 (1 H, m, CH), 1.82-1.84 (1 H, m, CH), 1.51-1.53 (1 H, m, $CH_3CH_2CH$)), 1.33 (3 H, d, *J* = 2.5 Hz, $CH_3CHCOOMe(NH)$), 1.15-1.20 (1 H, m, $CH_3CH_2CH$), 0.93 (3 H, d, *J* = 5.0 Hz, $CH_3CH$), 0.87 (3 H, t, *J* = 5 Hz, $CH_3CH_2$); $^{13}$C NMR (100 MHz, DMSO): δ (ppm) = 172.8 (Cq), 168.2 (Cq), 56.8 ($CH_3$), 52.4 ($CH_3$), 48.1 (CH), 36.7 ($CH_3$), 24.3 ($CH_2$), 17.2 ($CH_3$), 14.7 (CH), 11.6 (CH); MSES: *m*/*z* = 217.2 $[M+H]^+$; HRMS (ES): Calcd for $C_{10}H_{21}N_2O_3$ 217.1552 ($[M+H]^+$), found 217.1545; FT-IR (solid): $\nu_{max}$ $cm^{-1}$ = 3355 (s), 2962 (m), 1672 (s), 1202 (s), 1134 (m), 720 (m).

**(9S,12S)-Methyl 9-((R)-sec-butyl)-2,2,12-trimethyl-4,7,10-trioxo-3-oxa-5,8,11-triazatridecan-13-oate**
**(87)**

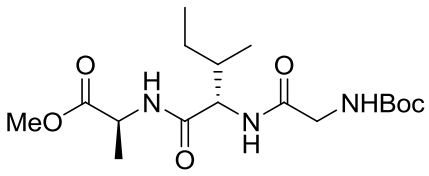


Boc protected glycine (1.10 g, 8.76 mmol) was dissolved in DMF (50 mL). *i*$Pr_2$NEt (4.3 mL, 24.33 mmol), DCC (4.30 g, 20.87 mmol), HOBt (3.40 g, 25.18 mmol) and **86** (1.80 g, 8.33 mmol) were added successively and the resulting solution was stirred at room temperature for 48 hrs. The solid residue from the reaction mixture was filtered off and the DMF was removed *in vacuo*. The resulting crude was dissolved in DCM (70 mL) and washed successively with aq. 1M $KHSO_4$ (20 mL), sat. $Na_2CO_3$ (20 mL) and brine (20 mL), and dried over $MgSO_4$. *In vacuo* removal of the solvent and purification the resulting crude product by column chromatography (1:100 MeOH/DCM) afforded **87** (2.30 g, 73%) as a white solid. MP = 122 -124 °C; $^{1}$H NMR (300 MHz, $CDCl_3$): δ (ppm) = 6.90 (1 H, s, NH), 6.84 (1 H, s, NH), 5.35 (1 H, d, *J* = 5.0 Hz, NH), 4.54 (1 H, m, CH), 4.37 (1 H, dd, *J* = 5.0 Hz, 2.5 Hz, CH), 3.82 (2 H, d, *J* = 2.5 Hz, $CH_2$), 3.74 (3 H, s, C$H_3$OOC), 1.86 (1 H, m, CH), 1.51 (1 H, m, $CH_3CH_2CH$ (Diastereotopic porton)), 1.44 (9 H, s, $C(CH_3)_3$), 1.40 (3 H, d, *J* = 5.0 Hz,

CHC*H*$_3$), 1.13-1.16 (1 H, m, CH$_3$C*H*$_2$CH (Diastereotopic porton)), 0.94 (3 H, d, *J* = 5.0 Hz CHC*H*$_3$), 0.89 (3 H, t, *J* = 5.0 Hz CH$_2$C*H*$_3$); $^{13}$C NMR (100 MHz, CDCl$_3$): δ (ppm) = 174.7 (Cq), 172.3 (Cq), 171.2 (Cq), 164.2 (Cq), 81.9 (Cq), 59.2 (CH$_3$), 54.1 (CH$_3$), 49.7 (CH), 46.0 (CH$_2$), 39.2 (CH), 29.9 (CH$_3$), 26.5 (CH$_2$), 19.6 (CH$_3$), 16.9 (CH), 12.9 (CH$_3$);MSES: *m*/*z* = 396.2 [M+Na]$^+$; HRMS (ES): Calcd for C$_{18}$H$_{33}$N$_2$O$_6$ 396.2111 ([M+H]$^+$), found 396.2104; FT-IR (solid): ν $_{max}$ cm$^{-1}$ = 3292 (w) (b), 2874 (w), 1635 (s), 1521 (s).

**(S)-Methyl 2-((2S,3R)-2-(2-aminoacetamido)-3-methylpentanamido)propanoate (88)**

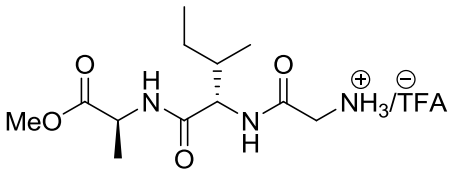


Compound **87** (1.00 g, 2.68 mmol) was dissolved in DCM (10 mL). 20% (v/v) TFA/DCM (10 mL) was added and the resulting solution was stirred for 5 hrs at room temperature. *In vacuo* drying of the reaction mixture after the addition of toluene (3 x 3 mL) followed by crystallization from diethyl ether afforded **88** (1.00 g, 100%) as a white solid. MP = 192 -194 $^{o}$C. $^1$H NMR (300 MHz, DMSO-*d*$_6$): δ (ppm) = 8.57 (1 H, d, *J* = 5.0 Hz, NH), 8.46 (1 H, d, *J* = 7.5 Hz, NH), 8.01 (2 H, s(b), NH$_2$), 4.21-4.32 (2 H, m, 2 x CH), 1.68-1.72 (1 H, m, CH), 1.45-1.47 (1 H, m, CH$_3$C*H*$_2$CH (a diasteriotopic proton)), 1.28 (3 H, d, *J* = 5.0 Hz, CHC*H*$_3$), 1.08-1.10 (1 H, m, CH$_3$C*H*$_2$CH (a diasteriotopic proton)), 0.88 (3 H, d, *J* = 5.0 Hz CHC*H*$_3$), 0.83 (3 H, t, *J* = 5.0 Hz CH$_2$C*H*$_3$); $^{13}$C NMR (100 MHz, DMSO-*d*$_6$): δ (ppm) = 171.6 (Cq), 169.3 (Cq), 164.5 (Cq), 55.3 (CH$_3$), 50.6 (CH), 46.4 (CH), 40.5 (CH$_2$), 37.5 (CH$_3$), 23.0 (CH$_2$), 15.6 (CH), 13.8 (CH$_3$), 9.8 (CH$_3$); MSES: *m*/*z* = 296.2 [M+Na]$^+$; HRMS (ES): Calcd for C$_{13}$H$_{25}$N$_2$O$_4$ 274.1768 ([M+H]$^+$), C$_{13}$H$_{24}$N$_2$NaO$_4$ 296.1587 ([M+Na]$^+$) found 274.1764, 296.1584; FT-IR (solid): ν $_{max}$ cm$^{-1}$ = 3280 (w), 2962 (w), 1683 (m), 1669 (s), 1558 (m), 1130 (m).

**(S)-Methyl 2-((2S,3R)-2-(2-(6-(((tert-butoxycarbonyl)amino)methyl)picolinamido)acetamido)-3-methylpentanamido)propanoate (89)**

Experimental

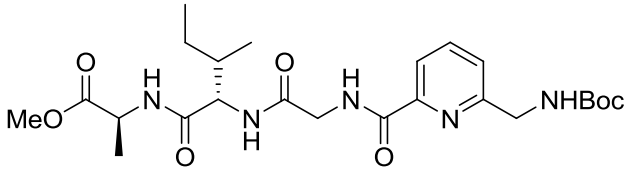

Compound **36** (0.70 g, 2.78 mmol) was dissolved in DCM (50 mL). *i*$Pr_2$NEt (1.76 mL, 10.12 mmol), EDC.HCl (1.3 g, 7.10 mmol), HOBt (1.2 g, 8.89 mmol) and **88** (0.80 g, 2.93 mmol) were added successively and the resulting solution was stirred at room temperature for 48 hrs. After addition of DCM (40 mL), the organic layer was washed with aq. 1M $KHSO_4$ (20 mL), sat. $Na_2CO_3$ (20 mL) and brine (20 mL), and dried over $MgSO_4$. *In vacuo* removal of the solvent and purification of the resulting crude by column chromatography ($SiO_2$, 1:100 MeOH/DCM) afforded **89** (1.00 g, 70%) as a white solid. MP = 188-190 $^oC$; $^1H$ NMR (300 MHz, DMSO-$d_6$): δ (ppm) = 8.89 (1 H, t, *J* = 2.5 Hz, NH), 8.47 (1 H, d, *J* = 5.0 Hz, NH), 8.02-7.95 (2 H, m, CH), 7.89 (1 H, d, *J* = 5.0 Hz, CH), 7.55 (1H, t, *J* = 2.5 Hz, NH), 7.48 (1 H, d, *J* = 5.0 Hz, NH), 4.33-4.22 (4 H, m, 2 H x $CH_2$), 4.01 (2 H, d, *J* = 2.5 Hz, $CH_2$), 3.60 (3 H, s, $CH_3$), 1.68-1.71 (1 H, m, CH), 1.45-1.48 (1 H, m, $CH_3C\mathit{H}_2CH$ (a diastereotopic proton))1.41 (9 H, s, 2 x $CH_3$), 1.28 (3 H, d, *J* = 5.0 Hz, $CHC\mathit{H}_3$), 1.05-1.12 (1 H, m, $CH_3C\mathit{H}_2CH$ (a diastereotopic proton)), 0.87 (3 H, d, *J* = 5.0 Hz $CHC\mathit{H}_3$), 0.82 (3 H, t, *J* = 5.0 Hz $CH_2C\mathit{H}_3$); $^{13}C$ NMR (100 MHz, DMSO-$d_6$): δ (ppm) = 172.8 (Cq), 170.9 (Cq), 168.2 (Cq), 163.8 (Cq), 158.3 (Cq), 155.9 (Cq), 148.8 (Cq), 138.4 (CH), 123.5 (CH), 120.0 (CH), 78.2 (Cq), 56.3 ($CH_3$), 51.7 (CH), 47.5 (CH), 45.3 ($CH_2$), 42.0 ($CH_2$), 40.2 ($CH_2$), 37.1 ($CH_3$), 28.2 ($CH_3$), 24.2 ($CH_3$), 16.7 (CH), 15.1 ($CH_3$), 11.0 ($CH_3$); MSES: *m*/*z* = 530.3 $[M+Na]^+$; HRMS (ES): Calcd for $C_{24}H_{37}N_5NaO_7$ 530.2591 ($[M+Na]^+$), found 530.2589; FT-IR (solid): $\nu_{max}$ $cm^{-1}$ = 3333 (w), 1685 (s), 1642 (s), 1527 (s), 1164 (s).

**(6-((2-(((2S,3R)-1-(((S)-1-Methoxy-1-oxopropan-2-yl)amino)-3-methyl-1-oxopentan-2-yl)amino)-2-oxoethyl)carbamoyl)pyridin-2-yl)methanaminium**
**(90)**

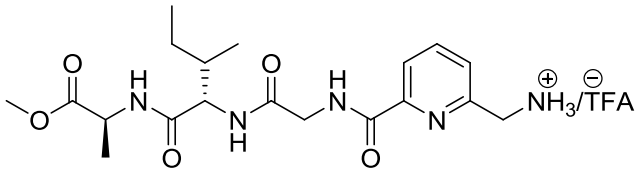

Experimental

Compound **89** (0.30 g, 0.59 mmol) was dissolved in DCM (10 mL). 20 % (v/v) TFA/DCM (10 mL) was added and the reaction mixture was stirred for 5 hrs at room temperature. *In vacuo* drying of the reaction mixture after the addition of toluene (3 x 3 mL) followed by crystallization from diethyl ether afforded **90** (0.29 g, 100%) as a white solid compound. MP = 160-162 $^{o}$C; $^{1}$H NMR (300 MHz, DMSO-$d_6$): δ (ppm) = 9.31 (1 H, t, *J* = 2.5 Hz, NH), 8.47 (1 H, d, *J* = 5.0 Hz, CH), 8.40 (2 H, s(broad), $NH_2$), 8.06 (1 H, *J* = 2.5 Hz, CH), 8.01 (1 H, s, NH), 7.99 (1 H, s(broad), NH), 7.67 (1 H, *J* = 5.0 Hz, CH), 4.33 (2 H, apparent quartet, $CH_2$), 4.24-4.39 (2 H, m, 2 x CH), 4.04 (2 H, *J* = 5.0 Hz, NHC$H_2$), 3.60 (3 H, s, $CH_3$), 1.71-1.73 (1 H, m, $CH_3CH_2CH$), 1.49-1.42 (1 H, m, $CH_3CH_2CH$ (a diastereotopic proton)), 1.28 (3 H, d, *J* = 5.0 Hz, $CH_3$), 1.05-1.12 (1 H, m, $CH_3CH_2CH$ (a diastereotopic proton)), 0.88 (3 H, d, *J* = 2.5 Hz $CHCH_3$), 0.83 (3 H, t, *J* = 2.5 Hz $CH_2CH_3$); $^{13}$C NMR (100 MHz, DMSO-$d_6$): δ (ppm) = 173.3 (Cq), 171.3 (Cq), 168.7 (Cq), 164.1 (Cq), 152.8 (Cq), 149.2 (Cq), 139.4 (CH), 125.4 (CH), 121.6 (CH), 56.8 ($CH_3$), 52.2 (CH), 48.0 (CH), 42.6 ($CH_2$), 42.3 ($CH_2$), 37.6 ($CH_3$), 24.6 ($CH_2$), 17.2 (CH), 15.5 ($CH_3$), 11.5 ($CH_3$); MSES: *m*/*z* = 430.2 $[M+Na]^+$; HRMS (ES): Calcd for $C_{19}H_{32}N_5O_4$ 408.2247 ($[M+H]^+$), found 408.2239; FT-IR (solid): $\nu_{max}$ $cm^{-1}$ = 3306w(b), 2957 (m), 1745 (m), 1654 (s), 1521 (s), 1366 (m).

**(*S*)-Methyl 2-((2*S*,3*R*)-2-(2-(6-(3-(((benzyloxy)carbonyl)imino)-7-oxo-11,14,17,20-tetraoxa-2,4,8-triazahenicosyl)picolinamido)acetamido)-3-methylpentanamido)propanoate**
**(91)**

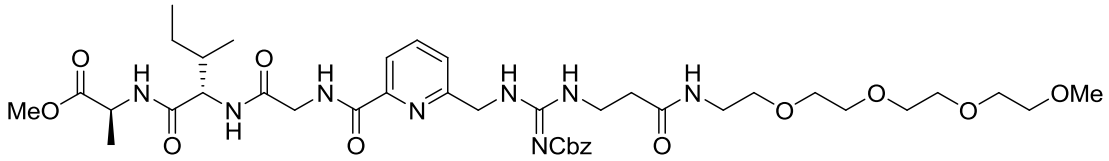


Compound **90** (0.70 g, 1.49 mmol) was dissolved in DCM (50 mL) and cooled to 0 $^{o}$C. $Et_3N$ (0.60 mL) and EDC.HCl (0.70 g, 3.83 mmol) were added to the reaction mixture. A DCM solution of **74** (0.70 g, 1.49 mmol) was slowly added and the resulting solution was stirred for 30 mins at 0 $^{o}$C and then overnight at room temperature. *In vacuo* drying of the reaction mixture and purification of the resulting crude by column chromatography ($SiO_2$, 1:50 MeOH/DCM) afforded **91** (0.76 g, 60%) as a white solid. MP = 102-104 $^{o}$C; H NMR (400 MHz, DMSO-$d_6$): δ (ppm) = 10.26 (1 H, s, NH),

9.86 (1 H, s, NH), 9.25 (1 H, s, NH), 8.12 (1 H, d, *J* = 2.5 Hz, NH), 7.42 (2 H, d, *J* = 5.0 Hz, CH), 7.32-7.36 (3 H, m, 3 x CH), 7.27-7.30 (3 H, m, 3 x CH), 6.93 (1 H, s(b), NH), 6.58 (1 H, s, NH), 5.15 (2 H, s, $CH_2$), 4.72 (2 H, s, $CH_2$), 4.47-4.54 (1 H, m, CH), 4.31-4.35 (1 H, m , CH), 4.12 (2 H, s, $CH_2$), 3.70 (3 H, s, $CH_3$), 3.54-3.70 (21 H, m, $CH_3$ + 9 x $CH_2$), 3.36 (3 H, s, $CH_3$), 2.46-2.52 (2 H, m, $CH_2$), 1.92-1.95 (1 H, m, $CH_3CH_2CH$), 1.45-1.50 (1 H, m, diastereotopic proton, $CH_3CH_2CH$), 1.06-1.15 (1 H, m, diastereotopic proton, $CH_3CH_2CH$), 0.91 (3 H, d, *J* = 5.0 Hz, $CHCH_3$), 0.87 (3 H, t, *J* = 5.0 Hz $CH_2CH_3$); $^{13}$C NMR (100 MHz, DMSO-$d_6$): δ (ppm) = 173.4 (Cq), 170.8 (Cq), 129.1 (CH), 128.4 (CH), 128.0 (CH), 72.9 ($CH_2$), 70.9 ($CH_2$), 70.8 ($CH_2$), 70.7 ($CH_2$), 70.3 ($CH_2$), 69.8 ($CH_2$), 59.4 ($CH_3$), 58.1 (CH), 52.8 (CH), 48.5 ($CH_3$), 46.4 ($CH_3$), 44.6 ($CH_2$), 37.4 ($CH_3$), 25.1 ($CH_2$), 18.4 (CH), 15.8 ($CH_3$), 11.8 ($CH_3$); MSES: *m*/*z* = 867.7 $[M+Na]^+$; HRMS (ES): Calcd for $C_{40}H_{61}N_8O_{12}$ 845.4409 ($[M+H]^+$), found 845.4392; FT-IR (solid): $\nu_{max}$ $cm^{-1}$ = 3276 (w), 2876 (w), 2364 (w), 1636 (s), 1541 (m).

**(S)-2-((2S,3R)-2-(2-(6-(3-(((Benzyloxy)carbonyl)imino)-7-oxo-11,14,17,20-tetraoxa-2,4,8-triazahenicosyl)picolinamido)acetamido)-3-methylpentanamido)propanoic acid**
**(92)**

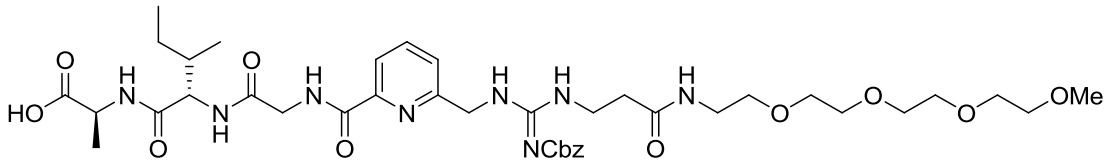


Compound **91** (0.20 g, 0.24 mmol) was dissolved in THF (30 mL) and added to a suspension of $Me_3SiOK$ (0.47 g, 0.4 mmol) in THF (25 mL) under nitrogen. After overnight stirring, DCM (50 mL) and $H_2O$ (50 mL) were added and the reaction mixture was cooled to 0 $^oC$. Citric acid (0.1 M) was added dropwise until the pH was 6-7 and further stirred for 1hr. *In vacuo* drying of the organic phase and purification of the resulting crude by column chromatography ($SiO_2$, 3:10 MeOH/DCM → 1:20 MeOH/DCM) afforded **92** (0.13 g, 54%) as a white solid. MP = 118 - 120 $^oC$; $^1$H NMR (400 MHz, DMSO-$d_6$): δ (ppm) = 12.40 (1 H, s(broad), COO*H*), 8.91 (1 H, s, NH), 8.32 (1 H, d, *J* = 5.0 Hz, CH), 8.10 (1 H, s, NH), 7.99 (1 H, d, *J* = 5.0 Hz, CH), 7.93 (1 H, m, CH), 7.52 (borad, NH), 7.31 (5 H, m, CH), 4.94 (2 H, s, $CH_2$), 4.60 (2 H, d, *J* = 5.0 Hz, $CH_2$), 4.23-4.31 (1 H, m, CH), 4.13-4.21 (1 H, m, CH), 4.01 (2 H, d, *J* =

5.0 Hz, $CH_2$), 3.51-3.49 (2 H, m, 1 x $CH_2$ (overlapped with water peak)), 3.38-3.42 (4 H, m, 2 x $CH_2$), 3.16-3.23 (6 H, m, 3 x $CH_2$), 2.39 (2 H, s, $CH_2$), 2.09 (4 H, s, 2 x $CH_2$), 1.70-171 (1 H, m, $CH_3CH_2CH$), 1.42-147 (1 H, m, diastereotopic proton, $CH_3CH_2CH$), 1.26 (3 H, d, $J$ = 5.0 Hz, $CH_3$), 1.02-1.10 (1 H, m, diastereotopic proton, $CH_3CH_2CH$), 0.86 (3 H, d, $J$ = 5.0 Hz, $CHCH_3$), 0.79 (3 H, t, $J$ = 5.0 Hz $CH_2CH_3$); $^{13}$C NMR (100 MHz, DMSO-$d_6$): δ (ppm) = 175.3 (Cq), 172.1 (Cq), 171.9 (Cq), 169.5 (Cq), 165.1 (Cq), 129.6 (CH), 129.1 (CH), 128.8 (CH), 72.6 ($CH_2$), 71.1 ($CH_2$), 70.9 ($CH_2$), 70.4 ($CH_2$), 66.9 ($CH_2$), 59.4 ($CH_3$), 57.7 (CH), 46.7 (CH), 43.4 ($CH_2$), 40.0($CH_2$), 38.5 ($CH_3$), 32.0 (CH), 25.6 ($CH_2$), 18.3 ($CH_3$), 16.5 ($CH_3$); MSES: $m/z$ = 831.5.60 $[M+H]^+$, 854.7 $[M+Na]^+$; HRMS (ES): Calcd for $C_{39}H_{58}N_8NaO_{12}$ 853.4072 ($[M+Na]^+$), found 853.4080; FT-IR (solid): $\nu_{max}$ $cm^{-1}$ = 3300 (w), 2989 (w), 1710 (w), 1635 (s), 1101 (s).

**(S)-2-((2S,3R)-2-(2-(6-(3-Imino-7-oxo-11,14,17,20-tetraoxa-2,4,8-triazahenicosyl)picolinamido)acetamido)-3-methylpentanamido)propanoic acid (82)**

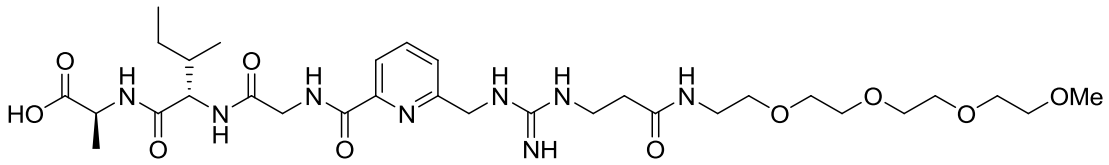


Compound **92** (300 mg, 0.36 mmol) was dissolved in MeOH (50 mL). Pd/C (38 mg, 0.36 mmol) was added and the reaction mixture was stirred for 4 hrs at room temperature under hydrogen (1 atm). The reaction mixture was filtered through celite and dried *in vacuo*. Purification of the resulting solid by precipitation from MeOH using $Et_2O$ afforded **82** (170 mg, 85%) as a white solid. MP = 220-222 $^oC$; $[\alpha]_D^{25}$ =-4.2 $^o$ (*c* 0.2, MeOH); $^1$H NMR (400 MHz, DMSO-$d_6$): δ (ppm) = 9.76 (1 H, s, NH), 8.90 (1 H, s, NH), 8.79 (1 H, s, NH), 8.25 (1 H, s, NH), 8.10 (1 H, s, NH), 8.03-7.96 (3 H, m, 2 x CH + NH), 7.60 (1 H, d, $J$ = 7.5 Hz, CH), 7.55 (1 H, s, NH), 4.52 (2 H, m, $CH_2$), 4.12-4.18 (1 H, m, CH), 4.02-4.03 (2 H, m, $CH_2$), 3.82 (1 H, m, CH), 3.33-3.43 (16 H, m, 8 x $CH_2$), 3.23-3.19 (5 H, m, $CH_2$ + $CH_3$), 2.36 (2 H, s, $CH_2$), 1.84 (1 H, m, CH), 1.42 (1 H, m, $CH_3CH_2$ (a diastereotopic proton)), 1.16-1.18 (4 H, m, $CH_3$ + $CH_3CH_2$ (a diastereotopic proton)), 0.81-0.87 (6 H, m, $CH_3CH_2$ + $CH_2CH(CH)CH_3$); $^{13}$C NMR (100 MHz, DMSO-$d_6$): δ (ppm) = 170.7 (Cq), 170.0 (Cq), 169.5 (Cq), 164.1 (Cq), 157.0 (Cq), 155.8 (Cq), 139.2 (CH), 125.4 (CH), 121.2 (CH), 71.7 ($CH_2$),

70.0 ($CH_2$), 70.2 ($CH_2$), 70.0 ($CH_2$), 69.4 ($CH_2$), 58.5 (CH), 49.7 (CH), 45.9 ($CH_2$), 43.0 ($CH_3$), 39.4 ($CH_2$), 39.1 ($CH_2$), 38.0 ($CH_2$), 36.4 ($CH_3$), 35.1 ($CH_2$), 24.9 ($CH_2$), 19.5 ($CH_3$), 16.1 ($CH_3$), 11.8 (CH); MSES: *m*/*z* = 697.60 $[M+H]^+$, 719.6 $[M+Na]^+$; HRMS (ES): Calcd for $C_{31}H_{52}N_8NaO_{10}$ 719.3704 ($[M+Na]^+$), found 719.3700; FT-IR (solid): $\nu_{max}$ $cm^{-1}$ = 3300 (w), 1662 (s), 1082 (m).

**(R)-Methyl 2-((S)-2-amino-4-methylpentanamido)-4-methylpentanoate (97)**

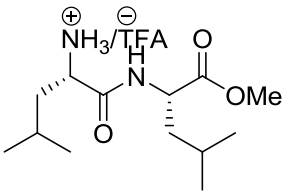


Compound **96** (2.50 g, 6.98 mmol) was dissolved in DCM (10 mL). 20% (v/v) TFA/DCM (20 mL) was added and the reaction mixture was stirred for 5 hrs at room temperature. *In vacuo* drying of the reaction mixture after the addition of toluene (3 x 3 mL) followed by crystallization from diethyl ether afforded **97** (2.50 g, 100%) as a white solid compound. MP = 172-174 ˚C; $^1$H NMR (400 MHz, DMSO-$d_6$): δ (ppm) = 8.81 (1 H, d, *J* = 5.0 Hz, NH), 8.19 (2 H, s, $NH_2$), 4.31-4.37 (1 H, m, C*H*$CH_2CH(CH_3)_2$), 3.80 (1 H, m, C*H*$CH_2CH(CH_3)_2$), 3.75 (3 H, s, COOC*H*$_3$), 1.68-1.69 (2 H, m, 2 x $CHCH_2CH(CH_3)_2$), 1.49-1.59 (4 H, m, 2 x $CHCH_2CH(CH_3)_2$), 0.86-0.95 (12 H, m, $CH(CH_3)_2$); $^{13}$C NMR (100 MHz, DMSO-$d_6$): δ (ppm) = 172.3 (Cq), 169.2 (Cq), 52.0 (CH), 50.6 (CH), 50.4 ($CH_3$), 40.1 ($CH_2$), 38.9 ($CH_2$), 24.0 ($CH_3$), 23.4 ($CH_3$), 22.7 ($CH_3$), 22.6 ($CH_3$), 21.9 (CH), 21.2 (CH); MSES: *m*/*z* = 259.3 $[M+H]^+$; HRMS (ES): Calcd for $C_{13}H_{27}N_2O_3$ 259.2023 ($[M+H]^+$), found 259.2017; FT-IR (solid): $\nu_{max}$ $cm^{-1}$ = 3350 (w), 2957 (w), 1725 (m), 1664 (s), 1522 (s), 1183 (s), 1136 (s).

**(R)-Methyl 2-((S)-2-(4-(((tertbutoxycarbonyl)amino)methyl)benzamido)-4-methylpentanamido)-4-methylpentanoate (98)**

Experimental

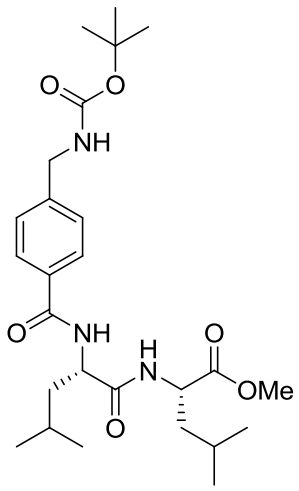

Boc-protected-*p*-methylamino benzoic acid (0.50 g, 1.99 mmol) was dissolved in DMF (5 mL). A solution of HOBt (0.81 g, 6.00 mmol) and DCC (0.82 g, 3.98 mmol) in DMF (10 mL) was added dropwise to the reaction mixture at 0 $^{o}$C and was stirred for 1 hr at room temperature. Compound **97** (0.50 g, 1.99 mmol) and *i*$Pr_2$NEt (1.2 mL, 6.90 mmol) were then added successively and the resulting solution was further stirred at room temperature for 12 hrs. The reaction mixture was added to EtOAc (20 mL), the resulting white precipitate (dicyclohexyl urea) was filtered off and the filtrate was washed with aq. 10% $NaHCO_3$ (10 mL), aq. 10% citric acid (10 mL) and water (10 mL). The organic layer was then dried over $MgSO_4$ and concentrated *in vacuo*. Purification of the resulting crude by column chromatography ($SiO_2$, 1:100 MeOH/DCM) afforded **98** (0.5g, 51%) as white solid. MP = 98-103 ˚C; $^{1}$H NMR (400 MHz, $CDCl_3$): δ (ppm) = 8.32 (1 H, d, *J* = 5.0 Hz, NH), 8.25 (1 H, d, *J* = 5.0 Hz, NH), 7.82 (2 H, d, *J* = 5.0 Hz, CH), 7.43 (1 H, t, *J* = 2.5 Hz, NHBoc), 7.30 (2 H, d, *J* = 5.0 Hz, CH), 4.52-4.58 (1 H, m, C*H*$CH_2CH(CH_3)_2$), 4.26-4.32 (1 H, m, C*H*$CH_2CH(CH_3)_2$), 4.16 (2 H, d, *J* = 5.0 Hz, C*H*$_2$NH), 3.60 (3 H, s, COOC*H*$_3$), 1.49-1.73 (6 H, m, 2 x $CHCH_2CH(CH_3)_2$ + 2 x $CHCH_2CH(CH_3)_2$), 1.39 (9 H, s, $OC(CH_3)_3$), 0.82-0.92 (12 H, m, $CH(CH_3)_2$); $^{13}$C NMR (100 MHz, $CDCl_3$): δ (ppm) = 173.1 (Cq), 172.7 (Cq), 166.3 (Cq), 156.0 (Cq), 143.8 (Cq), 132.8 (Cq), 127.7 (CH), 126.7 (CH), 78.1 (Cq), 52.0 (CH), 51.6 (CH), 50.4 ($CH_3$), 43.4 ($CH_2$), 40.5 ($CH_2$), 40.1 ($CH_2$), 24.7 ($CH_3$), 24.6 ($CH_3$), 24.4 ($CH_3$), 23.4 ($CH_3$), 23.0 ($CH_3$), 21.7 (CH), 21.2 (CH); MSES: *m*/*z* = 514.4 $[M+Na]^+$; HRMS (ES): Calcd for $C_{26}H_{41}N_3NaO_6$ 514.2893 ($[M+Na]^+$), found 514.2877; FT-IR (solid): $\nu_{max}$ $cm^{-1}$ = 3290 (w), 2954 (w), 1633 (s),1537 (s), 1503 (m), 1164 (s).

Experimental

Compound **99**

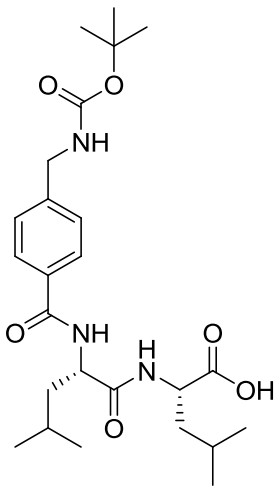

Compound **98** (0.20 g, 0.41 mmol) was dissolved in THF (15 mL) and added to $Me_3SiOK$ (78 mg, 0.61 mmol) suspended in THF (25 mL) under nitrogen. After overnight stirring, DCM (20 mL) and $H_2O$ (20 mL) were added and the reaction mixture was cooled to 0 ˚C. Citric acid (0.1 M) was added dropwise until the pH was 6-7 and further stirred for 1hr. *In vacuo* drying of the organic phase and purification of the resulting crude product by column chromatography ($SiO_2$, 1:20 MeOH/DCM) afforded **99** (0.15 g, 77%) as a white solid. MP = 172-174 ˚C; $^1$H NMR (400 MHz, $CDCl_3$): δ (ppm) = 8.33 (1 H, d, *J* = 5.0 Hz, NH), 8.08 (1 H, d, *J* = 5.0 Hz, NH), 7.83 (2 H, d, *J* = 5.0 Hz, CH), 7.43 (1 H, s(b), NHBoc), 7.31 (2 H, d, *J* = 5.0 Hz, CH), 4.53-4.59 (1 H, m, CH), 4.20-4.26 (1 H, m, CH), 4.16 (2 H, d, *J* = 5.0 Hz, NHC$H_2$), 1.65-1.68 (3 H, m, $CHCH_2CH(CH_3)_2$ + $CHCH_2CH(CH_3)_2$), 1.48-1.56 (3 H, m, $CHCH_2CH(CH_3)_2$ + $CHCH_2CH(CH_3)_2$), 1.40 (9 H, s, $OC(CH_3)_3$), 0.82-0.92 (12 H, m, 2 x $CH(CH_3)_2$); $^{13}$C NMR (100 MHz, $CDCl_3$): δ (ppm) = 174.5 (Cq), 172.9 (Cq), 166.6 (Cq), 156.4 (Cq), 144.2 (Cq), 132.2 (Cq), 128.1 (CH), 127.2 (CH), 78.5 (Cq), 52.1 (CH), 50.8 (CH), 43.8 ($CH_2$), 40.9 ($CH_2$), 40.4 ($CH_2$), 28.8 ($CH_3$), 24.9 ($CH_3$), 24.9 ($CH_3$), 23.7 ($CH_3$), 23.5 ($CH_3$), 22.1 (CH), 22.0 (CH); MSES: *m*/*z* = 500.3 $[M+Na]^+$; HRMS (ES): Calcd for $C_{25}H_{39}N_3NaO_6$ 500.2737 ($[M+Na]^+$), found 500.2733; FT-IR (solid): $\nu_{max}$ $cm^{-1}$ = 3268 (w), 2960 (w), 2361 (m), 2017 (m), 1716 (m),1698 (m), 1540 (s), 1508 (m).

**Methyl 2-(4-((R)-2-((S)-2-(4-(((tert-butoxycarbonyl)amino)methyl)benzamido)-4-methylpentanamido)-4-methylpentanamido)phenyl)acetate**
**(100)**

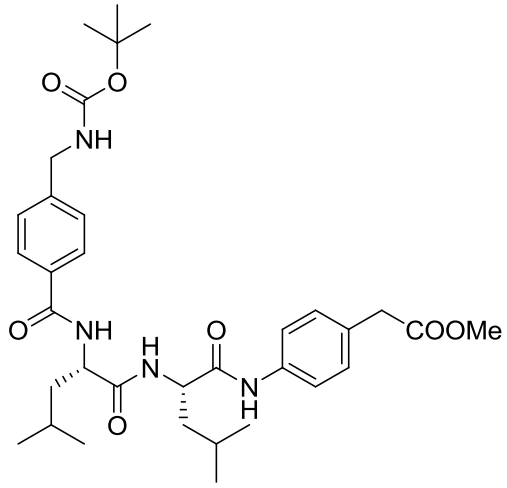


Compound **99** (0.40 g, 0.84 mmol) was dissolved in DCM (20 mL). *i*$Pr_2$NEt (0.5 mL, 2.94 mmol), EDC.HCl (0.4 g, 2.19 mmol), HOBt (0.34 g, 2.52 mmol) and *p*-amino benzylcarboxylic acid methyl ester (0.14 g, 0.84 mmol), previously dissolved in DMF (5 mL), were added successively and the resulting solution was stirred at room temperature for 72 hrs. DCM (30 mL) and aq. 1M $KHSO_4$ (20 mL) were added to the reaction mixture. The organic layer was separated, washed with sat. $Na_2CO_3$ (20 mL) and brine (20 mL) successively, and dried over $MgSO_4$. *In vacuo* removal of the solvent and purification of the resulting crude by column chromatography ($SiO_2$, 1:20 MeOH/DCM) afforded **100** (0.5 g, 95%) as a white solid. MP = 102-104 ˚C; $^1$H NMR (400 MHz, DMSO- $d_6$): δ (ppm) = 8.51 (1 H, t, *J* = 5.0 Hz, NH), 8.05(1 H, d, *J* = 5.0 Hz, NH), 8.05 (1 H, d, *J* = 5.0 Hz, NH), 7.85 (1 H, d, *J* = 5.0 Hz, CH), 7.65 (2 H, d, *J* = 5.0 Hz, CH), 7.55 (1 H, d, *J* = 5.0 Hz, CH), 7.43 (1 H, t, *J* = 2.5 Hz, N*H*Boc), 7.32 (2 H, d, *J* = 5.0 Hz, CH), 7.18-7.21 (2 H, m, CH), 4.40-4.52 (2 H, m, 2 x C*H*$CH_2$CH$(CH_3)_2$), 4.17 (2 H, d, *J* = 5.0 Hz, NHC$H_2$), 3.60-3.62 (5 H, m, C$H_2$COOMe + COOC$H_3$), 1.51-1.72 (6 H, m, 2 x CHC$H_2$C*H*$(CH_3)_2$ + 2 x CHC$H_2$CH$(CH_3)_2$), 1.40 (9 H, s, OC(C$H_3)_3$), 0.85-0.95 (12 H, m, 2 x CH(C$H_3)_2$); $^{13}$C NMR (100 MHz, DMSO-$d_6$): δ (ppm) = 172.4 (Cq), 171.5 (Cq), 170.8 (Cq), 166.5 (Cq), 155.6 (Cq), 143.8 (Cq), 137.4 (Cq), 137.3 (Cq), 129.3 (CH), 127.3 (CH), 126.4 (CH), 119.1 (CH), 77.7 (Cq), 52.5 ($CH_3$), 52.0 (CH), 51.6 ($CH_3$), 51.4 ($CH_3$), 42.9 ($CH_2$), 40.5 ($CH_2$), 40.2 ($CH_2$), 39.8 ($CH_2$), 28.0 ($CH_3$), 24.2 ($CH_3$), 22.9 ($CH_3$), 22.6

(CH), 21.0 (CH); MSES: *m/z* = 647.5 $[M+Na]^+$; HRMS (ES): Calcd for $C_{34}H_{48}N_4NaO_7$ 647.3421 ($[M+Na]^+$), found 647.3418; FT-IR (solid): $\nu_{max}$ $cm^{-1}$ = 3309 (w), 2956 (w), 2361 (m), 2333 (m), 1697 (s), 1671 (s), 1636 (s), 1522 (m),1509 (m),1169 (m).

**Methyl 2-(4-((*R*)-2-((*S*)-2-(4-(aminomethyl)benzamido)-4-methylpentanamido)-4-methylpentanamido)phenyl)acetate (101)**

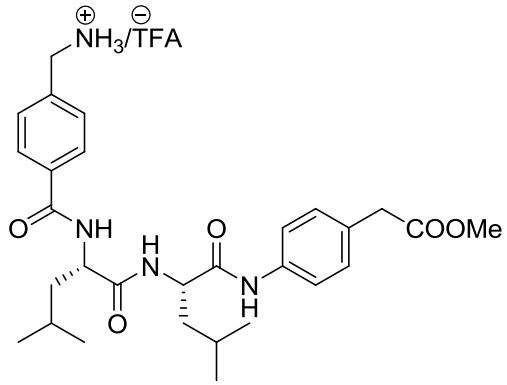


Compound **100** (0.40 g, 0.64 mmol) was stirred in 20% (v/v) TFA/DCM (20 mL) at room temperature for 3 hrs. *In vacuo* drying of the reaction mixture after the addition of toluene (3 x 3 mL) followed by precipitation from diethyl ether afforded **101** (0.40 g, 100%) as a white solid compound. MP =134-136 ˚C; $^1$H NMR (400 MHz, DMSO-$d_6$): δ (ppm) = 9.76 (1 H, s, NH), 8.60 (1 H, d, *J* = 5.0 Hz, NH), 8.52 (1 H, t, *J* = 5.0 Hz, NH), 8.22 (2 H, s(b), $NH_2$), 7.93-7.96 (2 H, m, CH), 7.63 (1 H, d, *J* = 5.0 Hz, CH), 7.52 (2 H, d, *J* = 5.0 Hz, CH), 7.17-7.20 (2 H, m, CH), 4.40-4.52 (2 H, m, 2 x C*H*$CH_2$CH$(CH_3)_2$), 4.10 (2 H, d, *J* = 5.0 Hz, $CH_2$), 3.60-3.62 (5 H, m, C$H_2$COOMe + COOC$H_3$), 1.52-1.80 (6 H, m, 2 x CHC$H_2$C*H*$(CH_3)_2$ + 2 x CHC$H_2$CH$(CH_3)_2$), 0.85-0.95 (12 H, m, 2 x CH(C$H_3)_2$); $^{13}$C NMR (100 MHz, DMSO-$d_6$): δ (ppm) = 171.4 (Cq), 170.7 (Cq), 169.90 (Cq), 136.6 (Cq), 136.3 (Cq), 129.8 (CH), 128.7 (CH), 128.0 (CH), 119.5 (CH), 119.5 (CH), 53.0 ($CH_3$), 52.3 (CH), 52.1 (CH), 42.0 ($CH_2$), 40.7 ($CH_2$), 40.3 ($CH_2$), 39.7 ($CH_2$), 24.9 ($CH_3$), 23.3 ($CH_3$), 22.3 ($CH_3$), 22.1 ($CH_3$), 21.9 (CH), 21.6 (CH); MSES: *m/z* = 525.4 $[M+H]^+$; HRMS (ES): Calcd for $C_{29}H_{41}N_4O_5$ 525.3077 ($[M+H]^+$), found 525.3071; FT-IR (solid): $\nu_{max}$ $cm^{-1}$ = 3275 (m), 2956 (m), 2360 (m), 2026 (m), 1648 (s), 1540 (s), 1520 (s), 1199 (m), 1176 (m), 1137 (m).

**Methyl 2-(4-((R)-2-((S)-2-(4-((6-(((tert-butoxycarbonyl)amino)methyl)picolinamido)methyl)benza mido)-4-methylpentanamido)-4-methylpentanamido)phenyl)acetate (102)**

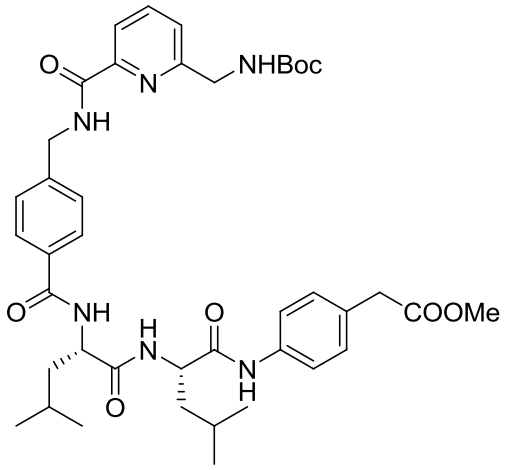


Compound **36** (0.20 g, 0.80 mmol) was dissolved in DCM (20 mL). *i*$Pr_2$NEt (0.6 mL, 2.80 mmol), EDC.HCl (0.37 g, 2.02 mmol), HOBt (0.32 g, 2.37 mmol) and **101** (0.40 g, 0.76 mmol), previously dissolved in DMF (5 mL), were added successively to the reaction mixture which was stirred at room temperature for 48 hrs. DCM (20 mL) and aq. 1M $KHSO_4$ (15 mL) were added to the reaction mixture. The organic layer was separated, washed with sat. $Na_2CO_3$ (15 mL) and brine (15 mL) successively, and dried over $MgSO_4$. *In vacuo* removal of the solvent and purification of the resulting crude by column chromatography ($SiO_2$, 1:25 MeOH/DCM) afforded **102** (0.40 g, 66%) as a white solid. MP = 69-70 ˚C; $^1$H NMR (400 MHz, DMSO-$d_6$): δ (ppm) = 9.89 (1 H, s, NH), 9.76 (1 H, s, NH), 9.35 (1 H, s(b), NH), 8.51 (1 H, t, *J* = 5.0Hz, N*H*Boc), 7.85-7.97 (4 H, m, CH), 7.63-7.65 (1 H, d, *J* = 5.0 Hz, CH), 7.53-7.55 (1 H, m, CH), 7.47-7.49 (1 H, m, CH), 7.40-7.42 (2 H, m, CH), 7.17-7.20 (2 H, m, CH), 4.33-4.59 (6 H, m, 2 x $CHCH_2CH(CH_3)_2$ + $CH_2NH$ + $CH_2NHBoc$), 3.59-3.61 (5 H, m, $CH_2COO$ + $COOCH_3$), 1.48-1.69 (6 H, m, 2 x $CHCH_2CH(CH_3)_2$ + 2 x $CHCH_2CH(CH_3)_2$), 1.39 (9 H, s, $OC(CH_3)_3$), 0.85-0.94 (12 H, m, 2 x $CH(CH_3)_2$); $^{13}$C NMR (100 MHz, DMSO-$d_6$): δ (ppm) = 172.7 (Cq), 171.9 (Cq), 171.1 (Cq), 166.8 (Cq), 164.2 (Cq), 158.4 (Cq), 156.0 (Cq), 149.2 (Cq), 143.2 (Cq), 143.1 (Cq), 138.5 (Cq), 137.7 (Cq), 132.6 (Cq), 129.8 (CH), 129.5 (CH), 127.8 (CH), 127.2 (CH), 123.7 (CH), 120.3 (CH), 119.5 (CH), 119.4 (CH), 78.3 (Cq), 52.8 ($CH_3$), 51.9 (CH), 51.8 (CH), 45.3 ($CH_2$), 42.3 ($CH_2$), 41.0 ($CH_2$), 39.5 ($CH_2$), 39.3 ($CH_2$), 28.4 ($CH_3$), 24.6 ($CH_3$), 23.3 ($CH_3$), 22.1 ($CH_3$), 21.8 ($CH_3$), 21.6 (CH), 21.4 (CH); MSES: *m*/*z* =

781.7 $[M+Na]^+$; FT-IR (solid): $\nu_{max}$ $cm^{-1}$ = 3301w, 2955w, 1716 (m), 1677 (m), 1633 (m), 1598 (m), 1526 (s), 1409 (s), 1276 (s), 1250 (s), 1170 (s).

**(6-((4-(((S)-1-(((R)-1-((4-(2-Methoxy-2-oxoethyl)phenyl)amino)-4-methyl-1-oxopentan-2-yl)amino)-4-methyl-1-oxopentan-2-yl)carbamoyl)benzyl)carbamoyl)pyridin-2-yl)methanaminium (103)**

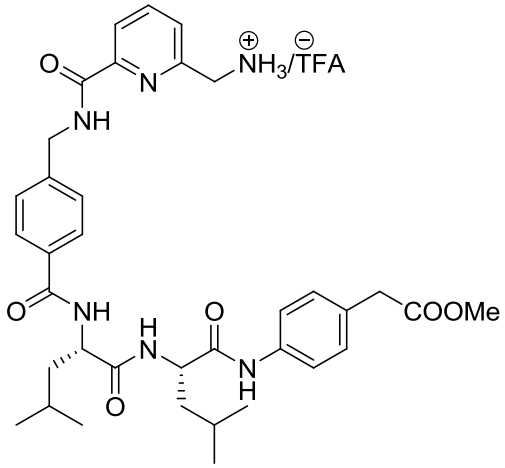


Compound **102** (0.44 g, 0.52 mmol) was stirred in 20% (v/v) TFA/DCM (20 mL) at room temperature for 3h. *In vacuo* drying of the reaction mixture after the addition of toluene (3 x 3 mL) followed by precipitation from diethyl ether afforded **103** (0.40 g, 100%) as a white solid compound. MP = 128-130 ˚C; $^1$H NMR (400 MHz, DMSO-$d_6$): δ (ppm) = 9.91 (1 H, s, NH), 9.79 (1 H, s, NH), 9.68 (1 H, t, $J$ = 5.0 Hz, NH), 8.50-8.53 (2 H, m, CH + NH), 8.36 (s(b), NH), 8.03-8.10 (2 H, m, CH + NH), 7.87-7.89 (2 H, m, CH), 7.61-7.68 (1 H, m, CH), 7.52-7.55 (1 H, m, CH), 7.41-7.43 (2 H, m, CH), 7.17-7.20 (2 H, m, CH), 4.64 (2 H, d, $J$ = 2.5 Hz, C$H_2$NH$_2$), 4.43-4.52 (2 H, m, 2 x C$H$CH$_2$CH(CH$_3$)$_2$), 4.34 (2 H, d, $J$ = 5.0 Hz, NHC$H_2$), 3.59-3.61 (5 H, m, C$H_2$COO + COOC$H_3$), 1.55-1.69 (6 H, m, 2 x CHCH$_2$C$H$(CH$_3$)$_2$ + 2 x CHC$H_2$CH(CH$_3$)$_2$), 0.85-0.94 (12 H, m, 2 x CH(C$H_3$)$_2$); $^{13}$C NMR (100 MHz, DMSO-$d_6$): δ (ppm) = 172.5 (Cq), 171.7 (Cq), 170.9 (Cq), 166.5 (Cq), 163.6 (Cq), 152.3 (Cq), 148.8 (Cq), 142.8 (Cq), 139.0 (CH), 137.5 (Cq), 132.5 (Cq), 129.6 (CH), 127.7 (CH), 126.9 (CH), 124.9 (CH), 121.2 (CH), 119.3 (CH), 119.2 (CH), 52.5 (CH$_3$), 51.8 (CH), 51.6 (CH), 42.1 (CH$_2$), 42.0 (CH$_2$), 40.8 (CH$_2$), 40.4 (CH$_2$), 24.4 (CH$_3$), 23.1 (CH$_3$), 22.9 (CH$_3$), 22.8(CH$_3$), 21.8 (CH), 21.2 (CH) (One CH$_2$ peak overlap with solvent peak); MSES: $m/z$ = 659.5 $[M+H]^+$; HRMS (ES): Calcd for

$C_{36}H_{47}N_6O_6$ 659.3557 ([M+H]$^+$), found 659.3565; FT-IR (solid): $\nu_{max}$ cm$^{-1}$ = 3292 (w), 2957 (w), 1658 (s), 1535 (s), 1200 (m), 1231 (m), 1175 (m), 1137 (m).

**Methyl 2-(4-((R)-2-((S)-2-(4-((6-(3-(((benzyloxy)carbonyl)imino)-7-oxo-11,14,17,20-tetraoxa-2,4,8-triazahenicosyl)picolinamido)methyl)benzamido)-4-methylpentanamido)-4-methylpentanamido)phenyl)acetate**
**(104)**

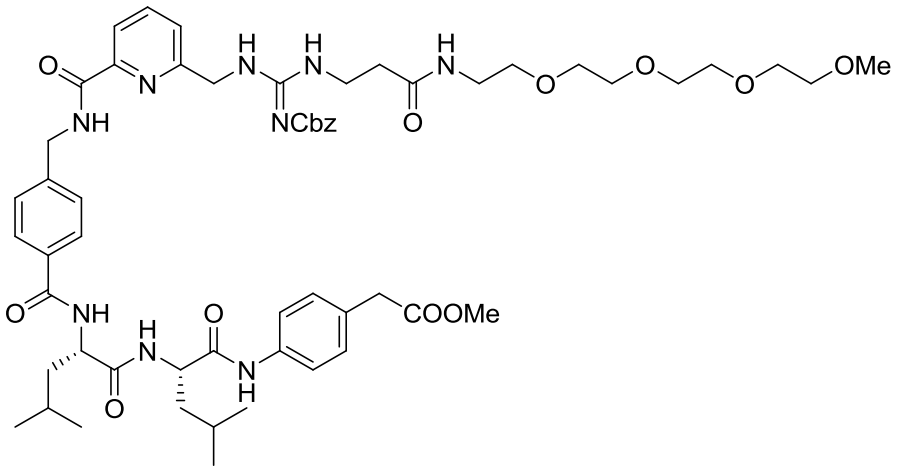


Compound **103** (0.35 g, 0.53 mmol) was dissolved in DCM (40 mL). $Et_3N$ (0.22 mL, 1.59 mmol) and EDC (0.24 g, 1.30 mmol) were added to the reaction mixture which was stirred until it formed a clear solution. Compound **74** (0.25 g, 0.53 mmol) was added and the resulting solution was further stirred for 48 hrs at room temperature. *In vacuo* removal of the solvent and purification of the resulting crude product by column chromatography ($SiO_2$, 1:2 MeOH/DCM) afforded **104** (0.40 g, 86%) as a white solid. MP = 86-88 ˚C; $^1$H NMR (400 MHz, DMSO-$d_6$): δ (ppm) = 10.06 (1 H, s, NH), 9.89 (1 H, s, NH), 9.76 (1 H, s, NH), 9.38 (1 H, s, NH), 8.49-8.51 (1 H, m, CH), 7.91-8.05 (4 H, m, 3 x CH + NH), 7.83-7.84 (2 H, d, *J* = 2.5 Hz, CH), 7.62-7.64 (1 H, d, *J* = 5.0 Hz, CH), 7.52-7.54 (2 H, d, *J* = 5.0 Hz, CH), 7.24-7.28 (5 H, m, CH), 7.17-7.19 (2 H, d, *J* = 5.0 Hz, CH), 4.87 (2 H, s, $CH_2$), 4.59 (4 H, m, 2 x $CH_2$), 4.39-4.50 (2H, m, 2 x C*H*$CH_2$CH$(CH_3)_2$), 3.58-3.59 (5 H, m, $CH_2$ + $CH_3$), 3.38-3.46 (15 H, m, 6 x $CH_2$ + $CH_3$), 3.19-3.23 (6 H, m, 3 x $CH_2$), 2.36 (2 H, s, $CH_2$), 1.55-1.68 (6 H, m, 2 x CH$CH_2$C*H*$(CH_3)_2$ + 2 x CHC*H*$_2$CH$(CH_3)_2$), 0.85-0.95 (12 H, m, 2 x CH(C*H*$_3)_2$); $^{13}$C NMR (100 MHz, DMSO-$d_6$): δ (ppm) = 172.5 (Cq), 172.2 (Cq), 171.7 (Cq), 170.9 (Cq), 170.6 (Cq), 166.6 (Cq), 166.3 (Cq), 137.7 (Cq), 137.6 (Cq), 129.5 (CH), 129.3 (CH), 129.3 (CH), 128.4 (CH), 127.9 (CH), 127.6 (CH),127.4 (CH), 126.9 (CH), 119.3 (CH), 119.2 (CH), 71.2 ($CH_2$), 69.7 ($CH_2$), 69.7 ($CH_2$), 69.5

($CH_2$), 69.0 ($CH_2$), 65.4 ($CH_2$), 58.0 ($CH_3$), 51.7 (CH), 51.6 (CH), 42.2 ($CH_2$), 42.2 ($CH_2$), 40.4 ($CH_2$), 38.5 ($CH_2$), 37.2 ($CH_2$), 24.4 ($CH_3$), 24.4 ($CH_3$), 23.1 ($CH_3$), 21.8 ($CH_3$), 21.6 ($CH_3$), 21.4 (CH), 21.2 (CH); MSES: *m*/*z* =1119.0 $[M+Na]^+$; FT-IR (solid): $\nu_{max}$ $cm^{-1}$ = 3282 (w), 2952 (w), 1736 (m), 1627 (s), 1571 (s), 1522 (s), 1310 (m), 1231 (m), 1100 (m).

**2-(4-((R)-2-((S)-2-(4-((6-(3-(((Benzyloxy)carbonyl)imino)-7-oxo-11,14,17,20-tetraoxa-2,4,8-triazahenicosyl)picolinamido)methyl)benzamido)-4-methylpentanamido)-4-methylpentanamido)phenyl)acetic acid (105)**

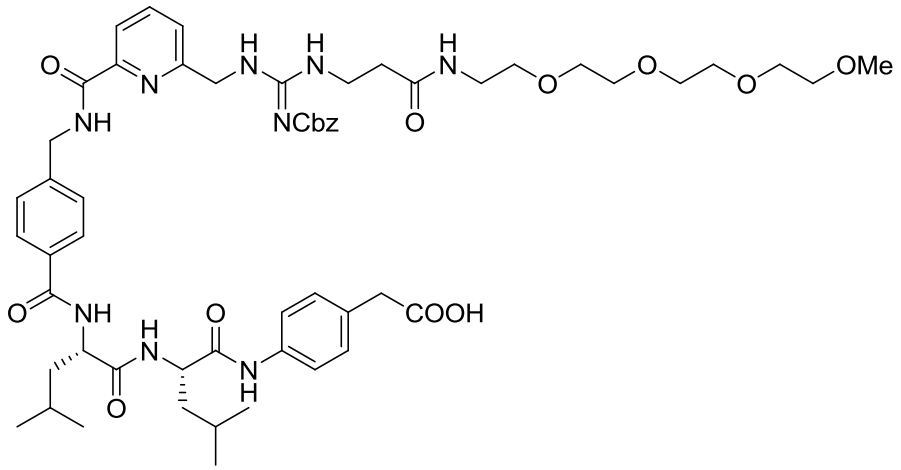


Compound **104** (0.31 g, 0.28 mmol) was dissolved in THF (30 mL) and added to $Me_3SiOK$ (54 mg, 0.42 mmol) suspended in THF (30 mL) under nitrogen. After overnight stirring, DCM (20 mL) and $H_2O$ (20 mL) were added and the reaction mixture was cooled to 0 ˚C. Citric acid (0.1 M) was added dropwise until the pH was 6-7. *In vacuo* removal of the organic phase and purification of the resulting crude product by column chromatography ($SiO_2$, 3:50 MeOH/DCM) afforded **105** (0.25g, 83%) as a white solid. MP = 101-102 ˚C; $^1H$ NMR (400 MHz, DMSO): δ (ppm) = 10.25(1 H, s(b), NH), 10.06 (1 H, s, NH), 9.87 (1 H, s, NH), 9.76 (1 H, s, NH), 9.38 (1 H, s, NH), 8.96 (1 H, s(b), NH), 8.49 (1 H, m, CH), 7.97-8.05 (2 H, m, CH + NH), 7.83-7.85 (2 H, d, *J* = 2.5 Hz, CH), 7.61-7.63 (1 H, d, *J* = 5.0 Hz, CH), 7.52-7.54 (2 H, d, *J* = 5.0 Hz, CH), 7.39-7.41 (2 H, d, *J* = 5.0 Hz, CH), 7.24-7.27 (5 H, m, CH), 7.16-7.18 (2 H, d, *J* = 5.0 Hz, CH), 4.87 (2 H, s, $CH_2$), 4.59 (4 H, s, 2 x $CH_2$), 4.40-4.50 (2 H, m, 2 x C*H*$CH_2CH(CH_3)_2$), 3.46-3.49 (17 H, overlapped with water peak, 7 x $CH_2$ + $CH_3$), 3.18-3.21 (6 H, m, 3 x $CH_2$), 2.36 (2 H, s, $CH_2$), 1.55-1.68 (6 H, m, 2 x

$CHCH_2CH(CH_3)_2$ + 2 x $CHCH_2CH(CH_3)_2$), 0.86-0.93 (12 H, m, 2 x $CH(CH_3)_2$); $^{13}C$ NMR (100 MHz, DMSO-$d_6$): δ (ppm) = 172.7 (Cq), 172.5 (Cq), 172.2 (Cq), 170.9 (Cq), 170.6 (Cq), 166.6 (Cq), 142.9 (Cq), 137.7 (Cq), 137.3 (Cq), 132.4 (Cq), 130.0 (Cq), 129.5 (CH), 128.2 (CH), 127.9 (CH), 127.6 (CH), 127.4 (CH), 126.9 (CH), 119.3 (CH), 119.1 (CH), 71.2 ($CH_2$), 69.7 ($CH_2$), 69.6 ($CH_2$), 69.5 ($CH_2$), 69.0 ($CH_2$), 65.4 ($CH_2$), 58.0 ($CH_3$), 52.6 (CH), 51.7 (CH), 42.2 ($CH_2$), 24.4 ($CH_3$), 23.1 ($CH_3$), 22.7 ($CH_3$), 21.8 ($CH_3$), 21.6 (CH), 21.2 (CH), (3 x $CH_2$ peaks overlap with solvent peak); MSES: *m/z* =1104.9 $[M+Na]^+$; Anal.Calcd for $C_{56}H_{75}N_9O_{13}$: C, 62.15; H, 6.98; N,11.64. Found: C, 61.19; H, 7.15; N,11.15. FT-IR (solid): $\nu_{max}$ $cm^{-1}$ = 3282 (m) (b), 2951(w), 1736 (m), 1633 (s), 1532 (s), 1310 (m), 1234 (m), 1085 (m).

**2-(4-((R)-2-((S)-2-(4-((6-(3-Imino-7-oxo-11,14,17,20-tetraoxa-2,4,8-triazahenicosyl)picolinamido)methyl)benzamido)-4-methylpentanamido)-4-methylpentanamido)phenyl)acetic acid**
**(93)**

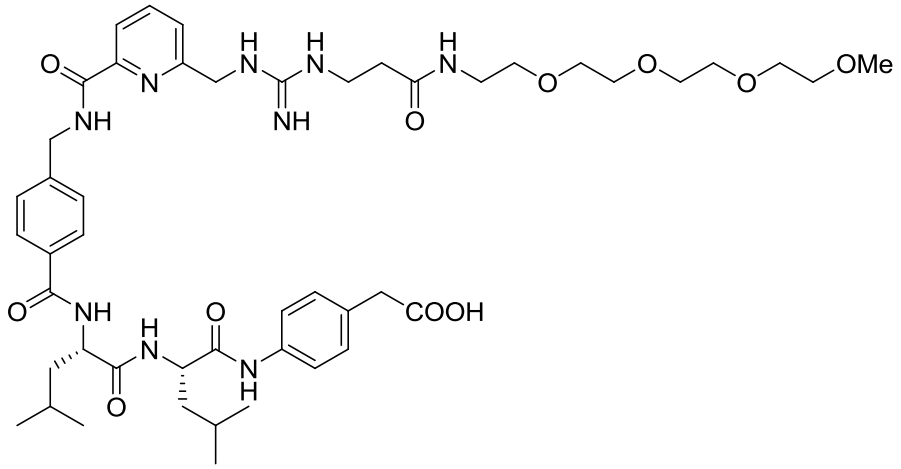


Compound **105** (0.20 g, 0.18 mmol) was dissolved in MeOH (20 mL). Pd/C (20 mg, 0.18 mmol) was added and the reaction mixture was stirred for 8 hrs at room temperature under hydrogen (1 atm). The reaction mixture was filtered through celite and dried *in vacuo*. Purification of the resulting solid by precipitation from MeOH using $Et_2O$ afforded **93** (150 mg, 79%) as a white solid. MP = 121-123 ˚C; -4.2 $^o$ (*c* 0.2, MeOH); $^1H$ NMR (400 MHz, DMSO-$d_6$): δ (ppm) = 9.50-9.61 (1 H, s(b), NH), 9.39 (1 H, s, NH), 8.72 (2 H, s(b), 2 x NH), 8.15 (1 H, m, CH), 7.97-8.05 (2 H, m, CH), 7.83-7.85 (2 H, d, *J* = 2.5 Hz, CH), 7.54 (2 H, s(b), *J* = 5.0 Hz, CH), 7.34-7.36 (2 H, m, CH), 7.01-7.07 (2 H, d, *J* = 5.0 Hz, CH), 4.30-4.65 (6 H, m, 2 x $CHCH_2CH(CH_3)_2$ + 2 x $CH_2$), 3.33-3.41 (17 H, overlapped with water peak, $CH_2$ +

$CH_3$), 3.18-3.22 (6 H, m, 3 x $CH_2$), 2.36 (2 H, s, $CH_2$), 1.59-1.63 (6 H, m, 2 x C*H*$CH_2CH(CH_3)_2$ + 2 x CHC*H*$_2CH(CH_3)_2$), 0.85-0.95 (12 H, m, 2 x CH(C*H*$_3)_2$); $^{13}$C NMR (100 MHz, DMSO-*d*$_6$): δ (ppm) = 176.3 (Cq), 172.2 (Cq), 170.5 (Cq), 170.3 (Cq), 163.8 (Cq), 156.2 (Cq), 143.1 (Cq), 136.0 (Cq), 134.2 (Cq), 132.1 (CH), 129.2 (CH), 129.1 (CH), 127.7 (CH), 127.6 (CH), 127.0 (CH), 126.8 (CH), 120.7 (CH), 119.1 (CH), 119.0 (CH), 71.2 ($CH_2$), 69.7 ($CH_2$), 69.7 ($CH_2$), 69.5 ($CH_2$), 69.0 ($CH_2$), 58.0 ($CH_3$), 54.9 (CH), 52.0 (CH), 44.6 ($CH_2$), 41.5 ($CH_2$), 40.1 ($CH_2$), 38.6 ($CH_2$), 34.8 ($CH_2$), 24.6 ($CH_3$), 23.4 ($CH_3$), 22.6 ($CH_3$), 22.6 ($CH_3$), 21.9 (CH), 21.1 (CH); MSES: *m*/*z* = 970.8[M+Na]$^+$; HRMS (ES): Calcd for $C_{48}H_{70}N_9O_{11}$ 948.5196 ([M+H]$^+$), found 948.5164; FT-IR (solid): $\nu_{max}$ cm$^{-1}$ = 3270 (m) (b), 2952 (w), 1642 (s), 1528 (s).

**(6R, 9R, 12R)-Methyl 6, 9, 12-triisobutyl-2,2-dimethyl-4,7,10-trioxo-3-oxa-5,8,11-triazatridecan-13-oate**
**(107)**

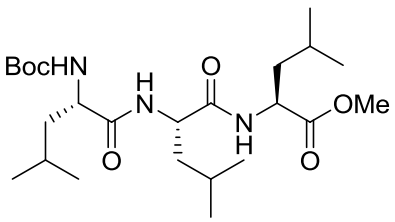


Boc-Leu-OH (0.54 mg, 2.15 mmol) was dissolved in DMF (5 mL). A solution of HOBt (395 mg, 2.58 mmol) and DCC (444 mg, 2.15 mmol) in DMF (10 mL) was added dropwise to the reaction mixture at 0 $^o$C which was stirred for 1 hr at room temperature. Compound **106** (523 mg, 2.15 mmol) and *i*$Pr_2$EtN (1.33 g, 10.3 mmol) were added successively at 0 $^o$C and the resulting solution was further stirred at room temperature for 12 hrs. The reaction mixture was added to EtOAc (25 mL), the resulting white precipitate (dicyclohexyl urea) was filtered off and the filtrate was washed with aq. 10% $NaHCO_3$ (10 mL), aq. 10% citric acid (10 mL) and water (10 mL) successively. The organic layer was dried over $MgSO_4$ concentrated *in vacuo*. Purification of the resulting crude product by column chromatography ($SiO_2$, 15:85 EtOAc/PE) afforded **107** (0.66 mg, 65%) as a white solid. MP = 153 - 154 $^o$C. $^1$H-NMR (300 MHz, $CDCl_3$): δ(ppm) = 6.69 (1 H, d, *J* = 6.6 Hz, N*H*), 6.61 (1 H, d, *J* = 7.7 Hz, N*H*), 4.99 (1 H, m, N*H*), 4.58 - 4.51 (1 H, m, C*H*$CH_2CH(CH_3)_2$), 4.48 - 4.41 (1 H, m, C*H*$CH_2CH(CH_3)_2$), 4.07 (1 H, m, C*H*$CH_2CH(CH_3)_2$), 3.69 (3 H, s, COOC*H*$_3$), 1.69 - 1.51 (9 H, m, 3 x CHC*H*$_2CH(CH_3)_2$ + 3 x $CHCH_2$C*H*$(CH_3)_2$), 1.41

(9 H, s, OC($CH_3$)$_3$), 0.91 - 0.87 (18 H, m, 3 x CH($CH_3$)$_2$); $^{13}$C-NMR (75 MHz, $CDCl_3$): δ(ppm) = 173.1 (Cq), 172.7 (Cq), 171.5 (Cq), 155.7 (Cq), 80.1 (Cq), 53.0 (CH), 52.2 (CH), 51.6 (CH), 50.7 ($CH_3$), 41.3 ($CH_2$), 41.0 ($CH_2$), 40.6 ($CH_2$), 28.3 ($CH_3$), 24.7 (CH), 24.6 (CH), 22.9 (CH), 22.8 ($CH_3$), 22.1 ($CH_3$), 21.8 ($CH_3$); MSES: *m*/*z* = 494.4 $[M+Na]^+$; HRMS (ES): Calcd for $C_{24}H_{45}N_3NaO_6$ 494.3206 ($[M+Na]^+$), found 494.3201; FT-IR (solid): $\nu_{max}$ $cm^{-1}$ = 3292 (w)(b), 2956 (m), 1751 (m), 1643 (s), 1539 (m),1367 (m).

**(S)-1-(((R)-1-(((R)-1-Methoxy-4-methyl-1-oxopentan-2-yl)amino)-4-methyl-1-oxopentan-2-yl)amino)-4-methyl-1-oxopentan-2-aminium**
**(108)**

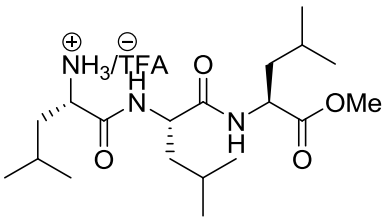


Compound **107** (0.5 g, 1.02 mmol) was stirred in 20% v/v TFA/DCM (20 mL) at room temperature for 3 hrs. *In vacuo* drying of the reaction mixture after the addition of toluene (3 x 3 mL) followed by crystallization from diethyl ether afforded **108** (0.50 g, 100%) as a white solid compound. MP = 200-202˚C; $^1$H NMR (400 MHz, $CDCl_3$): δ (ppm) = 8.61 (1 H, d, *J* = 5.0 Hz, NH), 8.44 (1 H, d, *J* = 5.0 Hz, NH), 8.13 (2 H, s(b), $NH_2$), 4.27-4.33 (2 H, m, CH), 3.78 (1 H, m, CH), 3.61 (3 H, s, COOC$H_3$), 1.40-1.70 (9 H, m, 3 x $CH_2$C*H*($CH_3$)$_2$ + 3 x C$H_2$CH($CH_3$)$_2$), 0.81-0.93 (18 H, m, 3 x CH(C$H_3$)$_2$); $^{13}$C NMR (100 MHz, DMSO-$d_6$): δ (ppm) = 173.9 (Cq), 172.7 (Cq), 169.7 (Cq), 53.0 (CH), 52.1 (CH), 51.9 (CH), 51.2 ($CH_3$), 41.4 ($CH_2$), 40.8 ($CH_2$), 39.9 ($CH_2$), 25.4 ($CH_3$), 25.1 ($CH_3$), 24.7 ($CH_3$), 24.1 ($CH_3$), 23.8 ($CH_3$), 23.3 (CH), 23.2 (CH), 22.2 (CH); MSES: *m*/*z* = 372.4 $[M+H]^+$; HRMS (ES): Calcd for $C_{19}H_{37}N_3NaO_4$ 371.2862 ($[M+Na]^+$), found 371.2859; FT-IR (solid): $\nu_{max}$ $cm^{-1}$ = 3287 (w), 2962 (w), 1697 (s), 1651 (s), 1518 (m), 1198 (m),1134 (s).

**(R)-methyl 2-((R)-2-((S)-2-(4-(((*Tert*-butoxycarbonyl)amino)methyl)benzamido)-4-methylpentanamido)-4-methylpentanamido)-4-methylpentanoate (109)**

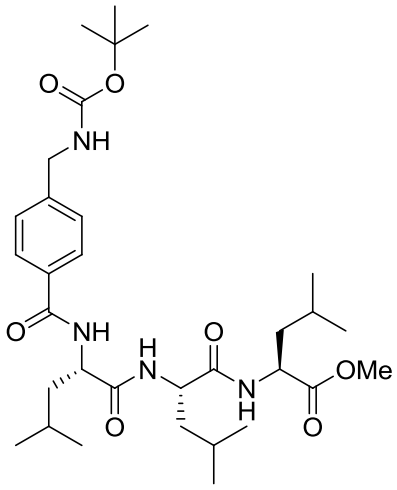

Boc-Protected *p*-methyl aminobenzoic acid (1.00 g, 3.98 mmol) was dissolved in DCM (30 mL). *i*$Pr_2$EtN (1.80 g, 13.7 mmol), EDC.HCl (1.84 g, 9.84 mmol), HOBt (1.6 g, 11.85 mmol) and compound **108** (1.50 g, 3.86 mmol), previously dissolved in DMF (5 mL), were added successively and the resulting solution was stirred at room temperature for 72 hrs. DCM (40 mL) and aq. 1M $KHSO_4$ (30 mL) were added to the reaction mixture. The organic layer was separated, washed with sat. $Na_2CO_3$ (30 mL) and brine (30 mL), and dried over $MgSO_4$. *In vacuo* removal of the solvent and purification of the resulting crude by column chromatography ($SiO_2$, 1:20 MeOH/DCM) afforded **109** (1.30 g, 55%) as a white solid. MP = 102-104 ˚C; $^1$H NMR (400 MHz, $CDCl_3$): δ (ppm) = 8.37 (1 H, d, *J* = 5.0 Hz, NH), 8.13 (1 H, d, *J* = 5.0 Hz, NH), 7.93(1 H, d, *J* = 5.0 Hz, NH), 7.83 (2 H, d, *J* = 5.0 Hz, CH), 7.43 (1 H, t, *J* = 2.5 Hz, NHBoc), 7.31 (2 H, d, *J* = 5.0 Hz, CH), 4.47-4.51 (1 H, m, C*H*$CH_2CH(CH_3)_2$), 4.33-4.37 (1 H, m, C*H*$CH_2CH(CH_3)_2$), 4.26-4.27 (1 H, m, C*H*$CH_2CH(CH_3)_2$), 4.17 (2 H, d, *J* = 5.0 Hz, C$H_2$NH), 3.60 (3 H, s, COOC$H_3$), 1.46-1.70 (9 H, m, 3 x $CHCH_2CH(CH_3)_2$) + 3 x $CHCH_2CH(CH_3)_2$), 1.40 (9 H, s, 3 x $OC(CH_3)_3$), 0.82-0.91 (18 H, m, 3 x $CH(CH_3)_2$); $^{13}$C NMR (100 MHz, DMSO-$d_6$): δ (ppm) = 172.5 (Cq), 172.0 (Cq), 171.9 (Cq), 166.2 (Cq), 155.8 (Cq), 143.6 (Cq), 132.5 (Cq), 127.5 (CH), 126.5 (CH), 77.9 (Cq), 51.9 (CH), 51.7 (CH), 51.1 (CH), 50.1 ($CH_3$), 43.1 ($CH_2$), 41.1 ($CH_2$), 40.4 ($CH_2$), 40.0 ($CH_2$), 28.2 ($CH_3$), 24.4 ($CH_3$), 24.1 ($CH_3$), 23.0 ($CH_3$), 22.9 ($CH_3$), 22.7 ($CH_3$), 21.8 (CH), 21.5 (CH), 21.2 (CH);

MSES: *m/z* = 627.5 $[M+Na]^+$; HRMS (ES): Calcd for $C_{32}H_{52}N_4NaO_7$ 627.3734 ($[M+Na]^+$), found 627.3727; FT-IR (solid): $\nu_{max}$ $cm^{-1}$ = 3269 (w), 2955 (w), 2361 (m), 1633 (s), 1538 (s), 1161 (s).

**(R)-2-((R)-2-((S)-2-(4-(((*Tert*-butoxycarbonyl)amino)methyl)benzamido)-4-methylpentanamido)-4-methylpentanamido)-4-methylpentanoic acid (110)**

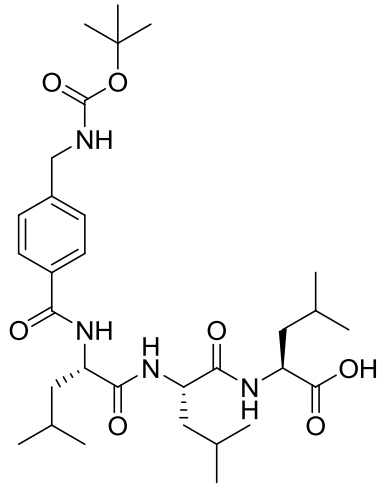

Compound **109** (1.1 g, 1.80 mmol) was dissolved in THF (30 mL) and added to $Me_3SiOK$ (0.35 g, 2.73 mmol) suspended in THF (30 mL) under nitrogen. After overnight stirring, DCM (20 mL) and $H_2O$ (20 mL) were added and the reaction mixture was cooled to 0 °C. Citric acid (0.1 M) was added dropwise until the pH was 6-7. The organic phase was separated and dried over $MgSO_4$. *In vacuo* removal of the organic solvent afforded **110** (1.00 g, 94%) as a white solid. MP = 120-122 °C; $^1$H NMR (400 MHz, DMSO-$d_6$): δ (ppm) = 12.43 (1 H, s(b), COOH), 8.37 (1 H, d, *J* = 5.0 Hz, NH), 7.95 (1 H, d, *J* = 5.0 Hz, NH), 7.93 (1 H, d, *J* = 5.0 Hz, NH), 7.82 (2 H, d, *J* = 5.0 Hz, CH), 7.43 (1 H, t, *J* = 2.5 Hz, N*H*Boc), 7.31 (2 H, d, *J* = 5.0 Hz, CH), 4.46-4.52 (1 H, m, C*H*$CH_2CH(CH_3)_2$), 4.31-4.37 (1 H, m, C*H*$CH_2CH(CH_3)_2$), 4.15-4.22 (3 H, m, C*H*$CH_2CH(CH_3)_2$ + NHC$H_2$), 1.42-1.68 (9 H, m, 3 x $CHCH_2CH(CH_3)_2$ + 3 x $CHCH_2CH(CH_3)_2$), 1.39 (9 H, s, $C(CH_3)_3$), 0.80-0.91 (18 H, m, 3 x $CH(CH_3)_2$); $^{13}$C NMR (100 MHz, DMSO-$d_6$): δ (ppm) = 173.8 (Cq), 171.9 (Cq), 171.8 (Cq), 166.2 (Cq), 155.8 (Cq), 143.6 (Cq), 132.6 (Cq), 127.5 (CH), 126.5 (CH), 77.8 (Cq), 51.9 (CH), 51.7 (CH), 50.1 (CH), 43.1 ($CH_2$), 40.7 ($CH_2$), 40.1 ($CH_2$), 39.8 ($CH_2$), 28.2 ($CH_3$), 24.4 ($CH_3$), 24.2 ($CH_3$), 24.0 ($CH_3$), 23.0 ($CH_3$), 22.8 ($CH_3$), 21.7 (CH), 21.4 (CH), 21.3 (CH); MSES: *m/z* = 613.5 $[M+Na]^+$; HRMS (ES): Calcd for

$C_{31}H_{51}N_4O_7$ 591.3757 ($[M+H]^+$), found 591.3756; FT-IR (solid): $\nu_{max}$ $cm^{-1}$ = 3274 (m), 2957 (m), 2360 (m), 2339 (m), 2019 (m), 1974 (m), 1635 (s), 1539 (s), 1164 (s).

**Methyl 2-(4-((R)-2-((R)-2-((S)-2-(4-(((tert-butoxycarbonyl)amino)methyl)benzamido)-4-methylpentanamido)-4-methylpentanamido)-4-methylpentanamido)phenyl)acetate**
**(111)**

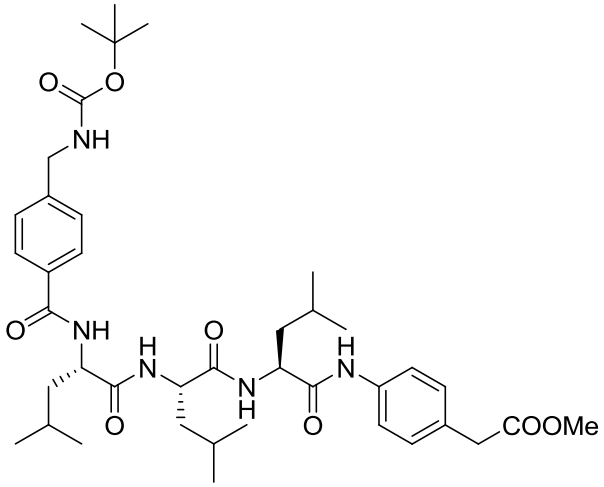


Compound **110** (1.00 g, 1.69 mmol) was dissolved in DCM (20 mL). *i*$Pr_2$EtN (1.1 mL, 5.60 mmol), EDC.HCl (0.80 g, 4.37 mmol), HOBt (0.70 g, 5.19 mmol) and *p*-amino benzylcarboxylic acid methyl ester (0.30 g, 1.82 mmol), previously dissolved in DMF (5 mL), were added successively and the resulting solution was stirred at room temperature for 72 hours. DCM (40 mL) and aq. 1M $KHSO_4$ (20 mL) were added to the reaction mixture. The organic layer was separated, washed with sat. $Na_2CO_3$ (20 mL) and brine (20 mL) successively, and dried over $MgSO_4$. *In vacuo* removal of the solvent and purification of the resulting crude product by column chromatography ($SiO_2$, 1:25 MeOH/DCM) afforded **111** (1.00 g, 80%) as a white solid. MP = 118-120 ˚C; $^1$H NMR (400 MHz, DMSO): δ (ppm) = 9.77 (1 H, s, NH), 8.22 (1 H, d, *J* = 5.0 Hz, NH), 8.13 (1 H, d, *J* = 5.0 Hz, NH), 7.89 (1 H, d, *J* = 5.0 Hz, NH), 7.81-7.84 (2 H, m, 2 x CH), 7.53-7.59 (2 H, m, 2 x CH), 7.43 (1 H, t, *J* = 2.5 Hz, N*H*Boc), 7.29-7.32 (2 H, m, 2 x CH), 7.13-7.19 (2 H, m, 2 x CH), 4.23-4.49 (3 H, m, 3 x C*H*$CH_2$CH$(CH_3)_2$), 4.16 (2 H, *J* = 2.5 Hz, NHC$H_2$), 3.60-3.61 (5 H, m, C$H_2$COOMe + COOC$H_3$), 1.46-1.70 (9 H, m, 3 x $CHCH_2CH(CH_3)_2$ + 3 x $CHCH_2CH(CH_3)_2$), 1.39 (9 H, s, C$(CH_3)_3$), 0.82-0.92 (18 H, m, 3 x CH$(CH_3)_2$); $^{13}$C NMR (100 MHz, DMSO-$d_6$): δ (ppm) = 172.7 (Cq), 172.2 (Cq), 172.1 (Cq), 171.4 (Cq), 171.2 (Cq), 166.9 (Cq),

156.3 (Cq), 144.1 (Cq), 138.0 (Cq), 130.0 (CH), 128.0 (CH), 119.9 (CH), 119.7 (CH), 78.4 (Cq), 52.5 (CH), 52.3 (CH), 52.1 (CH), 51.5 ($CH_3$), 43.6 ($CH_2$), 41.3 ($CH_2$), 40.9 ($CH_2$), 40.7 ($CH_2$), 40.1 ($CH_2$), 28.7 ($CH_3$), 24.7 ($CH_3$), 23.6 ($CH_3$), 23.4 ($CH_3$), 23.3 ($CH_3$), 22.0 (CH), 21.9 (CH), 21.7 (CH); **MSES:** *m/z* = 760.6 $[M+Na]^+$; HRMS (ES): Calcd for $C_{39}H_{59}N_5NaO_7$ 760.4262 ($[M+Na]^+$), found 760.4243; FT-IR (solid): $\nu_{max}$ $cm^{-1}$ = 3274 (m), 2956 (m), 2360 (m), 2019 (m), 1634 (s), 1538 (s), 1520 (s), 1164 (w).

**(4-(((S)-1-(((R)-1-(((R)-1-((4-(2-Methoxy-2-oxoethyl)phenyl)amino)-4-methyl-1-oxopentan-2-yl)amino)-4-methyl-1-oxopentan-2-yl)amino)-4-methyl-1-oxopentan-2-yl)carbamoyl)phenyl)methanaminium**
**(112)**

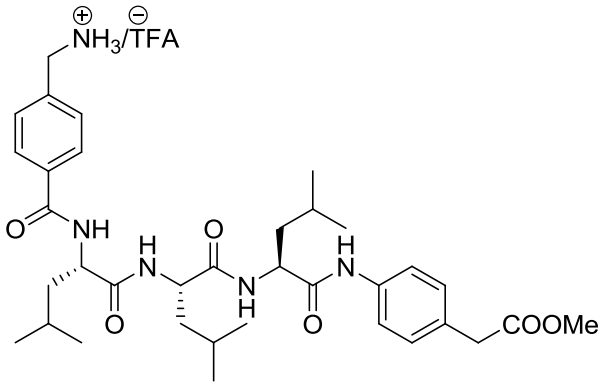


Compound **111** (1.0 g, 1.40 mmol) was stirred in 20% (v/v) TFA/DCM (20 mL) at room temperature for 3 hrs. *In vacuo* drying of the reaction mixture after the addition of toluene (3 x 3 mL) followed by precipitation from diethyl ether afforded **112** (1.00 g, 100%) as a white solid compound. MP = 128-130 ˚C; $^1$H NMR (400 MHz, DMSO-$d_6$):δ (ppm) = 9.92 (1 H, s, NH), 9.80 (1 H, s, NH), 8.50-8.53 (1 H, m, NH), 8.24 (2 H, s(b), $NH_2$), 8.05 (1 H, d, *J* = 5.0 Hz, NH), 7.89-7.94 (2 H, m, 2 x CH), 7.51-7.58 (4 H, m, 4 x CH), 7.14-7.19 (2 H, m, 2 x CH), 4.20-4.52 (3 H, m, 3 x $CH_2CH(CH_3)_2$), 4.11 (2 H, apparent triplate, *J* = 2.5 Hz, $CH_2$), 3.60-3.61 (5 H, m, $CH_2COOCH_3$ + $COOCH_3$), 1.46-1.70 (9 H, m, 3 x $CHCH_2CH(CH_3)_2$ + 3 x $CHCH_2CH(CH_3)_2$), 0.80-0.92 (18 H, m, 3 x $CH(CH_3)_2$); $^{13}$C NMR (100 MHz, DMSO-$d_6$): δ (ppm) = 174.6 (Cq), 174.2 (Cq), 172.1 (Cq), 173.9 (Cq), 173.1 (Cq), 168.2 (Cq), 160.4 (Cq), 139.8 (Cq), 136.2 (Cq), 131.4 (CH), 130.7 (CH), 120.0 (CH), 121.6 (CH), 121.4 (CH), 52.4 (CH), 52.1 (CH), 51.5 (CH), 42.4 ($CH_2$), 41.3 ($CH_2$), 41.0 ($CH_2$), 40.0 ($CH_2$), 26.6 ($CH_3$), 26.4 ($CH_3$), 25.3 ($CH_3$), 25.2 ($CH_3$), 25.0 ($CH_3$), 24.0 ($CH_3$), 23.8 ($CH_3$), 23.7

(CH), 23.6 (CH), 23.4 (CH); MSES: *m/z* = 660.5 $[M+Na]^+$; HRMS (ES): Calcd for $C_{35}H_{52}N_5O_6$ 638.3917 ($[M+H]^+$), found 638.3907; FT-IR (solid): $\nu_{max}$ $cm^{-1}$ = 3271 (w), 2956 (w), 2360 (m), 2340 (m), 1636 (s), 1536 (s), 1199 (s), 1139 (s).

**Compound 113a**

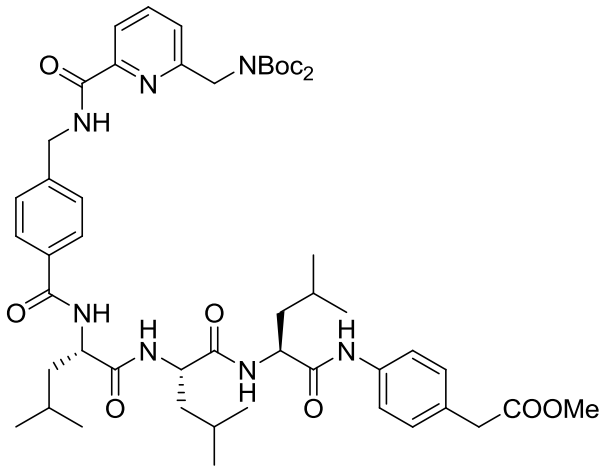


Compound **36** (0.42 g, 1.20 mmol) was dissolved in DCM (30 mL). *i*$Pr_2$EtN (0.73 mL, 4.20 mmol), EDC.HCl (0.55 g, 3.00 mmol), HOBt (0.49 g, 3.60 mmol) and **112** (0.75 g, 1.20 mmol) were successively added to the reaction mixture which was stirred for 24 hours at room temperature. DCM (40 mL) and aq. 1M $KHSO_4$ (20 mL) were added to the reaction mixture. The organic layer was separated, washed with sat. $Na_2CO_3$ (20 mL) and brine (20 mL), and dried over $MgSO_4$. *In vacuo* removal of the organic solvent and purification of the resulting crude by column chromatography ($SiO_2$, 1:50 MeOH/DCM) afforded **113a** (0.70 g, 60%) as a white solid compound. MP = 92-94 ˚C; $^1$H NMR (400 MHz, $CDCl_3$): δ (ppm) = 9.90 (1 H, s, NH), 9.77 (1 H, s, NH), 8.83 (1 H, t, *J* = 2.5 Hz, NH), 8.43 (1 H, d, *J* = 2.5 Hz, NH), 7.94-8.03 (3 H, m, 2 x CH + NH), 7.83-7.86 (2 H, m, CH), 7.52-7.59 (2 H, m, CH), 7.36-7.43 (3 H, m, CH), 7.12-7.19 (2 H, m, CH), 4.87 (2 H, s, $CH_2$), 4.59 (2 H, d, *J* = 2.5 Hz, $CH_2$), 4.47-4.52 (1 H, m, C*H*$CH_2$CH$(CH_3)_2$), 4.22-4.39 (2 H, m, 2 x C*H*$CH_2$CH$(CH_3)_2$), 3.61 (5 H, m, $CH_2$ + COOC*H*$_3$), 1.46-1.70 (9 H, m, 3 x $CHCH_2CH(CH_3)_2$ + 3 x $CHCH_2CH(CH_3)_2$), 1.33 (18 H, s, 2 x OC(C*H*$_3)_3$), 0.81-0.91 (18 H, m, 3 x CH(C*H*$_3)_2$); $^{13}$C NMR (100 MHz, $CDCl_3$): δ (ppm) = 172.9 (Cq), 172.5 (Cq), 172.1 (Cq), 171.2 (Cq), 166.7 (Cq), 166.6 (Cq), 164.1 (Cq), 157.3 (Cq), 152.6 (Cq), 149.2 (Cq), 142.9 (Cq), 139.2 (CH), 138.1 (Cq), 133.3 (Cq), 130.0 (CH), 129.7 (CH), 128.1 (CH), 127.5 (CH), 123.4 (CH),

120.7 (CH), 119.9 (CH), 119.7 (CH), 82.1 (Cq), 51.8 (CH), 51.6 (CH), 51.4 (CH), 50.2 ($CH_2$), 42.2 ($CH_2$), 40.4 ($CH_2$), 39.4 ($CH_2$), 27.9 ($CH_3$), 24.9 ($CH_3$), 24.7 ($CH_3$), 23.6 ($CH_3$), 23.5 ($CH_3$), 23.2 ($CH_3$), 22.3 ($CH_3$), 22.1 ($CH_3$), 22.0 (CH), 21.9 (CH), 21.7 (CH); MSES: *m*/*z* = 995 $[M+Na]^+$; HRMS (ES): Calcd for $C_{52}H_{73}N_7NaO_{11}$ 994.5266 ($[M+Na]^+$), found 994.5246; FT-IR (solid): $\nu_{max}$ $cm^{-1}$ = 3294 (w), 2955 (w), 1739 (s), 1634 (s), 1518 (s), 1366 (s), 1227 (s), 1141 (m).

**(6-((4-(((S)-1-(((R)-1-(((R)-1-((4-(2-Methoxy-2-oxoethyl)phenyl)amino)-4-methyl-1-oxopentan-2-yl)amino)-4-methyl-1-oxopentan-2-yl)amino)-4-methyl-1-oxopentan-2-yl)carbamoyl)benzyl)carbamoyl)pyridin-2-yl)methanaminium**
**(113)**

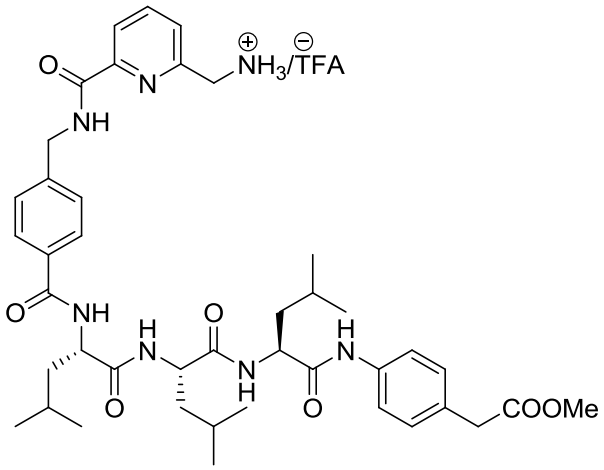


Compound **113a** (0.70 g, 0.72 mmol) was stirred in 20% (v/v) TFA/DCM (20 mL) at room temperature for 3 hrs. *In vacuo* drying of the reaction mixture after the addition of toluene (3 x 3 mL) followed by precipitation from diethyl ether afforded **113** (0.70 g, 100%) as a white solid compound. MP = 122-127 ˚C; $^1$H NMR (400 MHz, DMSO-$d_6$): δ (ppm) = 9.92 (1 H, s, NH), 9.79 (1 H, s, NH), 9.68 (1 H, t, *J* = 5.0 Hz, NH), 8.42 (1 H, d, *J* = 5.0 Hz, CH), 8.35 (1 H, s, $NH_2$), 8.03-8.10 (2 H, m, CH + NH), 7.85-7.85 (2 H, m, CH), 7.66-7.68 (1 H, m, CH), 7.52-7.58 (2 H, m, CH), 7.39-7.42 (2 H, m, CH), 7.13-7.19 (2 H, m, CH), 4.63 (2 H, d, *J* = 5.0 Hz, NHC$H_2$), 4.47-4.52 (1 H, m, C*H*$CH_2CH(CH_3)_2$), 4.31-4.43 (4 H, m, 2 x C*H*$CH_2CH(CH_3)_2$ + $CH_2$), 3.59-3.63 (5 H, m, C$H_2$COOMe + COOC$H_3$), 1.46-1.69 (9 H, m, 3 x $CHCH_2CH(CH_3)_2$ + 3 x $CHCH_2CH(CH_3)_2$), 0.81-0.91 (18 H, m, 3 x $CH(CH_3)_2$); $^{13}$C NMR (100 MHz, DMSO-$d_6$): δ (ppm) = 172.2 (Cq), 172.1 (Cq), 171.8 (Cq), 171.3 (Cq), 166.5 (Cq), 164.0 (Cq), 152.7 (Cq), 149.1 (Cq), 143.1 (Cq), 139.4 (CH), 133.2 (Cq), 130.0 (CH),

129.9 (CH), 128.1 (CH), 127.2 (CH), 125.3 (CH), 121.7 (CH), 119.6 (CH), 119.6 (CH), 52.1 (CH), 51.8 (CH), 51.2 (CH), 42.3 ($CH_2$), 42.2 ($CH_2$), 40.2 ($CH_2$), 39.8 ($CH_2$), 39.4 ($CH_2$), 24.6 ($CH_3$), 24.4 ($CH_3$), 23.3 ($CH_3$), 23.0 ($CH_3$), 23.0 ($CH_3$), 22.0 ($CH_3$), 21.8 ($CH_3$), 21.7 (CH), 21.4 (CH), 21.4 (CH), ($CH_2$ peak overlap with solvent peaks); MSES: *m*/*z* = 772.6 $[M+H]^+$; HRMS (ES): Calcd for $C_{42}H_{58}N_7O_7$ 772.4396 ($[M+H]^+$), found 772.4408; FT-IR (solid): $\nu_{max}$ $cm^{-1}$ = 3289 (w), 2958 (w), 1638 (m), 1535 (s), 1170 (s).

**Methyl 2-(4-((R)-2-((R)-2-((S)-2-(4-((6-(3-(((benzyloxy)carbonyl)imino)-7-oxo-11,14,17,20-tetraoxa-2,4,8-triazahenicosyl)picolinamido)methyl)benzamido)-4-methylpentanamido)-4-methylpentanamido)-4-methylpentanamido)phenyl)acetate**
**(114)**

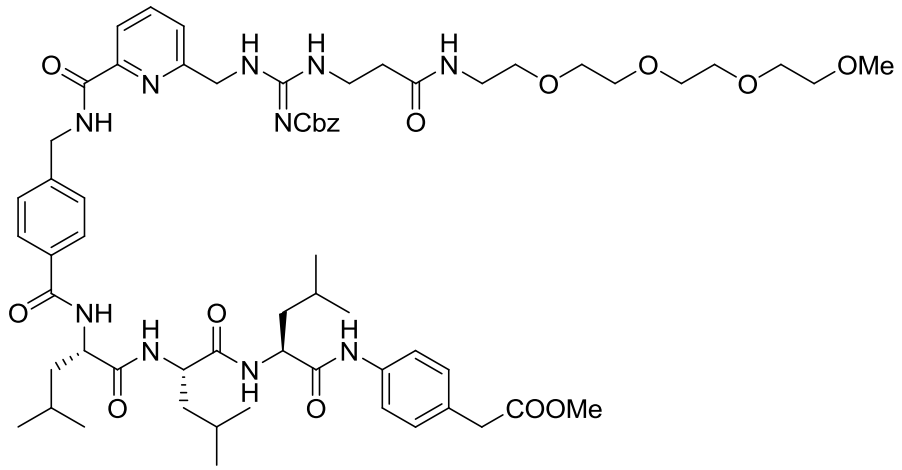


Compound **113** (0.60 g, 0.70 mmol) was dissolved in DCM (50 mL). $Et_3N$ (0.30 mL, 2.1 mmol) and EDC.HCl (0.32 g, 1.75 mmol) were added and the reaction mixture was stirred until it formed a clear solution. Compound **74** (0.33 g, 0.70 mmol) was added and the resulting solution was further stirred for 48 hrs at room temperature. *In vacuo* removal of the solvent and purification of the resulting crude product by column chromatography ($SiO_2$, 1:20 MeOH/DCM) afforded **114** (0.60 g, 71%) as a white solid. MP = 102-107 ˚C; $^1$H NMR (400 MHz, DMSO-$d_6$): δ (ppm) = 9.94 (1 H, s, NH), 9.90 (1 H, s, NH), 9.80 (1 H, s, NH), 9.38 (1 H, s, NH), 8.42-8.44 (1 H, m, CH), 8.16-8.19 (1 H, m, CH), 7.92-8.04 (4 H, m, 1 x CH + NH), 7.81-7.84 (2 H, m, CH), 7.52-7.60 (3 H, m, CH), 7.37-7.40 (2 H, m, CH), 7.23-7.28 (5 H, m, CH), 7.17-7.19 (2 H, d, *J* = 5.0 Hz, CH), 4.89 (2 H, s, $CH_2$), 4.60 (5 H, m, $CH_2$ + $CH_3$), 4.24-

4.49 (3 H, m, 3 x C*H*$CH_2CH(CH_3)_2$), 3.58-3.61 (5 H, m, $CH_2$ + $CH_3$), 3.38-3.49 (14 H, overlapped with water peak, 7 x $CH_2$), 3.17-3.23 (6 H, m, 3 x $CH_2$), 2.37 (2 H, s, $CH_2$), 1.40-1.66 (9 H, m, 3 x $CHCH_2CH(CH_3)_2$ + 3 x $CHCH_2CH(CH_3)_2$), 0.81-0.91 (18 H, m, 6 x $CH_3$); $^{13}$C NMR (100 MHz, DMSO-$d_6$): δ (ppm) = 172.7 (Cq), 172.2 (Cq), 170.8 (Cq), 166.5 (Cq), 166.4 (Cq), 137.5 (Cq), 129.5 (CH), 129.5 (CH), 129.2 (CH), 128.2 (CH), 127.6 (CH), 127.6 (CH), 127.4 (CH), 126.9 (CH), 119.4 (CH), 119.2 (CH), 71.2 ($CH_2$), 69.7 ($CH_2$), 69.7 ($CH_2$), 69.5 ($CH_2$), 69.0 ($CH_2$), 58.0 ($CH_3$), 51.9 (CH), 51.6 (CH), 50.7 (CH), 42.2 ($CH_2$), 40.4 ($CH_2$), 38.5 ($CH_2$), 24.4 ($CH_3$), 24.2 ($CH_3$), 23.1 ($CH_3$), 23.0 ($CH_3$), 22.7 ($CH_3$), 21.8 ($CH_3$), 21.5 (CH), 21.5 (CH), 21.1 (CH), $CH_2$ peaks overlap with solvent peaks; **FT-IR** (solid): $\nu_{max}$ $cm^{-1}$ = 278 (w), 2954 (w), 1627 (s), 1572 (s), 1529 (m), 1311 (m), 1164 (m).

**2-(4-((R)-2-((R)-2-((S)-2-(4-((6-(3-(((benzyloxy)carbonyl)imino)-7-oxo-11,14,17,20-tetraoxa-2,4,8-triazahenicosyl)picolinamido)methyl)benzamido)-4-methylpentanamido)-4-methylpentanamido)-4-methylpentanamido)phenyl)acetic acid**
**(115)**

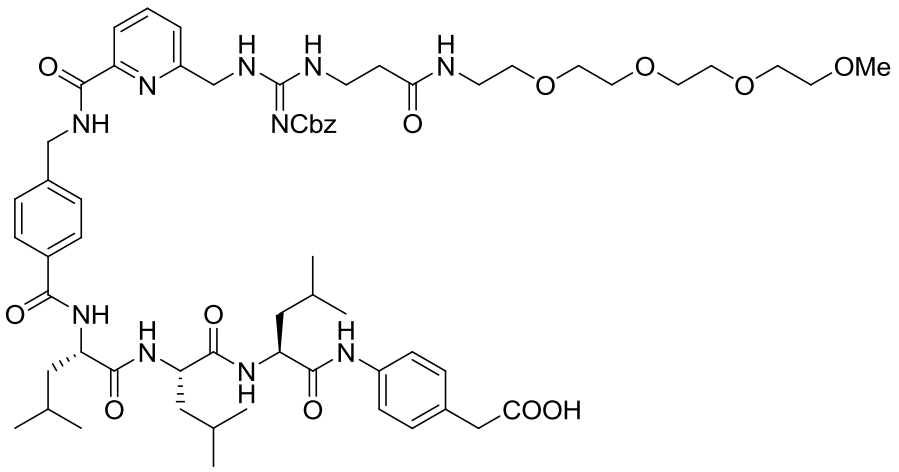


Compound **114** (0.50 g, 0.40 mmol) was dissolved in THF (30 mL) and added to $Me_3SiOK$ (77 mg, 0.66 mmol) suspended in THF (30 mL) under nitrogen. After overnight stirring, DCM (20 mL) and $H_2O$ (20 mL) were added and the reaction mixture was cooled to 0 °C. Citric acid (0.1 M) was added dropwise until the pH was 6-7. The organic phase was separated and dried over $MgSO_4$. *In vacuo* removal of the solvent and purification of the resulting crude by column chromatography ($SiO_2$, 3:50 MeOH/DCM) afforded **115** (0.35 g, 73%) the target compound as a white solid. MP =

112-114˚C; $^{1}$H NMR (400 MHz, DMSO-$d_6$): δ (ppm) = 9.77 (1 H, s, NH), 9.34 (1 H, s, NH), 8.39-8.41 (1 H, m, CH), 8.12-8.14 (1 H, m, CH), 7.99-8.01 (2 H, m(b), NH), 7.81-7.84 (2 H, m, CH), 7.51-7.57 (3 H, m, CH), 7.38-7.41 (2 H, m, CH), 7.28-7.31 (5 H, m, CH), 7.12-7.18 (2 H, m, CH), 4.95 (2 H, s, $CH_2$), 4.23-4.63 (6 H, m, 3 x C*H*$CH_2$CH$(CH_3)_2$ + $CH_3$), 3.36-3.49 (18 H, overlapped with water peak, 9 x $CH_2$), 3.16-3.23 (6 H, m, 3 x $CH_2$), 2.39 (2 H, s, $CH_2$), 1.46-1.65 (9 H, m, 3 x CHCH$_2$C*H*$(CH_3)_2$ + 3 x CHC*H*$_2$CH$(CH_3)_2$), 0.81-0.90 (18 H, m, 3 x CH(C*H*$_3)_2$); $^{13}$C NMR (100 MHz, DMSO-$d_6$): δ (ppm) = 172.9 (Cq), 172.6 (Cq), 171.4 (Cq), 170.9 (Cq), 137.6 (CH), 130.1 (Cq), 129.7 (CH), 128.5 (CH), 127.8 (CH), 127.1 (CH), 126.9 (CH), 119.5 (CH), 71.4 ($CH_2$), 70.1 ($CH_2$), 69.9 ($CH_2$), 69.7 ($CH_2$), 69.2 ($CH_2$), 58.2 ($CH_3$), 52.0 (CH), 42.8 ($CH_2$), 40.3 ($CH_2$), 38.8 ($CH_2$), 24.4 ($CH_3$), 23.3 ($CH_3$), 23.0 ($CH_3$), 23.0 (CH), 22.0 (CH), 21.7 (CH) ($CH_2$ peaks overlap with DMSO solvent peak); MSES**:** *m*/*z* = 1196.1 $[M+H]^+$; FT-IR (solid): $\nu_{max}$ cm$^{-1}$ = 3268 (m) (b), 2950 (w), 1736 (m),1632 (s), 1529 (s), 1367 (m), 1231 (s), 1091 (m).

**2-(4-((R)-2-((R)-2-((S)-2-(4-((6-(3-Imino-7-oxo-11,14,17,20-tetraoxa-2,4,8-triazahenicosyl)picolinamido)methyl)benzamido)-4-methylpentanamido)-4-methylpentanamido)-4-methylpentanamido)phenyl)acetic acid (94)**

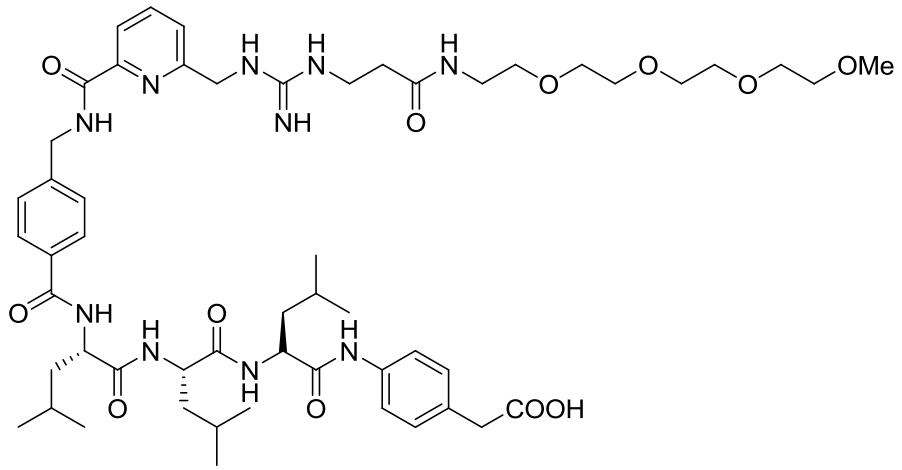


Compound **115** (0.3g, 0.25 mmol) was dissolved in MeOH (20 mL) under $N_2$. Pd/C (26 mg, 0.2 mmol) was added and the reaction mixture was stirred for 10 hrs at room temperature under hydrogen. The reaction mixture was filtered through celite and dried *in vacuo*. Purification of the resulting solid by precipitation from MeOH using $Et_2O$ afforded **94** (200 mg, 75%) as a white solid. MP = 123-125 ˚C; -8.5 $^{o}$ (*c* 0.2, MeOH); $^{1}$H NMR (400 MHz, DMSO-$d_6$): δ (ppm) = 9.87 (1 H, s, NH), 9.81 (1 H,

s(b), NH), 9.64 (1 H, s, NH), 9.58 (1 H, s(b), NH), 8.98 (1 H, s(b), NH), 8.41-8.43 (1 H, d, *J* = 5.0 Hz, NH), 8.32-8.36 (1 H, t, *J* = 5.0 Hz, NH), 8.13-8.17 (2 H, m, CH + NH), 7.98-8.02 (3 H, m, 2 x CH + NH), 7.82-7.84 (2 H, m, CH), 7.51-7.53 (3 H, m, CH), 7.36-7.40 (2 H, m, CH), 7.14-7.16 (1 H, d, *J* = 5.0 Hz, CH), 6.86 (1 H, s(b), NH), 4.17-4.64 (7 H, m, 3 x CH + 2 x $CH_2$), 3.22-3.42 (21 H, overlapped with water peak, $CH_2$ + $CH_3$), 2.37 (2 H, s, $CH_2$), 1.50-1.68 (9 H, m, 3 x CH + 3 x $CH_2$), 0.84-0.90 (18 H, m, 6 x $CH_3$); $^{13}$C NMR (100 MHz, DMSO-$d_6$): δ (ppm) = 172.7 (Cq), 171.9 (Cq), 170.7 (Cq), 170.3 (Cq), 166.5 (Cq), 164.0 (Cq), 149.3 (Cq), 142.8 (Cq), 138.6 (CH), 132.7 (Cq), 129.5 (Cq), 129.2 (CH), 127.6 (CH), 127.0(CH), 126.6 (CH), 120.8 (CH), 119.1 (CH), 71.2 ($CH_2$), 69.7 ($CH_2$), 69.7 ($CH_2$), 69.5 ($CH_2$), 69.0 ($CH_2$), 58.0 ($CH_3$), 54.9 (CH), 52.0 (CH), 45.4 ($CH_2$), 42.1 ($CH_2$), 40.2 ($CH_2$), 39.8 ($CH_2$), 38.6 ($CH_2$), 37.6 ($CH_2$), 34.6 ($CH_3$), 24.4 ($CH_3$), 23.2 ($CH_3$), 23.1 ($CH_3$), 22.6 ($CH_3$), 22.1 ($CH_3$), 21.6 ($CH_3$), 21.5 (CH), 21.2 (CH), 21.0 (CH); MSES**:** *m*/*z* = 1084.0 $[M+Na]^+$; FT-IR (solid): $\nu_{max}$ $cm^{-1}$ = 3291 (m) (b), 2953 (w), 1634 (s), 1532 (s), 1086 (m).

**Methyl 6-((N-((Benzyloxy)carbonyl) carbamimidoyl)carbamoyl)picolinate (119)**

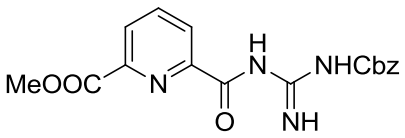


A solution of PyBOP (4.30 g, 8.25 mmol) and NMM (2 mL, 18.20 mmol) in dry DMF (15 mL) was added to a solution of **118** (1 g, 5.49 mmol), Cbz guanidine (1.60 g, 8.25 mmol), and DMF (5 mL). The reaction mixture was stirred at room temperature overnight. Water (100 mL) was added to the reaction mixture and extracted with DCM (3 x 100 mL). The combined organic layer was washed with brine (50 mL) and dried over $MgSO_4$. *In vacuo* removal of the organic solvent and purification of the resulting crude by column chromatography ($SiO_2$, 3:7, EA/DCM) afforded **119** (1.80 g, 92%) as a light yellow solid. MP = 144-146 ˚C; $^1$H NMR (300 MHz, DMSO-$d_6$): δ (ppm) = 8.30 (1 H, dd, *J* = 8.5 Hz, 1.2 Hz, CH), 8.26 (1 H, dd, *J* = 8.9 Hz, 1.2 Hz, CH), 8.00 (1 H, t, *J* = 8.5 Hz, CH), 7.40-7.20 (5 H, m, CH), 5.10 (2 H, s, $CH_2$), 3.95 (3 H, s, $CH_3$); $^{13}$C NMR (75 MHz, DMSO-$d_6$): δ (ppm) = 165.1 (Cq), 164.7 (Cq), 162.4 (Cq), 162.8 (Cq), 158.0 (Cq), 148.2 (Cq), 147.5 (Cq), 140.0 (CH), 139.7 (CH), 128.5 (CH), 128.3 (CH), 127.7 (CH), 126.3 (CH), 66.0 ($CH_2$), 52.8 ($CH_3$); MSES: *m*/*z*

= 379.2 $[M+Na]^+$, HRMS (ES): Calcd for $C_{17}H_{17}N_4O_5$ ($[M+H]^+$) 357.1199, found 357.1198; FT-IR (solid): $\nu_{max}$ $cm^{-1}$ = 3405 (w), 3367 (w), 3030 (w), 2945 (w), 1722 (m), 1696 (m), 1655 (s), 1560 (m), 1434 (m), 1246 (m), 741 (s), 686 (s).

**6-((N-((benzyloxy)carbonyl)carbamimidoyl)carbamoyl)picolinic acid (120)**

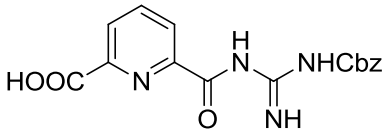


Compound **119** (100 mg, 0.28 mmol) was dissolved in 2% $H_2O/CH_3CN$ (15 mL). $Et_3N$ (0.12 mL, 0.84 mmol) and LiBr (0.24 g, 2.80 mmol) were added successively to the reaction mixture which was stirred for three days at room temperature. Water (20 mL) and EA (20 mL) were added and the reaction mixture was directly acidified with 2 M HCl. The organic phase was extracted with water and dried over $MgSO_4$. *In vacuo* removal of the organic solvent then afforded **120** (81 mg, 85 %) as a white solid. MP = 241- 243 ˚C; $^1$H NMR (300 MHz, DMSO-$d_6$): δ (ppm) = 9.15 (1 H, s, NH), 8.28-8.40 (3 H, m, CH), 7.30-7.37 (5 H, m, CH), 5.09 (2 H, s, $CH_2$); $^{13}$C NMR (75 MHz, DMSO-$d_6$): δ (ppm) = 165.2 (Cq), 155.5 (Cq), 153.0 (Cq), 147.7 (Cq), 147.5 (Cq), 140.9 (CH), 129.3 (CH), 129.0 (CH), 128.9 (CH), 128.6 (CH), 127.0 (CH), 68.9 ($CH_2$); MSES: *m*/*z* = 343.2 $[M+H]^+$; HRMS (ES): Calcd for $C_{16}H_{15}N_4O_5$ 343.1042 ($[M+H]^+$), found 343.1042; FT-IR (solid): $\nu_{max}$ $cm^{-1}$ = 3000w(b), 1698m, 1655 (s), 1533 (m), 1529 (s), 1132 (m), 746 (s), 694 (s).

**Methyl 4-((6-((N-((benzyloxy)carbonyl)carbamimidoyl)carbamoyl)picolinamid o)methyl)benzoate (121)**

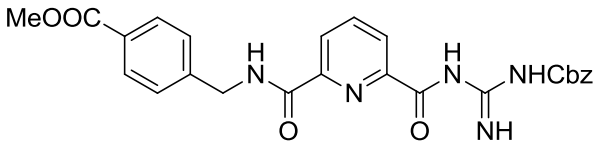


Compound **120** (0.30 g, 0.88 mmol) was dissolved in DCM (50 mL). *i*$Pr_2NEt$ (0.35 mL, 2.00 mmol), EDC.HCl (0.37 g, 1.93 mmol) and HOBt (0.32 g, 2.40 mmol) were successively added to the reaction mixture. 4-(Aminomethyl) benzoic acid methyl ester (0.20 g, 1.00 mmol) dissolved in DCM:DMF (1:1) (10 mL) was added and the resulting solution was stirred for 24 hrs at room temperature. After the addition of aq.

1M $KHSO_4$ (40 mL), the organic layer was separated and washed with sat. $Na_2CO_3$ (40 mL) and brine (40 mL). The organic layer was dried over $MgSO_4$ and the solvent was removed *in vacuo*. Purification of the resulting crude by column chromatogrpahy ($SiO_2$, 1:2 PE/DCM → 1:50 MeOH/DCM) afforded **121** (0.30 g, 70%) as a white solid compound. MP = 226-228 ˚C; $^1$H NMR (300 MHz, DMSO-$d_6$): δ (ppm) = 12.50 (1 H, s, NH), 9.93 (1 H, s, NH), 8.96 (2 H, s, NH), 8.30-8.33 (3 H, m, CH), 7.93 (2 H, d, *J* = 9.7 Hz , CH), 7.49 (2 H, d, *J* = 9.7 Hz , CH), 7.37-7.47 (5 H, m, CH), 5.00 (2 H, s, $CH_2$), 4.72 (2 H, d, *J* = 6.9 Hz, $CH_2$), 3.83 (3 H, s, $CH_3$); $^{13}$C NMR (75 MHz, DMSO-$d_6$): δ (ppm) = 166.5 (Cq), 163.6 (Cq), 158.6 (Cq), 149.3 (Cq), 145.2 (Cq), 140.8 (CH), 137.4 (Cq), 129.8 (CH), 128.8 (CH), 128.1 (CH), 127.9 (CH), 127.7 (CH), 126.6 (CH), 126.2 (CH), 66.2 ($CH_2$), 52.5 ($CH_3$), 42.6 ($CH_2$); MSES: *m*/*z* = 512.4 $[M+Na]^+$; HRMS (ES): Calcd for $C_{25}H_{24}N_5O_6$ 490.1726, found 490.1723 ($[M+H]^+$); FT-IR (solid): $\nu_{max}$ $cm^{-1}$ = 3318 (m), 1649 (s), 1535 (w), 1422 (m), 1381 (m), 1353 (m), 1135 (m), 841 (m), 807 (m), 728 (s), 686 (s), 594 (s), 1384 (s), 1281 (s), 759 (w), 629 (w).

**Benzyl 4-((6-((N'-((benzyloxy)carbonyl)carbamimidoyl)carbamoyl)picoli namido)methyl)benzoate (123)**

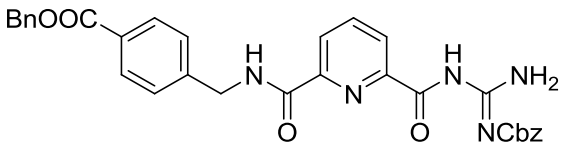


Compound **120** (0.20 g, 0.58 mmol) was dissolved in DCM (30 mL). *i*$Pr_2$NEt (0.23 mL, 1.30 mmol), EDC.HCl (0.24 g, 1.30 mmol) and HOBt (0.21 g, 1.56 mmol) were successively added to the reaction mixture. 4-(Aminomethyl) benzoic acid benzyl ester (0.15 g, 0.62 mmol) was added to the reaction mixture which was stirred for 24 hrs at room temperature. After the addition of 1M $KHSO_4$ (20 mL); the organic layer was separated and washed with sat. $Na_2CO_3$ (20 mL) and brine (20 mL) successively. The organic layer was dried over $MgSO_4$ and the solvent was removed *in vacou*. Purification of the resulting crude by column chromatogrpahy ($SiO_2$, DCM → 1:50 MeOH/DCM) afforded **123** (0.15 mg, 40%) as a white solid. MP = 238-240 ˚C. $^1$H NMR (400 MHz, DMSO-$d_6$): δ (ppm) = 12.50 (1 H, s, NH), 9.90 (1 H, s, NH), 8.94 (2 H, s, NH), 8.37-8.34 (3 H, m, CH), 7.94 (2 H, d, *J* = 5.3 Hz , CH), 7.49 (2 H, d, *J* =

5.3 Hz , CH), 7.46-7.25 (10 H, m, CH), 5.33 (2 H, s, $CH_2$), 4.77 (2 H,s, $CH_2$), 4.71 (2 H, d, *J* = 5.4 Hz, C*H*$_2$NH); $^{13}$C NMR (100 MHz, DMSO-*d*$_6$): δ (ppm) = 165.5 (Cq), 163.2 (Cq), 158.3 (Cq), 149.0 (Cq), 145.0 (Cq), 140.4 (CH), 137.0 (Cq), 136.3 (Cq), 129.5 (CH), 128.6 (CH), 128.9 (CH), 128.4 (CH), 128.2 (CH), 128.0 (CH), 127.7 (CH), 127.5 (CH), 127.4 (CH), 126.3 (CH), 125.8 (Cq), 66.1 ($CH_2$), 65.8 ($CH_2$), 42.3 ( $CH_2$ ); MSES: *m*/*z* = 566.10 $[M+H]^+$; HRMS (ES): Calcd for $C_{31}H_{28}N_5O_6$ 566.2039 ($[M+H]^+$), found 566.2039; FT-IR (solid): $\nu_{max}$ cm$^{-1}$ = 3379w, 3032 (w), 1727 (m), 1709 (m), 1676 (m), 1625 (m), 1300 (s), 1269 (m).

**4-((6-(Carbamimidoylcarbamoyl)picolinamido)methyl)benzoic acid (116)**

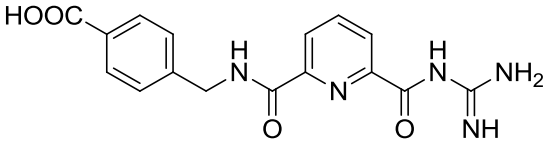


Compound **123** (80 mg, 0.14 mmol) was dissolved in DCM/ MeOH (1:1) (20 mL). Pd/C (10 mg) was added and the reaction mixture was stirred overnight at room temperature under hydrogen (1 atm). The reaction mixture was filtered through celite and dried *in vacuo.* Purification of the resulting solid by precipitation from $Et_2O$/MeOH afforded **116** (25 mg, 52%) as a pale yellow solid. MP > 300 ˚C; $^1$H NMR (400 MHz, DMSO-*d*$_6$): δ (ppm) = 12.57 (1 H, s, NH), 10.71 (1 H, s, NH), 9.43 (1 H, s, NH), 8.62 (2 H, s, NH), 8.40-8.30 (3 H, m, CH), 7.89 (2 H, d, *J* = 5.4 Hz , CH), 7.52 (2 H, d, *J* = 5.4 Hz , CH), 4.60 (2 H, d, *J* = 4.1 Hz, C*H*$_2$NH); $^{13}$C NMR (100 MHz, DMSO-*d*$_6$) δ (ppm) = 166.0 (Cq), 161.4 (Cq), 148.0 (Cq), 143.4 (Cq), 139.0 (CH), 128.0 (CH), 126.3 (CH), 125.4 (CH), 124.7 (CH), 40.9 ($CH_2$); HRMS (ES): Calcd for $C_{16}H_{16}N_5O_4$ 342.1202 ($[M+H]^+$), found 342.1199; FT-IR (solid): $\nu_{max}$ cm$^{-1}$ = 3050 (m) broad, 2360 (m), 2157 (m), 1719 (s), 1670 (s), 1541 (s), 1319 (s), 1234 (s),742 (s).

**6-((4-((Benzyloxy)carbonyl)benzyl)carbamoyl)picolinic acid (125)**

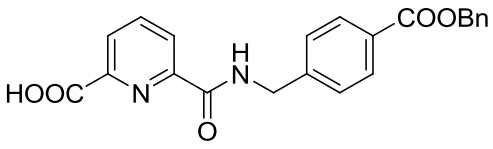

Pyridine-2, 6-dicarboxylic acid (1.40 g, 8.30 mmol) was dissolved in DCM (30 mL) and dry DMF (10 mL). *i*$Pr_2NEt$ (0.72 mL, 4.15 mmol), EDC.HCl (0.76 g, 4.15 mmol) and HOBt (0.56 g, 4.15 mmol) were successively added to the reaction mixture. 4-(Aminomethyl) benzoic acid benzyl ester (1.00 g, 4.15 mmol) dissolved in DCM (10 mL) was added and the resulting was stirred for 24 hours at room temperature. Aq. 1M $KHSO_4$ (30 mL) was added, the organic layer separated, and washed with sat. $Na_2CO_3$ (30 mL) and brine (30 mL). The organic layer was dried over $MgSO_4$ and the solvent was removed *in vacuo*. Purification of the resulting crude product by column chromatography ($SiO_2$, 1:20 MeOH/DCM) afforded **125** (80 mg, 40 %) as a white solid. MP = 250-252 ˚C; $^1$H NMR (400 MHz, $CDCl_3$): δ (ppm) = 9.26 (1 H, t, *J* = 3.8 Hz, NH), 8.27 (1 H, d, *J* = 4.7 Hz, CH), 8.17 (1 H, d, , *J* = 5.0 Hz, CH), 7.89 (1 H, t, *J* = 5.0 Hz, CH), 7.72 (2 H, d, *J* = 6.7 Hz, CH), 7.32-7.14 (5 H, m, CH), 7.15 (2 H, d, *J* = 6.7 Hz, CH), 5.21 (2 H, s, C*H*$_2$Ph), 4.50 (2 H, d, *J* = 3.8 Hz, NHC*H*$_2$); $^{13}$C NMR (100 MHz, $CDCl_3$): δ (ppm) = 165.2 (Cq), 164.0 (Cq), 163.7 (Cq), 162.9 (Cq), 162.5 (Cq), 148.0 (Cq), 144.6 (CH), 142.3 (Cq), 138.5 (CH), 134.8 (Cq), 128.9 (CH), 128.0 (CH), 127.0 (CH), 126.5 (CH), 126.0 (CH), 125.4 (CH), 65.8 ($CH_2$), 42.2 ($CH_2$); MSES: *m*/*z* = 414.0 $[M+Na]^+$; FT-IR (solid): $\nu_{max}$ $cm^{-1}$ = 2843 (b), 1694 (s), 1449 (m), 1429 (m), 1138 (s).

Compound **129**

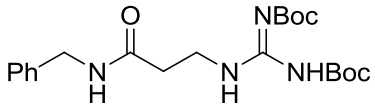


The amine (**41a**) (22 mg, 0.12 mmol) was dissolved in DMF (2 mL). Compound **19** (37 mg, 0.12 mmol) dissolved in THF (5 mL) was added to the reaction mixture and the resulting solution was stirred at room temperature for 3 days. *In vacuo* drying of the reaction mixture and purification of the resulting crude by column chromatography (1:100, MeOH/DCM) afforded **129** (35 mg, 70%) as a yellowish oily liquid. $^1$H NMR (400 MHz, $CDCl_3$): δ (ppm) = 11.27 (1 H, s, NH), 8.94 (1 H, s, NH), 7.91 (1 H, s, NH), 7.23-7.12 (5 H, m, CH), 4.35 (2 H, d, *J* = 3.5 Hz , CH), 3.72-3.68 (2 H, m, $CH_2$), 2.51 (2 H, t, *J* = 3.8 Hz , $CH_2$), 1.54 (9 H, s, C(C*H*$_3$)$_3$), 1.40 (9 H, s, C(C*H*$_3$)$_3$); $^{13}$C NMR (100 MHz, $CDCl_3$): δ (ppm) = 170.0 (Cq), 154.7 (Cq), 151.6

(Cq), 137.4 (Cq), 127.7 (CH), 126.7 (CH), 126.3 (CH), 83.0 (Cq), 82.4 (Cq), 42.5 ($CH_2$), 35.4 ($CH_2$), 30.4 ($CH_2$), 27.1 ($CH_3$), 27.0 ($CH_3$); MSES: *m*/*z* = 421.2 $[M+H]^+$; FT-IR (solid): $\nu_{max}$ $cm^{-1}$ = 3322 (w), 2980 (w), 2360 (w), 1786 (m), 1723 (m), 1618 (s), 1132 (s), 747 (s).

**_N_-Benzyl-3-guanidinopropanamide (130)**

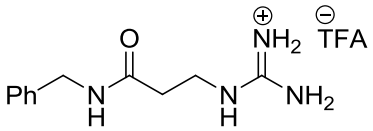


Compound **129** (50 mg, 0.12 mmol) was dissolved in 20% TFA/DCM (5 mL). The resulting solution was left stirring overnight at room temperature. The solvent was removed *in vacuo* and the residual TFA was removed by the addition of toluene (1 mL) and further evaporation *in vacou*. Triturating the resulting gummy material by the addition of diethylether afforded **130** (26 mg, 100%) as a white solid. MP = 120-123 $^oC$; $^1H$ NMR (400 MHz, $CDCl_3$): δ (ppm) = 8.49 (1 H, t, *J* = 3.5 Hz, NH), 7.49 (1 H, t, *J* = 3.5 Hz, NH), 7.32-7.21 (5 H, m, CH), 4.28 (2 H, d, *J* = 3.8 Hz, $CH_2$), 2.42 (2 H, t, *J* = 4.1 Hz, $CH_2$), (one $CH_2$ peak has overlapped with the water peak). $^{13}C$ NMR (100 MHz, $CDCl_3$): δ (ppm) = 170.5 (Cq), 157.3 (Cq), 139.7 (Cq), 128.8 (CH), 127.7 (CH), 127.3 (CH), 42.6 ($CH_2$), 37.6 ($CH_2$), 34.8 ($CH_2$); MSES: *m*/*z* = 221.2 $[M+H]^+$; FT-IR (solid): $\nu_{max}$ $cm^{-1}$ = 3375 (w), 3271 (w), 1683 (s), 1638 (s), 1616 (s), 1171 (s), 1135 (s).

**Methyl 4-((5-((N-((benzyloxy)carbonyl)carbamimidoyl)carbamoyl)-1H-pyrrole-2-carboxamido)methyl)benzoate (142)**

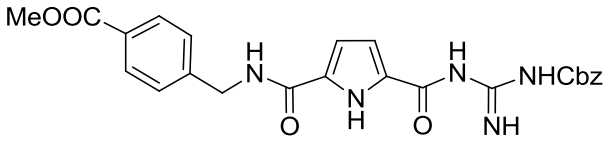


Compound **141** (0.18 g, 0.55 mmol) was dissolved in dry DCM (50 mL). *i*$Pr_2$NEt (0.6 mL, 1.40 mmol), EDC.HCl (0.26 g, 1.38 mmol) and HOBt (0.22 g, 1.65 mmol) were successively added to the reaction mixture. 4-(Aminomethyl) benzoic acid methyl ester (0.11 g, 0.55 mmol) dissolved in DCM : DMF (1:1) (10 mL) was added to the

reaction mixture which was stirred for 24 hrs at room temperature. Aq. 1M $KHSO_4$ (30 mL) was added, the organic layer separated, and washed with aq sat. $Na_2CO_3$ (30 mL) and brine (30 mL) successively. The organic layer was dried over $MgSO_4$ and the solvent was evaporated *in vacuo*. Purification of the resulting crude by column chromatography ($SiO_2$, 1:100-1:50 MeOH/DCM) afforded **142** (0.20 g, 76%) as a white solid. MP = 210-211˚C; $^1$H NMR (400 MHz, DMSO-$d_6$): δ (ppm) = 11.15 (1 H, s, NH), 9.39 (1 H, s, NH), 9.00 (1 H, t, *J* = 3.5 Hz, NH), 8.80 (1 H, s, NH), 7.94 (2 H, d, *J* = 5.0 Hz, CH), 7.45 (2 H, d, *J* = 5.0 Hz, CH), 7.31-7.40 (6 H, m, CH), 6.95 (1 H, m, CH), 5.15 (2 H, s, OC$H_2$Ph), 4.55 (2 H, d, *J* = 3.8 Hz, NHC$H_2$), 3.85 (3 H, s, C$H_3$COO); $^{13}$C NMR (100 MHz, DMSO- $d_6$): δ (ppm) =180.6 (Cq), 166.3 (Cq), 159.9 (Cq), 145.3 (Cq), 129.6 (CH), 128.7 (CH), 128.5 (CH), 128.1 (CH), 127.9 (CH), 127.7 (CH), 112.4 (CH), 66.4 ($CH_3$), 52.3 ($CH_2$), 42.2 ($CH_2$); MSES: *m*/*z* = 500.2 $[M+Na]^+$; HRMS (ES): Calcd for $C_{24}H_{24}N_5O$ ($[M+H]^+$) 478.1726, found 478.1729; FT-IR (solid): $\nu_{max}$ $cm^{-1}$ = 3395 (w), 3370 (m), 2970 (b), 1715 (m), 1673 (m), 1641 (m), 1616 (w),1532 (m), 1263 (s), 752 (m).

**4-((5-((*N*-((Benzyloxy)carbonyl)carbamimidoyl)carbamoyl)-1*H*-pyrrole-2-carboxamido)methyl)benzoic acid**
**(143)**

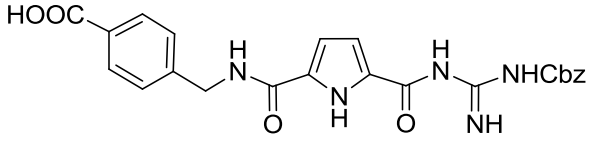


Compound **142** (0.19 g, 0.40 mmol) was dissolved in THF (20 mL) and added to $Me_3SiOK$ (65 mg, 0.5 mmol) suspended in THF (10 mL) under $N_2$. The reaction mixture was stirred for 72 hrs at room temperature. DCM (30 mL) and $H_2O$ (30 mL) were added and the reaction mixture was cooled to 0 ˚C. Citric acid (0.1 M aqeous) was added dropwise until the pH was 6-7 and further stirred for 1 hr. *In vacuo* drying of the organic phase and purification of the resulting crude by column chromatography ($SiO_2$, 1:20 MeOH/DCM) afforded **143** (0.16 g, 86%) as a white solid. MP = 294-296 ˚C; $^1$H NMR (400 MHz, DMSO-$d_6$): δ (ppm) = 11.83 (1 H, s, NH), 9.36 (1 H, s, NH), 8.97 (1 H, t, *J* = 3.8 Hz, NH), 8.76 (1 H, s, NH), 7.90 (2 H, d, *J* = 5.0 Hz, CH), 7.31-7.42 (7 H, m, CH), 6.97 (1 H, s, CH), 6.87 (1 H, s, CH), 5.12 (2 H, s, $CH_2$), 4.52 (2 H, d, *J* = 3.8 Hz, $CH_2$); $^{13}$C NMR (100 MHz, DMSO-$d_6$): δ (ppm)

= 180.6 (Cq), 171.7 (Cq), 167.6 (Cq), 160.1 (Cq), 159.4 (Cq), 145.0 (Cq), 129.9 (CH), 128.9 (CH), 128.3 (CH), 128.1 (CH), 127.7 (CH), 112.4 (CH), 66.6 ($CH_2$), 42.4 ($CH_2$); MSES: *m*/*z* = 464.1 $[M+H]^+$; FT-IR (solid): $\nu_{max}$ $cm^{-1}$ = 3077m(b), 2949m(b), 1726s, 1666s, 1283s, 1109m, 848m, 749m, 756m, 635m.

**Benzyl 4-((5-((*N*-((benzyloxy)carbonyl)carbamimidoyl)carbamoyl)-1*H*-pyrrole-2-carboxamido)methyl)benzoate**

**(144)**

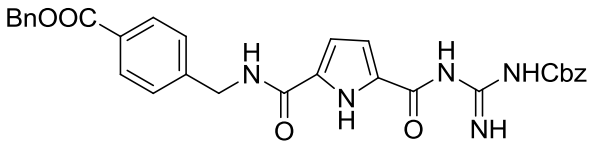


Compound **141** (1.10 g, 3.33 mmol) was dissolved in dry DCM (50 mL). *i*$Pr_2NEt$ (1.43 mL, 1.40 mmol), EDC.HCl (1.29 g, 8.33 mmol) and HOBt (1.1 g, 8.3 mmol) were successively added to the reaction mixture. 4-(Aminomethyl) benzoic acid benzyl ester (0.90 g, 4.00 mmol) dissolved in DCM (25 mL) was added to the reaction mixture which was stirred for 24 hrs at room temperature. Aq. 1 M $KHSO_4$ (30 mL) was added and the organic layer separated and washed with sat. aq $Na_2CO_3$ (30 mL) and brine (30 mL). The organic layer was dried over $MgSO_4$ and the solvent was evaporated *in vacuo*. Purification of the resulting crude by column chromatography ($SiO_2$, 1:100-1:50 MeOH/DCM) afforded **144** (0.73 g, 40%) as a white solid. MP = 215-216 ˚C; $^1$H NMR (400 MHz, DMSO-*d*$_6$): δ (ppm) = 11.16 (1 H, s, NH), 9.35 (1 H, s, NH), 9.00 (1 H, s, NH), 8.76 (1 H, s, NH), 7.96 (2 H, d, *J* = 5.35 Hz, CH), 7.46-7.36 (12 H, m, CH), 6.97 (1 H, s, CH), 6.86 (1 H, s, CH), 5.33 (2 H, s, $CH_2$), 5.12 (2 H, s, $CH_2$), 4.52 (2 H, s, $CH_2$); $^{13}$C NMR (100 MHz, DMSO-*d*$_6$): δ (ppm) = 165.5 (Cq), 159.7 (Cq), 145.3 (Cq), 136.3 (Cq), 129.3 (CH), 128.6 (CH), 128.5 (CH), 128.3 (CH), 128.2 (CH), 128.0 (CH), 127.6 (CH), 66.1 ($CH_2$ ), 42.0 ($CH_2$); HRMS (ES): Calcd for $C_{30}H_{28}N_5O_6$ ($[M+H]^+$) 554.2039, found 554.2024; FT-IR (solid): $\nu_{max}$ $cm^{-1}$ = 3345 (w), 3222 (m), 2957 (w)(b), 1720 (m), 1674 (m), 1641 (m), 1324 (s), 1262 (s), 1237 (s).

**4-((5-(Carbamimidoylcarbamoyl)-1*H*-pyrrole-2-carboxamido)methyl)benzoic acid**
**(133)**

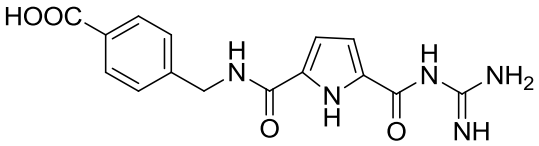


Compound **144** (90 mg, 0.2 mmol) was dissolved in DCM/ MeOH (1:4) (10 mL). Pd/C (10 mg) was added to the reaction mixture which was stirred under hydrogen (1 atm) overnight at room temperature. The reaction mixture was filtered through celite and dried *in vacuo.* Purification of the resulting solid by precipitation from $Et_2O$/MeOH afforded **133** (30 mg, 45%) as a pale yellow solid. MP > 250 ˚C; $^1$H NMR (400 MHz, DMSO-$d_6$): δ (ppm) = 12.35 (1 H, s, NH), 11.85 (1 H, s, NH), 9.05 (1 H, t, *J* = 3.8 Hz, N*H*$CH_2$), 8.44 (2 H, d, *J* = 5.0 Hz, NH), 7.92 (2 H, d, *J* = 5.0 Hz , CH), 7.43 (2 H, d, *J* = 5.0 Hz, CH), 7.37 (1 H, s(broad), CH), 6.91 (1 H, d, *J* = 2.2 Hz, CH), 4.54 (2 H, d, *J* = 2.5 Hz, NHC$H_2$); $^{13}$C NMR (100 MHz, DMSO-$d_6$): δ (ppm) = 167.6 (Cq), 159.9 (Cq), 144.8 (Cq), 129.9 (CH), 127.8 (CH), 113.0 (CH), 42.5 ($CH_2$); MSES: *m*/*z* = 330.2 $[M+H]^+$; HRMS (ES): Calcd for $C_{15}H_{16}N_5O_4$ 330.1202 ($[M+H]^+$), found 330.1198; FT-IR (solid): $\nu_{max}$ $cm^{-1}$ = 2979 (w)(b), 2362 (w), 1590 (m), 1552 (s).

N.B Compounds **31a** [128], **32** [129], **40** [130], **48** [131], **61** [132], **96** [134], **118** [70], **127** [125], **128** [125], **135** [133], **136** [96], **138** [96], **139** [96], **140** [96] and **141** [96] were prepared according to literature procedures and their spectroscopic data are consistent with the reported literature data.

# Appendices

## Appendix A- ITC dilution data

*ITC data of guandinium carboxylate **29***

[monomer] = 20 mM
Solvent = DMSO
$K_{dim}[M^{-1}]$ = 38
$\Delta G_{dim}$ [kJ $mol^{-1}$] = -9.0
$\Delta H_{dim}$ [kJ $mol^{-1}$] = -6.0
$T\Delta S_{dim}$ [kJ $mol^{-1}$] = 3.0

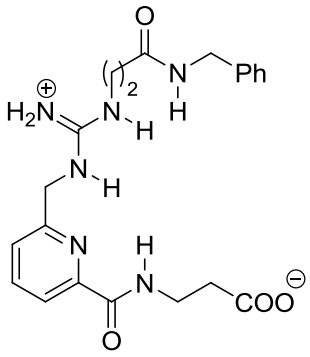

**29**

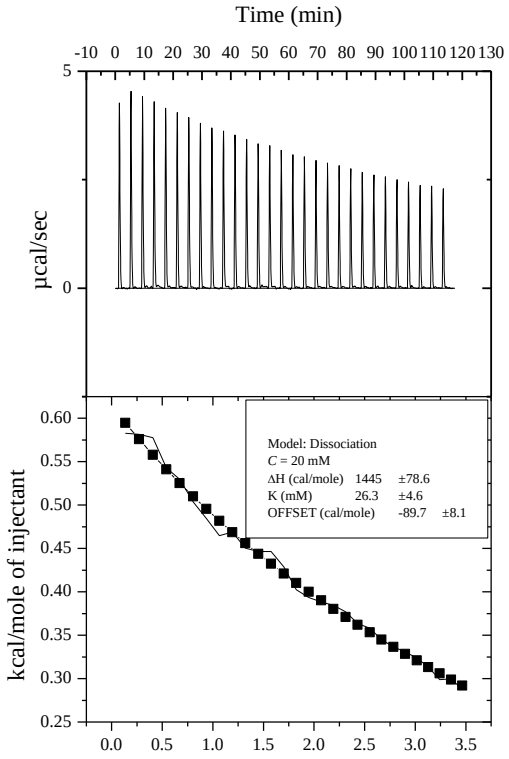


Guanidinium-carboxylate **29** in DMSO

ITC final figure

| Inj. No. | Molar ratio | Cal/mol of injected **29** |
|---|---|---|
| 1 | 0.13639 | 582.8645 |
| 2 | 0.27184 | 581.477 |
| 3 | 0.40635 | 577.5922 |
| 4 | 0.53993 | 543.001 |
| 5 | 0.67257 | 529.6865 |
| 6 | 0.80427 | 503.7762 |
| 7 | 0.93504 | 484.5144 |
| 8 | 1.06487 | 464.8826 |
| 9 | 1.19377 | 468.9053 |
| 10 | 1.32173 | 450.2652 |
| 11 | 1.44875 | 446.5529 |
| 12 | 1.57484 | 446.3665 |
| 13 | 1.69998 | 428.9436 |
| 14 | 1.8242 | 402.567 |
| 15 | 1.94747 | 393.5152 |
| 16 | 2.06981 | 388.3179 |
| 17 | 2.19122 | 384.3716 |
| 18 | 2.31168 | 376.9056 |
| 19 | 2.43121 | 363.5502 |
| 20 | 2.54981 | 358.2004 |
| 21 | 2.66747 | 344.9901 |
| 22 | 2.78419 | 336.5519 |
| 23 | 2.89997 | 330.9379 |
| 24 | 3.01482 | 323.6815 |
| 25 | 3.12873 | 313.4672 |
| 26 | 3.24171 | 298.826 |
| 27 | 3.35375 | 299.794 |
| 28 | 3.46485 | 287.4068 |
| 29 | 0.13639 | 582.8645 |

*ITC data of guanidinium-carboxylate **30***

[monomer] = 10 mM
Solvent = DMSO
$K_{dim}[M^{-1}]$ = 400
$\Delta G_{dim}$ [kJ $mol^{-1}$] = -14.9
$\Delta H_{dim}$ [kJ $mol^{-1}$] = -11.1
$T\Delta S_{dim}$ [kJ $mol^{-1}$] = 3.7

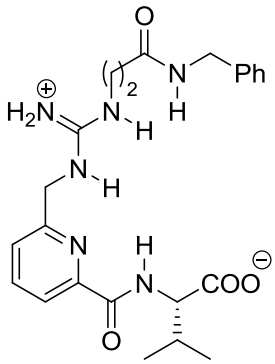

**30**

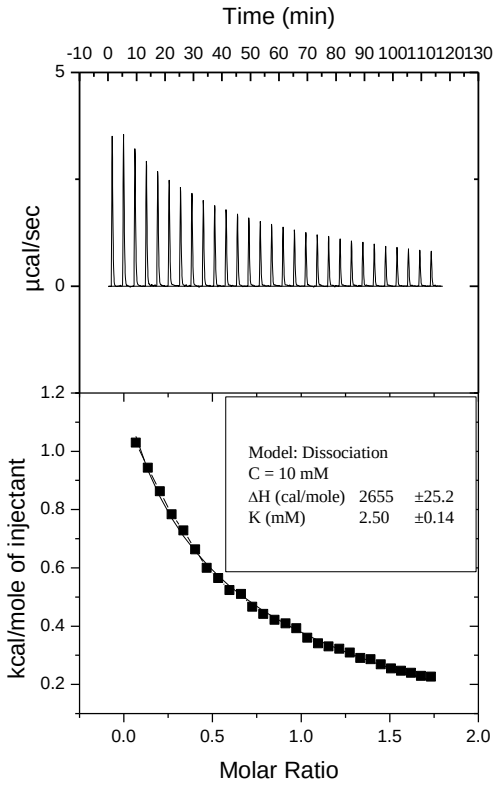


Guanidinium-carboxylate **30** in DMSO

ITC final figure

| Inj. No. | Molar ratio | Cal/mol of injected **30** |
|---|---|---|
| 1 | 0.06819 | 1029.967 |
| 2 | 0.13592 | 943.0357 |
| 3 | 0.20318 | 862.9701 |
| 4 | 0.26996 | 783.4125 |
| 5 | 0.33628 | 728.5454 |
| 6 | 0.40214 | 662.9338 |
| 7 | 0.46752 | 600.3399 |
| 8 | 0.53244 | 564.5805 |
| 9 | 0.59688 | 523.2009 |
| 10 | 0.66086 | 510.01 |
| 11 | 0.72437 | 466.0615 |
| 12 | 0.78742 | 441.7893 |
| 13 | 0.84999 | 421.3278 |
| 14 | 0.9121 | 409.2686 |
| 15 | 0.97374 | 392.2766 |
| 16 | 1.03491 | 360.3329 |
| 17 | 1.09561 | 340.3065 |
| 18 | 1.15584 | 330.0532 |
| 19 | 1.21561 | 322.0468 |
| 20 | 1.2749 | 308.9202 |
| 21 | 1.33373 | 291.0364 |
| 22 | 1.39209 | 286.0037 |
| 23 | 1.44999 | 268.8602 |
| 24 | 1.50741 | 254.5628 |
| 25 | 1.56437 | 246.7858 |
| 26 | 1.62085 | 239.9488 |
| 27 | 1.67687 | 229.4327 |
| 28 | 1.73242 | 226.5848 |
| 29 | 0.06819 | 1029.967 |

Appendices

*ITC data of guandinium-carboxylate **45***

[monomer] = 10 mM
Solvent = DMSO
$K_{dim}[M^{-1}]$ = 240
$\Delta G_{dim}$ [kJ $mol^{-1}$] = -13.6
$\Delta H_{dim}$ [kJ $mol^{-1}$] = -16.7
$T\Delta S_{dim}$ [kJ $mol^{-1}$] = -3.1

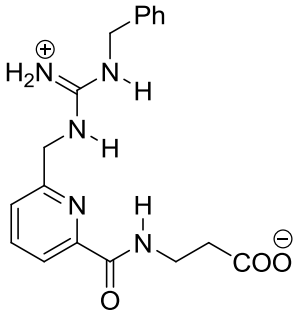


**45**

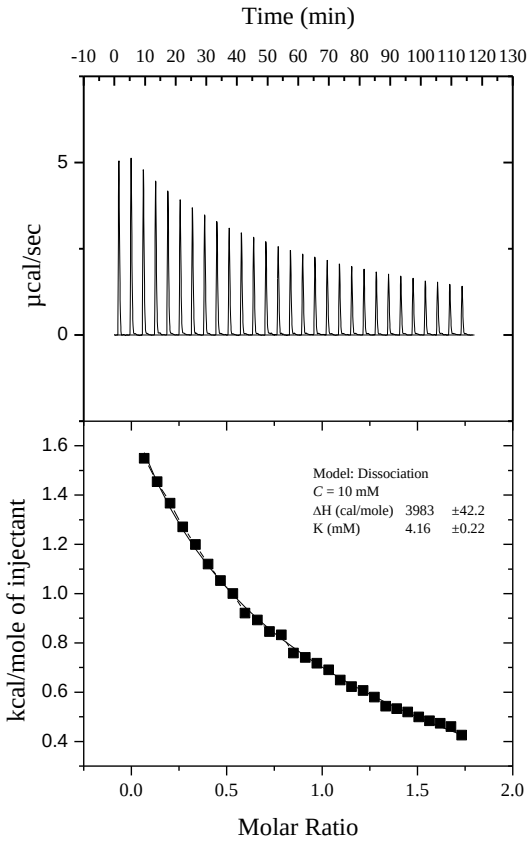


Guanidinium-carboxylate **45** in DMSO

ITC final figure

| Inj. No. | Molar ratio | Cal/mol of injected **45** |
|---|---|---|
| 1 | 0.06819 | 1548.599 |
| 2 | 0.13592 | 1454.206 |
| 3 | 0.20318 | 1366.935 |
| 4 | 0.26996 | 1270.348 |
| 5 | 0.33628 | 1199.276 |
| 6 | 0.40214 | 1120.013 |
| 7 | 0.46752 | 1053.079 |
| 8 | 0.53244 | 1000.365 |
| 9 | 0.59688 | 920.3925 |
| 10 | 0.66086 | 893.0963 |
| 11 | 0.72437 | 845.3409 |
| 12 | 0.78742 | 832.6059 |
| 13 | 0.84999 | 758.2611 |
| 14 | 0.9121 | 740.978 |
| 15 | 0.97374 | 717.3456 |
| 16 | 1.03491 | 690.3944 |
| 17 | 1.09561 | 649.0963 |
| 18 | 1.15584 | 621.6606 |
| 19 | 1.21561 | 606.4449 |
| 20 | 1.2749 | 580.0727 |
| 21 | 1.33373 | 542.835 |
| 22 | 1.39209 | 533.0577 |
| 23 | 1.44999 | 519.4099 |
| 24 | 1.50741 | 499.3891 |
| 25 | 1.56437 | 482.8966 |
| 26 | 1.62085 | 473.8048 |
| 27 | 1.67687 | 459.4052 |
| 28 | 1.73242 | 425.7022 |
| 29 | 0.06819 | 1548.599 |

Appendices

*ITC data of guandinium-carboxylate **45***

[monomer] = 20 mM
Solvent = 10% $H_2O$/DMSO
$K_{dim}[M^{-1}]$ = 54
$\Delta G_{dim}$ [kJ $mol^{-1}$] = -9.9
$\Delta H_{dim}$ [kJ $mol^{-1}$] = -6.2
$T\Delta S_{dim}$ [kJ $mol^{-1}$] = 3.6

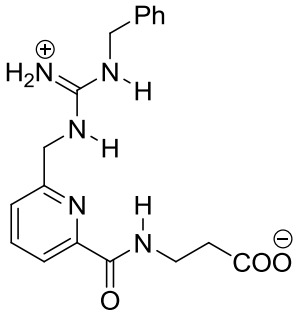


**45**

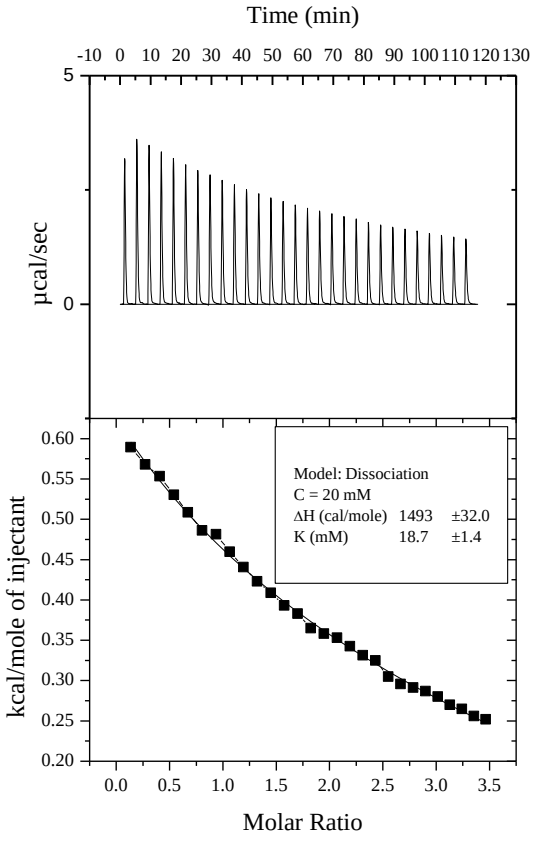


Guanidinium-carboxylate **45** in 10% $H_2O$/ DMSO

ITC final figure

| Inj. No. | Molar ratio | Cal/mol of injected **45** |
|---|---|---|
| 1 | 0.13639 | 589.4092 |
| 2 | 0.27184 | 568.0632 |
| 3 | 0.40635 | 553.2367 |
| 4 | 0.53993 | 530.2699 |
| 5 | 0.67257 | 508.6899 |
| 6 | 0.80427 | 486.0782 |
| 7 | 0.93504 | 481.2641 |
| 8 | 1.06487 | 459.8468 |
| 9 | 1.19377 | 440.573 |
| 10 | 1.32173 | 422.9418 |
| 11 | 1.44875 | 408.7186 |
| 12 | 1.57484 | 393.1313 |
| 13 | 1.69998 | 382.9138 |
| 14 | 1.8242 | 364.9136 |
| 15 | 1.94747 | 358.2289 |
| 16 | 2.06981 | 353.0942 |
| 17 | 2.19122 | 342.6911 |
| 18 | 2.31168 | 331.2941 |
| 19 | 2.43121 | 324.8235 |
| 20 | 2.54981 | 304.8985 |
| 21 | 2.66747 | 295.6677 |
| 22 | 2.78419 | 291.3028 |
| 23 | 2.89997 | 286.7959 |
| 24 | 3.01482 | 279.9466 |
| 25 | 3.12873 | 270.0848 |
| 26 | 3.24171 | 264.846 |
| 27 | 3.35375 | 255.8926 |
| 28 | 3.46485 | 251.892 |
| 29 | 0.13639 | 589.4092 |

Appendices

*ITC data of guandinium-carboxylate **46***

[monomer] = 4 mM
Solvent = DMSO
$K_{dim}[M^{-1}]$ = 4608
$\Delta G_{dim}$ [kJ $mol^{-1}$] = -20.9
$\Delta H_{dim}$ [kJ $mol^{-1}$] = -21.7
$T\Delta S_{dim}$ [kJ $mol^{-1}$] = -0.9

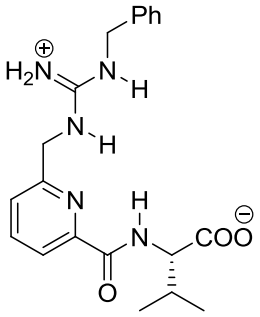

**46**

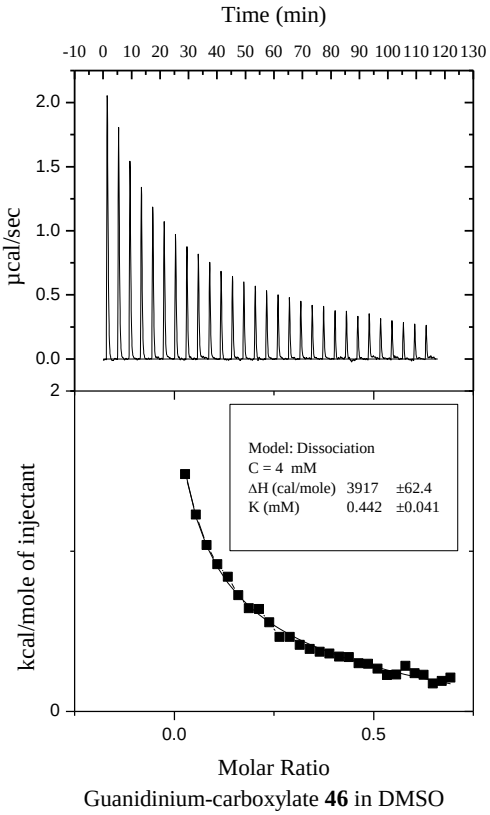


Guanidinium-carboxylate **46** in DMSO

ITC final figure

| Inj. No. | Molar ratio | Cal/mol of injected **46** |
|---|---|---|
| 1 | 0.02728 | 1481.307 |
| 2 | 0.05437 | 1228.54 |
| 3 | 0.08127 | 1039.061 |
| 4 | 0.10799 | 918.9863 |
| 5 | 0.13451 | 839.599 |
| 6 | 0.16085 | 724.6821 |
| 7 | 0.18701 | 643.8358 |
| 8 | 0.21297 | 639.4556 |
| 9 | 0.23875 | 555.7509 |
| 10 | 0.26435 | 465.2519 |
| 11 | 0.28975 | 465.1578 |
| 12 | 0.31497 | 415.3962 |
| 13 | 0.34 | 389.6998 |
| 14 | 0.36484 | 372.077 |
| 15 | 0.38949 | 361.4618 |
| 16 | 0.41396 | 341.1894 |
| 17 | 0.43824 | 338.6941 |
| 18 | 0.46234 | 299.645 |
| 19 | 0.48624 | 297.6352 |
| 20 | 0.50996 | 267.0348 |
| 21 | 0.53349 | 226.6123 |
| 22 | 0.55684 | 229.9116 |
| 23 | 0.57999 | 284.9057 |
| 24 | 0.60296 | 237.2871 |
| 25 | 0.62575 | 228.2035 |
| 26 | 0.64834 | 173.537 |
| 27 | 0.67075 | 189.493 |
| 28 | 0.69297 | 211.6555 |
| 29 | 0.02728 | 1481.307 |

Appendices

*ITC data of guanidinium-carboxylate **46***

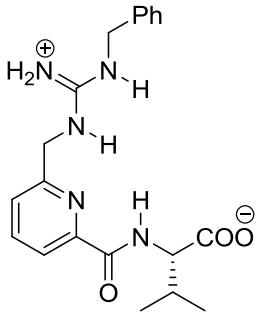


**46**

[monomer] = 20 mM
Solvent = 10% $H_2O$/DMSO
$K_{dim}[M^{-1}]$ = 54
$\Delta G_{dim}$ [kJ $mol^{-1}$] = -9.9
$\Delta H_{dim}$ [kJ $mol^{-1}$] = -5.6
$T\Delta S_{dim}$ [kJ $mol^{-1}$] = 4.2

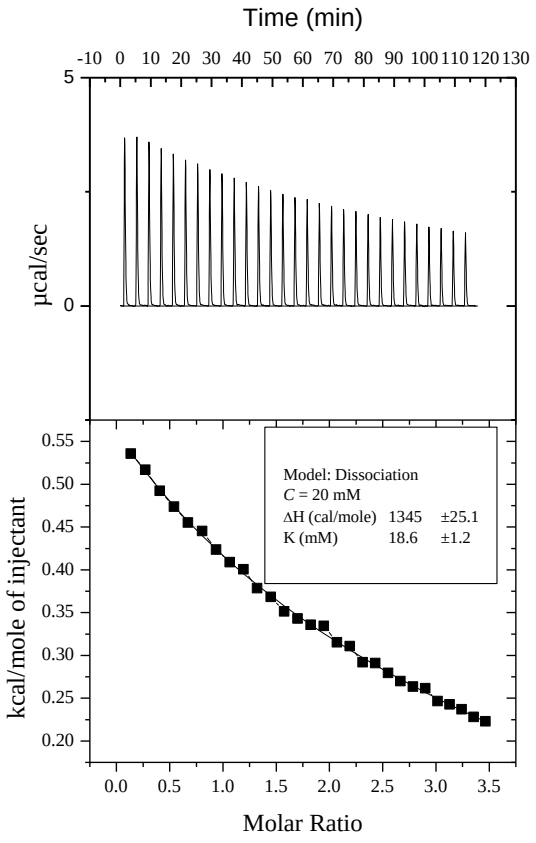


Guanidinium-carboxylate 4**6** in 10% $H_2O$/DMSO

ITC final figure

| Inj. No. | Molar ratio | Cal/mol of injected **46** |
|---|---|---|
| 1 | 0.13639 | 535.6104 |
| 2 | 0.27184 | 516.776 |
| 3 | 0.40635 | 492.168 |
| 4 | 0.53993 | 473.7907 |
| 5 | 0.67257 | 455.1108 |
| 6 | 0.80427 | 445.283 |
| 7 | 0.93504 | 423.4051 |
| 8 | 1.06487 | 409.0048 |
| 9 | 1.19377 | 400.5563 |
| 10 | 1.32173 | 378.4534 |
| 11 | 1.44875 | 368.1346 |
| 12 | 1.57484 | 351.5004 |
| 13 | 1.69998 | 342.9795 |
| 14 | 1.8242 | 335.7038 |
| 15 | 1.94747 | 334.5311 |
| 16 | 2.06981 | 315.2711 |
| 17 | 2.19122 | 310.8289 |
| 18 | 2.31168 | 292.0199 |
| 19 | 2.43121 | 291.0248 |
| 20 | 2.54981 | 279.3251 |
| 21 | 2.66747 | 270.0351 |
| 22 | 2.78419 | 263.3474 |
| 23 | 2.89997 | 261.6277 |
| 24 | 3.01482 | 246.5664 |
| 25 | 3.12873 | 242.7272 |
| 26 | 3.24171 | 236.9132 |
| 27 | 3.35375 | 227.9059 |
| 28 | 3.46485 | 223.0008 |
| 29 | 0.13639 | 535.6104 |

Appendices

*ITC data of guanidinium-carboxylate **53***

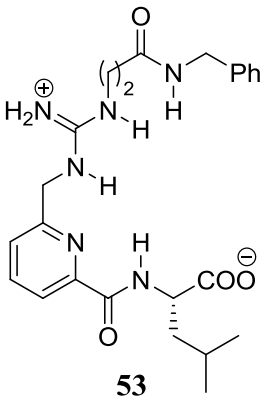

**53**

[monomer] = 10 mM
Solvent = DMSO
$K_{dim}[M^{-1}]$ = 952
$\Delta G_{dim}$ [kJ $mol^{-1}$] = -17.0
$\Delta H_{dim}$ [kJ $mol^{-1}$] = -16.7
$T\Delta S_{dim}$ [kJ $mol^{-1}$] = 0.3

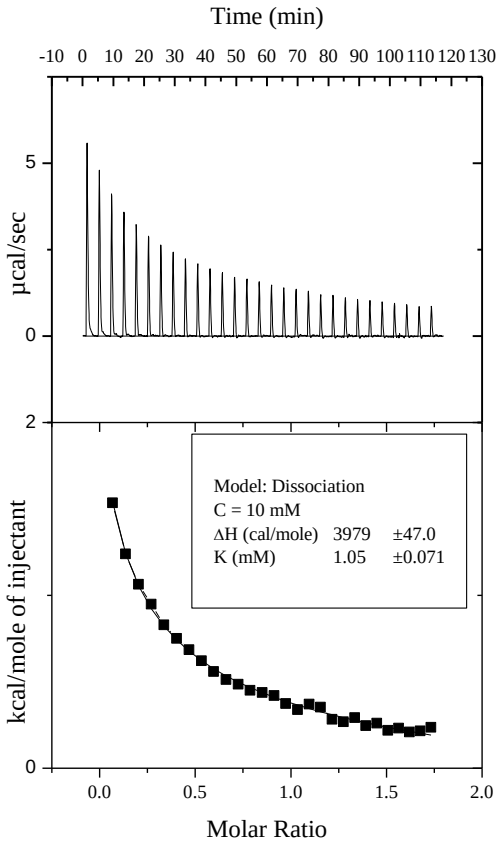


Guanidinium-carboxylate **53** in DMSO

ITC final figure

| Inj. No. | Molar ratio | Cal/mol of injected **53** |
|---|---|---|
| 1 | 0.06819 | 1535.011 |
| 2 | 0.13592 | 1240.399 |
| 3 | 0.20318 | 1063.472 |
| 4 | 0.26996 | 948.9337 |
| 5 | 0.33628 | 828.7126 |
| 6 | 0.40214 | 751.2859 |
| 7 | 0.46752 | 685.924 |
| 8 | 0.53244 | 621.5231 |
| 9 | 0.59688 | 558.6093 |
| 10 | 0.66086 | 513.2643 |
| 11 | 0.72437 | 486.0624 |
| 12 | 0.78742 | 450.8132 |
| 13 | 0.84999 | 438.1397 |
| 14 | 0.9121 | 419.8108 |
| 15 | 0.97374 | 373.6592 |
| 16 | 1.03491 | 338.5508 |
| 17 | 1.09561 | 369.954 |
| 18 | 1.15584 | 353.4904 |
| 19 | 1.21561 | 283.2167 |
| 20 | 1.2749 | 267.9879 |
| 21 | 1.33373 | 293.1073 |
| 22 | 1.39209 | 245.786 |
| 23 | 1.44999 | 261.0369 |
| 24 | 1.50741 | 219.0222 |
| 25 | 1.56437 | 231.5258 |
| 26 | 1.62085 | 209.8938 |
| 27 | 1.67687 | 215.0006 |
| 28 | 1.73242 | 236.2752 |
| 29 | 0.06819 | 1535.011 |

Appendices

*ITC data of guanidinium-carboxylate **53***

[monomer] = 20 mM
Solvent = 10% $H_2O$/DMSO
$K_{dim}[M^{-1}]$ = 73
$\Delta G_{dim}$ [kJ $mol^{-1}$] = -10.6
$\Delta H_{dim}$ [kJ $mol^{-1}$] = -8.6
$T\Delta S_{dim}$ [kJ $mol^{-1}$] = 2.0

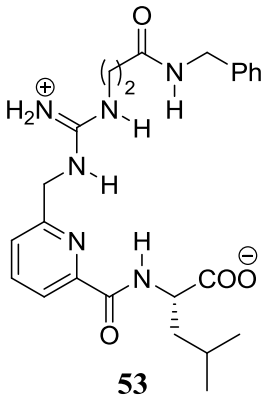

**53**

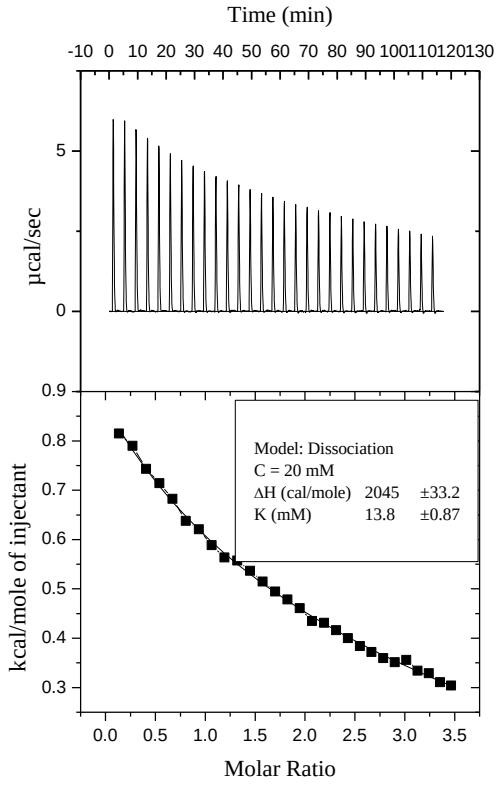


Guanidinium-carboxylate 53 in 10% $H_2O$/DMSO

ITC final figure

| Inj. No. | Molar ratio | Cal/mol of injected **53** |
|---|---|---|
| 1 | 0.13639 | 814.7614 |
| 2 | 0.27184 | 789.8495 |
| 3 | 0.40635 | 743.4171 |
| 4 | 0.53993 | 714.1899 |
| 5 | 0.67257 | 682.7087 |
| 6 | 0.80427 | 637.575 |
| 7 | 0.93504 | 620.7341 |
| 8 | 1.06487 | 588.3947 |
| 9 | 1.19377 | 563.4242 |
| 10 | 1.32173 | 557.417 |
| 11 | 1.44875 | 536.7141 |
| 12 | 1.57484 | 514.8635 |
| 13 | 1.69998 | 494.3066 |
| 14 | 1.8242 | 478.3506 |
| 15 | 1.94747 | 460.8538 |
| 16 | 2.06981 | 434.6123 |
| 17 | 2.19122 | 431.3305 |
| 18 | 2.31168 | 415.9101 |
| 19 | 2.43121 | 400.2346 |
| 20 | 2.54981 | 384.1484 |
| 21 | 2.66747 | 371.9534 |
| 22 | 2.78419 | 359.3785 |
| 23 | 2.89997 | 350.9882 |
| 24 | 3.01482 | 356.0036 |
| 25 | 3.12873 | 333.9854 |
| 26 | 3.24171 | 328.686 |
| 27 | 3.35375 | 310.7691 |
| 28 | 3.46485 | 304.0664 |
| 29 | 0.13639 | 814.7614 |

Appendices

*ITC data of guanidinium-carboxylate **53***

[monomer] = 40 mM
Solvent = 50% $H_2O$/DMSO
$K_{dim}[M^{-1}]$ = 13
$\Delta G_{dim}$ [kJ $mol^{-1}$] = -6.4
$\Delta H_{dim}$ [kJ $mol^{-1}$] = -1.8
$T\Delta S_{dim}$ [kJ $mol^{-1}$] = 4.6

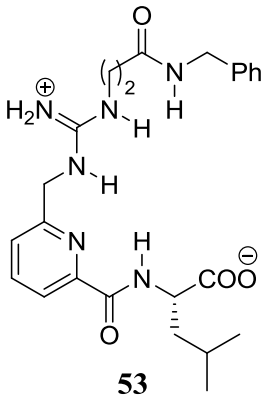

**53**

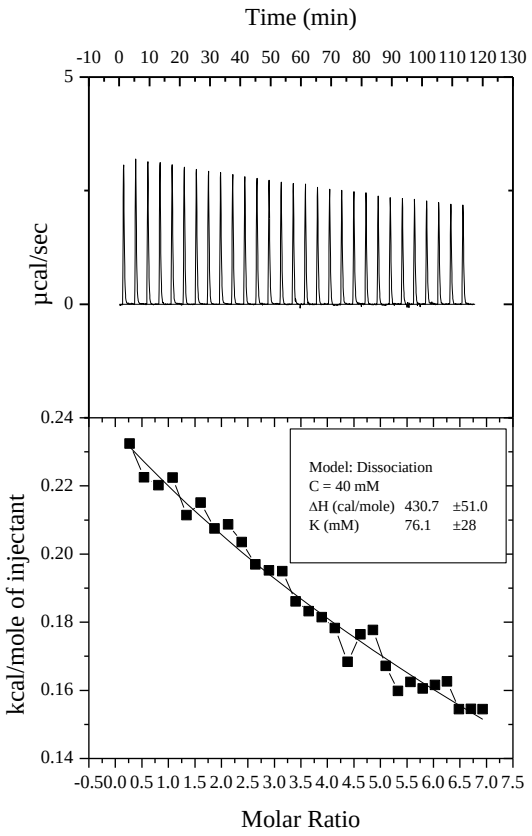


Guanidinium-carboxylate **53** in 50% $H_2O$/DMSO

ITC final figure

| Inj. No. | Molar ratio | Cal/mol of injected **53** |
|---|---|---|
| 1 | 0.27277 | 232.4499 |
| 2 | 0.54367 | 222.4874 |
| 3 | 0.8127 | 220.2105 |
| 4 | 1.07986 | 222.4285 |
| 5 | 1.34514 | 211.4203 |
| 6 | 1.60855 | 215.0561 |
| 7 | 1.87008 | 207.5 |
| 8 | 2.12975 | 208.6904 |
| 9 | 2.38754 | 203.4767 |
| 10 | 2.64345 | 196.9539 |
| 11 | 2.8975 | 195.1989 |
| 12 | 3.14967 | 194.9533 |
| 13 | 3.39997 | 186.0931 |
| 14 | 3.64839 | 183.1811 |
| 15 | 3.89495 | 181.4643 |
| 16 | 4.13963 | 178.278 |
| 17 | 4.38243 | 168.3892 |
| 18 | 4.62337 | 176.4388 |
| 19 | 4.86243 | 177.672 |
| 20 | 5.09962 | 167.1739 |
| 21 | 5.33493 | 159.8071 |
| 22 | 5.56837 | 162.4328 |
| 23 | 5.79994 | 160.5358 |
| 24 | 6.02964 | 161.5837 |
| 25 | 6.25746 | 162.5643 |
| 26 | 6.48341 | 154.4675 |
| 27 | 6.70749 | 154.5085 |
| 28 | 6.92969 | 154.455 |
| 29 | 0.27277 | 232.4499 |

Appendices

*ITC data of guanidinium-carboxylate **53***

[monomer] = 40 mM
Solvent = 75% $H_2O$/DMSO
$K_{dim}[M^{-1}]$ = 5
$\Delta G_{dim}$ [kJ $mol^{-1}$] = -4.0
$\Delta H_{dim}$ [kJ $mol^{-1}$] = -2.3
$T\Delta S_{dim}$ [kJ $mol^{-1}$] = 1.7

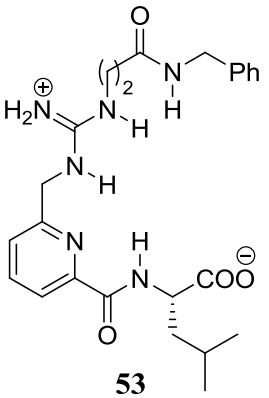

**53**

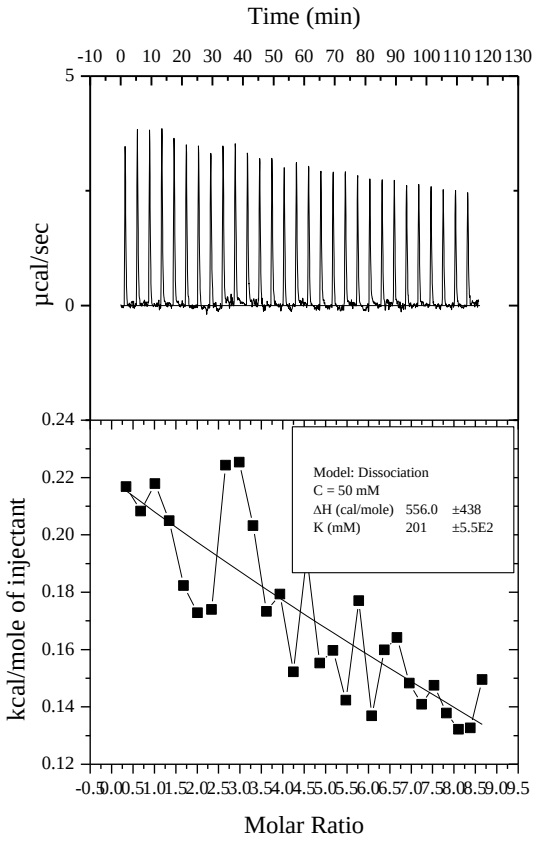


Guanidinium-carboxylate **53** in 75% $H_2O$/DMSO

ITC final figure

| Inj. No. | Molar ratio | Cal/mol of injected **53** |
|---|---|---|
| 1 | 0.34097 | 216.8087 |
| 2 | 0.67959 | 208.2562 |
| 3 | 1.01588 | 217.8864 |
| 4 | 1.34982 | 204.9368 |
| 5 | 1.68142 | 182.27 |
| 6 | 2.01069 | 172.7955 |
| 7 | 2.33761 | 173.9801 |
| 8 | 2.66218 | 224.2853 |
| 9 | 2.98442 | 225.3709 |
| 10 | 3.30432 | 203.1723 |
| 11 | 3.62187 | 173.2495 |
| 12 | 3.93709 | 179.3489 |
| 13 | 4.24996 | 152.1873 |
| 14 | 4.56049 | 192.7629 |
| 15 | 4.86868 | 155.2425 |
| 16 | 5.17453 | 159.6459 |
| 17 | 5.47804 | 142.3568 |
| 18 | 5.77921 | 177.0456 |
| 19 | 6.07804 | 136.8977 |
| 20 | 6.37452 | 159.8666 |
| 21 | 6.66866 | 164.1536 |
| 22 | 6.96047 | 148.3184 |
| 23 | 7.24993 | 140.9159 |
| 24 | 7.53705 | 147.4637 |
| 25 | 7.82183 | 137.8061 |
| 26 | 8.10427 | 132.2024 |
| 27 | 8.38436 | 132.6134 |
| 28 | 8.66212 | 149.5444 |
| 29 | 0.34097 | 216.8087 |

Appendices

*ITC data of guanidinium-carboxylate **57***

[monomer] = 3 mM
Solvent = DMSO
$K_{dim}[M^{-1}]$ = 4032
$\Delta G_{dim}$ [kJ $mol^{-1}$] = -20.6
$\Delta H_{dim}$ [kJ $mol^{-1}$] = -13.8
$T\Delta S_{dim}$ [kJ $mol^{-1}$] = 6.8

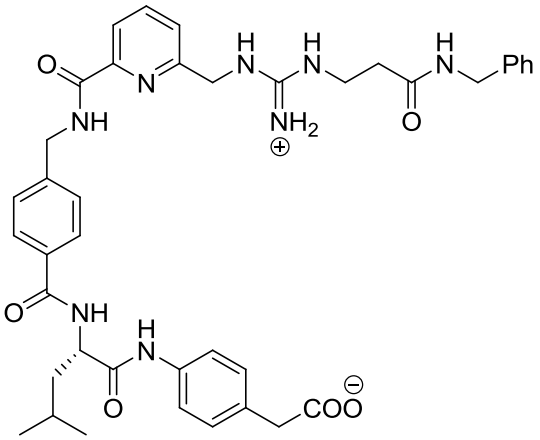

**57**

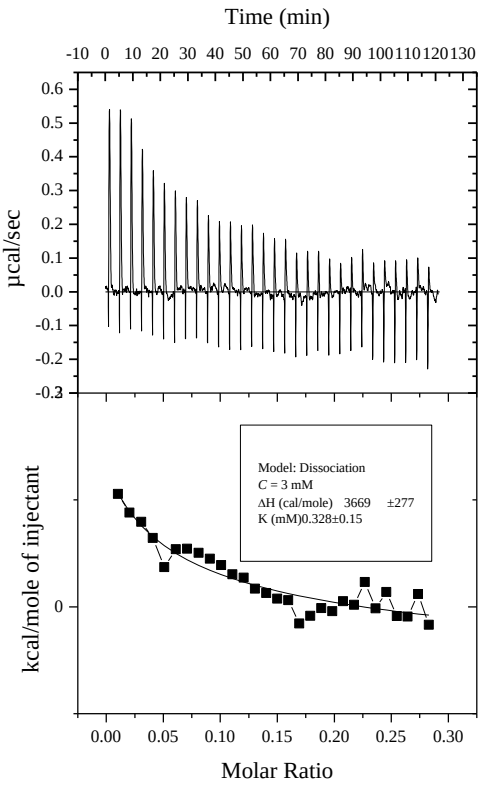


Guanidinium-carboxylate **57** in DMSO

ITC final figure

| Inj. No. | Molar ratio | Cal/mol of injected **57** |
|---|---|---|
| 1 | 0.01025 | 1070.74 |
| 2 | 0.02046 | 966.5833 |
| 3 | 0.03063 | 963.6294 |
| 4 | 0.04078 | 680.2051 |
| 5 | 0.05088 | 607.1643 |
| 6 | 0.06095 | 498.8218 |
| 7 | 0.07099 | 609.2261 |
| 8 | 0.08099 | 515.3998 |
| 9 | 0.09095 | 533.7236 |
| 10 | 0.10089 | 208.4286 |
| 11 | 0.11078 | 420.8158 |
| 12 | 0.12064 | 156.9195 |
| 13 | 0.13047 | 115.0583 |
| 14 | 0.14026 | 300.1156 |
| 15 | 0.15001 | 381.3619 |
| 16 | 0.15973 | 168.2936 |
| 17 | 0.16942 | 219.2553 |
| 18 | 0.17907 | 261.4352 |
| 19 | 0.18868 | 304.3861 |
| 20 | 0.19826 | 220.2145 |
| 21 | 0.2078 | 1.96792 |
| 22 | 0.21731 | 131.5099 |
| 23 | 0.22679 | 206.0906 |
| 24 | 0.23623 | 94.74537 |
| 25 | 0.24563 | -35.7505 |
| 26 | 0.255 | 112.7255 |
| 27 | 0.26433 | 32.87384 |
| 28 | 0.27363 | 171.4396 |
| 29 | 0.28289 | 215.9282 |

Appendices

*ITC data of guanidinium-carboxylate **57***

[monomer] = 20 mM
Solvent = 10% $H_2O$/DMSO
$K_{dim}[M^{-1}]$ = 336
$\Delta G_{dim}$ [kJ $mol^{-1}$] = -14.4
$\Delta H_{dim}$ [kJ $mol^{-1}$] = -3.7
$T\Delta S_{dim}$ [kJ $mol^{-1}$] = 10.8

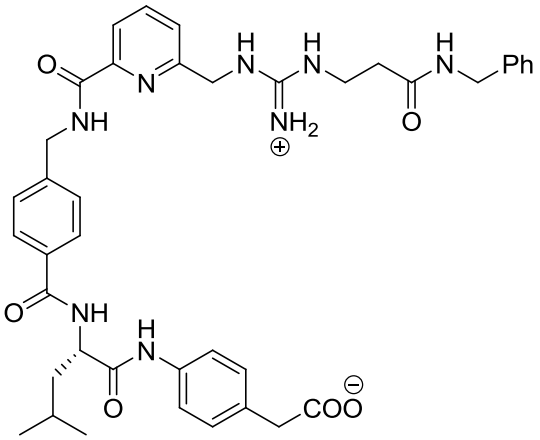

**57**

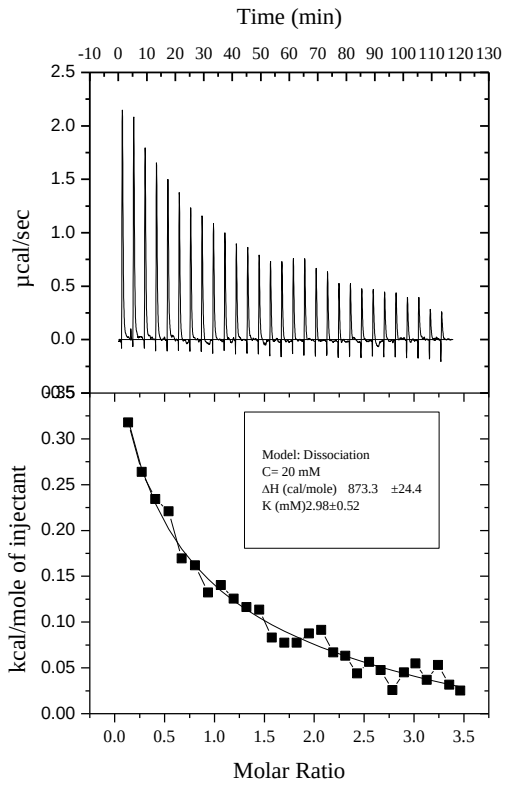


Guanidinium-carboxylate **57** in10%$H_2O$/ DMSO

ITC final figure

| Inj. No. | Molar ratio | Cal/mol of injected **57** |
|---|---|---|
| 1 | 0.13639 | 317.9293 |
| 2 | 0.27184 | 263.9745 |
| 3 | 0.40635 | 234.2109 |
| 4 | 0.53993 | 220.7908 |
| 5 | 0.67257 | 169.3606 |
| 6 | 0.80427 | 161.9809 |
| 7 | 0.93504 | 132.3573 |
| 8 | 1.06487 | 140.2771 |
| 9 | 1.19377 | 125.5838 |
| 10 | 1.32173 | 116.3109 |
| 11 | 1.44875 | 113.3768 |
| 12 | 1.57484 | 82.90507 |
| 13 | 1.69998 | 77.52011 |
| 14 | 1.8242 | 77.49117 |
| 15 | 1.94747 | 87.57144 |
| 16 | 2.06981 | 91.41337 |
| 17 | 2.19122 | 66.71729 |
| 18 | 2.31168 | 63.28454 |
| 19 | 2.43121 | 43.81419 |
| 20 | 2.54981 | 56.41177 |
| 21 | 2.66747 | 47.52595 |
| 22 | 2.78419 | 25.71653 |
| 23 | 2.89997 | 45.02554 |
| 24 | 3.01482 | 54.84943 |
| 25 | 3.12873 | 36.8154 |
| 26 | 3.24171 | 53.23039 |
| 27 | 3.35375 | 31.56108 |
| 28 | 3.46485 | 25.16868 |
| 29 | 0.13639 | 317.9293 |

Appendices

*ITC data of guanidinium-carboxylate **57***

[monomer] = 10 mM
Solvent = 50% $H_2O$/DMSO
$K_{dim}[M^{-1}]$ = 334
$\Delta G_{dim}$ [kJ $mol^{-1}$] = -14.5
$\Delta H_{dim}$ [kJ $mol^{-1}$] = -0.6
$T\Delta S_{dim}$ [kJ $mol^{-1}$] = 13.9

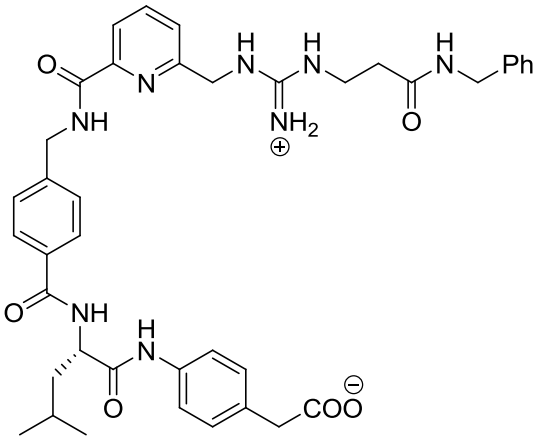

**57**

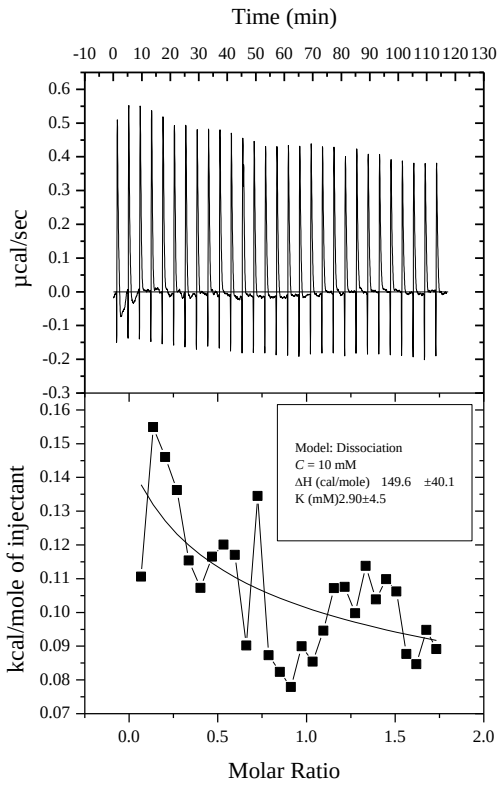


Guanidinium-carboxylate **57** in 50%$H_2O$/DMSO

ITC final figure

| Inj. No. | Molar ratio | Cal/mol of injected **57** |
|---|---|---|
| 1 | 0.06819 | 110.6255 |
| 2 | 0.13592 | 154.8958 |
| 3 | 0.20318 | 146.0179 |
| 4 | 0.26996 | 136.2531 |
| 5 | 0.33628 | 115.3443 |
| 6 | 0.40214 | 107.2727 |
| 7 | 0.46752 | 116.493 |
| 8 | 0.53244 | 120.0475 |
| 9 | 0.59688 | 117.0199 |
| 10 | 0.66086 | 90.14614 |
| 11 | 0.72437 | 134.5073 |
| 12 | 0.78742 | 87.33339 |
| 13 | 0.84999 | 82.37251 |
| 14 | 0.9121 | 77.86754 |
| 15 | 0.97374 | 89.95909 |
| 16 | 1.03491 | 85.4027 |
| 17 | 1.09561 | 94.55916 |
| 18 | 1.15584 | 107.1945 |
| 19 | 1.21561 | 107.5672 |
| 20 | 1.2749 | 99.7082 |
| 21 | 1.33373 | 113.7951 |
| 22 | 1.39209 | 103.8491 |
| 23 | 1.44999 | 109.8129 |
| 24 | 1.50741 | 106.2173 |
| 25 | 1.56437 | 87.70996 |
| 26 | 1.62085 | 84.66482 |
| 27 | 1.67687 | 94.81133 |
| 28 | 1.73242 | 89.12951 |
| 29 | 0.06819 | 110.6255 |

Appendices

*ITC data of guanidinium-carboxylate* ***67***

[monomer] = 3 mM
Solvent = DMSO
$K_{dim}[M^{-1}]$ = 7692
$\Delta G_{dim}$ [kJ $mol^{-1}$] = -22.2
$\Delta H_{dim}$ [kJ $mol^{-1}$] = -4.7
$T\Delta S_{dim}$ [kJ $mol^{-1}$] = 17.5

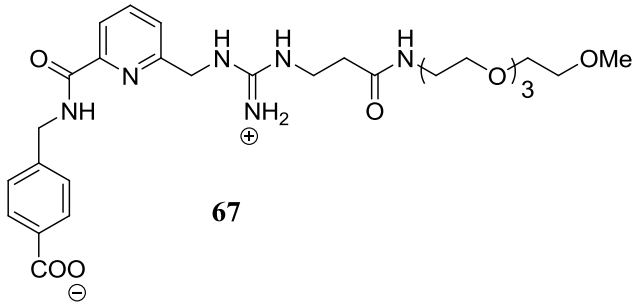

**67**

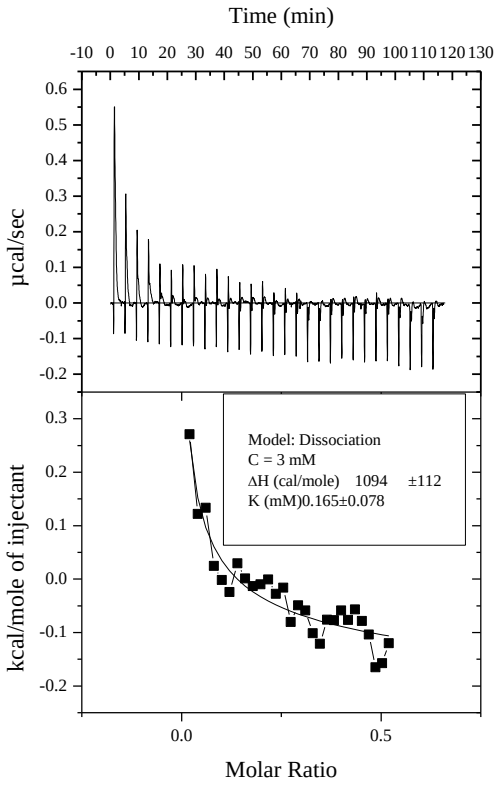


Guanidinium-carboxylate **67** in DMSO

ITC final figure

| Inj. No. | Molar ratio | Cal/mol of injected **67** |
|---|---|---|
| 1 | 0.02046 | 270.7547 |
| 2 | 0.04078 | 122.0604 |
| 3 | 0.06095 | 133.2901 |
| 4 | 0.08099 | 24.61232 |
| 5 | 0.10089 | -1.69407 |
| 6 | 0.12064 | -24.0811 |
| 7 | 0.14026 | 29.24413 |
| 8 | 0.15973 | 0.88459 |
| 9 | 0.17907 | -13.1276 |
| 10 | 0.19826 | -9.99776 |
| 11 | 0.21731 | -0.90787 |
| 12 | 0.23623 | -27.4382 |
| 13 | 0.255 | -16.1238 |
| 14 | 0.27363 | -80.437 |
| 15 | 0.29212 | -49.0432 |
| 16 | 0.31047 | -58.8897 |
| 17 | 0.32868 | -101.461 |
| 18 | 0.34675 | -121.283 |
| 19 | 0.36468 | -76.2555 |
| 20 | 0.38247 | -77.178 |
| 21 | 0.40012 | -58.8989 |
| 22 | 0.41763 | -76.5828 |
| 23 | 0.435 | -56.9363 |
| 24 | 0.45222 | -78.2048 |
| 25 | 0.46931 | -103.647 |
| 26 | 0.48626 | -165.308 |
| 27 | 0.50306 | -157.386 |
| 28 | 0.51973 | -120.05 |
| 29 | 0.02046 | 270.7547 |

Appendices

*ITC data of guanidinium-carboxylate* ***67***

[monomer] = 20 mM
Solvent = 10% $H_2O$/DMSO
$K_{dim}[M^{-1}]$ = 495
$\Delta G_{dim}$ [kJ $mol^{-1}$] = -15.4
$\Delta H_{dim}$ [kJ $mol^{-1}$] = -9.8
$T\Delta S_{dim}$ [kJ $mol^{-1}$] = 5.6

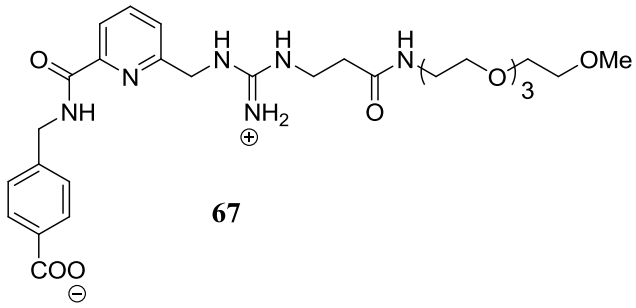

**67**

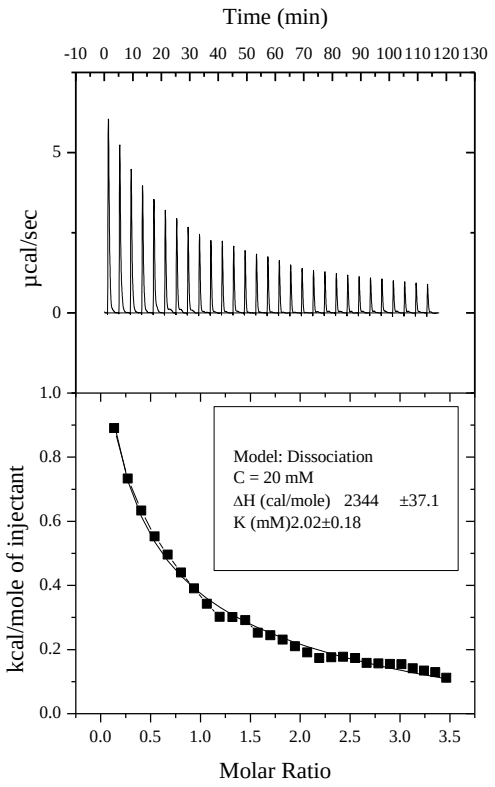


Guanidinium-carboxylate **67** in10%$H_2O$/ DMSO

ITC final figure

| Inj. No. | Molar ratio | Cal/mol of injected **67** |
|---|---|---|
| 1 | 0.13639 | 890.3695 |
| 2 | 0.27184 | 733.2514 |
| 3 | 0.40635 | 633.3786 |
| 4 | 0.53993 | 553.0476 |
| 5 | 0.67257 | 495.993 |
| 6 | 0.80427 | 439.7383 |
| 7 | 0.93504 | 390.357 |
| 8 | 1.06487 | 342.4304 |
| 9 | 1.19377 | 302.1241 |
| 10 | 1.32173 | 301.2538 |
| 11 | 1.44875 | 291.6009 |
| 12 | 1.57484 | 252.1471 |
| 13 | 1.69998 | 244.1995 |
| 14 | 1.8242 | 230.7084 |
| 15 | 1.94747 | 210.0998 |
| 16 | 2.06981 | 191.2566 |
| 17 | 2.19122 | 173.1413 |
| 18 | 2.31168 | 175.6001 |
| 19 | 2.43121 | 177.6385 |
| 20 | 2.54981 | 173.4444 |
| 21 | 2.66747 | 157.7729 |
| 22 | 2.78419 | 156.7273 |
| 23 | 2.89997 | 154.9719 |
| 24 | 3.01482 | 154.4555 |
| 25 | 3.12873 | 141.5913 |
| 26 | 3.24171 | 134.3133 |
| 27 | 3.35375 | 129.2073 |
| 28 | 3.46485 | 111.4981 |
| 29 | 0.13639 | 890.3695 |

Appendices

*ITC data of guanidinium-carboxylate* ***67***

[monomer] = 20 mM
Solvent = 20% $H_2O$/DMSO
$K_{dim}[M^{-1}]$ = 57
$\Delta G_{dim}$ [kJ $mol^{-1}$] = -10.0
$\Delta H_{dim}$ [kJ $mol^{-1}$] = - 4.6
$T\Delta S_{dim}$ [kJ $mol^{-1}$] = 5.4

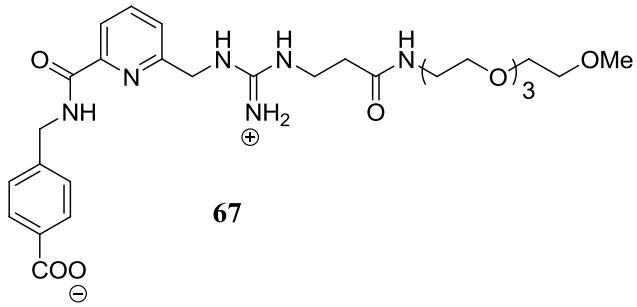

**67**

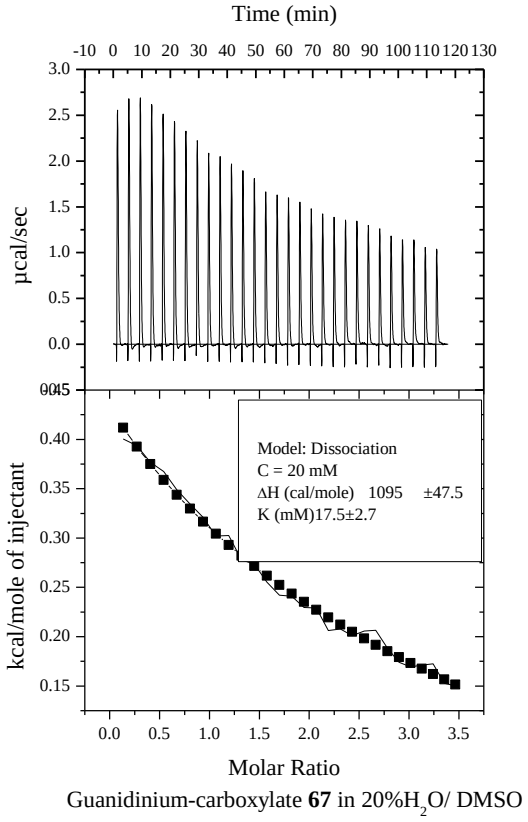


Guanidinium-carboxylate **67** in 20%$H_2O$/ DMSO

ITC final figure

| Inj. No. | Molar ratio | Cal/mol of injected **67** |
|---|---|---|
| 1 | 0.13639 | 400.5412 |
| 2 | 0.27184 | 393.583 |
| 3 | 0.40635 | 376.9221 |
| 4 | 0.53993 | 367.4068 |
| 5 | 0.67257 | 348.912 |
| 6 | 0.80427 | 334.4894 |
| 7 | 0.93504 | 321.0904 |
| 8 | 1.06487 | 302.1076 |
| 9 | 1.19377 | 302.4781 |
| 10 | 1.32173 | 277.8551 |
| 11 | 1.44875 | 273.5147 |
| 12 | 1.57484 | 255.4022 |
| 13 | 1.69998 | 242.163 |
| 14 | 1.8242 | 240.9809 |
| 15 | 1.94747 | 229.5505 |
| 16 | 2.06981 | 229.1133 |
| 17 | 2.19122 | 206.3608 |
| 18 | 2.31168 | 207.7092 |
| 19 | 2.43121 | 200.9869 |
| 20 | 2.54981 | 205.7332 |
| 21 | 2.66747 | 206.5932 |
| 22 | 2.78419 | 188.2099 |
| 23 | 2.89997 | 174.0106 |
| 24 | 3.01482 | 169.3128 |
| 25 | 3.12873 | 171.1624 |
| 26 | 3.24171 | 172.5926 |
| 27 | 3.35375 | 152.7597 |
| 28 | 3.46485 | 150.1991 |
| 29 | 0.13639 | 400.5412 |

Appendices

*ITC data of guanidinium-carboxylate **78***

[monomer] = 3 mM
Solvent = DMSO
$K_{dim}[M^{-1}]$ = 5076
$\Delta G_{dim}$ [kJ $mol^{-1}$] = -21.1
$\Delta H_{dim}$ [kJ $mol^{-1}$] = - 11.7
$T\Delta S_{dim}$ [kJ $mol^{-1}$] = 9.4

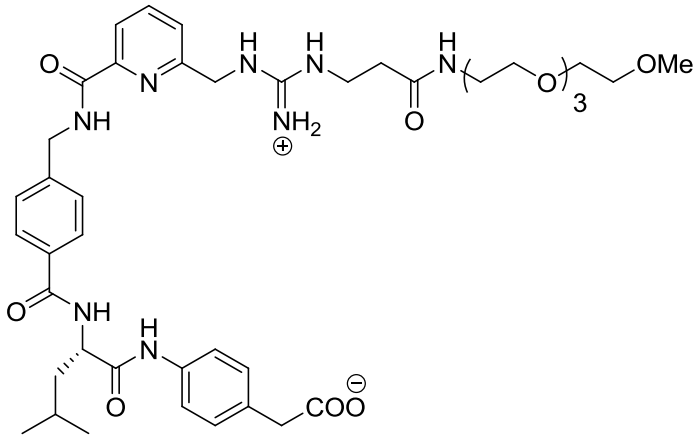

**78**

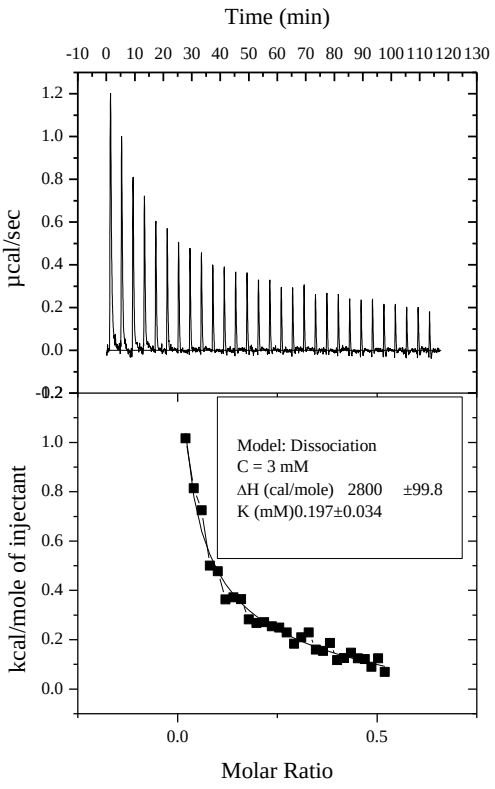


Guanidinium-carboxylate **78** in DMSO

ITC final figure

| Inj. No. | Molar ratio | Cal/mol of injected **78** |
|---|---|---|
| 1 | 0.02046 | 1015.751 |
| 2 | 0.04078 | 813.6497 |
| 3 | 0.06095 | 723.9875 |
| 4 | 0.08099 | 500.2608 |
| 5 | 0.10089 | 477.0202 |
| 6 | 0.12064 | 363.3647 |
| 7 | 0.14026 | 371.7165 |
| 8 | 0.15973 | 364.2035 |
| 9 | 0.17907 | 281.83 |
| 10 | 0.19826 | 267.6187 |
| 11 | 0.21731 | 270.9691 |
| 12 | 0.23623 | 254.2144 |
| 13 | 0.255 | 248.626 |
| 14 | 0.27363 | 229.4177 |
| 15 | 0.29212 | 183.9683 |
| 16 | 0.31047 | 209.9109 |
| 17 | 0.32868 | 228.8116 |
| 18 | 0.34675 | 159.5333 |
| 19 | 0.36468 | 154.7319 |
| 20 | 0.38247 | 186.6366 |
| 21 | 0.40012 | 116.6147 |
| 22 | 0.41763 | 125.0727 |
| 23 | 0.435 | 147.1851 |
| 24 | 0.45222 | 123.9258 |
| 25 | 0.46931 | 120.8954 |
| 26 | 0.48626 | 90.46449 |
| 27 | 0.50306 | 124.2907 |
| 28 | 0.51973 | 69.66365 |
| 29 | 0.02046 | 1015.751 |

Appendices

*ITC data of guanidinium-carboxylate **78***

[monomer] = 10 mM
Solvent = 5% $H_2O$/DMSO
$K_{dim}[M^{-1}]$ = 862
$\Delta G_{dim}$ [kJ $mol^{-1}$] = -16.7
$\Delta H_{dim}$ [kJ $mol^{-1}$] = -10.3
$T\Delta S_{dim}$ [kJ $mol^{-1}$] = 6.4

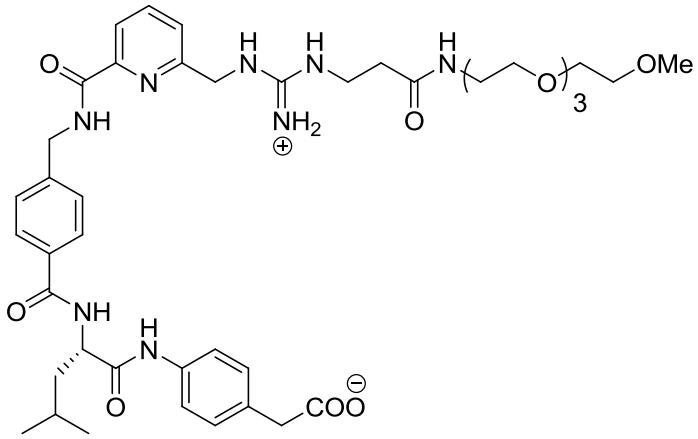

**78**

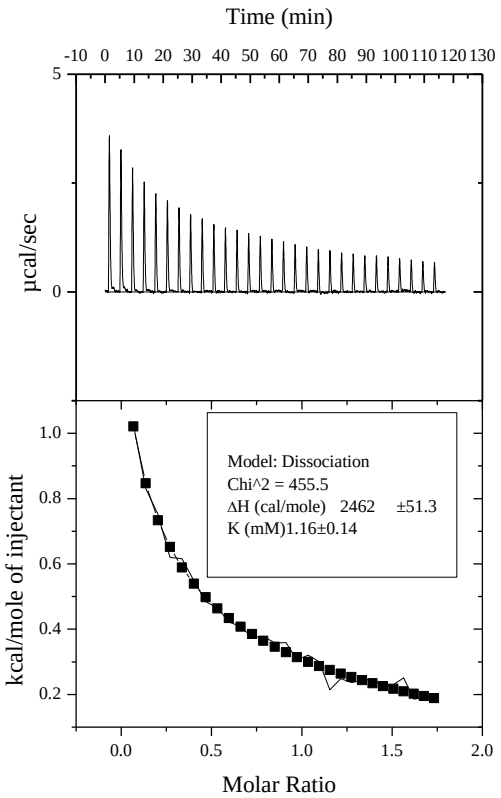


Guanidinium-carboxylate **78** in 5%$H_2O$/DMSO

ITC final figure

| Inj. No. | Molar ratio | Cal/mol of injected **78** |
|---|---|---|
| 1 | 0.06819 | 1026.049 |
| 2 | 0.13592 | 831.0022 |
| 3 | 0.20318 | 751.5362 |
| 4 | 0.26996 | 620.0662 |
| 5 | 0.33628 | 616.0074 |
| 6 | 0.40214 | 548.0316 |
| 7 | 0.46752 | 484.3801 |
| 8 | 0.53244 | 465.8637 |
| 9 | 0.59688 | 421.5469 |
| 10 | 0.66086 | 408.3777 |
| 11 | 0.72437 | 374.6027 |
| 12 | 0.78742 | 378.1343 |
| 13 | 0.84999 | 358.3461 |
| 14 | 0.9121 | 358.6175 |
| 15 | 0.97374 | 306.2486 |
| 16 | 1.03491 | 320.4483 |
| 17 | 1.09561 | 300.6358 |
| 18 | 1.15584 | 214.3444 |
| 19 | 1.21561 | 248.4988 |
| 20 | 1.2749 | 236.7443 |
| 21 | 1.33373 | 241.8786 |
| 22 | 1.39209 | 248.4592 |
| 23 | 1.44999 | 222.1031 |
| 24 | 1.50741 | 230.1554 |
| 25 | 1.56437 | 251.1154 |
| 26 | 1.62085 | 185.5107 |
| 27 | 1.67687 | 190.1331 |
| 28 | 1.73242 | 180.1535 |
| 29 | 0.06819 | 1026.049 |

Appendices

*ITC data of guanidinium-carboxylate **78***

[monomer] = 10 mM
Solvent = 10% $H_2O$/DMSO
$K_{dim}[M^{-1}]$ = 156
$\Delta G_{dim}$ [kJ $mol^{-1}$] = -12.5
$\Delta H_{dim}$ [kJ $mol^{-1}$] = -7.4
$T\Delta S_{dim}$ [kJ $mol^{-1}$] = 5.1

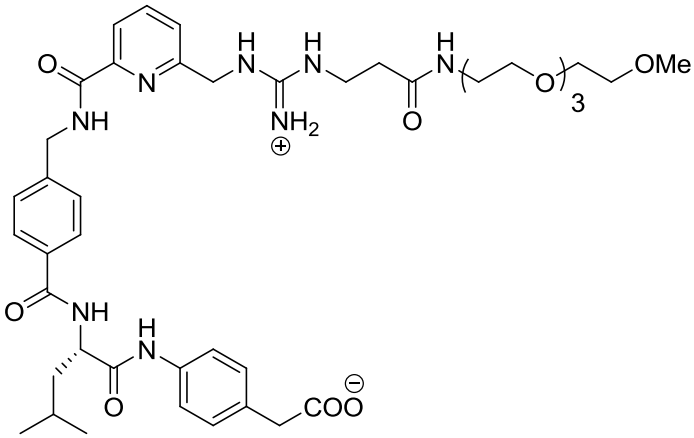

**78**

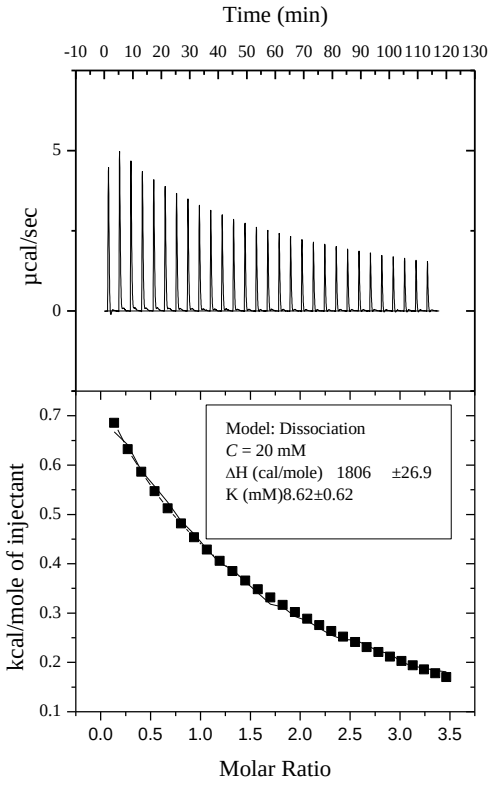


Guanidinium-carboxylate **78** in 10% $H_2O$/DMSO

ITC final figure

| Inj. No. | Molar ratio | Cal/mol of injected **78** |
|---|---|---|
| 1 | 0.13639 | 711.9548 |
| 2 | 0.27184 | 650.3678 |
| 3 | 0.40635 | 580.3131 |
| 4 | 0.53993 | 558.9752 |
| 5 | 0.67257 | 513.0282 |
| 6 | 0.80427 | 485.0643 |
| 7 | 0.93504 | 451.1931 |
| 8 | 1.06487 | 423.1163 |
| 9 | 1.19377 | 403.6405 |
| 10 | 1.32173 | 376.7011 |
| 11 | 1.44875 | 365.3502 |
| 12 | 1.57484 | 341.0457 |
| 13 | 1.69998 | 331.5105 |
| 14 | 1.8242 | 311.5874 |
| 15 | 1.94747 | 299.2547 |
| 16 | 2.06981 | 286.4118 |
| 17 | 2.19122 | 275.6302 |
| 18 | 2.31168 | 266.4468 |
| 19 | 2.43121 | 259.3672 |
| 20 | 2.54981 | 244.1421 |
| 21 | 2.66747 | 227.3492 |
| 22 | 2.78419 | 218.781 |
| 23 | 2.89997 | 217.3703 |
| 24 | 3.01482 | 206.0993 |
| 25 | 3.12873 | 201.3442 |
| 26 | 3.24171 | 194.7789 |
| 27 | 3.35375 | 187.6458 |
| 28 | 3.46485 | 182.1243 |
| 29 | 0.13639 | 711.9548 |

Appendices

*ITC data of guanidinium-carboxylate* ***82***

[monomer] = 10 mM
Solvent = DMSO
$K_{dim}[M^{-1}]$ = 357
$\Delta G_{dim}$ [kJ $mol^{-1}$] = -14.6
$\Delta H_{dim}$ [kJ $mol^{-1}$] = -3.1
$T\Delta S_{dim}$ [kJ $mol^{-1}$] = 11.5

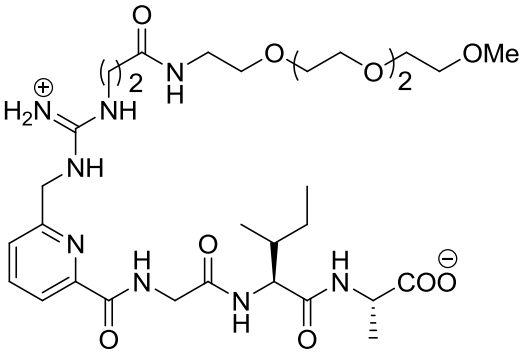

**82**

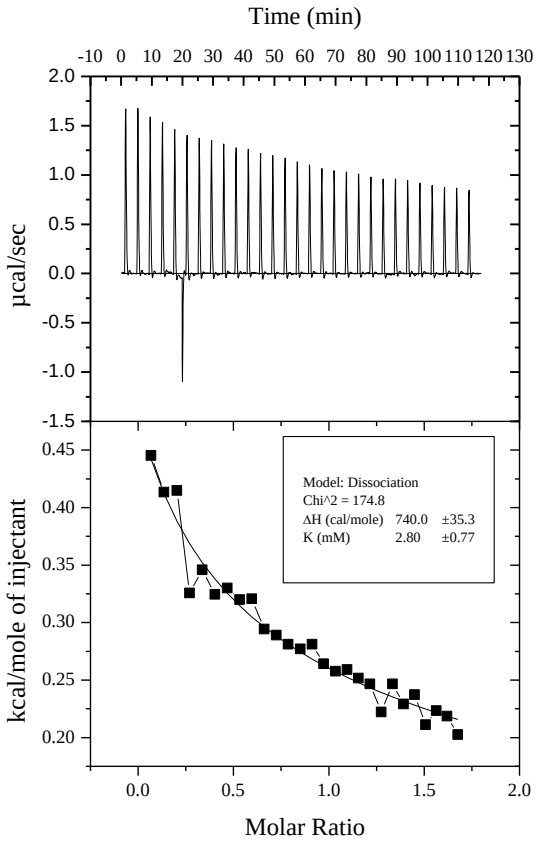


Guanidinium-carboxylate **82** in DMSO

ITC final figure

| Inj. No. | Molar ratio | Cal/mol of injected **82** |
|---|---|---|
| 1 | 0.06819 | 445.2186 |
| 2 | 0.13592 | 413.3985 |
| 3 | 0.20318 | 414.7525 |
| 4 | 0.26996 | 325.6465 |
| 5 | 0.33628 | 345.946 |
| 6 | 0.40214 | 324.4266 |
| 7 | 0.46752 | 330.103 |
| 8 | 0.53244 | 320.0542 |
| 9 | 0.59688 | 320.623 |
| 10 | 0.66086 | 294.4177 |
| 11 | 0.72437 | 289.0147 |
| 12 | 0.78742 | 281.1459 |
| 13 | 0.84999 | 277.0877 |
| 14 | 0.9121 | 281.1414 |
| 15 | 0.97374 | 264.1301 |
| 16 | 1.03491 | 257.748 |
| 17 | 1.09561 | 259.0549 |
| 18 | 1.15584 | 251.6177 |
| 19 | 1.21561 | 246.6774 |
| 20 | 1.2749 | 222.2816 |
| 21 | 1.33373 | 246.6756 |
| 22 | 1.39209 | 229.0389 |
| 23 | 1.44999 | 237.3561 |
| 24 | 1.50741 | 211.1446 |
| 25 | 1.56437 | 223.3512 |
| 26 | 1.62085 | 218.6038 |
| 27 | 1.67687 | 202.6463 |
| 28 | 0.06819 | 445.2186 |
| 29 | 0.13592 | 413.3985 |

Appendices

*ITC data of guanidinium-carboxylate* ***82***

[monomer] = 20 mM
Solvent = 10% $H_2O$/DMSO
$K_{dim}[M^{-1}]$ = 78
$\Delta G_{dim}$ [kJ $mol^{-1}$] = -10.8
$\Delta H_{dim}$ [kJ $mol^{-1}$] = -2.7
$T\Delta S_{dim}$ [kJ $mol^{-1}$] = 8.1

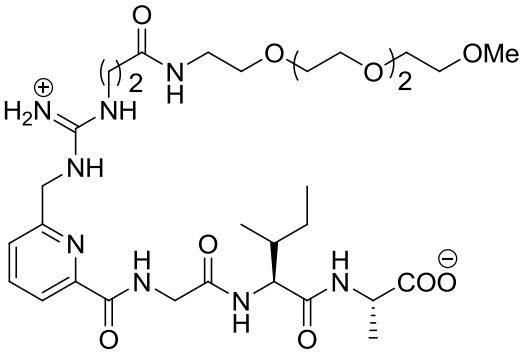

**82**

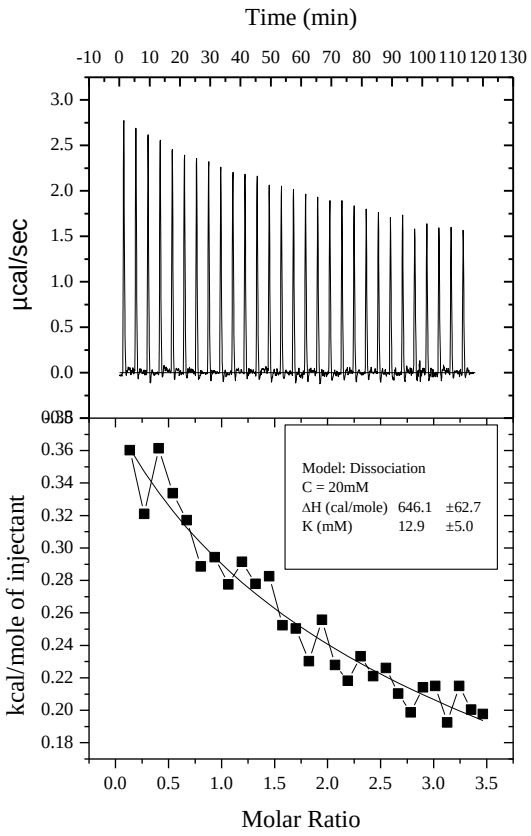


Guanidinium-carboxylate **82** in 10% $H_2O$/DMSO

ITC final figure

| Inj. No. | Molar ratio | Cal/mol of injected **82** |
|---|---|---|
| 1 | 0.13639 | 360.1677 |
| 2 | 0.27184 | 321.0363 |
| 3 | 0.40635 | 361.4471 |
| 4 | 0.53993 | 333.6741 |
| 5 | 0.67257 | 317.1002 |
| 6 | 0.80427 | 288.6113 |
| 7 | 0.93504 | 294.2549 |
| 8 | 1.06487 | 277.4665 |
| 9 | 1.19377 | 291.4978 |
| 10 | 1.32173 | 277.8912 |
| 11 | 1.44875 | 282.6107 |
| 12 | 1.57484 | 252.3568 |
| 13 | 1.69998 | 250.2703 |
| 14 | 1.8242 | 230.2727 |
| 15 | 1.94747 | 255.72 |
| 16 | 2.06981 | 227.8381 |
| 17 | 2.19122 | 218.101 |
| 18 | 2.31168 | 233.2753 |
| 19 | 2.43121 | 221.0632 |
| 20 | 2.54981 | 225.9528 |
| 21 | 2.66747 | 210.2339 |
| 22 | 2.78419 | 198.6501 |
| 23 | 2.89997 | 214.1101 |
| 24 | 3.01482 | 215.0317 |
| 25 | 3.12873 | 192.4871 |
| 26 | 3.24171 | 214.8893 |
| 27 | 3.35375 | 200.3798 |
| 28 | 3.46485 | 197.6202 |
| 29 | 0.13639 | 360.1677 |

Appendices

*ITC data of guanidinium-carboxylate* ***82***

[monomer] = 40 mM
Solvent = 50% $H_2O$/DMSO
$K_{dim}[M^{-1}]$ = 24
$\Delta G_{dim}$ [kJ $mol^{-1}$] = -7.8
$\Delta H_{dim}$ [kJ $mol^{-1}$] = -1.4
$T\Delta S_{dim}$ [kJ $mol^{-1}$] = 6.5

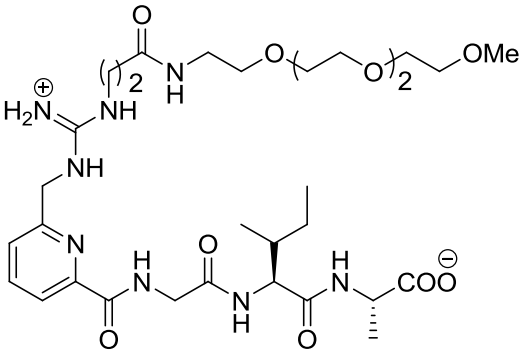

**82**

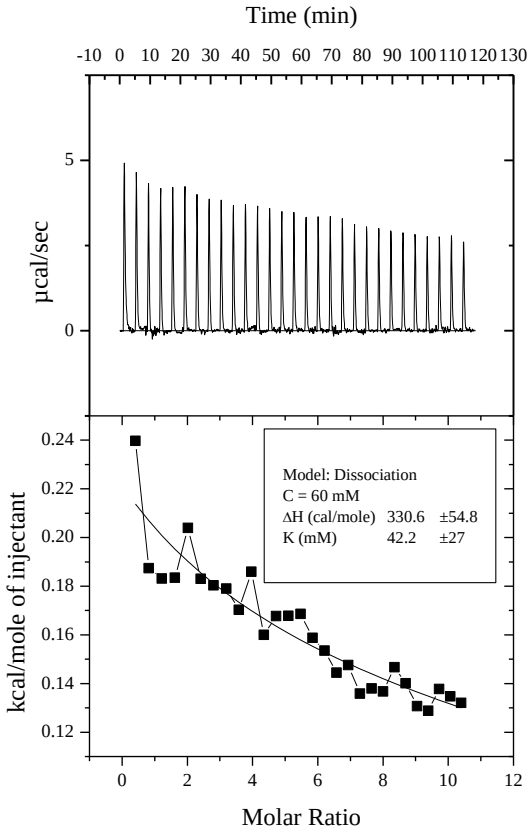


Guanidinium-carboxylate **82** in 10% $H_2O$/DMSO

ITC final figure

| Inj. No. | Molar ratio | Cal/mol of injected **82** |
|---|---|---|
| 1 | 0.40916 | 239.6855 |
| 2 | 0.81551 | 187.3761 |
| 3 | 1.21905 | 183.1618 |
| 4 | 1.61979 | 183.4541 |
| 5 | 2.01771 | 203.8911 |
| 6 | 2.41282 | 183.0415 |
| 7 | 2.80513 | 180.3327 |
| 8 | 3.19462 | 179.0225 |
| 9 | 3.58131 | 170.2817 |
| 10 | 3.96518 | 185.8982 |
| 11 | 4.34625 | 159.9951 |
| 12 | 4.72451 | 167.676 |
| 13 | 5.09995 | 167.8052 |
| 14 | 5.47259 | 168.6434 |
| 15 | 5.84242 | 158.8081 |
| 16 | 6.20944 | 153.4551 |
| 17 | 6.57365 | 144.4317 |
| 18 | 6.93505 | 147.5993 |
| 19 | 7.29364 | 135.8326 |
| 20 | 7.64942 | 137.9379 |
| 21 | 8.0024 | 136.7784 |
| 22 | 8.35256 | 146.7226 |
| 23 | 8.69991 | 140.0552 |
| 24 | 9.04446 | 130.714 |
| 25 | 9.38619 | 128.815 |
| 26 | 9.72512 | 137.7476 |
| 27 | 10.06124 | 134.7008 |
| 28 | 10.39454 | 132.0201 |
| 29 | 0.40916 | 239.6855 |

Appendices

*ITC data of guanidinium-carboxylate **93***

[monomer] = 20 mM
Solvent = 75% $H_2O$/DMSO
$K_{dim}[M^{-1}]$ = 27
$\Delta G_{dim}$ [kJ $mol^{-1}$] = -8.1
$\Delta H_{dim}$ [kJ $mol^{-1}$] = -4.1
$T\Delta S_{dim}$ [kJ $mol^{-1}$] = 4.0

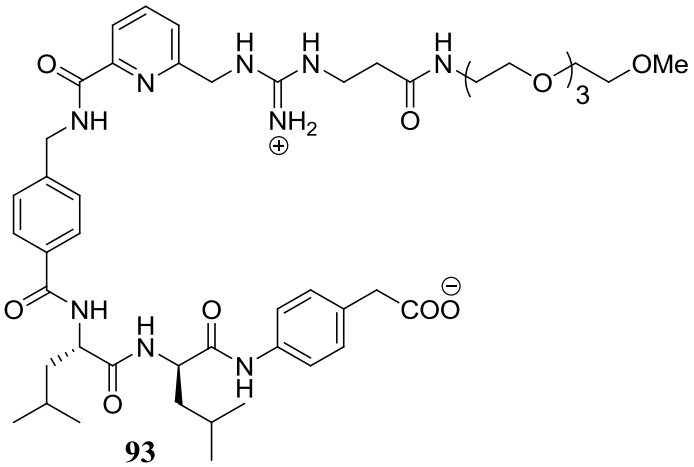

**93**

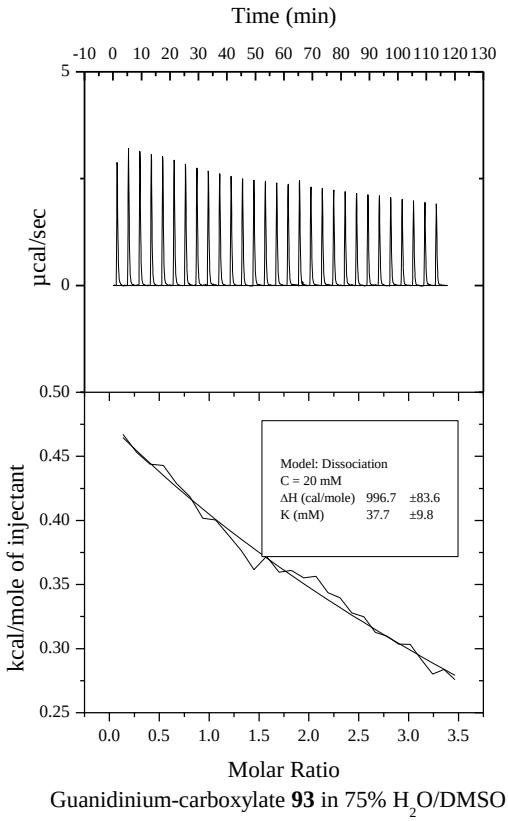


Guanidinium-carboxylate **93** in 75% $H_2O$/DMSO

ITC final figure

| Inj. No. | Molar ratio | Cal/mol of injected **93** |
|---|---|---|
| 1 | 0.13639 | 467.2507 |
| 2 | 0.27184 | 453.2614 |
| 3 | 0.40635 | 443.86 |
| 4 | 0.53993 | 442.8732 |
| 5 | 0.67257 | 428.848 |
| 6 | 0.80427 | 418.7716 |
| 7 | 0.93504 | 401.7638 |
| 8 | 1.06487 | 400.3926 |
| 9 | 1.19377 | 388.655 |
| 10 | 1.32173 | 376.5334 |
| 11 | 1.44875 | 361.6381 |
| 12 | 1.57484 | 371.9674 |
| 13 | 1.69998 | 359.7162 |
| 14 | 1.8242 | 361.1065 |
| 15 | 1.94747 | 355.2 |
| 16 | 2.06981 | 356.4061 |
| 17 | 2.19122 | 343.7182 |
| 18 | 2.31168 | 339.632 |
| 19 | 2.43121 | 327.8597 |
| 20 | 2.54981 | 324.959 |
| 21 | 2.66747 | 312.7782 |
| 22 | 2.78419 | 309.7764 |
| 23 | 2.89997 | 303.4462 |
| 24 | 3.01482 | 303.2519 |
| 25 | 3.12873 | 291.3745 |
| 26 | 3.24171 | 280.1756 |
| 27 | 3.35375 | 283.6748 |
| 28 | 3.46485 | 275.6988 |
| 29 | 0.13639 | 467.2507 |

Appendices

*ITC data of guanidinium-carboxylate **94***

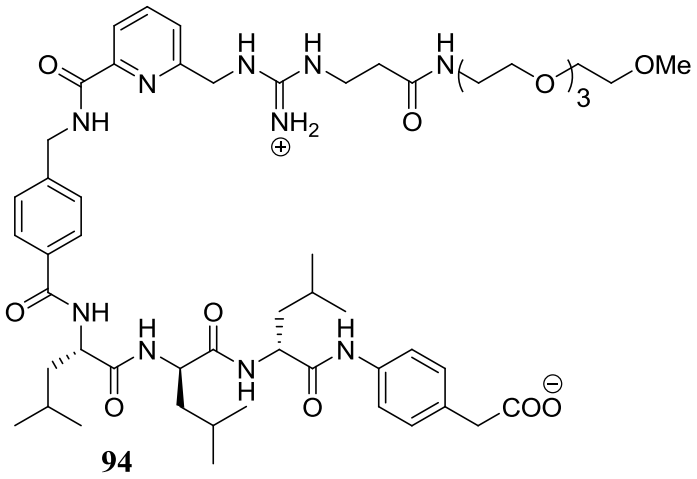

**94**

[monomer] = 10 mM
Solvent = 75% $H_2O$/DMSO
$K_{dim}[M^{-1}]$ = 127
$\Delta G_{dim}$ [kJ $mol^{-1}$] = -12.0
$\Delta H_{dim}$ [kJ $mol^{-1}$] = -33.4
$T\Delta S_{dim}$ [kJ $mol^{-1}$] = -21.4

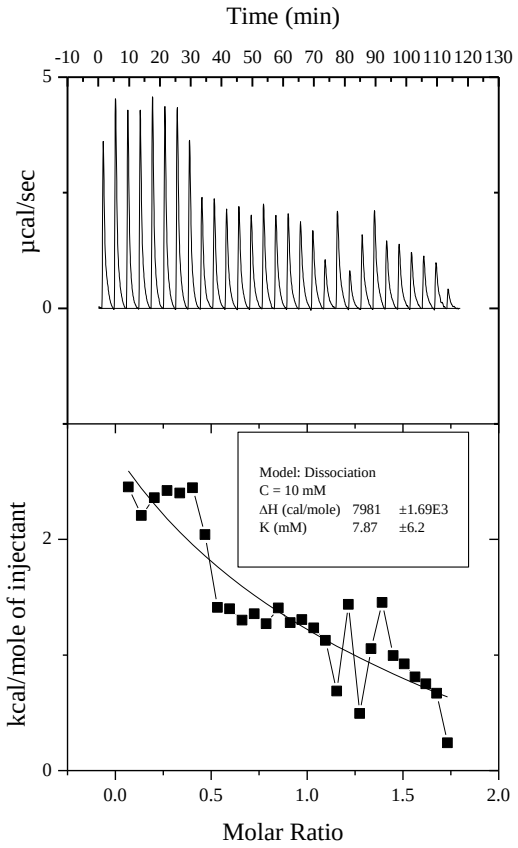


Guanidinium-carboxylate **94** in 75% $H_2O$/DMSO

ITC final figure

| Inj. No. | Molar ratio | Cal/mol of injected **94** |
|---|---|---|
| 1 | 0.06819 | 2454.375 |
| 2 | 0.13592 | 2206.454 |
| 3 | 0.20318 | 2360.827 |
| 4 | 0.26996 | 2422.016 |
| 5 | 0.33628 | 2400.899 |
| 6 | 0.40214 | 2447.049 |
| 7 | 0.46752 | 2040.727 |
| 8 | 0.53244 | 1411.053 |
| 9 | 0.59688 | 1399.769 |
| 10 | 0.66086 | 1301.594 |
| 11 | 0.72437 | 1355.388 |
| 12 | 0.78742 | 1270.49 |
| 13 | 0.84999 | 1405.375 |
| 14 | 0.9121 | 1280.655 |
| 15 | 0.97374 | 1305.084 |
| 16 | 1.03491 | 1233.042 |
| 17 | 1.09561 | 1125.997 |
| 18 | 1.15584 | 687.4067 |
| 19 | 1.21561 | 1437.231 |
| 20 | 1.2749 | 494.0954 |
| 21 | 1.33373 | 1055.312 |
| 22 | 1.39209 | 1453.526 |
| 23 | 1.44999 | 994.3124 |
| 24 | 1.50741 | 922.6757 |
| 25 | 1.56437 | 809.7317 |
| 26 | 1.62085 | 751.0828 |
| 27 | 1.67687 | 669.5469 |
| 28 | 1.73242 | 239.3349 |
| 29 | 0.06819 | 2454.375 |

Appendices

*ITC data of guanidinium-carboxylate **116***

[monomer] = 3 mM
Solvent = DMSO
$K_{dim}[M^{-1}]$ = 1002
$\Delta G_{dim}$ [kJ $mol^{-1}$] = -17.1
$\Delta H_{dim}$ [kJ $mol^{-1}$] = -8.5
$T\Delta S_{dim}$ [kJ $mol^{-1}$] = 8.6

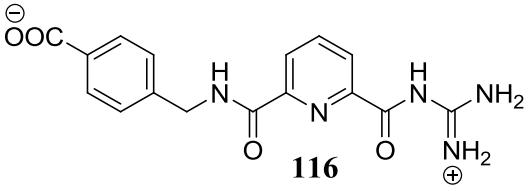


**116**

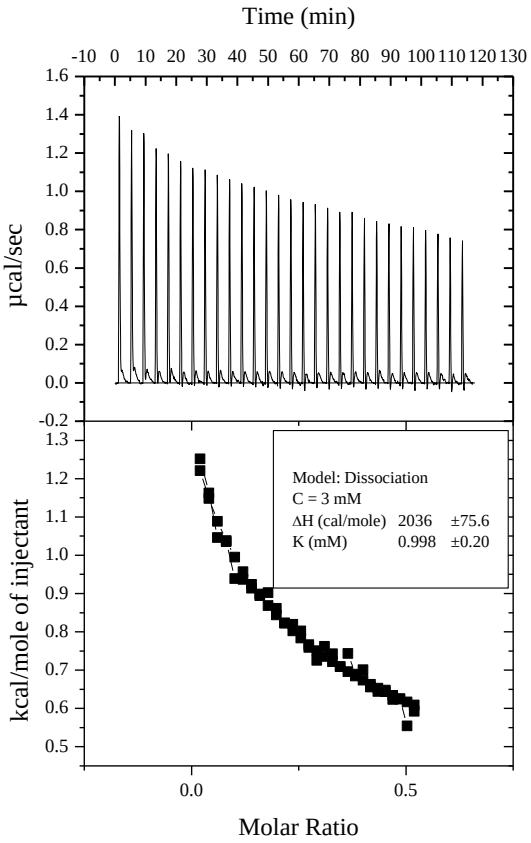


Guanidinium-carboxylate **116** in DMSO

ITC final figure

| Inj. No. | Molar ratio | Cal/mol of injected **116** |
|---|---|---|
| 1 | 0.02046 | 1251.285 |
| 2 | 0.04078 | 1162.246 |
| 3 | 0.06095 | 1045.685 |
| 4 | 0.08099 | 1035.119 |
| 5 | 0.10089 | 939.1429 |
| 6 | 0.12064 | 936.9648 |
| 7 | 0.14026 | 913.3319 |
| 8 | 0.15973 | 898.8061 |
| 9 | 0.17907 | 902.1655 |
| 10 | 0.19826 | 861.3918 |
| 11 | 0.21731 | 823.2552 |
| 12 | 0.23623 | 819.6478 |
| 13 | 0.255 | 801.8791 |
| 14 | 0.27363 | 758.7807 |
| 15 | 0.29212 | 725.4847 |
| 16 | 0.31047 | 762.1949 |
| 17 | 0.32868 | 742.3539 |
| 18 | 0.34675 | 708.7523 |
| 19 | 0.36468 | 742.9584 |
| 20 | 0.38247 | 689.4308 |
| 21 | 0.40012 | 700.6147 |
| 22 | 0.41763 | 655.7673 |
| 23 | 0.435 | 643.8494 |
| 24 | 0.45222 | 647.8605 |
| 25 | 0.46931 | 623.2526 |
| 26 | 0.48626 | 624.2542 |
| 27 | 0.50306 | 554.4971 |
| 28 | 0.51973 | 592.6216 |
| 29 | 0.02046 | 1251.285 |

Appendices

*ITC data of guanidinium-carboxylate **116***

[monomer] = 10 mM
Solvent = 10% $H_2O$/DMSO
$K_{dim}[M^{-1}]$ = 2695
$\Delta G_{dim}$ [kJ $mol^{-1}$] = -19.6
$\Delta H_{dim}$ [kJ $mol^{-1}$] = -6.7
$T\Delta S_{dim}$ [kJ $mol^{-1}$] = 12.9

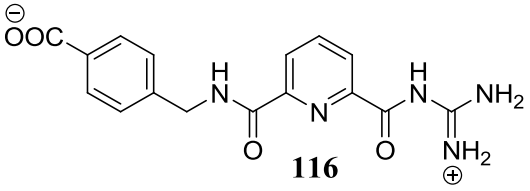


**116**

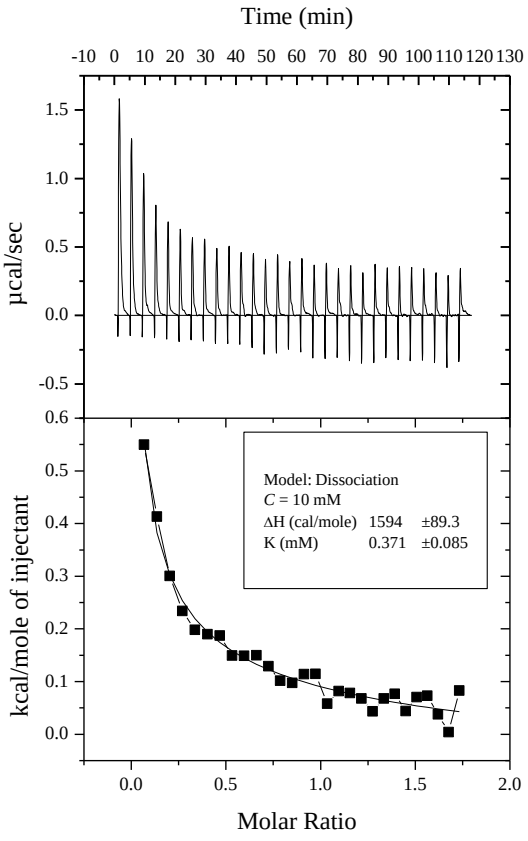


Guanidinium-carboxylate **116** in 10%$H_2O$/ DMSO

ITC final figure

| Inj. No. | Molar ratio | Cal/mol of injected **116** |
|---|---|---|
| 1 | 0.06819 | 549.7635 |
| 2 | 0.13592 | 413.1658 |
| 3 | 0.20318 | 300.4874 |
| 4 | 0.26996 | 234.0588 |
| 5 | 0.33628 | 198.4033 |
| 6 | 0.40214 | 190.0672 |
| 7 | 0.46752 | 187.0514 |
| 8 | 0.53244 | 149.3284 |
| 9 | 0.59688 | 148.7519 |
| 10 | 0.66086 | 150.093 |
| 11 | 0.72437 | 129.3041 |
| 12 | 0.78742 | 101.3938 |
| 13 | 0.84999 | 97.44372 |
| 14 | 0.9121 | 114.1193 |
| 15 | 0.97374 | 114.6592 |
| 16 | 1.03491 | 58.02614 |
| 17 | 1.09561 | 81.76825 |
| 18 | 1.15584 | 78.34983 |
| 19 | 1.21561 | 68.03227 |
| 20 | 1.2749 | 43.60338 |
| 21 | 1.33373 | 68.01357 |
| 22 | 1.39209 | 76.55501 |
| 23 | 1.44999 | 44.10678 |
| 24 | 1.50741 | 70.33935 |
| 25 | 1.56437 | 72.94642 |
| 26 | 1.62085 | 37.99424 |
| 27 | 1.67687 | 4.09021 |
| 28 | 1.73242 | 82.68496 |
| 29 | 0.06819 | 549.7635 |

Appendices

*ITC data of guanidinium-carboxylate **133***

[monomer] = 3 mM
Solvent = DMSO
$K_{dim}[M^{-1}]$ = 1767
$\Delta G_{dim}$ [kJ $mol^{-1}$] = -18.5
$\Delta H_{dim}$ [kJ $mol^{-1}$] = -19.5
$T\Delta S_{dim}$ [kJ $mol^{-1}$] = -0.9

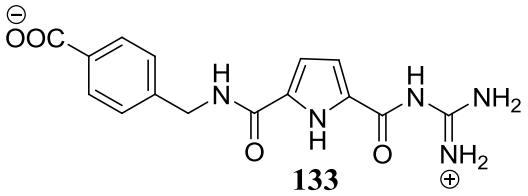


**133**

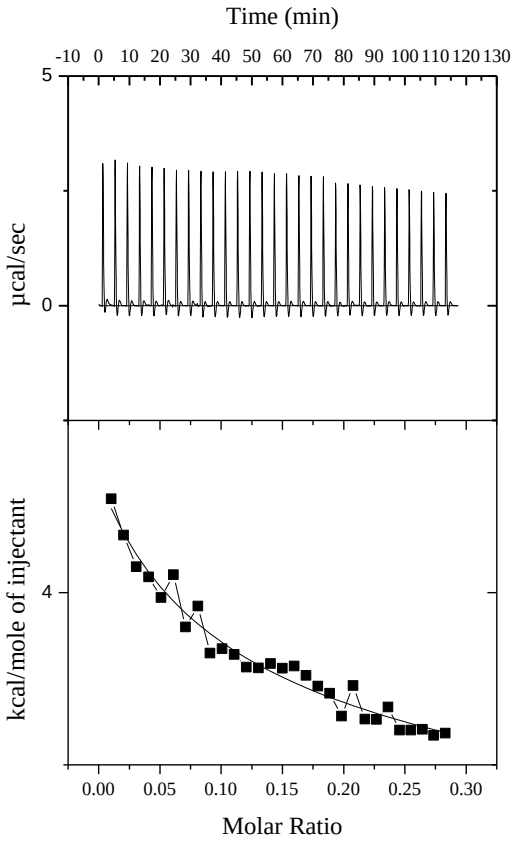


Guanidinium-carboxylate **133** in DMSO

ITC final figure

| Inj. No. | Molar ratio | Cal/mol of injected **133** |
|---|---|---|
| 1 | 0.01025 | 4544.97 |
| 2 | 0.02046 | 4333.193 |
| 3 | 0.03063 | 4150.022 |
| 4 | 0.04078 | 4091.449 |
| 5 | 0.05088 | 3970.88 |
| 6 | 0.06095 | 4104.563 |
| 7 | 0.07099 | 3800.997 |
| 8 | 0.08099 | 3922.435 |
| 9 | 0.09095 | 3648.704 |
| 10 | 0.10089 | 3673.324 |
| 11 | 0.11078 | 3641.177 |
| 12 | 0.12064 | 3567.185 |
| 13 | 0.13047 | 3562.207 |
| 14 | 0.14026 | 3588.404 |
| 15 | 0.15001 | 3560.526 |
| 16 | 0.15973 | 3574.128 |
| 17 | 0.16942 | 3519.308 |
| 18 | 0.17907 | 3457.449 |
| 19 | 0.18868 | 3414.729 |
| 20 | 0.19826 | 3282.165 |
| 21 | 0.2078 | 3459.297 |
| 22 | 0.21731 | 3265.843 |
| 23 | 0.22679 | 3263.845 |
| 24 | 0.23623 | 3335.185 |
| 25 | 0.24563 | 3201.162 |
| 26 | 0.255 | 3201.374 |
| 27 | 0.26433 | 3206.477 |
| 28 | 0.27363 | 3170.465 |
| 29 | 0.28289 | 3183.144 |

Appendices

*ITC data of guanidinium-carboxylate **133***

[monomer] = 10 mM
Solvent = 10% $H_2O$/DMSO
$K_{dim}[M^{-1}]$ = 7634
$\Delta G_{dim}$ [kJ $mol^{-1}$] = -22.2
$\Delta H_{dim}$ [kJ $mol^{-1}$] = -2.8
$T\Delta S_{dim}$ [kJ $mol^{-1}$] = 19.4

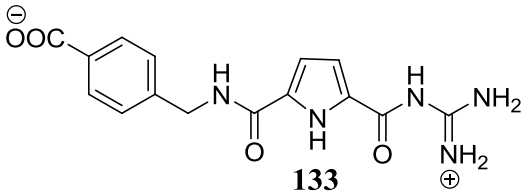


**133**

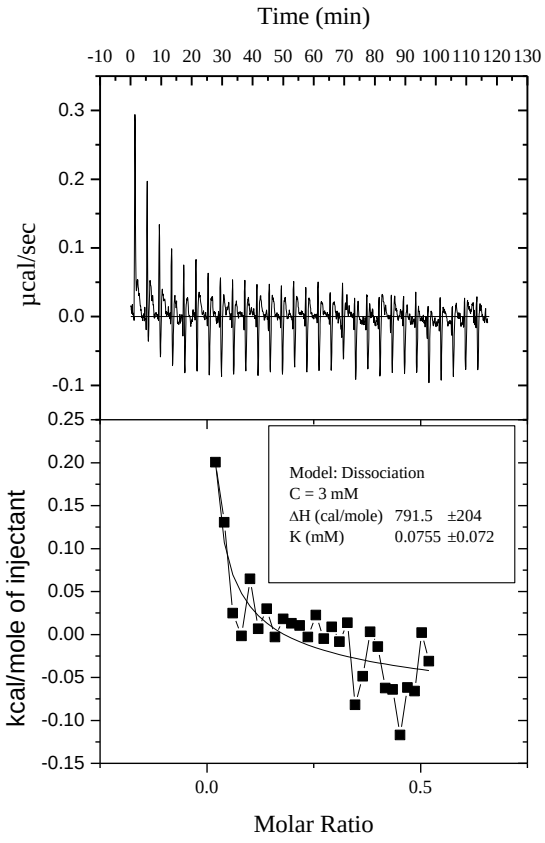


Guanidinium-carboxylate **133** in DMSO

ITC final figure

| Inj. No. | Molar ratio | Cal/mol of injected **133** |
|---|---|---|
| 1 | 0.04092 | 71.34053 |
| 2 | 0.08155 | 42.79089 |
| 3 | 0.12191 | 41.54887 |
| 4 | 0.16198 | 41.2283 |
| 5 | 0.20177 | 14.95972 |
| 6 | 0.24128 | 27.1825 |
| 7 | 0.28051 | 16.92545 |
| 8 | 0.31946 | -20.834 |
| 9 | 0.35813 | 11.32559 |
| 10 | 0.39652 | 14.75362 |
| 11 | 0.43462 | -0.88948 |
| 12 | 0.47245 | 2.49588 |
| 13 | 0.51 | 23.66004 |
| 14 | 0.54726 | 16.35735 |
| 15 | 0.58424 | 12.72356 |
| 16 | 0.62094 | 16.75129 |
| 17 | 0.65737 | -0.4407 |
| 18 | 0.69351 | 3.74826 |
| 19 | 0.72936 | -13.8684 |
| 20 | 0.76494 | -0.63128 |
| 21 | 0.80024 | 15.5098 |
| 22 | 0.83526 | 11.06631 |
| 23 | 0.86999 | 9.99491 |
| 24 | 0.90445 | -4.50713 |
| 25 | 0.93862 | -21.3629 |
| 26 | 0.97251 | -8.3646 |
| 27 | 1.00612 | 26.97792 |
| 28 | 1.03945 | 14.81587 |
| 29 | 0.04092 | 71.34053 |

# Appendix B- NMR dilution data

*NMR dilution data of guanidinium-carboxylate* ***45***

| Conc.(mM) | NH $^{1}$ (ppm) | NH $^{2}$ (ppm) |
|---|---|---|
| 56 | 10.00 | 10.00 |
| 50 | 10.04 | 9.94 |
| 44 | 10.09 | 9.90 |
| 38 | 10.12 | 9.83 |
| 32 | 10.17 | 9.75 |
| 26 | 10.19 | 9.69 |
| 20 | 10.24 | 9.63 |
| 14 | 10.31 | 9.42 |
| 8 | 10.46 | 9.19 |
| 2 | 10.75 | 8.80 |

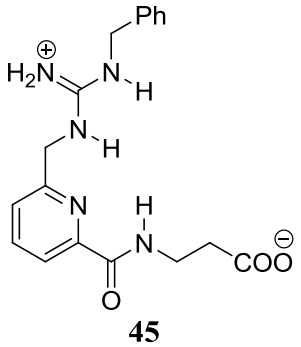


**45**

a)

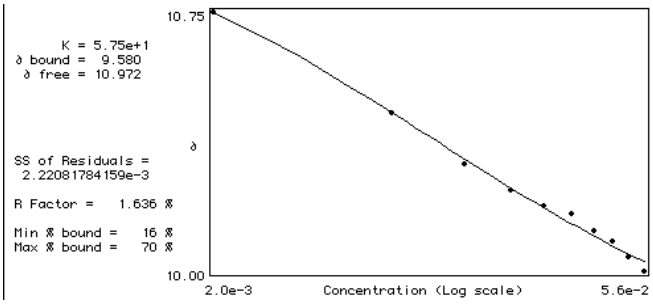


b)

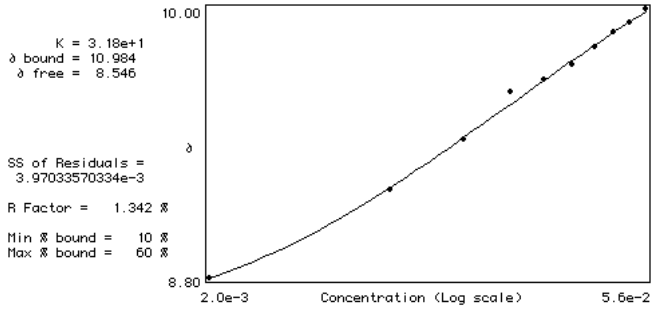


c)

a) 1H NMR dilution data for two NH protons ($NH^1$ and $NH^2$) in compound **45** recorded in DMSO at 298 K.

b) c) The curve shows the fit to the dimerization isotherm. The data span 10%–70% bound and were used to determine the bound and free chemical shifts and the dimerisation constant.

Appendices

*NMR dilution data of guanidinium-carboxylate* ***53***

| Con. (mM) | $NH^1$(ppm) | $NH^2$ (ppm) |
|---|---|---|
| 40.60 | 8.80 | - |
| 20.60 | 8.81 | - |
| 12.10 | 8.90 | - |
| 7.70 | 8.90 | - |
| 5.14 | 8.95 | - |
| 3.58 | 8.99 | - |
| 2.55 | 9.09 | 7.80 |
| 1.85 | 9.18 | 7.76 |
| 1.35 | 9.17 | 7.75 |
| 0.99 | 9.20 | 7.73 |
| 0.72 | 9.27 | 7.70 |
| 0.51 | 9.30 | 7.68 |
| 0.35 | 9.42 | 7.65 |
| 0.23 | 9.45 | 7.61 |
| 0.13 | 9.51 | 7.58 |

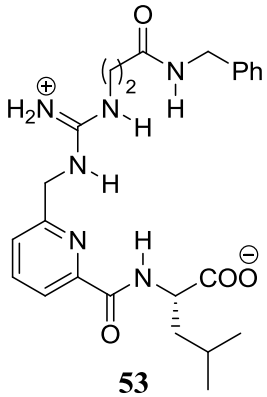


**53**

a)

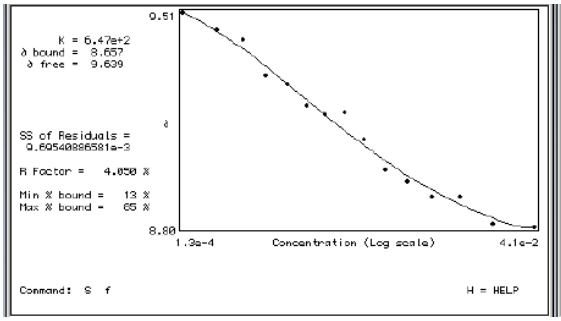


b)

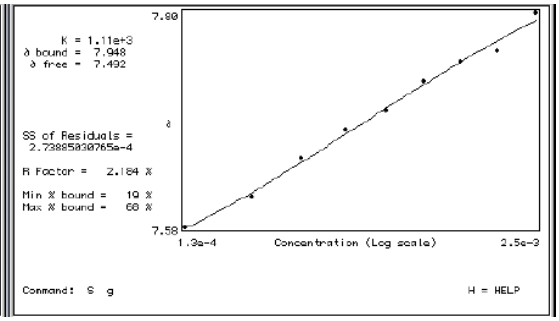


c)

a) $^1$H NMR dilution data for two NH protons ($NH^1$ and $NH^2$) in compound **53** recorded in DMSO at 298 K.

b) c) The curve shows the fit to the dimerization isotherm. The data span 10%–65% bound and were used to determine the bound and free chemical shifts and the dimerisation constant.

Appendices

*NMR dilution data of guanidinium-carboxylate* ***78***

| Conc. (mM) | $NH^1$ (ppm) | $NH^2$(ppm) |
|---|---|---|
| 23.3 | 9.69 | - |
| 14.0 | 9.66 | - |
| 9.10 | 9.61 | - |
| 6.20 | - | - |
| 4.40 | 9.56 | - |
| 3.16 | 9.55 | - |
| 2.30 | 9.53 | 7.79 |
| 1.73 | 9.49 | 7.76 |
| 1.29 | 9.49 | 7.75 |
| 0.96 | 9.47 | 7.74 |
| 0.71 | 9.44 | 7.72 |
| 0.52 | 9.42 | 7.70 |
| 0.36 | 9.40 | 7.69 |
| 0.24 | 9.38 | 7.67 |
| 0.14 | 9.36 | 7.66 |

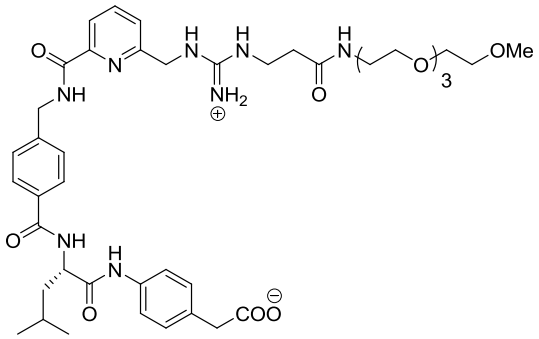


**78**

a)

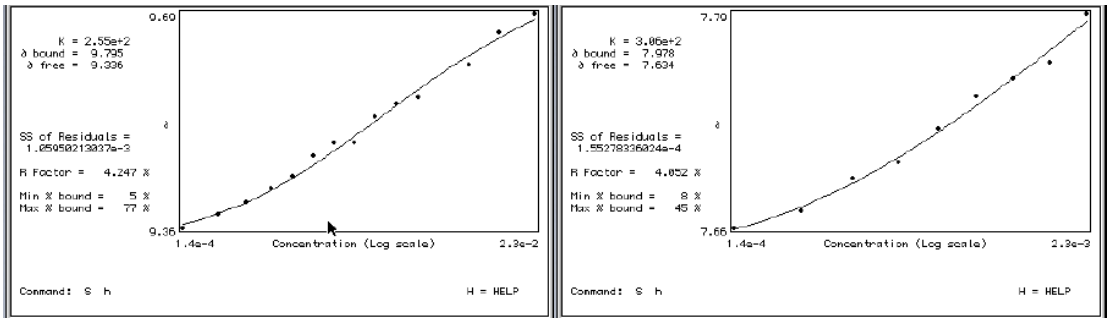


b) c)

a) $^1$H NMR dilution data for two NH protons ($NH^1$ and $NH^2$) in compound **78** recorded in DMSO at 298 K.

b) c) The curve shows the fit to the dimerization isotherm. The data span 5%–77% bound and were used to determine the bound and free chemical shifts and the dimerisation constant.

Appendices

*NMR dilution data of guanidinium-carboxylate **82***

| Conc. (mM) | NH (ppm) |
|---|---|
| 33.8 | 7.55 |
| 18.4 | 7.52 |
| 11 | 7.5 |
| 6.9 | 7.48 |
| 4.5 | 7.45 |
| 2.9 | 7.44 |
| 1.9 | 7.44 |
| 1.2 | 7.43 |
| 0.7 | 7.42 |
| 0.4 | 7.40 |

a)

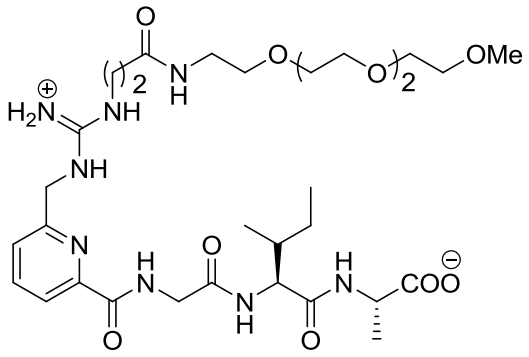

**82**

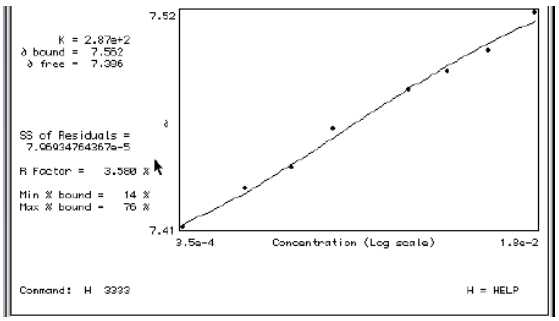


b)

a) $^{1}$H NMR dilution data for two NH protons (NH$^{1}$ and NH$^{2}$) in compound **78** recorded in DMSO at 298 K.

b) The curve shows the fit to the dimerization isotherm. The data span 14%–76% bound and were used to determine the bound and free chemical shifts and the dimerisation constant.

# Appendix C

*X-ray crystal data of guanidinium-carboxylate* ***45***

**Table 15.** Crystal data and structure refinement details.

| | |
|---|---|
| Identification code | **2008sot0404 (BT/5029/37)** |
| Empirical formula | $C_{18}H_{21}N_5O_3$ |
| Formula weight | 355.40 |
| Temperature | 120(2) K |
| Wavelength | 0.71073 Å |
| Crystal system | Monoclinic |
| Space group | $P2_1/n$ |
| Unit cell dimensions | $a$ = 8.4729(3) Å |
| | $b$ = 19.3608(6) Å |
| | $c$ = 11.2976(5) Å |
| | $\beta$ = 105.552(2)° |
| Volume | 1785.43(12) Å$^3$ |
| $Z$ | 4 |
| Density (calculated) | 1.322 Mg / m$^3$ |
| Absorption coefficient | 0.093 mm$^{-1}$ |
| *F(000)* | 752 |
| Crystal | Lozenge; Colourless |
| Crystal size | 0.12 × 0.03 × 0.02 mm$^3$ |
| $\theta$ range for data collection | 3.26 – 25.03° |
| Index ranges | $-9 \le h \le 10$, $-22 \le k \le 23$, $-13 \le l \le 13$ |
| Reflections collected | 16301 |
| Independent reflections | 3131 [$R_{int}$ = 0.1008] |
| Completeness to $\theta$ = 25.03° | 99.7 % |
| Absorption correction | Semi–empirical from equivalents |
| Max. and min. transmission | 0.9981 and 0.9789 |
| Refinement method | Full-matrix least-squares on $F^2$ |
| Data / restraints / parameters | 3131 / 1 / 254 |
| Goodness-of-fit on $F^2$ | 1.097 |
| Final $R$ indices [$F^2 > 2\sigma(F^2)$] | *R1* = 0.0880, *wR2* = 0.1467 |
| $R$ indices (all data) | *R1* = 0.1430, *wR2* = 0.1725 |
| Largest diff. peak and hole | 0.400 and –0.390 e Å$^{-3}$ |

**Diffractometer:** *Nonius KappaCCD* area detector ($\phi$ scans and $\omega$ scans to fill *asymmetric unit* ). **Cell determination:** DirAx (Duisenberg, A.J.M.(1992). J. Appl. Cryst. 25, 92-96.) **Data collection:** Collect (Collect: Data collection software, R. Hooft, Nonius B.V., 1998). **Data reduction and cell refinement**: *Denzo* (Z. Otwinowski & W. Minor, *Methods in Enzymology* (1997) Vol. **276**: *Macromolecular Crystallography*, part A, pp. 307–326; C. W. Carter, Jr. & R. M. Sweet, Eds., Academic Press). **Absorption correction**: Sheldrick, G. M. SADABS - Bruker Nonius area detector scaling and absorption correction - V2.10 S**tructure solution**: *SHELXS97* (G. M. Sheldrick, Acta Cryst. (1990) A**46** 467–473). S**tructure refinement**: *SHELXL97* (G. M. Sheldrick (1997), University of Göttingen, Germany). **Graphics:** Cameron - A Molecular Graphics Package. (D. M. Watkin, L. Pearce and C. K. Prout, Chemical Crystallography Laboratory, University of Oxford, 1993).

**Special details**: All hydrogen atoms were placed in idealised positions and refined using a riding model, those of the hetero atoms were located in the difference map and refined.

**Table 16.** Atomic coordinates [$\times 10^4$], equivalent isotropic displacement parameters [$Å^2 \times 10^3$] and site occupancy factors. $U_{eq}$ is defined as one third of the trace of the orthogonalized $U^{ij}$ tensor.

| Atom | *x* | *y* | *z* | $U_{eq}$ | *S.o.f.* |
|---|---|---|---|---|---|
| O1 | 7404(4) | 1596(2) | 8954(3) | 32(1) | 1 |
| O2 | 6704(4) | 1061(2) | 7161(3) | 34(1) | 1 |
| O3 | 11727(4) | –410(2) | 7551(3) | 30(1) | 1 |
| N1 | 9354(5) | 209(2) | 7061(3) | 26(1) | 1 |
| N2 | 10385(4) | 977(2) | 5455(3) | 24(1) | 1 |
| N3 | 10155(5) | 2350(2) | 3158(3) | 26(1) | 1 |
| N4 | 9055(5) | 1661(2) | 1432(4) | 29(1) | 1 |
| N5 | 10304(5) | 2700(2) | 1257(3) | 27(1) | 1 |
| C1 | 7415(5) | 1082(2) | 8279(4) | 25(1) | 1 |
| C2 | 8369(6) | 450(2) | 8866(4) | 27(1) | 1 |
| C3 | 8557(6) | –88(2) | 7935(4) | 28(1) | 1 |
| C4 | 10839(5) | 51(2) | 6966(4) | 24(1) | 1 |
| C5 | 11423(5) | 489(2) | 6064(4) | 23(1) | 1 |
| C6 | 12968(5) | 382(2) | 5899(4) | 26(1) | 1 |
| C7 | 13459(5) | 796(2) | 5065(4) | 29(1) | 1 |
| C8 | 12394(5) | 1295(2) | 4430(4) | 28(1) | 1 |
| C9 | 10880(5) | 1371(2) | 4647(4) | 23(1) | 1 |
| C10 | 9644(5) | 1918(2) | 4036(4) | 27(1) | 1 |
| C11 | 9823(5) | 2225(2) | 1959(4) | 24(1) | 1 |
| C12 | 10721(5) | 2520(2) | 131(4) | 29(1) | 1 |
| C13 | 12100(5) | 1997(2) | 302(4) | 28(1) | 1 |
| C14 | 13348(6) | 1966(3) | 1386(4) | 36(1) | 1 |
| C15 | 14617(6) | 1498(3) | 1534(5) | 46(1) | 1 |
| C16 | 14683(6) | 1064(3) | 579(5) | 46(1) | 1 |
| C17 | 13462(6) | 1095(3) | –511(5) | 42(1) | 1 |
| C18 | 12179(6) | 1557(2) | –650(5) | 35(1) | 1 |

Appendices

**Table 17**

Bond Length's (Å) and Angles(°)

| | | | |
|---|---|---|---|
| O1–C1 | 1.256(5) | C17–C18 | 1.385(7) |
| O2–C1 | 1.246(5) | C4–N1–C3 | 125.9(4) |
| O3–C4 | 1.239(5) | C9–N2–C5 | 117.8(4) |
| N1–C4 | 1.327(6) | C11–N3–C10 | 124.9(4) |
| N1–C3 | 1.456(5) | C11–N5–C12 | 122.4(4) |
| N2–C9 | 1.340(5) | O2–C1–O1 | 124.2(4) |
| N2–C5 | 1.348(5) | O2–C1–C2 | 118.2(4) |
| N3–C11 | 1.329(6) | O1–C1–C2 | 117.6(4) |
| N3–C10 | 1.449(5) | C1–C2–C3 | 113.2(4) |
| N4–C11 | 1.327(6) | N1–C3–C2 | 110.6(3) |
| N5–C11 | 1.347(5) | O3–C4–N1 | 125.2(4) |
| N5–C12 | 1.451(6) | O3–C4–C5 | 120.2(4) |
| C1–C2 | 1.517(6) | N1–C4–C5 | 114.6(4) |
| C2–C3 | 1.520(6) | N2–C5–C6 | 123.1(4) |
| C4–C5 | 1.507(6) | N2–C5–C4 | 116.9(4) |
| C5–C6 | 1.386(6) | C6–C5–C4 | 120.0(4) |
| C6–C7 | 1.383(6) | C7–C6–C5 | 118.2(4) |
| C7–C8 | 1.384(6) | C6–C7–C8 | 119.0(4) |
| C8–C9 | 1.377(6) | C9–C8–C7 | 119.4(4) |
| C9–C10 | 1.519(6) | N2–C9–C8 | 122.5(4) |
| C12–C13 | 1.519(6) | N2–C9–C10 | 113.8(4) |
| C13–C18 | 1.387(6) | C8–C9–C10 | 123.7(4) |
| C13–C14 | 1.388(6) | N3–C10–C9 | 114.6(4) |
| C14–C15 | 1.383(7) | N4–C11–N3 | 123.4(4) |
| C15–C16 | 1.380(8) | N4–C11–N5 | 119.1(4) |
| C16–C17 | 1.381(7) | N3–C11–N5 | 117.5(4) |
| | | N5–C12–C13 | 114.1(4) |
| | | C18–C13–C14 | 118.4(4) |
| | | C18–C13–C12 | 120.4(4) |
| | | C14–C13–C12 | 121.2(4) |
| | | C15–C14–C13 | 121.2(5) |
| | | C16–C15–C14 | 119.9(5) |
| | | C15–C16–C17 | 119.5(5) |
| | | C16–C17–C18 | 120.5(5) |
| | | C17–C18–C13 | 120.5(5) |

**Table 18** Hydrogen coordinates [$\times 10^4$] and isotropic displacement parameters [$Å^2 \times 10^3$].

| Atom | *x* | *y* | *z* | $U_{eq}$ | *S.o.f.* |
|---|---|---|---|---|---|
| H2A | 7804 | 238 | 9437 | 32 | 1 |
| H2B | 9471 | 597 | 9354 | 32 | 1 |
| H3A | 9217 | –480 | 8367 | 33 | 1 |
| H3B | 7464 | –267 | 7489 | 33 | 1 |
| H6 | 13670 | 34 | 6347 | 32 | 1 |
| H7 | 14511 | 739 | 4931 | 35 | 1 |
| H8 | 12704 | 1583 | 3849 | 33 | 1 |
| H10A | 8606 | 1686 | 3610 | 32 | 1 |
| H10B | 9418 | 2218 | 4682 | 32 | 1 |
| H12A | 11042 | 2945 | –232 | 35 | 1 |
| H12B | 9735 | 2331 | –462 | 35 | 1 |
| H14 | 13330 | 2273 | 2039 | 43 | 1 |
| H15 | 15442 | 1474 | 2292 | 56 | 1 |
| H16 | 15562 | 746 | 671 | 55 | 1 |
| H17 | 13503 | 796 | –1170 | 51 | 1 |
| H18 | 11346 | 1574 | –1405 | 42 | 1 |
| H91 | 8870(60) | 560(20) | 6720(40) | 30(14) | 1 |
| H93 | 10890(60) | 2730(30) | 3460(50) | 44(14) | 1 |
| H94 | 8830(60) | 1390(20) | 1800(40) | 27(15) | 1 |
| H95 | 10760(60) | 3110(30) | 1620(40) | 38(14) | 1 |
| H99 | 7940(50) | 1600(20) | 9710(20) | 36 | 1 |

Appendices

Table 19 Hydrogen bonds [Å and °].

| *D*–H···*A* | *d*(*D*–H) | *d*(H···*A*) | *d*(*D*···*A*) | ∠(*DHA*) |
|---|---|---|---|---|
| N1–H91···O2 | 0.83(5) | 2.25(5) | 2.813(5) | 125(4) |
| N3–H93···O1$^{i}$ | 0.97(5) | 1.80(5) | 2.772(5) | 174(4) |
| N4–H94···O3$^{ii}$ | 0.73(5) | 2.13(5) | 2.834(5) | 163(5) |
| N5–H95···O2$^{i}$ | 0.94(5) | 1.81(5) | 2.749(5) | 173(4) |
| O1–H99···N4$^{iii}$ | 0.853(19) | 1.93(2) | 2.776(5) | 175(5) |

Symmetry transformations used to generate equivalent atoms:
(i) x+1/2,–y+1/2,z–1/2 (ii) –x+2,–y,–z+1 (iii) x,y,z+1

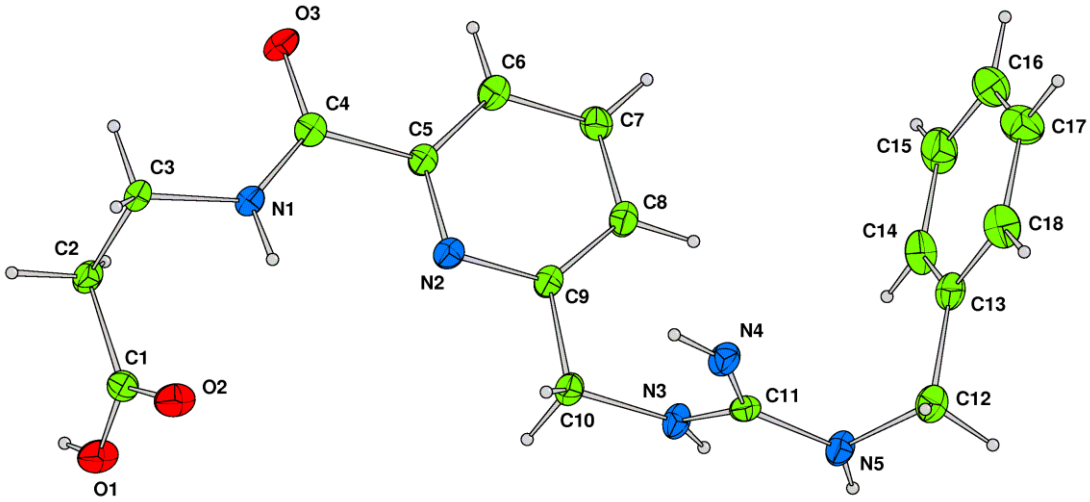


Thermal ellipsoids drawn at the 45% probability level

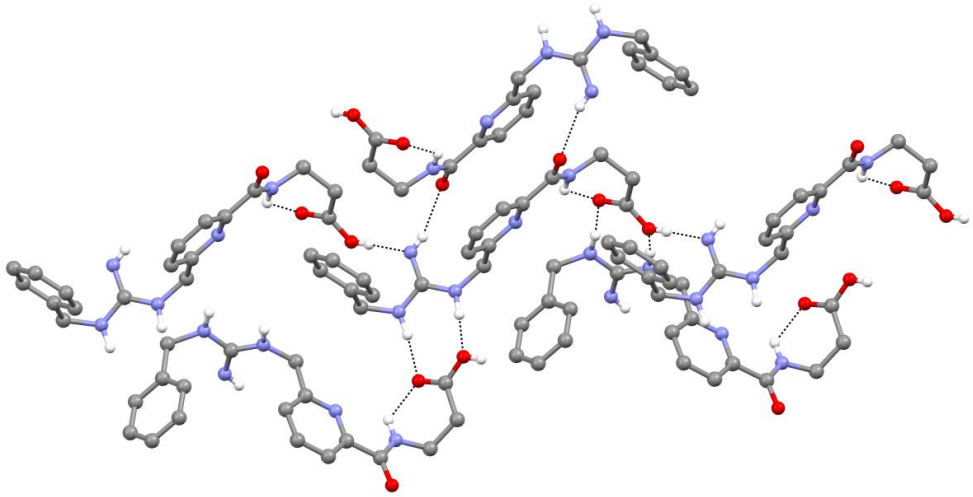

Part of the 3D hydrogen bonding network

# References


1. H. Schneider, *Angew. Chem. Int. Ed.* **2009**, 48, 3924.
2. G. A. Jeffrey, W.Saenger, *Hydrogen Bonding in Biological Structures, Springer-Verlag*: **1991**.
3. A. Prokop, W. Wrasidlo, H. Lode, R. Herold, F. Lang , G. Henze, B. Dörken , T.Wieder, P.T. Daniel, *Oncogene*, **2000**, 22, 9107.
4. S. Wang, J. Wu, S.Yamamoto, H. Liu, *Biotechnol J.* **2008**, 3, 2, 165.
5. C. Ross, M. A. Poireri, *Nature Medicine*. **2004**, 10, S10.
6. J. N. Martin, E. M. Muñoz, C. Schwergold, F. Souard, J. L. Asensio, J. Jiménez-Barbero, J .Cañada, C. Vicent, *J. Am. Chem. Soc*. **2005**, 127, 9518.
7. E. Di Cera, *Chem. Rev*. **1998**, 98, 1563.
8. M.M.Conn, J. Rebek, *Chem. Rev*. **1997**, 97, 674.
9. L. Jullien, H.Cottet, B. Hamelin, A. Jardy, *J. Phys. Chem.* **1999**, 103, 10866.
10. G.Storm, J. A. Crommelin, *PSTT*. **1998**, 1, 19.
11. S. Vemuri, C. T. Rhodes, *Pharm. Acta. Helv.* **1995**, 70, 95.
12. L. Sun, J. Gersdorff, D. Niethammer, P. Tian, H. Kurreck, *Angew. Chem. Int. Ed.* **1994**, 22, 2318.
13. C.A. Hunter, H.L. Anderson, *Angew. Chem. Int. Ed.* **2009**, 48, 7488.
14. A. E. Martell, R. D. Hancock, R. J. Motekaitis, *Coord. Chem. Rev*. **1994**, 133, 39.
15. J. M Daniel, S. D. Friess, S. Rajagopalan, S. Wendt, R. Zenobi, *Int. J. Mass Spectrom.* **2002**, 216, 1.
16. E. A. Meyer, R. K.Castellano, F.Diederich, *Angew. Chem., Int. Ed.* **2003**, 42, 1210.
17. G. A. Jeffrey, *An Introduction to Hydrogen Bonding*; Oxford University Press: New York, **1997**.
18. J. Sponer, P. Jurecka, P. Hobza, *J. Am. Chem. Soc*. **2004**, 126, 10142.
19. D. H. Williams, M. S. Westwall, *Chem. Soc. Rev*. **1998**, 27, 57.
20. A. Ranganathan, G. U. Kulkarni, C. N. R. Rao, *J. Phys. Chem. A.* **2003**, 107, 6073.
21. S. J. Brooks, P. R. Edwards, P. A. Gale, M. E. Light, *New J. Chem*. **2006**, 30, 65.
22. S. K. Chang, D. Van. Engen, E. Fan, A. D. Hamilton, *J. Am. Chem. Soc*. **1991**, 113, 7640.
23. C. Tanford, The Hydrophobic Effect. Wiley. New York: **1980**.
24. K. A. Dill, *Biochemistry.* **1990**, *29*, 7133.
25. I. Gitlin, J. D. Carbeck, G. M. Whitesides, *Angew. Chem. Int. Ed*. **2006**, 45, 3022.
26. S. M. Ngola, P. C. Kearney, S. Mecozzi, K. Russell, D. A. Dougherty, *J. Am. Chem. Soc.* **1999**, 121, 1192.
27. A. Camara-Campos, C. A. Hunter, S. Tomas, *Proc Natl Acad Sci U S A*. **2006**, 103, 3034.

References


28. N. Douteau-Guevel, A. W. Coleman, J. P. Morel, N. J. Morel- Desrosiers, *J. Chem. Soc., Perkin Trans. 2*, **1999**, 629.
29. G. Ercolani, *J. Am. Chem. Soc.* **2003**, 125, 16097.
30. C. A. Hunter, S. Tomas, *Chem. Biol*. **2003**, 10, 1023.
31. M. Lovatt, A.Cooper, P.Camilleri, *Eur Biophys J.* **1996**, 24, 354.
32. P. J. Carter, G. Winter, A. J. Wilkinson, A. R. Fersht, *Cell.* **1984**, 38, 835.
33. S. L. Cockroft, C. A. Hunter *Chem. Soc. Rev.* **2007**, 36, 172.
34. L. J. Prins, D. N. Reinhoudt, P. Timmerman, *Angew. Chem. Int. Ed.*, **2001**, 40, 2383.
35. L. R. Pratt, A. Pohorille, *Chem. Rev.* **2002**, 102, 2671.
36. C. A. Hunter, K. R. Lawson, J. Perkins, C. J. Urch, *J. Chem. Soc., Perkin Trans. 2*. **2001**, 651.
37. K. A. Schug, W. Lindner, *Chem. Rev*. **2005**, 102, 67.
38. R. J. Fitzmaurice, M. Y. Graham, D. David, J.D. Kilburn, *J. Chem. Soc., Perkin Trans.1*. **2002**, 841.
39. F.P. Schmidtchen, M. Berger, *Chem. Rev.* **1997**, 97, 1609.
40. C. L. Hannon, E. V. Anslyn, *Bioorg. Chem. Front.*, **1993**, 3, 193.
41. R. Zenobi, *Int. J. Mass Spectrom.* **2002**, 216, 202, 1.
42. J. Georges, *Spectrochim. Acta.* **1995**. 51A, 6, 985.
43. H. W. Gmeiner, C. D. Poulter, *J. Am. Chem. Soc.* **1988**, 110, 23, 1641.
44. L. Katz, S. Penman, *J. Mol. Biol.* **1966**, 15, 220.
45. M. Berger, F. P. Schmidtchen, *J. Am. Chem. Soc*. **1999**, 121, 9986.
46. B. R Linton, M. S. Goodman, E. Fan, S. A.van Arman, A. D. Hamilton, *J. Org. Chem.* **2001**, 66, 7313.
47. B. Meyer, T. Peters, *Angew. Chem., Int. Ed.* **2003**, 42, 864.
48. M. Czekalla, H. Stephan, B. Habermann, J. Trepte, K. Gloe, F. P. Schmidtchen, *Thermochim. Acta.* **1998**, 313, 137.
49. I. Jelesarov, H. R. Bosshard, *J. Mol. Recognit*. **1999**, 12, 3.
50. A. Ababou, J. E. Ladbury, *J. Mol. Recognit*. **2006**, 19, 79.
51. M. Berger, F. P. Schmidtchen, *Angew. Chem., Int. Ed.* **1998**, 37, 2694.
52. M. Haj-Zaroubi, N. W Mitzel, F. P. Schmidtchen, *Angew. Chem., Int. Ed*. **2002**, 41, 104.
53. I. Jelesarov, H. R. Bosshard, *J. Mol. Recognit*. **1999**, 12, 3.
54. L. Baranauskienė, V. Petrikaitė, J. Matulienė, M. Daumantas, *Int. J. Mol. Sci.* **2009**, 10.
55. M. Bello, G. Perez-Hernandez, D. A. Fernandez-Velasco, R. Arreguın-Espinosa, E. Garcıa-Hernandez, *Protiens: Struct. Funct. Bioinf.* **2008**, 70, 1475.
56. D. McPhail, A. Cooper, *J. Chem. Soc. Faraday Trans*. **1997**, 93, 2283.
57. A. Arnaud, L. Bouteiller, *Langmuir.* **2004**, 20, 16, 6858.
58. A. R. Fersht, *Trends Biochem. Sci*. **1987**, 12, 301.
59. R. J. Fitzmaurice, F. Gaggini, N. Srinivasan, J. D. Kilburn, *Org. Biomol. Chem*. **2007**, 5, 1706.
60. D. A. Dougherty, *Chem. Rev.* **1997**, 97, 1303.

References


61. C. Schmuck, *Chem. Eur. J*., **2000**, 6, 709.
62. E. Palagiano, S. De Marino, L. Minale, R. Riccio, F. Zollo, M. Iorizzi, J. B. Carre, C. Debitus, L. Lucarain, J. Provost, *Tetrahedron*. **1995**, 51, 3675.
63. G. T. Anderson, M. D. Alexander, S. D. Taylor, D. B. Smithrud, S. J. Benkovic, S. Weinreb, *J. Org. Chem.* **1996**, 61, 125.
64. J. Klein, A. Medlik, *Chem. Commun.* **1973**, 275.
65. A. Gleich, F. P. Schmidtchen, P. Mikulcik, G. Mueller, *J. Chem. Soc., Chem. Commun.* **1990**, 55.
66. G. Mueller, J. Riede, F. P. Schmidtchen, *Angew. Chem.* **1988**, 100, 1574.
67. P. Blondeau, M. Segura, R. Pe´rez-Ferna´ndez, J. de Mendoza, *Chem. Soc. Rev.* **2007**, 36, 198.
68. C. L. Hannon, E. V. Anslyn, *The Guanidinium Group: Its Biological Role, Synthetic Analogs. In Bioorganic Chemistry Frontiers*, Eds. Springer: Heidelberg, **1993**, 193.
69. S. Mangani, M. Ferraroni, A. Bianchi, K. Bowman-James, E. Garcia-Espana, *Supramolecular Chemistry of Anions*, Wiley/VCH, NewYork, **1997**.
70. C. Schmuck, U. Machon, *Chem. Eur. J.*, **2005**, 11, 1109.
71. J. S. Albert, M. S. Goodman, A. D. Hamilton, *J. Am. Chem. Soc.* **1995**, 117, 1143.
72. A. Echvarren, A. Gala´n, J. M. Lehn, J.De Mendoza, *J. Am.Chem. Soc.* **1989**, 111, 4994.
73. F. P. Schmidtchen, *Tetrahedron Lett*. **1989**, 30, 4493.
74. K. B. Jensen, T. M. Braxmeier, M. Demarcus, J. G. Frey, J. D. Kilburn, *Chem. Eur. J.* **2002**, 8,1300.
75. M. Haj-Zaroubi, N. W. Mitzel, F. P. Schmidtchen, *Angew. Chem., Int. Ed.* **2002**, 41, 104.
76. C. Schmuck, *Chem. Commun*. **1999**, 843.
77. A. Klug, *Angew. Chem*. **1983**, 95, 579.
78. C. Schmuck, L.Geiger, *J. Am. Chem. Soc.* **2005**, 127, 10486.
79. M. Davies, M. Bonnat, F. Guillier, J. D. Kilburn , M. Bradley, *J. Org. Chem.* **1998**, 63, 8696.
80. S. Bartoli, T. M. Abdul Malik, S. Dixon, J. D. Kilburn, *Org. Biomol. Chem.* **2008**, 6, 2340.
81. S. Y. Chang, H. S. Kim, K. J. Chang, K. S. Jeong, *Org. Lett.* **2004**, 6, 181.
82. J. D. Harper, C. M. Lieber, P. T. Lansbury, *Chem. Biol*. **1997**, 4, 951.
83. J. M. Lehn, *Supramolecular Chemistry: Concepts and Perspectives*, VCH, Weinheim, **1995**.
84. M. Sara, D. Mikael, K. Staffan. *Tetrahedron Lett.* **2007**, *48*, *2497*.
85. A. Hossain, H.-J. Schneider, *J. Am. Chem. Soc.* **1998**, 120, 11208.
86. C. Schmuck, *Eur. J. Org. Chem*., **1999**, 2397.
87. R. Fornasier, D. Milani, P. Scrimin, U. Tonellato, *J. Chem. Soc., Perkin Trans. 2*., **1986**, 233.
88. M. I. Ashiq, B. F. Tesfatsion, F. Gaggini, S. Dixon, J. D. Kilburn, *Chem. Eur. J.* **2010**, 16, 12387.

References


89. J. Rebek, *Angew. Chem*. **2005**, 117, 2104.
90. H. Hofmeier, U. S. Schubert, *Chem. Commun.* **2005**, 2423.
91. G. D. Pantos, P. Pengo, J. K. M. Sanders, *Angew. Chem., Int. Ed.* **2007**, 46, 2138.
92. R. Thomas, C. Schmuck, *Chem. Commun*. **2008**, 801.
93. J. P. Glusker, *Top. Curr. Chem.* **1998**, 198, 1.
94. J. L. Cook, C. A. Hunter, C. M. R. Low, A. Perez-Velasco, J. G.Winter, *Angew. Chem., Int. Ed*. **2007**, 46, 3706.
95. S. Leininger, B. Olenyuk , P. J. Stang, Chem. Rev. 2000, 100, 853.
96. C. Schmuck, *Eur. J. Org. Chem*., **2008**, 2, 324.
97. C. Schmuck , W. Wienand, *J. Am. Chem. Soc.* **2003**, 125, 452.
98. A. Brown, *Int. J. Mol. Sci.* **2009**, 10, 3457.
99. E. Zerovnik, *Eur. J. Biochem.* **2002,** 269, 3362.
100. P.T. Lansbury, *Curr. Opin. Chem. Biol.* **1997**, 1, 260.
101. C.Soto, *J. Mol. Med.* **1999**, 5, 343.
102. T.L. Lowe, A. Strzelec, L. L. Kiessling, R. M. Murphy, *Biochemistry*. **2001**, 40, 7882.
103. J. T. Jarret, E. P. Berger, P. T. Lansbury, *Biochemistry*. **1993**, 32, 4693.
104. C. Schmuck, M. Heil, *Org. Biomol. Chem.* **2003**, 1, 633.
105. C. Schmuck, T. Rehm, K. Klein, F.Grohn, *Angew. Chem. Int. Ed.* **2007**, 46, 1693.
106. J. P. Behr, J. M. Lehn, *J. Am. Chem. Soc.* **1973**, 95, 6108.
107. C. Urban, C. Schmuck, *Chem. Eur. J.* **2010**, 16, 9502.
108. A. G. Street, S. L. Mayo, *Proc Natl Acad Sci U S A.* **1999**, 96, 9074.
109. R. Fornasier, D. Milani, P. Scrimin, U. Tonellato, *J. Chem. Soc., Perkin Trans. 2*. **1986**, 233.
110. M. Sara, D. Mikael, K. Staffan, *Tetrahedron Lett.* **2007**, 48, 2497.
111. T. R. Kelly, M. H. Kim, *J. Am. Chem. Soc.* **1994**, 116, 7072.
112. J.C. Manimala, E. V. Anslyn, *Tet.Lett*. **2002**, 43, 565.
113. M. I. Ashiq, I. Hussain, S. Dixon, M. E. Light, J. D. Kilburn, *Acta Cryst.* **2010**, C66, o455.
114. P.W. Baures, J. R. Rush, A. V. Wiznycia, J. Desper, B. A. Helfrich, A. M. Beatty, *Cryst. Growth Des*, **2002**, 2, 653.
115. N. B. Perry, J. W. Blunt, H. G. Munro, *Magn Reson Chem*, **1989**, 27, 624.
116. H. M. Fooks, A. C. R. Martin, D. N. Woolfson, R. B Sessions, E. G. Hutchinson, *J. Mol. Biol.* **2006**, 356, 32.
117. S. Levin, J. S. Nowick, *J. Am. Chem. Soc.*, **2007**, 129, 13043.
118. H. Adams, C. A. Hunter, K. R. Lawson, J. Perkins, S. E. Spey, C. J. Urch, J. M. Sanderson, *Chem. Eur. J.* **2001**, 7, 4863.
119. G. Li, V. S. Bhosale, T. Wang, S. Hackbarth, B. Roeder, U. Siggel, J. Fuhrhop, *J. Am. Chem. Soc.*, **2003**, 125, 10693.
120. C. A. Hunter, *Chem. Soc. Rev.*, **1994**, 23, 101.
121. H. D.Matheka, H. L. Bachrach, *J. Virol*. **1975**,16, 1248.

122. S. Xu, J. Sun, D. Ke, G. Song , W. Zhang, C. Zhan, *J. Colloid Interface Sci*. **2010**, 349, 142.
123. R. Fuchs, C. P. Hagan, *J. Phys. Chem*, **1973**, 77, 1787.
124. C. Schmuck, *Coordin Chem Rev*, **2006**, 250, 3053.
125. S. B. Michael, W. youling,G. R. Matsueda, *Tet. Lett*., **1993**, 34, 3389 -3392.
126. S. B. Michael, W. youling, G.R.Matsueda, *J. Org. Chem.*, **1992**, 57, 2497.
127. G. M. Kyne, M. E. Light, M. B. Hursthouse, J. deMendoza, J. D. Kilburn, *J. Chem. Soc., Perkin Trans. 1*, **2001**, 1258.
128. B.Su, J.Zaho, Y.Cui, Y.Liang, W. Sun, *Synthetic Commun*, **2005**, 35, 2317.
129. L. J. Charbonniere, N.Weibel, P.Retailleau, R. Ziessel, *Chem. Eur. J.* **2007**, 13, 346.
130. E.Guénin, M.onteil, N.Bouchemal, T.rangé, *Eur.J Org. Chem*. **2007**, 3380.
131. B. R.Linton, A. J. Carr, B. P.Orner, A. D. Hamilton, *J. Org. Chem.* **2000**, 65, 1566.
132. T.Kasagami, I. Kim, H. Tsai, K. Nishi, B.D.Hammock, C. Morisseau, *Bioorg. Med. Chem. Lett*, **2009**, 19, 1784.
133. J. W. Harbuck, H. Rapoport, *J. Org. Chem*. **1972**, 37, 3618.
134. M.Wehner, D.Janssen, G. Schäfer, T. Schrader, *Eur. J. Org. Chem.* **2006**, *1*, 138.
135. A. P. Bisson, C. A. Hunter, J. C. Morales, K. Young, *Chem. Eur. J.*, **1998**, 4, 845.
136. M. I. Asgiq, PhD thesis, University of Southampton, **2010**.
137. C. Schmuck, T. Rehm, L. Geiger, M. Schäfer, *J. Org. Chem.*, **2007**, 72, 6162.

Appendices